Early Inhibition of the MAPK Pathway Prevents Optic Nerve Glioma Formation in a *Nf1*-Deficient Mouse Model

by

Emmanuelle Sterline Jecrois

A dissertation submitted in partial fulfillment
of the requirements for the degree of
Doctor of Philosophy
(Neuroscience)
in the University of Michigan
2018

Doctoral Committee:

Professor Roman Giger, Co-Chair
Adjunct Associate Professor Yuan Zhu, Co-Chair
Professor Peter Hitchcock
Associate Professor Bing Ye

Emmanuelle S. Jecrois

ejecrois@umich.edu

ORCID iD: 0000-0003-0313-0444

Dedication

This thesis is dedicated to my late father, Clement Jecrois. Thank you for understanding the importance of education and instilling it in your daughter.

Acknowledgements

First and foremost, I would like to acknowledge God without whom this dissertation would never have been possible. Thank you for granting me the serenity to accept the things I cannot change, the courage to change the things that I can and the wisdom to know the difference.

Next, I would like to thank the people who have always believed in me and supported me no matter what, my family: my mother, Immacula Bertrand, my sister, Stephanie Bertrand, my step-mother Miracuse Sinence, and my aunts, uncles, and cousins.

I would like to thank my dissertation mentor, Dr. Yuan Zhu, for his full support and expert guidance during my study and research. His wisdom and hard-work have always been a great motivation to me. I would like to express my appreciation to my committee members: Dr. Roman Giger, Dr. Peter Hitchcock and Dr. Bing Ye. Thank you for your helpful advice and feedback throughout my graduate studies as well as insight into my personal career development. I would especially like to thank Dr. Roman Giger for agreeing to serve as my co-chair during my time in Washington, D.C.

I am also grateful to past Zhu Laboratory members, particularly Dr. SunJung Kim, Dr. Yuan Wang and Dr. Miriam Bornhorst for their encouragement and contributions to my dissertation project. I would also like to thank current lab members Wang Zheng, Yuting Huang, Daniel Treisman, Chaoyang Li, Yinghua Li, Patrick Mateas, Hongmei Mao and other lab members for their friendship, support, insight and scientific discussions during my graduate career.

Lastly, I owe many thanks to our former Neuroscience program director Dr. Edward Stuenkel and current director Dr. Audrey Seasholtz, who have provided great motivation and have kept my best interests in the fore even while I was off-campus. Furthermore, I am grateful for program

administrators Rachel Harbach and Valerie Smith for creating a friendly and welcoming environment through their hard-work and dedication.

Table of Contents

List of Figures

List of Tables

Abstract

Low-grade pilocytic astrocytomas are the most common type of glioma found in children. Children with the inherited tumor predisposition syndrome, Neurofibromatosis type 1 (NF1), are especially prone to develop optic pathway gliomas (OPGs) primarily involving the anterior visual pathway composed of the optic nerve, chiasm and tracts. These tumors usually manifest in patients younger than 7 years of age, with the peak incidence between years 4 and 5. Despite the benign nature of these tumors, a subset of OPGs will develop and cause vision loss and other endocrine problems. Although treatment with non-alkylating chemotherapeutic agents has resulted in efficient disease stabilization, their ability to maintain or improve vision remains unclear. Despite recent advances in understanding how NF1 regulates neural stem and glial precursor cells in the brain, it remains uncertain which cell population(s) is (are) most affected by *Nf1* loss in OPGs. In addition, there is urgent need to define therapeutic windows to develop effective preventative and therapeutic strategies before visual deterioration.

This thesis focuses on understanding the timing and mechanism(s) of how loss of *Nf1* contributes to the formation of OPG by using a genetically engineered mouse (GEM) model of NF1-OPG. In this model, *Nf1* was inactivated in neural stem and progenitor cell populations during embryonic development. The resulting mutant pups ($Nf1^{hGFAP}$CKO) display hyperplastic lesions in the prechiasmatic optic nerves that develop into OPGs with high penetrance. A detailed analysis of the natural history of OPGs in $Nf1^{hGFAP}$CKOs yielded several important findings. *Nf1* loss in the developing optic nerve leads to the expansion of an abnormal glial cell population that expresses both GFAP and Olig2, and over-activates RAS/MEK/ERK signaling as well as glia restricted progenitor cells which, persist throughout gliomagenesis. Importantly, MEKi treatment during a critical developmental window (P0.5-P21) is sufficient to prevent the formation of OPG in $Nf1^{hGFAP}$CKO mice and rescue retinal ganglion cells (RGC) loss. Likewise, genetic inactivation

of *Mek1/2* rescues the formation of OPG and the death of RGCs in a dose-dependent manner. Collectively, this study clearly demonstrates that OPGs are a developmental defect with Erk-dependent glial cell expansion occurring during the early postnatal period (Phase I) followed by an immune response, nerve degeneration and Bax-mediated RGC apoptosis (Phase II) and identifies a critical period for neuroprotective intervention before irreversible neurological deficits. Lastly, we have developed a preclinical model to test for the biological effects of MEK inhibitor-based preventative therapies, which allows us to screen for the optimal dose and delivery method.

Chapter I: Introduction

1.1 Pediatric low-grade gliomas

Brain tumors are the most frequently encountered solid tumors in childhood (Surawicz et al. 1998; Surawicz et al. 1999). Low-grade gliomas (LGGs) constitute the largest fraction of these tumors, accounting for more than 50% of all pediatric central nervous system tumors (Rickert and Paulus 2001). They are the leading cause of cancer-related death in children under the age of 14. Pediatric LGGs represent a heterogeneous group of tumors and are classified as World Health Organization (WHO) grade I or II, low-grade glial neoplasms, based on their morphological features and constitutive cell type such as astrocytic, oligodendroglial, mixed oligoastrocytic neuronal, or mixed glial-neuronal morphology (Table 1). Although this classification is designed to include every tumor, separation between variants is often difficult and even arbitrary, especially when the tumors display overlapping histology for multiple categories. Pleomorphic xanthoastrocytomas (PXAs) account for one of the rarest histopathological entities of pediatric LGGs. They typically arise in the supratentorial regions and are comprised of large pleomorphic as well as spindle and lipidized cells in a dense pericellular reticulin network. Pediatric diffuse astrocytoma (DA) is an umbrella group comprised of tumors with diffusely infiltrating components that rarely undergo malignant transformation and offer better overall prognosis. The group of mixed neuro-glial neuroepithelial LGGs is predominantly found in the cortical regions of the temporal lobe and is characterized by columns made up of bundles of axons oriented perpendicular to the cortical surface and mature, dysplastic ganglion cells in combination with neoplastic glial cells. Oligodendrogliomas (ODs) and oligoastrocytomas (OAs) are more commonly found in adult population, but are extremely rare in children, representing less than 5% of pediatric LGG. The cerebellum is the most prevalent location for LGGs, and cerebellar low-grade gliomas account for 15% to 25% of all pediatric central nervous system tumors. They are followed by hemispheric

(cerebral) gliomas (10% - 15%), gliomas of the deep midline structures (10% - 15%), optic pathway gliomas (5%), and brain stem gliomas (2% - 4%) (Freeman, Farmer, and Montes 1998).

Table 1: Different subtypes of pediatric LGGs based on WHO classification

Astrocytic tumors	Grade (WHO)
Pilocytic astrocytoma (PA)	I
Diffuse astrocytoma (DA)	II
Pilomyxoid astrocytoma (PMA)	II
Pleomorphic xanthoastrocytoma (PXA)	II
Oligodendroglial oligoastrocytic tumors	
Oligodendroglioma (OD)	II
Oligoastrocytoma (OA)	II
Neuronal, mixed neuro-glial neuroepithelial tumors	
Ganglioglioma (GG)	I
Angiocentric glioma (AG)	I
Desmoplastic infantile tumor	I
Dysembryoplastic neuroepithelial tumor (DNT)	I

Pilocytic astrocytomas (PAs) are the most common among pediatric LGGs, accounting for 85% of these tumors. The term "pilocytic" has been used to describe astrocytoma variants at least partially comprised of cells with hair-like, bipolar processes. PAs are defined by WHO as grade I and typically arise in the cerebellum, optic pathway, and brainstem (Ostrom et al. 2014; Pfister and Witt 2009). PAs are classically characterized by the presence of Rosenthal fibers, biphasic architecture with areas of disaggregated cells or small cysts alternating with more compact regions, vascular proliferation, and eosinophilic granular. On magnetic resonance imaging (MRI), PAs appear as well-circumscribed tumors, hyper intense on T2 weighted with a large cystic component. Pilocytic astrocytomas that involve the optic pathways, optic nerve, and chiasm typically form fusiform masses with distinct nuclear pleomorphism. Consistent with their classification as low-grade glial neoplasms, they have low cell density, contain very few mitotic figures, are often indolent or slow-growing and do not undergo malignant transformation. This is in contrast to adult low-grade gliomas that have a more aggressive phenotype. They often lack palisading necrosis

and pronounced nuclear atypia but harbor large number of microglia. Immunoreactivity for proteins associated with glial lineage cells, including glial fibrillary acidic protein (GFAP) and oligodendroglial marker Olig2 has been observed in these tumors.

Unlike the adult population, the majority of pediatric PAs have an excellent prognosis with overall 10-year survival reported to be over 90% (Burkhard et al. 2003). However, the prognosis is worse for tumors in the hypothalamic/chiasmatic, deep midline, and brain stem regions because they have minimal potential for resection and therefore, less favorable progression-free and overall survival. Nonetheless, PAs rarely progress to malignancy, with the vast majority, even after multiple recurrences, maintaining their WHO grade I designation. In addition to pilocytic astrocytomas that develop sporadically (without any known genetic inheritance), these tumors can also develop in association with the hereditary tumor predisposition syndrome Neurofibromatosis type 1 (NF1). PAs in the NF1 pediatric population display unique features that distinguish them from their sporadic counterpart. The cerebellum is the organ of predilection in sporadic PAs, whereas those in children with NF1 predominate in the optic pathways (optic nerve, chiasm, tracks, and radiations). The differences in brain location impact the presenting signs and symptoms- optic pathway PAs are associated with visual impairment and early onset puberty, whereas cerebellum and brainstem PAs induce headaches and hydrocephalus. Importantly, PAs in children with NF1 tend to arise at earlier ages than those in the sporadic population.

1.2 Molecular genetics of PA

Comprehensive genomic and genetic studies, using high-throughput genetic sequencing and gene expression profiling, performed in recent years have determined a number of mutations and genetic alterations associated with pediatric PAs. Besides a relatively normal karyotype, these tumors contain few regions of chromosomal loss or gain. The majority of PAs present alterations in the RAS/RAF/MEK/ERK pathway, which is responsible for modulating cell growth, proliferation, and apoptosis in both normal and tumor cells. The most frequent genetic alterations observed in PAs are tandem duplication at 7q34, which produces a fusion between *KIAA1549* and *BRAF* genes, leading to the expression of an abnormal fusion transcript *KIAA1549-BRAF* and loss of *NF1* gene expression. As many as 60–94% of PAs exhibit the *KIAA1549-BRAF* fusion, most

commonly in those Pas arising in the cerebellum (Bergthold et al. 2014). Expression of this fusion protein results in loss of the BRAF auto regulatory domain at the amino-terminus and constitutive activation of the RAS-ERK pathway (Jacob et al. 2009). Another gene fusion that also results in constitutive activation of the BRAF kinase, *FAM131B-BRAF,* has been described in PAs (Cin et al. 2011). A further seven gene partners for *BRAF* fusions have been found in small numbers of cases (*RNF130*, *CLCN6*, *MKRN1*, *GNA11*, *QKI*, *FZR1* and *MACF1*), which have all resulted in the loss of the N-terminal regulatory region of the BRAF protein and the retention of the kinase domain. These arise by various genetic mechanisms, including deletions and translocations (Forshew et al. 2009; Jones et al. 2013; Zhang et al. 2013). Non-fusion mutations of the *BRAF* gene, including the well-known V600E mutation and a number of small insertions which activate BRAF kinase signaling, have also been identified in a subset of PA cases (Schindler et al. 2011). In addition to BRAF, fusion genes retaining the kinase domain in both NTRK2 (TrkB) and NTRK3 (TrkC) receptor tyrosine kinases have been described in some LGG histological subtypes (Jones et al. 2013). Recently, next-generation sequencing analyses have suggested a role for fibroblast growth factor receptor (FGFR) activation as a driver for some supratentorial PAs (Zhang et al. 2013). One interesting clinical observation is that the various MAPK mutations identified in LGGs are not uniformly spread across different tumor anatomical locations. For example, BRAF fusions are found readily in LGGs in the cerebellum but are less common in supratentorial locations. On the other hand, BRAF V600E and NRTK fusions are more prevalent in tumors located in the brain hemispheres.

Patients with NF1 have an increased risk of all gliomas, with PA being the most frequent form that occurs in about 15-20% of these patients, particularly on the optic pathway during early childhood (Listernick et al. 2007). NF1-associated PAs show complete loss of *NF1* expression, whereas histologically comparable PAs that arise sporadically in patients without NF1 still maintain *NF1* gene expression (Kluwe et al. 2001). Likewise, PAs have also been reported in a small number of patients with Noonan syndrome, which is characterized by mutations in RAS-ERK pathway genes, including *PTPN11*, *SOS1*, and *KRAS* (Collins, Jones, and Giannini 2015). These new insights regarding the underlying biological processes necessary for tumor growth and maintenance will open the door to a more targeted, molecularly based classification approach to therapy.

1.3 Neurofibromatosis type 1

Neurofibromatosis type 1 is sometimes referred to as Von Recklinghausen's disease based on the German physician, Friedrich Von Recklinghausen, who identified it in 1882. It is one of the most common monoallelic genetic disorders, with sporadic mutations arising in about half of cases and affects approximately 1 in 3500 individuals worldwide (Friedman 1999). NF1 displays an autosomal dominant pattern of inheritance and is caused by a germline mutation in a single gene *NF1*. Approximately 50% of all documented cases represent de novo mutations, as a result of the *NF1* gene having a large genomic footprint and an elevated rate of germ cell mutations (estimated 1 $x10^4$ per gamete per generation) (Huson, Harper, and Compston 1988). Beside its complete penetrance, the phenotypic expression of the disease is highly variable among afflicted individuals, even among family members who may carry the same genetic mutation. The high variability in phenotypic expression in NF1 could be due to modifier genes, such as protein-coding sequences, microRNA, and long noncoding RNA genes (Pasmant et al. 2012). This hypothesis was supported by cohort studies, which have shown that the clinical features tended to be similar in close relatives versus distant relatives. The incidence of the disease remains the same regardless of sex or ethnicity.

NF1 is characterized by the presence of benign peripheral nerve sheath tumors termed neurofibromas, pigmentary changes such as skinfold freckling, café-au-lait macules (CALMs), iris hamartomas (Lisch nodules) and gliomas involving the optic pathway (Table 2) (Gutmann et al. 1997). Optic pathway gliomas are not the only type of LGG that occur in children and adults with NF1. The brain stem and other midline structures can harbor low-grade gliomas, but these lesions are usually diagnosed later in childhood. Likewise, tumors can occur in corpus callosum and cerebral hemispheres often in adolescence or the teenage years. Similar to optic pathway gliomas, the natural history of these non-visual pathway tumors is erratic with some tumors growing for brief periods of time and then seemingly arresting, while others may become increasingly symptomatic over relatively brief periods of time, especially brain stem tumors. In addition to central nervous system (CNS) tumors, several types of peripheral nerve sheath tumors can arise in NF1 patients. They range from benign neurofibromas, including dermal and plexiform

neurofibromas, to malignant peripheral nerve sheath tumors (MPNSTs). In addition to being susceptible to PNS and CNS tumors, individuals with NF1 have an increased risk of developing leukemia, pheochromocytoma, gastrointestinal stromal tumors, early-onset breast cancer, and high-grade malignant glioblastoma (Stiller, Chessells, and Fitchett 1994; Sharif et al. 2007; Vlenterie et al. 2013). Between 30%-70% of NF1 children are diagnosed with learning disabilities, making it the most significant factor affecting quality of life among those patients (Hyman, Shores, and North 2005). Affected individuals are also prone to macrocephaly, seizures, short stature and skeletal defects, such as bone malformations and spinal curvature (scoliosis). At the moment, it is extremely difficult to predict which child or adult will develop any of these medical problems. Lastly, even when clinical abnormalities arise, an accurate prediction of the natural history of any particular disease feature is almost impossible because there are few predictors of disease progression or response to therapy.

Table 2: Onset of NF1 symptoms

Clinical Features	Congenital (0 - 2 years)	Preschool years (2 - 6 years)	Late childhood & Adolescent years (6 - 16 years)	Adulthood (16+ years)
Café-au-lait macules				
Lisch nodules				
Plexiform Neurofibromas				
Diffuse				
Nodular or Superficial				
Bony Lesion				
Tibial dysplasia				
Axillary or inguinal freckling				
Optic pathway glioma				
Learning disabilities				
Dermal neurofibromas				
Scoliosis				
MPNST				

1.4 Molecular and Genetic characterization of NF1 and neurofibromin

The *NF1* gene is located on chromosome 17q11.2 and spans 350 kilobases (kb) of genomic DNA (Marchuk et al. 1991). The gene encodes a 220-250kDA protein called neurofibromin which is predominantly expressed in neuronal and glial cells (Daston et al. 1992). Amino acid sequence analysis of neurofibromin protein has revealed that it encloses a functional GAP-related domain (GRD) that is homologous to members of the GTPase-activating protein (GAP) family (Xu et al. 1990). The protein neurofibromin is highly conserved within vertebrate species and has over 98% homology with the mouse homolog. Similar to other GAP members, neurofibromin is involved in precipitating the conversion of active RAS-GTP to its inactive form, RAS-GDP. Therefore, the protein functions as a negative regulator of the RAS-mediated signaling pathway, which is involved in cell proliferation and transformation, senescence.

Most of the mutations in NF1 have been identified as loss-of-function mutations. These include missense, nonsense, frameshift, and splice site mutations, insertions, deletions, large deletions, including *NF1* gene and possibly other neighboring genes, and translocations. Although patients with NF1 disease begin life with one functional and one mutated *NF1* allele, this heterozygous state alone is insufficient for tumor formation. Loss of heterozygosity (LOH), or 'second-hit' somatic mutations, through the inactivation of the remaining functional allele, thereby causing loss of neurofibromin protein expression, has been reported in a variety of NF1-associated tumors, including neurofibromas, malignant peripheral nerve sheath tumors, pheochromocytomas, and myeloid tumors (Glover et al. 1991; Xu et al. 1992; Legius et al. 1993; Shannon et al. 1994; Colman, Williams, and Wallace 1995; Serra et al. 2000). Based on these findings, the *NF1* gene has been classified as a tumor suppressor. Moreover, whole genome sequencing of NF1-PAs has revealed the presence of neoplastic cells with alterations affecting both *NF1* alleles (germline *NF1* gene mutation and somatically acquired *NF1* gene mutation)(Gutmann et al. 2013).

RAS-mediated signaling has two primary effector pathways: (1) the mitogen-activated protein kinase/extracellular-signal regulated kinase (MAPK/ERK) and (2) the phosphatidylinositol 3 kinase (PI3K)/AKT pathway (Cichowski and Jacks 2001). *RAS* genes, including *NRAS*, *HRAS*,

and *KRAS*, form a multigene family encoding guanosine nucleotide bound GTPases. The signaling pathway begins with the interaction between a ligand and a cell surface receptor, a receptor tyrosine kinase (RTK) (Figure 1). This is followed by activation of RAS by conversion of RAS-GDP into RAS-GTP. Neurofibromin negatively regulates this step through GTPase-activating protein activity by converting the active RAS-GTP to the inactive RAS-GDP. Active RAS interacts with many downstream mediators, most importantly by binding to the RAS-binding domain of BRAF or Raf-1 proto-oncogene, serine/threonine kinase (*RAF1*). This leads to homo and heterodimerization and activation of RAF, which then activates MEK, a serine/tyrosine/threonine kinase, via phosphorylation. Lastly, the extracellular signal-regulated kinases (ERK) is phosphorylated and activated. When activated, MEK accelerates progression through the cell cycle, leading to cell growth and differentiation. Of note, RAS/ERK pathway activation may be involved in cell differentiation and senescence (Jacob et al. 2011). The other effector pathway, P13K-AKT signaling pathway, which modulates the activity of the mammalian target of rapamycin (mTOR), was also found to be hyperactivated due to *NF1* loss (Kaul et al. 2015). In addition, a recent study has reported that neurofibromin differentially controls neural stem cells (NSCs) proliferation and multilineage differentiation through selective use of PI3K-AKT and RAF/MEK effector arms respectively (Chen, Gianino, and Gutmann 2015).

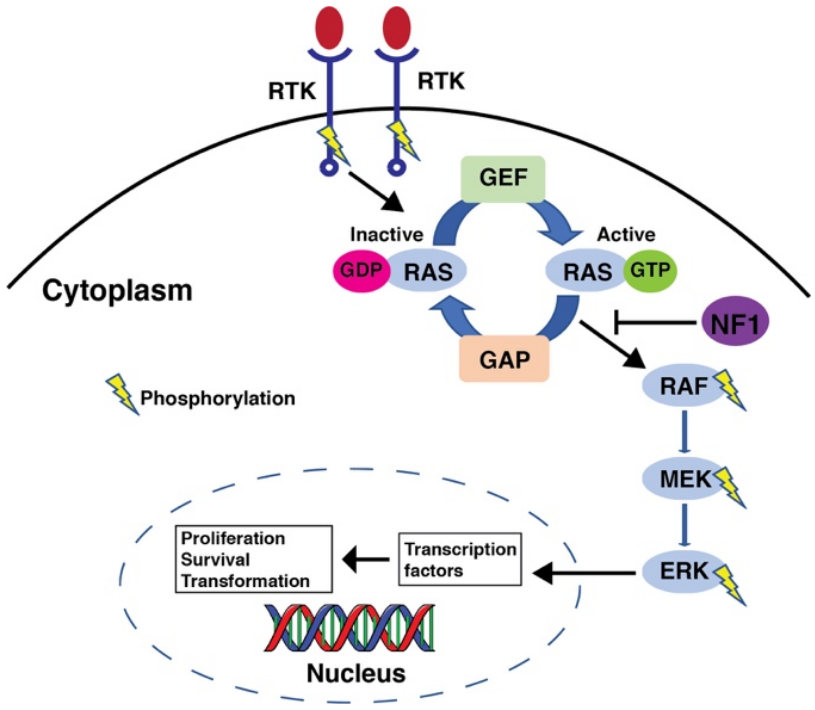

Figure 1. Overview of the MAPK-ERK signaling pathway.

Receptor tyrosine kinases (RTKs), when activated by a ligand, promote guanine nucleotide exchange to form activated RAS- GTP complex. Thus, a kinase cascade begins through MEK and ERK phosphorylation, resulting in the activation of transcription factors that drive genomic signature programs such as cell cycle progression, proliferation, survival, and transformation. NF1 functions as a GTPase activating protein (GAP) which stimulate GTP hydrolysis and formation of inactive RAS–GDP. Consequently, neurofibromin suppresses activation of the downstream effectors of RAS, negatively regulating the pathway. GDP=guanosine diphosphate. GTP, guanosine triphosphate. ERK, extracellular signal-regulated kinase. MEK, MAPK-ERK kinase.

1.5 NF1-associated Optic Pathway Glioma

Approximately 15% to 20% of NF1 patients develop low-grade gliomas predominantly involving the optic pathway (optic pathway glioma, OPG) (Listernick, Charrow, and Gutmann 1999; Listernick et al. 1997). OPGs behavior and aggressiveness correlate with the tumor site within the optic pathway. OPGs located in the hypothalamic region usually display pilomyxoid attributes and more aggressive behavior, often resulting in short stature, precocious puberty, hydrocephalus with related symptoms such as headaches and vomiting, larger head circumference, and learning and behavior deficits (Tihan et al. 1999; Fried et al. 2013). Gliomas that involve the optic chiasm will often result in slow visual loss in both eyes as well as swelling of the optic disc or atrophy, or bitemporal field deficits, proptosis with or without strabismus, and nystagmus. Patients with gliomas of the optic nerve proper tend to display painless optic disc swelling and visual loss in only one side and proptosis with or without strabismus. These tumors are usually benign and can sometime spontaneously regress (Parsa et al. 2001). In fact, patients with NF1-associated OPG tend to require less treatment and display a more passive disease progression with better clinical outcomes than sporadic OPGs. The mechanisms underlying the growth and occasional senescence of NF1-associated OPGs are still unclear. OPGs can be readily detected in imaging and present a wide range of neuroradiologic appearances such as enlargement of the chiasm, a fusiform shape or have a downward kink in the middle of their orbit.

Although there is lack of clear prognosis features, patient sex, age and tumor location have all been associated with an increased risk of clinical progression. It was reported that girls with NF1 are more likely to lose vision and require treatment for OPG than boys. In addition, girls with OPGs are up to 10 times more likely to experience visual decline than their male counterparts (Diggs-Andrews et al. 2014). NF1-OPGs that arise in postchiasmatic optic pathway tend to behave more aggressively than those in the optic nerve proper. Lastly, OPGs that develop in children younger than 2 years of age or after the age of 8 to 10 tend to be more aggressive than those in children between the ages of 2 to 8 (Listernick et al. 2004; Balcer et al. 2001).

1.6 Current NF1-OPG treatment and management

NF1-OPGs often behave in an unpredictable manner, requiring an increase in routine surveillance in all NF1 children. Annual eye exams are recommended for all children less than 10 years old, and after that every two years until the age of 18. Serial screenings for progressive visual loss, complete ophthalmic examinations for visual acuity, visual evoked potentials and magnetic resonance imaging (MRI) have all been used as tools to monitor OPG progression in NF1 patients. Treatment of diagnosed OPG is based on the radiographic and clinical progression of the tumor and still remains controversial due to high variability of the disease course. The major morbidity associated with these gliomas is visual loss with 30%-50% of NF1 children with OPG experiencing impaired visual acuity. However, the mechanism of visual loss in children with NF1-associated OPGs is poorly understood and has not been clearly related to tumor size or extent of the involvement of the visual pathway. Some patients with relatively small lesions can lose vision, while some with larger growing lesions may have well maintained vision. Many children with NF1-associated OPGs do not require treatment, because the tumors are asymptomatic or remain static. Even slow growing tumors often do not need to be treated, because they have a specific time window of development (usually up to age 7), and past this short window, the tumors may spontaneously arrest and on rare occasions even regress. Currently, it is impossible to determine which NF1 children have the greatest risk for developing NF1-OPG since baseline MRI is useless in predicting clinical outcome.

When treatment is required, it may only be needed for a limited period of time. Because of the location on the visual pathway, surgery is rarely a therapeutic option. Likewise, radiation is seldom utilized due to concerns of hormone deficits, cerebrovascular disease, secondary malignant neoplasms and cognitive impairment, especially in the pediatric population (Sharif et al. 2006; Murphy et al. 2015). Chemotherapy is now the front-line adjuvant therapy for children with progressive low-grade gliomas. The most common chemotherapeutic agents employed has been the combination of carboplatin and vincristine (Ater et al. 2016; Packer et al. 1997). This treatment regimen results in minimal long-term complications and achieves tumor stabilization in 80%–90% of patients. Although several international collaborative trials have demonstrated the ability of carboplatin and vincristine to control tumor growth, over a quarter of treated NF1 children lost vision despite stable radiographic studies (Fisher et al. 2012). Therefore, the primary benefit of novel intervention may be in improving visual outcome. Recently, several studies have employed the RNFL thickness as a useful biomarker of vision loss in children with NF1-OPGs. A reduction of the RNFL reflects axonal degeneration of retinal ganglion cells (RGCs), which represent the only neuronal population that connects the retina to the brain (Avery et al. 2015; Avery, Mansoor, Idrees, Biggs, et al. 2016; Avery, Mansoor, Idrees, Trimboli-Heidler, et al. 2016). Despite their success in controlling radiographically defined tumor growth, chemotherapeutic agents are not expected to regenerate RGCs or re-establish neuronal circuits.

Improvement in the understanding of the molecular alterations involved in OPG formation has led to molecularly targeted therapies, such as mTOR inhibitors and MEK inhibitors, to be incorporated into clinical trials. Inhibitors of the mTOR pathway, including rapamycin and RAD001, have been utilized following genetic engineered mouse modeling based research that suggested that mTOR hyperactivation was a major component of glioma growth. However, blocking mTOR hyperactivation with rapamycin coupled with Tarceva, an EGFR inhibitor, has primarily resulted in a static arrest of tumor growth (Yalon et al. 2013). MEK inhibitors are also actively being explored in children with NF1-OPGs. Early results from clinical trials are more encouraging, and tumor shrinkage was seen more frequently. Inhibiting MEK presents an attractive advantage because it represents a convergence point in the RAS/RAF/MEK/ERK pathway where a number of upstream signaling pathways can be blocked. Most MEK inhibitors are specific and do not inhibit many different protein kinases, although some are more specific

than others. The use of these MEK inhibitors, or other biologic agents, must be undertaken with careful toxicity monitoring including neurocognitive assessments since the long-term suppression of the RAS-MAPK pathway in young children may result in significant developmental issues. The most critical challenge for NF1-OPG is to develop preventive or early interventional therapies to be delivered before irreversible neurological deficits such as axonal degeneration and RGC loss occur (Listernick 2016). In order to achieve this goal, we need a better understanding of the full-course of NF1-OPG disease pathogenesis from a developmental defect to visual loss.

1.7 Insights from murine models of NF1-OPG

Due to the paucity of human glioma tissue available for analysis, the neurobiology of NF1-associated gliomas is only partially understood and has been greatly elucidated by the use of genetically engineered mouse (GEM) models. Moreover, there is an increasing need for preclinical mouse models that reflect the unique clinical features of NF1-OPG – monogenic disease, early window for development, and slow growth – to assess preventative and therapeutic intervention. GEM models have been developed which mimic NF1 LGGs and have resulted in important insights. Because of the essential role of neurofibromin during tissue development and organogenesis, mice harboring homozygous *Nf1* mutation ($Nf1^{-/-}$) are embryonic lethal and die of heart failure and cardiac defects (Brannan et al. 1994). Although the early lethality of $Nf1^{-/-}$ mutants has hampered the study of *Nf1* loss during late developmental stages and adulthood, these mice have nonetheless supplied very useful information and materials to help characterize *NF1* function in cell population involved in NF1-associated tumors. In contrast, mice with a heterozygous germline *Nf1* mutation ($Nf1^{+/-}$) are viable and fertile, and fail to develop common and early onset features of human NF1 such as neurofibromas and cafe-au-lait spots but are susceptible to the development of tumors, such as leukemia and pheochromocytomas and ultimately die by 15 to 18 months (Jacks et al. 1994).

Due to the limitation of *Nf1* germline homozygous and heterozygous deletion mouse models, researchers have developed tissue-specific *Nf1* conditional knockout (CKO) mice, which allow them to investigate the effect of *Nf1* deficiency in a small population of cells. For example, Dr. Yuan Zhu generated a GEM model of *Nf1*-OPG by targeting homozygous *Nf1* mutations ($Nf1^{-}$

$^{/-}$) to neural stem and progenitor cell populations during embryonic development using a Cre transgenic line under the control of human glial fibrillary acidic protein promoter (hGFAP-cre) (Anthony et al. 2004; Malatesta et al. 2003; Wang et al. 2012; Zhuo et al. 2001; Zhu et al. 2005). The resulting mutant pups (*Nf1*^{hGFAP}CKO) exhibited structural brain defects, ataxia, reduced body size and poor health. More importantly, the mutants show increased glial progenitor proliferation in the brain and develop OPGs in high penetrance with similar histopathological characteristics of human NF1-OPGs. The next attempt was led by Dr. David Gutmann, who generated another conditional *Nf1* mouse strain, using the GFAP-cre* transgene to inactivate *Nf1* in neuroglial progenitors at around E14 (Bajenaru et al. 2003). In this model, the mice develop low-grade gliomas of the optic nerve and chiasm by 3 months of age only when neighboring cells in the tumor environment were *Nf1* heterozygous (*Nf1*$^{+/-}$), not wild-type (*Nf1*$^{+/+}$). From these results, the researchers concluded that the heterozygosity of the surrounding cells play an important role in the tumor development. These tumors were characterized by low proliferative indices, microglial infiltration, and robust GFAP expression, and were detectable on MRI (Bajenaru et al. 2005). Moreover, these tumors led to subsequent time-dependent sequence of events: optic nerve dysfunction, retinal ganglion cell (RGC) loss, retinal nerve fiber layer thinning, and reduced visual acuity (Hegedus et al. 2009). These GEM models suggest that optic gliomagenesis requires somatic *Nf1* inactivation in a population of progenitor cells from specific brain regions during mid to late embryogenesis. This partly explains the propensity of gliomas to arise in the optic pathway and brainstem of NF1 patients and the predilection for these tumors to arise in young children during early childhood.

Although these GEMs have already yielded some important findings, there are several questions that still remain unanswered. The most promising opportunities for application of mouse *Nf1* optic glioma models in the future will be: 1- to determine the cell population(s) is(are) most affected by *Nf1* loss during early optic nerve development; 2- to define the mechanisms underlying tumor-associated visual decline; 3- to determine the optimal time to initiate preventive or early interventional treatments that can effectively prevent visual deterioration.

1.8 Optic nerve development in rodents

The optic nerve is part of the central nervous system and contain the same glial cell types found throughout the central white matter, in addition to the axons of retinal ganglion cells (RGCs). The optic nerve connects all RGCs from the retina to their targets in number of central regions known as retino-recipient targets, including the suprachiasmatic nuclei, the accessory optic nuclei, the pretectal nuclei, the ventral and dorsal lateral geniculate nuclei, the lateral geniculate nucleus (LGN) and the superior colliculus (SC), where the majority of RGCs project towards. Formation of the vertebrate eye begins with the asymmetrical, bilateral invagination from the anterior portion of the neural tube, the neuroepithelium of the ventral diencephalon of the embryonic brain. This, in turn, results in the formation of the proximal optic stalk and the distal optic vesicle, which further invaginates to create the bilayered optic cup. The inner layer of the optic cup gives rise to the neural retina and the retinal pigment epithelium (RPE) develops from the outer layer (between E9.5-E11.5 in the mouse) (Mui et al. 2005). Eventually, the optic stalk and the edge of the optic cup fuse to form the optic disc or optic nerve head (ONH). Lastly, axons of the RGCs project through the optic disc into the optic stalk towards their targets in the brain. This event signals the development of the optic nerve and occurs at approximately E15.5 in the mouse.

The adult optic nerve is comprised of two macroglia cell types: astrocytes and oligodendrocytes, which fold around the axons of RGCs and produce myelin and play an essential role in the efficiency and velocity of neuron impulse conduction. Microglia, the immunocompetent and phagocytic cells in the CNS, represent a small population in the nerve under normal conditions. Unlike other glial cells that originate from the ectodermal tissue, microglia are mesodermal in origin and are derived from yolk-sac progenitors at E7.5 and populate the brain during early development (Aguzzi, Barres, and Bennett 2013). Although astrocytes were initially thought to passively support and nurture neurons, numerous studies have shown that they play a role in almost all facets of development and function in CNS. Their functions range from maintenance of ionic homeostasis and blood-brain barrier to actively regulating neuron-to-neuron communication and synaptic plasticity. Furthermore, astrocyte dysfunction has been implicated in ocular pathologies such as coloboma, optic nerve dysplasia and glioma resulting in mild vision impairment to complete vision loss (Friedlander 2007). Studies with the rat optic nerve culture (Raff et al. 1983;

Raff, Abney, and Miller 1984; Miller et al. 1985) coupled with recent advances in genetic engineering and fate mapping have allowed for more detailed examination of the lineages of glial cells in the optic nerve. These studies have provided evidence of two spatially-restricted glial progenitor lineages that locate within the optic nerve at different developing stages (Figure 2).

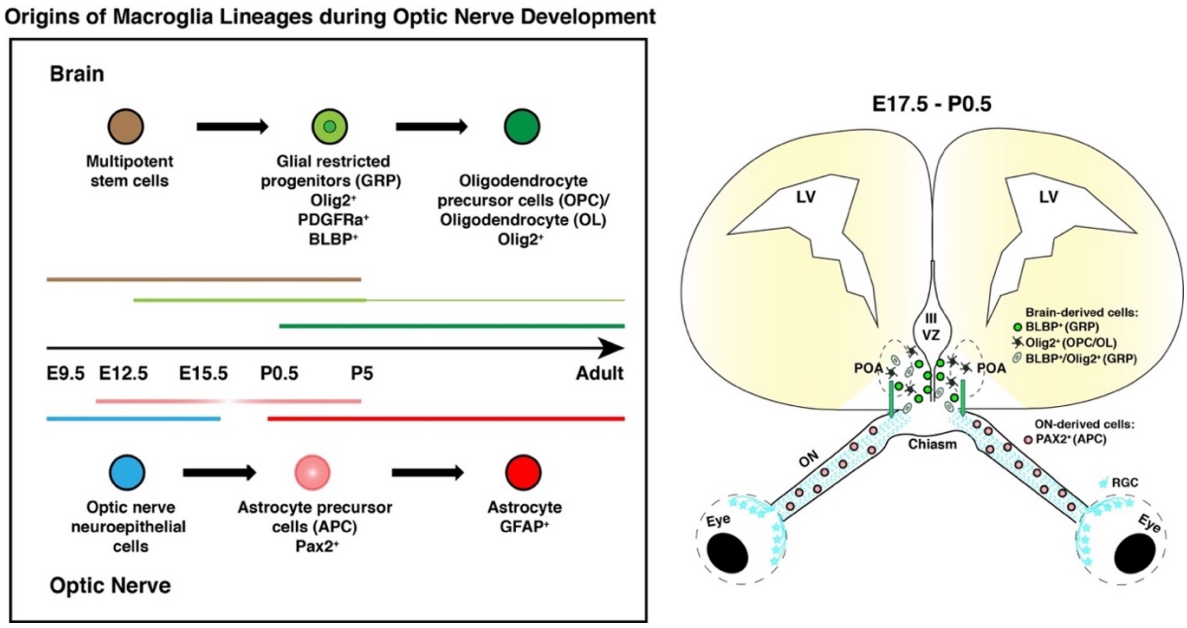

Figure 2: Anatomically distinct origins of astrocyte and oligodendrocyte lineages during optic nerve development in rodents. (See text for details)

During embryonic stages, neuroepithelial cells from the optic stalk generate $Pax2^+$ astrocyte precursor cells (APCs) that differentiate only into astrocytes (Mi and Barres 1999; Small, Riddle, and Noble 1987). Pax2 belongs to the Pax protein transcription factor characterized by a paired box (a DNA-binding element) and also plays a critical role in eye morphogenesis by defining retina-optic nerve boundaries (Schwarz et al. 2000). Specifically, Pax2 has been shown to suppress the neuronal fate and promote glial fate of optic nerve neuroepithelial cells (Soukkarieh et al. 2007). The peak differentiation period of optic stalk neuroepithelial cells into $Pax2^+$ APCs in rats is between E12 to E14 (Kuwabara 1975). This period coincides with the onset of Sonic hedgehog (Shh) expression from differentiating RGCs (Dakubo et al. 2003). It was demonstrated that RGC axons-derived Shh promotes astrocyte proliferation (Wallace and Raff 1999; Dakubo et

al. 2008). By E17, almost all neuroepithelial cells in the rat optic nerve are $Pax2^+$ cells. $Pax2^+$ precursors begin to rapidly generate $GFAP^+$ astrocytes by E19. The proximal-distal patterning of the optic nerve development is regulated by Shh signaling which suppresses Pax6 while simultaneously promoting Pax2 and Vax in optic stalk cells. Transgenic mice lacking Pax2 have helped to highlight the critical role of this transcription factor in optic stalk specification. These mice display incomplete optic fissure closure, abnormal axonal pathways, hyperpigmentation of the optic stalk, and optic nerve glia hypoplasia (Torres, Gomez-Pardo, and Gruss 1996; Macdonald et al. 1997).

Oligodendrocytes, however, are not locally generated in the optic nerve. They are derived from oligodendrocyte progenitor cells (OPCs), highly motile cells that migrate into the nerve from the chiasm towards the eye beginning at birth and populate the entire nerve (except lamina cribosa) by P3 (Small, Riddle, and Noble 1987; Ueda et al. 1999). Multiple lines of evidence have demonstrated that optic nerve OPCs mostly originate from the ventral brain, specifically the floor of the third ventricle (Small, Riddle, and Noble 1987; Ono et al. 1997; Gao and Miller 2006) and the preoptic area (Ono et al. 2017). Unlike other regions of the CNS where OPCs have been reported to differentiate into astrocytes in addition to oligodendrocytes (Ono et al. 2008; Tatsumi et al. 2008), there may be intrinsic inhibitor factors specifically localized in the optic nerve that prevent OPCs from yielding astrocytes.

1.9 Cell of origin for *Nf1*-OPG

Individuals with NF1 are born with one functional allele (wild-type) and one mutated allele in germline cells ("first-hit"). The most well-known genetic and molecular mechanism for tumor development is the biallelic inactivation of *NF1* gene, or loss of the remaining wild-type allele ("second-hit") (Gutmann et al. 2013; Lau et al. 2000). It is well documented that NF1-OPGs rarely develop in children over 7 years of age (peak incidence between 4 to 5 years) (Packer et al. 2017; Listernick 2016). These clinical observations suggest that complete *NF1* inactivation must occur in a transient neural stem and/or progenitor cell population during a critical time window of early nerve development. The high degree of heterogeneity in the clinical manifestations of NF1 disease in patients has reinforced the importance of determining the cell of origin of OPG. Previous studies

have shown that brain tumors with similar histopathological characteristics possess unique molecular features that correlate with their original progenitor cells (Taylor et al. 2005; Kalamarides et al. 2011). Furthermore, several labs have demonstrated that some brain cancers are initiated and maintained by a population of cells that exhibit stem cell-like characteristics such as multipotency and self-renewal (Galli et al. 2004; Hemmati et al. 2003; Singh et al. 2004; Wang et al. 2009). These studies have highlighted the importance of determining the cellular origin of OPG, which could yield useful information on the molecular basis for the development of the tumor, its regulatory mechanisms, changes in genetic profile and allow for improved response to therapeutic drugs.

There are multiple germinal zones in the brain such as the subventricular zone of the lateral ventricle (lv-SVZ), the III-VZ and the fourth ventricle and the optic nerve proper that could serve as site of origin for tumorigenesis. In principle, at least three cell types could serve as the cell of origin of NF1-OPG: 1- multipotent neural stem cells (NSCs), 2- glial-restricted progenitor (GRP) cells, and 3- mature dedifferentiated cells. The third option is also the least likely, considering the monogenic nature of this disease and the very low risk of malignancy associated with it. One aspect of NSCs, which makes them easily susceptible to oncogenic transformation, is their persistent proliferative activity during the brain's lifetime. A growing body of literature has shown that NSCs are one of the most susceptible cell types that can give rise to malignant glioma. Indeed, GEMs with various combinations of mutations in *p53*, *Pten* and *Nf1* tumor suppressor genes enable embryonic NSCs to develop malignant tumors with high penetrance (Wang et al. 2009; Zheng et al. 2008; Kwon et al. 2008). Recent studies provided some evidences to suggest multipotent NSCs are the cell of origin of NF1-OPG. The strongest argument comes from a group led Dr. David Gutmann (Lee, Gianino, and Gutmann 2012). In a study published in Cancer Cell, they supplied four lines of evidence supporting the hypothesis that NSCs within the germinal layer of the third ventricular zone (III-VZ) serve as a source or cell of origin for NF1-associated optic nerve glioma. First, they showed that cells in the III-VZ at E15.5 express markers for stem and progenitor cells, including Sox2, Nestin, BLBP, Ki67, are capable of forming self-renewing neurospheres, and undergo multilineage differentiation under culture conditions. Secondly, using microarray data and glioma-causing genetic modifications such as *p53*, *Pten* or *B-raf*, they proposed that cells from lateral ventricle SVZ (lv-SVZ) and III-VZ in E17.5 brains represent two different stem or

progenitor cell populations based on their distinct expression profiles and their differential responses *in vitro*. Thirdly, when *Nf1* was inactivated at E9.5 in BLBP-cre; *Nf1*$^{flox/flox}$ mice, the III-VZ, but not the lv-SVZ, showed increased numbers of Olig2 and GFAP expressing cells in the P8 brain and increased proliferation *in vitro*. Lastly, they claimed that *Nf1* deletion at E16.5 using and inducible GFAP-cre^{ER} mouse produced a single viable mutant mouse that developed optic glioma at 3 months whereas induction at P1-P3 or P14 did not induce tumors. Taken together, the Gutmann group concluded that neural stem/progenitor cells from the proliferating III-VZ during embryonic stages give rise to optic gliomas.

However, there are several major concerns with the conclusion from these findings. The definitive evidence demonstrating that E15.5 III-VZ cells are true neural stem cells is still lacking, because we do not know whether such cells are neurogenic *in vivo* or what type(s) of neurons would be generated from these putative neural stem cells. Furthermore, it is well documented that *in vitro* culture conditions do not necessarily reflect what happens *in vivo*. Secondly, hGFAP-cre is expressed in multi-potent neural stem cells and radial glial cells in the dorsal brain. However, the cre expression seems to be restricted to glia precursors already committed to the glial lineage in the ventral brain, including the III-VZ (Anthony et al. 2004; Malatesta et al. 2003; Zhuo et al. 2001; Yue et al. 2006). Although the pups induced at P1-P3 failed to develop optic gliomas, this could simply be attributed to fewer cells targeted by GFAP-cre^{ER}, and not necessarily due to late induction as the authors suggested. There was also a lack of reporter or lineage-tracing used to assess the percentage of recombined cells as well as the phenotype of *Nf1*$^{-/-}$ cells in these postnatally induced mice. However, the most significant caveat for this study was the failure to distinguish between the different origins of macroglia in the developing optic nerve. The authors incorrectly assumed that stem cells in the III-VZ migrate and differentiate into both oligodendrocytes and astrocytes in the optic nerve. As a consequence, the definitive evidence is lacking to conclude that neural stem cells from the III-VZ, but not glial-restricted precursors from either the brain or the nerve, are the cell of origin of NF1-OPGs. In a follow-up study, the Gutmann group generated an additional transgenic mouse, *Nf1*$^{flox/mut}$; Prom1-cre^{ER} by employing tamoxifen (TM)-inducible Cre system expressed from the endogenous prominin-1 (CD133) promoter, to specifically target *Nf1* loss into CD133^{+} neural stem cells in the brain at E15 (Solga et al. 2017). The resulting mutants developed OPGs by 3 months of age, similar to the latency in their GFAP-

cre* CKO mice. Although these observations suggest that neural stem cells could serve as cell of origin of OPGs, current Cre/LoxP conditional knockout system, targeting the stem cells will also inevitably target all the progeny derived from stem cells, making it extremely difficult to conclude which type(s) of cells (NSC or glia-restricted progenitors) is(are) most susceptible to *Nf1* loss.

Interestingly, the strongest evidence for glia-restricted progenitors as potential cell of origin for *Nf1*-OPGs also comes from Dr. Gutmann's group. In the same study as above published in the journal Oncotarget, they employed a cre transgenic mouse for somatic inactivation of *Nf1* in Olig2^{+} glial progenitors by E12. They reported that the $Nf1^{flox/mut}$; Olig2-cre mice develop OPGs with a delayed onset of 6 months compared to their conventional model which develop OPGs by 3 months of age. They concluded that both NSC/progenitors and pre-OPCs can serve as initiating cells for OPGs with different latencies for optic gliomagenesis (Solga et al. 2017). Taken together, these studies all suggest the embryonic III-VZ as the regional origin for all these OPGs initiating cells. It is important to note that when *Nf1* mutation is introduced in multi-potent NSCs, it becomes extremely difficult to distinguish whether the mutant stem cells or their more restricted progeny are more affected. It is well established that biallelic inactivation (or loss of heterozygosity, LOH) of the *NF1* gene is the rate-limiting step for NF1-OPG formation. However, it remains unclear whether the key LOH must occur in NSCs or glia-restricted precursors from either the brain or the optic nerve during development to initiate gliomagenesis. Therefore, investigating the role of *NF1* in the different cell lineages in the optic nerve could not only provide insights in the cellular targets for *NF1* mutation, but also advance our understanding of how *NF1* loss in these cells leads to tumor formation.

1.10 Summary and overall layout of this thesis

In this thesis, I use both conventional conditional knock-outs (CKOs) and the MADM system to study the entire tumorigenic process from early development to adult stage. In Chapter II, I demonstrate that *Nf1*-associated glial abnormalities established during neonatal stages can be found throughout tumor development and in late-stage OPGs. I also delineate the timing and developmental defects caused by *Nf1* loss that result in neurological deficits in late stages. Finally,

I provide evidences to support the MEK-Erk pathway as the signaling pathway responsible for tumor initiation and maintenance. In Chapter III, I use pharmacological inhibition in the *Nf1*^{hGFAP}CKO mouse model to demonstrate that transient MEK inhibition during a neonatal window (P0.5-P21) prevents OPG formation in a dose dependent fashion. In Chapter IV, I discuss how my findings advance the field of *Nf1*-OPGs, the clinical implications of these advances, and future directions for the field.

1.11 References

Aguzzi, A., B. A. Barres, and M. L. Bennett. 2013. 'Microglia: scapegoat, saboteur, or something else?', *Science*, 339: 156-61.

Anthony, T. E., C. Klein, G. Fishell, and N. Heintz. 2004. 'Radial glia serve as neuronal progenitors in all regions of the central nervous system', *Neuron*, 41: 881-90.

Ater, J. L., C. Xia, C. M. Mazewski, T. N. Booth, D. R. Freyer, R. J. Packer, R. Sposto, G. Vezina, and I. F. Pollack. 2016. 'Nonrandomized comparison of neurofibromatosis type 1 and non-neurofibromatosis type 1 children who received carboplatin and vincristine for progressive low-grade glioma: A report from the Children's Oncology Group', *Cancer*, 122: 1928-36.

Avery, R. A., A. Cnaan, J. S. Schuman, C. Trimboli-Heidler, C. L. Chen, R. J. Packer, and H. Ishikawa. 2015. 'Longitudinal Change of Circumpapillary Retinal Nerve Fiber Layer Thickness in Children With Optic Pathway Gliomas', *Am J Ophthalmol*, 160: 944-52 e1.

Avery, R. A., A. Mansoor, R. Idrees, E. Biggs, M. A. Alsharid, R. J. Packer, and M. G. Linguraru. 2016. 'Quantitative MRI criteria for optic pathway enlargement in neurofibromatosis type 1', *Neurology*, 86: 2264-70.

Avery, R. A., A. Mansoor, R. Idrees, C. Trimboli-Heidler, H. Ishikawa, R. J. Packer, and M. G. Linguraru. 2016. 'Optic pathway glioma volume predicts retinal axon degeneration in neurofibromatosis type 1', *Neurology*, 87: 2403-07.

Bajenaru, M. L., J. R. Garbow, A. Perry, M. R. Hernandez, and D. H. Gutmann. 2005. 'Natural history of neurofibromatosis 1-associated optic nerve glioma in mice', *Ann Neurol*, 57: 119-27.

Bajenaru, M. L., M. R. Hernandez, A. Perry, Y. Zhu, L. F. Parada, J. R. Garbow, and D. H. Gutmann. 2003. 'Optic nerve glioma in mice requires astrocyte Nf1 gene inactivation and Nf1 brain heterozygosity', *Cancer Res*, 63: 8573-7.

Balcer, L. J., G. T. Liu, G. Heller, L. Bilaniuk, N. J. Volpe, S. L. Galetta, P. T. Molloy, P. C. Phillips, A. J. Janss, S. Vaughn, and M. G. Maguire. 2001. 'Visual loss in children with neurofibromatosis type 1 and optic pathway gliomas: relation to tumor location by magnetic resonance imaging', *Am J Ophthalmol*, 131: 442-5.

Bao, S., Q. Wu, R. E. McLendon, Y. Hao, Q. Shi, A. B. Hjelmeland, M. W. Dewhirst, D. D. Bigner, and J. N. Rich. 2006. 'Glioma stem cells promote radioresistance by preferential activation of the DNA damage response', *Nature*, 444: 756-60.

Bergthold, G., P. Bandopadhayay, W. L. Bi, L. Ramkissoon, C. Stiles, R. A. Segal, R. Beroukhim, K. L. Ligon, J. Grill, and M. W. Kieran. 2014. 'Pediatric low-grade gliomas: how modern biology reshapes the clinical field', *Biochim Biophys Acta*, 1845: 294-307.

Brannan, C. I., A. S. Perkins, K. S. Vogel, N. Ratner, M. L. Nordlund, S. W. Reid, A. M. Buchberg, N. A. Jenkins, L. F. Parada, and N. G. Copeland. 1994. 'Targeted disruption of the neurofibromatosis type-1 gene leads to developmental abnormalities in heart and various neural crest-derived tissues', *Genes Dev*, 8: 1019-29.

Burkhard, C., P. L. Di Patre, D. Schuler, G. Schuler, M. G. Yasargil, Y. Yonekawa, U. M. Lutolf, P. Kleihues, and H. Ohgaki. 2003. 'A population-based study of the incidence and survival rates in patients with pilocytic astrocytoma', *J Neurosurg*, 98: 1170-4.

Chen, Y. H., S. M. Gianino, and D. H. Gutmann. 2015. 'Neurofibromatosis-1 regulation of neural stem cell proliferation and multilineage differentiation operates through distinct RAS effector pathways', *Genes Dev*, 29: 1677-82.

Cichowski, K., and T. Jacks. 2001. 'NF1 tumor suppressor gene function: narrowing the GAP', *Cell*, 104: 593-604.

Cin, H., C. Meyer, R. Herr, W. G. Janzarik, S. Lambert, D. T. Jones, K. Jacob, A. Benner, H. Witt, M. Remke, S. Bender, F. Falkenstein, T. N. Van Anh, H. Olbrich, A. von Deimling, A. Pekrun, A. E. Kulozik, A. Gnekow, W. Scheurlen, O. Witt, H. Omran, N. Jabado, V. P. Collins, T. Brummer, R. Marschalek, P. Lichter, A. Korshunov, and S. M. Pfister. 2011. 'Oncogenic FAM131B-BRAF fusion resulting from 7q34 deletion comprises an alternative mechanism of MAPK pathway activation in pilocytic astrocytoma', *Acta Neuropathol*, 121: 763-74.

Collins, V. P., D. T. Jones, and C. Giannini. 2015. 'Pilocytic astrocytoma: pathology, molecular mechanisms and markers', *Acta Neuropathol*, 129: 775-88.

Colman, S. D., C. A. Williams, and M. R. Wallace. 1995. 'Benign neurofibromas in type 1 neurofibromatosis (NF1) show somatic deletions of the NF1 gene', *Nat Genet*, 11: 90-2.

Dakubo, G. D., S. T. Beug, C. J. Mazerolle, S. Thurig, Y. Wang, and V. A. Wallace. 2008. 'Control of glial precursor cell development in the mouse optic nerve by sonic hedgehog from retinal ganglion cells', *Brain Res*, 1228: 27-42.

Dakubo, G. D., Y. P. Wang, C. Mazerolle, K. Campsall, A. P. McMahon, and V. A. Wallace. 2003. 'Retinal ganglion cell-derived sonic hedgehog signaling is required for optic disc and stalk neuroepithelial cell development', *Development*, 130: 2967-80.

Daston, M. M., H. Scrable, M. Nordlund, A. K. Sturbaum, L. M. Nissen, and N. Ratner. 1992. 'The protein product of the neurofibromatosis type 1 gene is expressed at highest abundance in neurons, Schwann cells, and oligodendrocytes', *Neuron*, 8: 415-28.

Diggs-Andrews, K. A., J. A. Brown, S. M. Gianino, J. B. Rubin, D. F. Wozniak, and D. H. Gutmann. 2014. 'Sex Is a major determinant of neuronal dysfunction in neurofibromatosis type 1', *Ann Neurol*, 75: 309-16.

Fisher, M. J., M. Loguidice, D. H. Gutmann, R. Listernick, R. E. Ferner, N. J. Ullrich, R. J. Packer, U. Tabori, R. O. Hoffman, S. L. Ardern-Holmes, T. R. Hummel, D. R. Hargrave, E. Bouffet, J. Charrow, L. T. Bilaniuk, L. J. Balcer, and G. T. Liu. 2012. 'Visual outcomes in children with neurofibromatosis type 1-associated optic pathway glioma following chemotherapy: a multicenter retrospective analysis', *Neuro Oncol*, 14: 790-7.

Forshew, T., R. G. Tatevossian, A. R. Lawson, J. Ma, G. Neale, B. W. Ogunkolade, T. A. Jones, J. Aarum, J. Dalton, S. Bailey, T. Chaplin, R. L. Carter, A. Gajjar, A. Broniscer, B. D.

Young, D. W. Ellison, and D. Sheer. 2009. 'Activation of the ERK/MAPK pathway: a signature genetic defect in posterior fossa pilocytic astrocytomas', *J Pathol*, 218: 172-81.

Freeman, C. R., J. P. Farmer, and J. Montes. 1998. 'Low-grade astrocytomas in children: evolving management strategies', *Int J Radiat Oncol Biol Phys*, 41: 979-87.

Fried, I., U. Tabori, T. Tihan, A. Reginald, and E. Bouffet. 2013. 'Optic pathway gliomas: a review', *CNS Oncol*, 2: 143-59.

Friedlander, M. 2007. 'Fibrosis and diseases of the eye', *J Clin Invest*, 117: 576-86.

Friedman, J. M. 1999. 'Epidemiology of neurofibromatosis type 1', *Am J Med Genet*, 89: 1-6.

Galli, R., E. Binda, U. Orfanelli, B. Cipelletti, A. Gritti, S. De Vitis, R. Fiocco, C. Foroni, F. Dimeco, and A. Vescovi. 2004. 'Isolation and characterization of tumorigenic, stem-like neural precursors from human glioblastoma', *Cancer Res*, 64: 7011-21.

Gao, L., and R. H. Miller. 2006. 'Specification of optic nerve oligodendrocyte precursors by retinal ganglion cell axons', *J Neurosci*, 26: 7619-28.

Glover, T. W., C. K. Stein, E. Legius, L. B. Andersen, A. Brereton, and S. Johnson. 1991. 'Molecular and cytogenetic analysis of tumors in von Recklinghausen neurofibromatosis', *Genes Chromosomes Cancer*, 3: 62-70.

Gutmann, D. H., A. Aylsworth, J. C. Carey, B. Korf, J. Marks, R. E. Pyeritz, A. Rubenstein, and D. Viskochil. 1997. 'The diagnostic evaluation and multidisciplinary management of neurofibromatosis 1 and neurofibromatosis 2', *JAMA*, 278: 51-7.

Gutmann, D. H., M. D. McLellan, I. Hussain, J. W. Wallis, L. L. Fulton, R. S. Fulton, V. Magrini, R. Demeter, T. Wylie, C. Kandoth, J. R. Leonard, A. Guha, C. A. Miller, L. Ding, and E. R. Mardis. 2013. 'Somatic neurofibromatosis type 1 (NF1) inactivation characterizes NF1-associated pilocytic astrocytoma', *Genome Res*, 23: 431-9.

Hegedus, B., B. Dasgupta, J. E. Shin, R. J. Emnett, E. K. Hart-Mahon, L. Elghazi, E. Bernal-Mizrachi, and D. H. Gutmann. 2007. 'Neurofibromatosis-1 regulates neuronal and glial cell differentiation from neuroglial progenitors in vivo by both cAMP- and Ras-dependent mechanisms', *Cell Stem Cell*, 1: 443-57.

Hegedus, B., F. W. Hughes, J. R. Garbow, S. Gianino, D. Banerjee, K. Kim, M. H. Ellisman, M. A. Brantley, Jr., and D. H. Gutmann. 2009. 'Optic nerve dysfunction in a mouse model of neurofibromatosis-1 optic glioma', *J Neuropathol Exp Neurol*, 68: 542-51.

Hemmati, H. D., I. Nakano, J. A. Lazareff, M. Masterman-Smith, D. H. Geschwind, M. Bronner-Fraser, and H. I. Kornblum. 2003. 'Cancerous stem cells can arise from pediatric brain tumors', *Proc Natl Acad Sci U S A*, 100: 15178-83.

Huson, S. M., P. S. Harper, and D. A. Compston. 1988. 'Von Recklinghausen neurofibromatosis. A clinical and population study in south-east Wales', *Brain*, 111 (Pt 6): 1355-81.

Hyman, S. L., A. Shores, and K. N. North. 2005. 'The nature and frequency of cognitive deficits in children with neurofibromatosis type 1', *Neurology*, 65: 1037-44.

Jacks, T., T. S. Shih, E. M. Schmitt, R. T. Bronson, A. Bernards, and R. A. Weinberg. 1994. 'Tumour predisposition in mice heterozygous for a targeted mutation in Nf1', *Nat Genet*, 7: 353-61.

Jacob, K., S. Albrecht, C. Sollier, D. Faury, E. Sader, A. Montpetit, D. Serre, P. Hauser, M. Garami, L. Bognar, Z. Hanzely, J. L. Montes, J. Atkinson, J. P. Farmer, E. Bouffet, C. Hawkins, U. Tabori, and N. Jabado. 2009. 'Duplication of 7q34 is specific to juvenile pilocytic astrocytomas and a hallmark of cerebellar and optic pathway tumours', *Br J Cancer*, 101: 722-33.

Jacob, K., D. A. Quang-Khuong, D. T. Jones, H. Witt, S. Lambert, S. Albrecht, O. Witt, C. Vezina, M. Shirinian, D. Faury, M. Garami, P. Hauser, A. Klekner, L. Bognar, J. P. Farmer, J. L. Montes, J. Atkinson, C. Hawkins, A. Korshunov, V. P. Collins, S. M. Pfister, U. Tabori, and N. Jabado. 2011. 'Genetic aberrations leading to MAPK pathway activation mediate oncogene-induced senescence in sporadic pilocytic astrocytomas', *Clin Cancer Res*, 17: 4650-60.

Jones, D. T., B. Hutter, N. Jager, A. Korshunov, M. Kool, H. J. Warnatz, T. Zichner, S. R. Lambert, M. Ryzhova, D. A. Quang, A. M. Fontebasso, A. M. Stutz, S. Hutter, M. Zuckermann, D. Sturm, J. Gronych, B. Lasitschka, S. Schmidt, H. Seker-Cin, H. Witt, M. Sultan, M. Ralser, P. A. Northcott, V. Hovestadt, S. Bender, E. Pfaff, S. Stark, D. Faury, J. Schwartzentruber, J. Majewski, U. D. Weber, M. Zapatka, B. Raeder, M. Schlesner, C. L. Worth, C. C. Bartholomae, C. von Kalle, C. D. Imbusch, S. Radomski, C. Lawerenz, P. van Sluis, J. Koster, R. Volckmann, R. Versteeg, H. Lehrach, C. Monoranu, B. Winkler, A. Unterberg, C. Herold-Mende, T. Milde, A. E. Kulozik, M. Ebinger, M. U. Schuhmann, Y. J. Cho, S. L. Pomeroy, A. von Deimling, O. Witt, M. D. Taylor, S. Wolf, M. A. Karajannis, C. G. Eberhart, W. Scheurlen, M. Hasselblatt, K. L. Ligon, M. W. Kieran, J. O. Korbel, M. L. Yaspo, B. Brors, J. Felsberg, G. Reifenberger, V. P. Collins, N. Jabado, R. Eils, P. Lichter, S. M. Pfister, and Project International Cancer Genome Consortium PedBrain Tumor. 2013. 'Recurrent somatic alterations of FGFR1 and NTRK2 in pilocytic astrocytoma', *Nat Genet*, 45: 927-32.

Kalamarides, M., A. O. Stemmer-Rachamimov, M. Niwa-Kawakita, F. Chareyre, E. Taranchon, Z. Y. Han, C. Martinelli, E. A. Lusis, B. Hegedus, D. H. Gutmann, and M. Giovannini. 2011. 'Identification of a progenitor cell of origin capable of generating diverse meningioma histological subtypes', *Oncogene*, 30: 2333-44.

Kaul, A., J. A. Toonen, P. J. Cimino, S. M. Gianino, and D. H. Gutmann. 2015. 'Akt- or MEK-mediated mTOR inhibition suppresses Nf1 optic glioma growth', *Neuro Oncol*, 17: 843-53.

Kim, E., Y. Wang, S. J. Kim, M. Bornhorst, E. S. Jecrois, T. E. Anthony, C. Wang, Y. E. Li, J. L. Guan, G. G. Murphy, and Y. Zhu. 2014. 'Transient inhibition of the ERK pathway prevents cerebellar developmental defects and improves long-term motor functions in murine models of neurofibromatosis type 1', *Elife*, 3.

Kluwe, L., C. Hagel, M. Tatagiba, S. Thomas, D. Stavrou, H. Ostertag, A. von Deimling, and V. F. Mautner. 2001. 'Loss of NF1 alleles distinguish sporadic from NF1-associated pilocytic astrocytomas', *J Neuropathol Exp Neurol*, 60: 917-20.

Kuwabara, T. 1975. 'Development of the optic nerve of the rat', *Invest Ophthalmol*, 14: 732-45.

Kwon, C. H., D. Zhao, J. Chen, S. Alcantara, Y. Li, D. K. Burns, R. P. Mason, E. Y. Lee, H. Wu, and L. F. Parada. 2008. 'Pten haploinsufficiency accelerates formation of high-grade astrocytomas', *Cancer Res*, 68: 3286-94.

Lau, N., M. M. Feldkamp, L. Roncari, A. H. Loehr, P. Shannon, D. H. Gutmann, and A. Guha. 2000. 'Loss of neurofibromin is associated with activation of RAS/MAPK and PI3-K/AKT signaling in a neurofibromatosis 1 astrocytoma', *J Neuropathol Exp Neurol*, 59: 759-67.

Lee, D. Y., S. M. Gianino, and D. H. Gutmann. 2012. 'Innate neural stem cell heterogeneity determines the patterning of glioma formation in children', *Cancer Cell*, 22: 131-8.

Lee, D. Y., T. H. Yeh, R. J. Emnett, C. R. White, and D. H. Gutmann. 2010. 'Neurofibromatosis-1 regulates neuroglial progenitor proliferation and glial differentiation in a brain region-specific manner', *Genes Dev*, 24: 2317-29.

Legius, E., D. A. Marchuk, F. S. Collins, and T. W. Glover. 1993. 'Somatic deletion of the neurofibromatosis type 1 gene in a neurofibrosarcoma supports a tumour suppressor gene hypothesis', *Nat Genet*, 3: 122-6.

Lim, D. A., S. Cha, M. C. Mayo, M. H. Chen, E. Keles, S. VandenBerg, and M. S. Berger. 2007. 'Relationship of glioblastoma multiforme to neural stem cell regions predicts invasive and multifocal tumor phenotype', *Neuro Oncol*, 9: 424-9.

Listernick, R. 2016. 'Predicting which NF1 optic pathway gliomas will require treatment', *Neurology*, 87: 2389-90.

Listernick, R., J. Charrow, and D. H. Gutmann. 1999. 'Intracranial gliomas in neurofibromatosis type 1', *Am J Med Genet*, 89: 38-44.

Listernick, R., R. E. Ferner, G. T. Liu, and D. H. Gutmann. 2007. 'Optic pathway gliomas in neurofibromatosis-1: controversies and recommendations', *Ann Neurol*, 61: 189-98.

Listernick, R., R. E. Ferner, L. Piersall, S. Sharif, D. H. Gutmann, and J. Charrow. 2004. 'Late-onset optic pathway tumors in children with neurofibromatosis 1', *Neurology*, 63: 1944-6.

Listernick, R., D. N. Louis, R. J. Packer, and D. H. Gutmann. 1997. 'Optic pathway gliomas in children with neurofibromatosis 1: consensus statement from the NF1 Optic Pathway Glioma Task Force', *Ann Neurol*, 41: 143-9.

Macdonald, R., J. Scholes, U. Strahle, C. Brennan, N. Holder, M. Brand, and S. W. Wilson. 1997. 'The Pax protein Noi is required for commissural axon pathway formation in the rostral forebrain', *Development*, 124: 2397-408.

Malatesta, P., M. A. Hack, E. Hartfuss, H. Kettenmann, W. Klinkert, F. Kirchhoff, and M. Gotz. 2003. 'Neuronal or glial progeny: regional differences in radial glia fate', *Neuron*, 37: 751-64.

Marchuk, D. A., A. M. Saulino, R. Tavakkol, M. Swaroop, M. R. Wallace, L. B. Andersen, A. L. Mitchell, D. H. Gutmann, M. Boguski, and F. S. Collins. 1991. 'cDNA cloning of the type 1 neurofibromatosis gene: complete sequence of the NF1 gene product', *Genomics*, 11: 931-40.

Mi, H., and B. A. Barres. 1999. 'Purification and characterization of astrocyte precursor cells in the developing rat optic nerve', *J Neurosci*, 19: 1049-61.

Miller, R. H., S. David, R. Patel, E. R. Abney, and M. C. Raff. 1985. 'A quantitative immunohistochemical study of macroglial cell development in the rat optic nerve: in vivo evidence for two distinct astrocyte lineages', *Dev Biol*, 111: 35-41.

Mui, S. H., J. W. Kim, G. Lemke, and S. Bertuzzi. 2005. 'Vax genes ventralize the embryonic eye', *Genes Dev*, 19: 1249-59.

Murphy, E. S., H. Xie, T. E. Merchant, J. S. Yu, S. T. Chao, and J. H. Suh. 2015. 'Review of cranial radiotherapy-induced vasculopathy', *J Neurooncol*, 122: 421-9.

Ono, K., H. Takebayashi, K. Ikeda, M. Furusho, T. Nishizawa, K. Watanabe, and K. Ikenaka. 2008. 'Regional- and temporal-dependent changes in the differentiation of Olig2 progenitors in the forebrain, and the impact on astrocyte development in the dorsal pallium', *Dev Biol*, 320: 456-68.

Ono, K., Y. Yasui, U. Rutishauser, and R. H. Miller. 1997. 'Focal ventricular origin and migration of oligodendrocyte precursors into the chick optic nerve', *Neuron*, 19: 283-92.

Ono, K., K. Yoshii, H. Tominaga, H. Gotoh, T. Nomura, H. Takebayashi, and K. Ikenaka. 2017. 'Oligodendrocyte precursor cells in the mouse optic nerve originate in the preoptic area', *Brain Struct Funct*, 222: 2441-48.

Ostrom, Q. T., H. Gittleman, P. Liao, C. Rouse, Y. Chen, J. Dowling, Y. Wolinsky, C. Kruchko, and J. Barnholtz-Sloan. 2014. 'CBTRUS statistical report: primary brain and central nervous system tumors diagnosed in the United States in 2007-2011', *Neuro Oncol*, 16 Suppl 4: iv1-63.

Packer, R. J., J. Ater, J. Allen, P. Phillips, R. Geyer, H. S. Nicholson, R. Jakacki, E. Kurczynski, M. Needle, J. Finlay, G. Reaman, and J. M. Boyett. 1997. 'Carboplatin and vincristine chemotherapy for children with newly diagnosed progressive low-grade gliomas', *J Neurosurg*, 86: 747-54.

Packer, R. J., S. Pfister, E. Bouffet, R. Avery, P. Bandopadhayay, M. Bornhorst, D. C. Bowers, D. Ellison, J. Fangusaro, N. Foreman, M. Fouladi, A. Gajjar, D. Haas-Kogan, C. Hawkins, C. Y. Ho, E. Hwang, N. Jabado, L. B. Kilburn, A. Lassaletta, K. L. Ligon, M. Massimino, S. V. Meeteren, S. Mueller, T. Nicolaides, G. Perilongo, U. Tabori, G. Vezina, K. Warren, O. Witt, Y. Zhu, D. T. Jones, and M. Kieran. 2017. 'Pediatric low-grade gliomas: implications of the biologic era', *Neuro Oncol*, 19: 750-61.

Parsa, C. F., C. S. Hoyt, R. L. Lesser, J. M. Weinstein, C. M. Strother, R. Muci-Mendoza, M. Ramella, R. S. Manor, W. A. Fletcher, M. X. Repka, J. A. Garrity, R. N. Ebner, M. L. Monteiro, R. M. McFadzean, I. V. Rubtsova, and W. F. Hoyt. 2001. 'Spontaneous regression of optic gliomas: thirteen cases documented by serial neuroimaging', *Arch Ophthalmol*, 119: 516-29.

Pasmant, E., M. Vidaud, D. Vidaud, and P. Wolkenstein. 2012. 'Neurofibromatosis type 1: from genotype to phenotype', *J Med Genet*, 49: 483-9.

Pfister, S., and O. Witt. 2009. 'Pediatric gliomas', *Recent Results Cancer Res*, 171: 67-81.

Raff, M. C., E. R. Abney, J. Cohen, R. Lindsay, and M. Noble. 1983. 'Two types of astrocytes in cultures of developing rat white matter: differences in morphology, surface gangliosides, and growth characteristics', *J Neurosci*, 3: 1289-300.

Raff, M. C., E. R. Abney, and R. H. Miller. 1984. 'Two glial cell lineages diverge prenatally in rat optic nerve', *Dev Biol*, 106: 53-60.

Rickert, C. H., and W. Paulus. 2001. 'Epidemiology of central nervous system tumors in childhood and adolescence based on the new WHO classification', *Childs Nerv Syst*, 17: 503-11.

Schindler, G., D. Capper, J. Meyer, W. Janzarik, H. Omran, C. Herold-Mende, K. Schmieder, P. Wesseling, C. Mawrin, M. Hasselblatt, D. N. Louis, A. Korshunov, S. Pfister, C. Hartmann, W. Paulus, G. Reifenberger, and A. von Deimling. 2011. 'Analysis of BRAF V600E mutation in 1,320 nervous system tumors reveals high mutation frequencies in pleomorphic xanthoastrocytoma, ganglioglioma and extra-cerebellar pilocytic astrocytoma', *Acta Neuropathol*, 121: 397-405.

Schwarz, M., F. Cecconi, G. Bernier, N. Andrejewski, B. Kammandel, M. Wagner, and P. Gruss. 2000. 'Spatial specification of mammalian eye territories by reciprocal transcriptional repression of Pax2 and Pax6', *Development*, 127: 4325-34.

Serra, E., T. Rosenbaum, U. Winner, R. Aledo, E. Ars, X. Estivill, H. G. Lenard, and C. Lazaro. 2000. 'Schwann cells harbor the somatic NF1 mutation in neurofibromas: evidence of two different Schwann cell subpopulations', *Hum Mol Genet*, 9: 3055-64.

Shannon, K. M., P. O'Connell, G. A. Martin, D. Paderanga, K. Olson, P. Dinndorf, and F. McCormick. 1994. 'Loss of the normal NF1 allele from the bone marrow of children with type 1 neurofibromatosis and malignant myeloid disorders', *N Engl J Med*, 330: 597-601.

Sharif, S., R. Ferner, J. M. Birch, J. E. Gillespie, H. R. Gattamaneni, M. E. Baser, and D. G. Evans. 2006. 'Second primary tumors in neurofibromatosis 1 patients treated for optic glioma: substantial risks after radiotherapy', *J Clin Oncol*, 24: 2570-5.

Sharif, S., A. Moran, S. M. Huson, R. Iddenden, A. Shenton, E. Howard, and D. G. Evans. 2007. 'Women with neurofibromatosis 1 are at a moderately increased risk of developing breast cancer and should be considered for early screening', *J Med Genet*, 44: 481-4.

Singh, S. K., C. Hawkins, I. D. Clarke, J. A. Squire, J. Bayani, T. Hide, R. M. Henkelman, M. D. Cusimano, and P. B. Dirks. 2004. 'Identification of human brain tumour initiating cells', *Nature*, 432: 396-401.

Small, R. K., P. Riddle, and M. Noble. 1987. 'Evidence for migration of oligodendrocyte--type-2 astrocyte progenitor cells into the developing rat optic nerve', *Nature*, 328: 155-7.

Solga, A. C., J. A. Toonen, Y. Pan, P. J. Cimino, Y. Ma, G. A. Castillon, S. M. Gianino, M. H. Ellisman, D. Y. Lee, and D. H. Gutmann. 2017. 'The cell of origin dictates the temporal course of neurofibromatosis-1 (Nf1) low-grade glioma formation', *Oncotarget*, 8: 47206-15.

Soukkarieh, C., E. Agius, C. Soula, and P. Cochard. 2007. 'Pax2 regulates neuronal-glial cell fate choice in the embryonic optic nerve', *Dev Biol*, 303: 800-13.

Stiller, C. A., J. M. Chessells, and M. Fitchett. 1994. 'Neurofibromatosis and childhood leukaemia/lymphoma: a population-based UKCCSG study', *Br J Cancer*, 70: 969-72.

Surawicz, T. S., F. Davis, S. Freels, E. R. Laws, Jr., and H. R. Menck. 1998. 'Brain tumor survival: results from the National Cancer Data Base', *J Neurooncol*, 40: 151-60.

Surawicz, T. S., B. J. McCarthy, V. Kupelian, P. J. Jukich, J. M. Bruner, and F. G. Davis. 1999. 'Descriptive epidemiology of primary brain and CNS tumors: results from the Central Brain Tumor Registry of the United States, 1990-1994', *Neuro Oncol*, 1: 14-25.

Tatsumi, K., H. Takebayashi, T. Manabe, K. F. Tanaka, M. Makinodan, T. Yamauchi, E. Makinodan, H. Matsuyoshi, H. Okuda, K. Ikenaka, and A. Wanaka. 2008. 'Genetic fate mapping of Olig2 progenitors in the injured adult cerebral cortex reveals preferential differentiation into astrocytes', *J Neurosci Res*, 86: 3494-502.

Taylor, M. D., H. Poppleton, C. Fuller, X. Su, Y. Liu, P. Jensen, S. Magdaleno, J. Dalton, C. Calabrese, J. Board, T. Macdonald, J. Rutka, A. Guha, A. Gajjar, T. Curran, and R. J. Gilbertson. 2005. 'Radial glia cells are candidate stem cells of ependymoma', *Cancer Cell*, 8: 323-35.

Tihan, T., P. G. Fisher, J. L. Kepner, C. Godfraind, R. D. McComb, P. T. Goldthwaite, and P. C. Burger. 1999. 'Pediatric astrocytomas with monomorphous pilomyxoid features and a less favorable outcome', *J Neuropathol Exp Neurol*, 58: 1061-8.

Torres, M., E. Gomez-Pardo, and P. Gruss. 1996. 'Pax2 contributes to inner ear patterning and optic nerve trajectory', *Development*, 122: 3381-91.

Ueda, H., J. M. Levine, R. H. Miller, and B. D. Trapp. 1999. 'Rat optic nerve oligodendrocytes develop in the absence of viable retinal ganglion cell axons', *J Cell Biol*, 146: 1365-74.

Vlenterie, M., U. Flucke, L. C. Hofbauer, H. J. Timmers, J. Gastmeier, D. E. Aust, W. T. van der Graaf, P. Wesseling, G. Eisenhofer, and J. W. Lenders. 2013. 'Pheochromocytoma and gastrointestinal stromal tumors in patients with neurofibromatosis type I', *Am J Med*, 126: 174-80.

Wallace, V. A., and M. C. Raff. 1999. 'A role for Sonic hedgehog in axon-to-astrocyte signalling in the rodent optic nerve', *Development*, 126: 2901-9.

Wang, Y., E. Kim, X. Wang, B. G. Novitch, K. Yoshikawa, L. S. Chang, and Y. Zhu. 2012. 'ERK inhibition rescues defects in fate specification of Nf1-deficient neural progenitors and brain abnormalities', *Cell*, 150: 816-30.

Wang, Y., J. Yang, H. Zheng, G. J. Tomasek, P. Zhang, P. E. McKeever, E. Y. Lee, and Y. Zhu. 2009. 'Expression of mutant p53 proteins implicates a lineage relationship between neural stem cells and malignant astrocytic glioma in a murine model', *Cancer Cell*, 15: 514-26.

Xu, G. F., P. O'Connell, D. Viskochil, R. Cawthon, M. Robertson, M. Culver, D. Dunn, J. Stevens, R. Gesteland, R. White, and et al. 1990. 'The neurofibromatosis type 1 gene encodes a protein related to GAP', *Cell*, 62: 599-608.

Xu, W., L. M. Mulligan, M. A. Ponder, L. Liu, B. A. Smith, C. G. Mathew, and B. A. Ponder. 1992. 'Loss of NF1 alleles in phaeochromocytomas from patients with type I neurofibromatosis', *Genes Chromosomes Cancer*, 4: 337-42.

Yalon, M., B. Rood, T. J. MacDonald, G. McCowage, R. Kane, S. Constantini, and R. J. Packer. 2013. 'A feasibility and efficacy study of rapamycin and erlotinib for recurrent pediatric low-grade glioma (LGG)', *Pediatr Blood Cancer*, 60: 71-6.

Yue, T., K. Xian, E. Hurlock, M. Xin, S. G. Kernie, L. F. Parada, and Q. R. Lu. 2006. 'A critical role for dorsal progenitors in cortical myelination', *J Neurosci*, 26: 1275-80.

Zhang, J., G. Wu, C. P. Miller, R. G. Tatevossian, J. D. Dalton, B. Tang, W. Orisme, C. Punchihewa, M. Parker, I. Qaddoumi, F. A. Boop, C. Lu, C. Kandoth, L. Ding, R. Lee, R. Huether, X. Chen, E. Hedlund, P. Nagahawatte, M. Rusch, K. Boggs, J. Cheng, J. Becksfort, J. Ma, G. Song, Y. Li, L. Wei, J. Wang, S. Shurtleff, J. Easton, D. Zhao, R. S. Fulton, L. L. Fulton, D. J. Dooling, B. Vadodaria, H. L. Mulder, C. Tang, K. Ochoa, C. G. Mullighan, A. Gajjar, R. Kriwacki, D. Sheer, R. J. Gilbertson, E. R. Mardis, R. K. Wilson, J. R. Downing, S. J. Baker, D. W. Ellison, and Project St. Jude Children's Research Hospital-Washington University Pediatric Cancer Genome. 2013. 'Whole-genome sequencing identifies genetic alterations in pediatric low-grade gliomas', *Nat Genet*, 45: 602-12.

Zheng, H., L. Chang, N. Patel, J. Yang, L. Lowe, D. K. Burns, and Y. Zhu. 2008. 'Induction of abnormal proliferation by nonmyelinating schwann cells triggers neurofibroma formation', *Cancer Cell*, 13: 117-28.

Zhu, Y., T. Harada, L. Liu, M. E. Lush, F. Guignard, C. Harada, D. K. Burns, M. L. Bajenaru, D. H. Gutmann, and L. F. Parada. 2005. 'Inactivation of NF1 in CNS causes increased glial progenitor proliferation and optic glioma formation', *Development*, 132: 5577-88.

Zhuo, L., M. Theis, I. Alvarez-Maya, M. Brenner, K. Willecke, and A. Messing. 2001. 'hGFAP-cre transgenic mice for manipulation of glial and neuronal function in vivo', *Genesis*, 31: 85-94.

Chapter II: *Nf1* loss leads to Erk-dependent abnormal glial cell expansion in the optic nerve followed by nerve degeneration and RGC loss

2.1 Introduction

Patients with the tumor predisposition syndrome, neurofibromatosis type 1 (NF1) have increased risks of developing benign and malignant tumors in the nervous system. Approximately 15% to 20% of NF1 patients develop low-grade gliomas predominantly involving the optic pathway (optic pathway glioma, OPG) and the incidence of high-grade malignant astrocytoma development in the brain is increased by more than 5-fold compared to the general population (Listernick, Charrow, and Gutmann 1999; Listernick et al. 1997). The major morbidity associated with these gliomas is visual loss with 30 to 50% of NF1 children with OPG experiencing impaired visual acuity. However, the mechanism of visual loss in children with NF1-OPGs is poorly understood and has not been clearly related to tumor size or extent of the involvement of the visual pathway. Some patients with relatively small lesions can lose vision, while some with larger growing lesions may have well maintained vision.

Individuals with NF1 are born with one functional allele (wild-type) and one mutated allele in germline cells ("first-hit"). The heterogeneity in disease manifestation in NF1 patients raises the possibility of two distinct genetic mechanisms. The first possibility could be due to haploinsufficiency where a single copy of the wild-type gene is insufficient to produce enough proteins to perform normal cell functions as opposed to two normal alleles of the gene. In support of this possibility, it was reported that a heterozygous null mutation in *Nf1* impeded long-term potentiation (LTP) and learning by increasing GABA release in the hippocampus (Cui et al. 2008). This phenotype was reverse with pharmacological inhibition of the RAS-MEK-ERK signaling pathway. Moreover, reduced neurofibromin expression in ($Nf1^{+/-}$) neural stem cells leads to increased stem cell proliferation *in vitro* (Dasgupta and Gutmann 2005). However,

haploinsufficiency alone is unlikely to be the basis for NF1-associated OPGs since *Nf1* heterozygous mice do not develop OPGs. The second possibility is the stochastic loss of the remaining wild-type *NF1* allele ("second-hit") in a subset of cells through a genetic event called loss of heterozygosity (LOH). As a result, the NF1-deficient cells are unable to produce the protein neurofibromin. One unique clinical feature of NF1-OPGs is that they arise in children younger than 7 years of age. This clinical observation suggests that the "second-hit" must occur in a transient neural stem and/or progenitor cell population during a critical window of early nerve development. As a result, NF1 deficiency would be transmitted to all subsequent progeny and alter mature cell function. Alternatively, LOH can directly impact neural/stem and progenitor cells by affecting their potential to produce mature, differentiated cells. Therefore, we hypothesize that there is a therapeutic window to target and eliminate this "putative" precursor cell most susceptible to neurofibromin loss and prevent OPG formation.

Due to the diagnosis of NF1-OPGs as pilocytic astrocytomas, it was generally assumed that astrocytes or astrocyte precursor cells (APCs) most likely serve as the cell of origin for these tumors. Recent studies using GEM models have suggested the III-VZ stem/progenitor cells as potential source for OPGs due to their capacity for self-renewal and multilineage differentiation. However, it appears that the onset of hGFAP-cre expression does not occur until after the neuronal-to-glial transition of neural stem cells in the ventral forebrain (E12.5), which occurs much earlier than the lateral ventricle zone in the dorsal forebrain (E17.5). Furthermore, it is well established that astrocytes in the optic nerve, unlike brain-derived oligodendrocytes, arise from locally generated neuroepithelial cells that produce APCs. These optic nerve-derived APCs only differentiate into mature astrocytes in the direction from the eye to the brain. To study optic nerve gliomagenesis, our lab generated GEM model by targeting homozygous *Nf1* mutations ($Nf1^{-/-}$) to neural stem and progenitor cell populations during embryonic development using a Cre transgenic line under the control of human glial fibrillary acidic protein promoter (hGFAP-cre)(Anthony et al. 2004; Malatesta et al. 2003; Wang et al. 2012; Zhuo et al. 2001; Zhu et al. 2005). The hGFAP promoter drives Cre recombinase expression in the majority of embryonic multipotent progenitors, which give rise to cell types such as neurons, oligodendrocytes and astrocytes in the brain. Furthermore, the Cre activity persists in developing astrocytes and progenitor cells in the SVZ at postnatal stages. Unpublished findings in the lab revealed that cre-mediated recombination does

not occur until E15.5 in the ventral brain. In an effort to investigate the role of *Nf1* during optic nerve development, our lab uncovered two major findings. 1) During neonatal stage, *Nf1* loss causes transcriptional activation of the basic helix-loop-helix (bHLH) transcription factor Olig2 in nerve-derived $Pax2^+$ APCs and the expansion $Pax2^+Olig2^+$ cells which later differentiate into $GFAP^+Olig2^+$ cells. 2) In the embryonic brain, *Nf1* inactivation leads to the expansion of $BLBP^+Olig2^+$ glia-restricted progenitors which migrate in the developing optic nerve. Taken together, these findings suggest that $Pax2^+Olig2^+$ cells and $BLBP^+$ progenitors represent the "putative" precursor cell populations that transiently exist during early optic nerve development and are uniquely susceptible to *Nf1* loss.

In this study, I establish the chronological sequence of cellular and molecular events that underlie optic glioma development following *Nf1*-associated glial abnormalities in the developing optic nerve. Investigation of the GEM $Nf1^{hGFAP}$CKOs revealed that they display hyperplastic lesions in the prechiasmatic optic nerves that were able to develop into OPGs with high penetrance. Importantly, the study of late-stage OPGs in $Nf1^{hGFAP}$CKOs revealed the expansion of an abnormal cell population that express both GFAP and Olig2 ($GFAP^+Olig2^+$) and over-activate RAS-MEK-ERK signaling as well as the persistence of glia-restricted progenitor cells. Analysis of the natural history of optic glioma formation determined that the abnormal glial cell expansion is established during neonatal development in mutant nerves. Using a MADM-based *Nf1*-OPG model, I confirmed that the oligodendrocyte lineage underwent the most dramatic expansion in the tumor. Lastly, genetic inactivation of *Mek1/2* rescues OPG formation and RGC loss in *Nf1*-OPG model in a dose dependent manner. Collectively, this study clearly demonstrates that OPGs are a developmental defect with Erk-dependent glial cell expansion occurring during the early postnatal period (Phase I), followed by an immune response, nerve degeneration and Bax-mediated RGC apoptosis (Phase II) and identifies a critical period for neuroprotective intervention before irreversible neurological deficits.

2.2 Results

2.2.1 $Nf1^{hGFAP}$CKOs develop OPGs in the prechiasmatic optic nerve characterized by increased cellularity, microglia infiltration, nerve degeneration and RGC loss.

Our lab previously showed that, in addition to brain structural abnormalities (enlarged corpus callosum, cerebellar defects), *Nf1*^{hGFAP}CKO mice develop OPGs in high penetrance by 2 months of age (Wang et al. 2012; Kim et al. 2014; Zhu et al. 2005). I decided to analyze the optic nerves from *Nf1*^{hGFAP}CKOs and their littermate controls at 6 months and older in order to characterize late-stage tumor in our model. Similar to other *Nf1*-OPG models, *Nf1*^{hGFAP}CKOs develop OPGs characterized by increase in volume (gross fusiform enlargement) at the distal nerve, in an area immediately adjacent to the chiasm (prechiasmatic area) (Figures 3A and 3A'). As revealed by Hematoxylin & Eosin (H&E) staining, *Nf1*^{hGFAP}CKOs show a significant increase in nerve diameter at the tumor site, which was supported by concurrent increase in cellularity with abnormal clusters of cells and increased cell density (Figures 3B-3E). Consistent with their classification as Grade I neoplasms with low proliferative index, late-stage *Nf1*-OPGs had few proliferating cells and the overall proliferative index (less that 1%) was not significantly higher than that of control nerves (Figures 3F, 3F'). However, these tumors do not fully recapitulate human tumors histopathological features such as Rosenthal fibers and eosinophilic granular bodies.

Previous studies have revealed that gliomas are composed of a heterogeneous mixture of neoplastic cells (*Nf1* mutant cells) and non-neoplastic cells (microglia and endothelial cells). Microglia have been shown to play critical role in brain tumor formation and progression by releasing pro-inflammatory factors as well as clearing the dead neurons by phagocytosis (Watters, Schartner, and Badie 2005). To determine the extent of microglia infiltration in OPGs from our GEM models, I performed double-labeling immunofluorescence for Iba1, a microglia/macrophage-specific calcium-binding protein, and GFAP in *Nf1*-OPGs of mice 6 months and older. The number of microglia was increased two-folds in *Nf1*-OPGs compared to age-matched controls. More importantly, the microglia in the OPGs exhibited bushy or amoeboid shape, suggesting they were at an activated status (Figures 4A and 4A'). Unlike normal nerves where microglia were evenly distributed, microglia in *Nf1*-OPGs tended to cluster in areas with intense GFAP staining. These findings indicate that *Nf1*-OPGs are associated with increased microglia infiltration, similar to their human counterparts. Interestingly, these microglia didn't express the tdTomato reporter gene, which labels cells that have undergone Cre-mediated

recombination. This observation suggested that the increase in microglia in the tumors is non-cell autonomous (Figure 4B). To determine whether *Nf1*-OPGs cause changes in axonal organization, I performed neurofilament staining (NF68k) on longitudinal sections of the optic nerve. Optic nerves of tumor-bearing mice contain areas completely void of axonal filament as well as areas with focal axonal fiber misalignment when compared to well-oriented axonal fiber projections in similar regions of control nerves (Figure 4C). In addition, *Nf1*-OPGs in aged mice display areas with severe myelin disruption and loss and the presence of spherical lamellar bodies, a phenotype of myelin degeneration (Figure 4D).

The obvious axonal injury observed at the tumor site may be reflective of RGC apoptosis. Damage to the optic nerve, composed of the axons of RGCs, can lead to their retrograde death and the subsequent loss of vision. To assess whether RGCs are lost in mice with late-stage gliomas, I performed retinal whole-mount staining using the RGC marker, Brn3a (Nadal-Nicolas et al. 2009). The retinas from control mice showed RGCs labeled with bright puncta throughout the RGC layer, with higher cell densities in the central region of the retina, proximal to the optic nerve head (ONH) compared to the peripheral (Figure 5A). In contrast, I observed substantial decrease in RGC cell density in a sectoral pattern in OPG-bearing mice, with the most obvious loss occurring in areas near the ONH (Figure 5A). To examine whether apoptosis contributes to the loss of RGCs observed in the retina of $Nf1^{hGFAP}$CKO mice, I performed terminal deoxynucleotidyl transferase deoxyuridine triphosphate nick end labeling (TUNEL) along with RBPMS, a specific marker for retinal ganglion cells on retinal cross-sections (Rodriguez, de Sevilla Muller, and Brecha 2014). The results confirmed that tumor-bearing mice showed a ~60% decrease in the number of RGCs compared to retinas of control mice (Figures 5B and 5B'). Similarly, there was ~11-fold increase in TUNEL-positive cell in the ganglion cell layer (GCL) of $Nf1^{hGFAP}$CKO mice (Figures 5B and 5B"). Next, I set out to determine whether this apoptosis is cell autonomous (due to Cre activity in RGC cells) or non-cell autonomous. The tdTomato reporter expression was examined in the retina along with RBPMS. Although there was clear evidence of Cre-mediated recombination in $GFAP^+$ astrocytes in the retina, tdTomato expression was not observed in $RBPMS^+$ RGCs in $Nf1^{hGFAP}$CKO retinas (Figure 6C). Taken together, these results indicate that late-stage prechiasmatic *Nf1*-OPGs cause severe nerve damage associated with non-cell autonomous RGC apoptosis.

2.2.2 GFAP$^+$Olig2$^+$ cells, that activate RAS-ERK signaling pathway, underwent the biggest expansion in late stage OPGs in *Nf1*^{hGFAP}CKOs.

Given its robust expression in human tumors, GFAP has long been used as the primary marker to classify pilocytic astrocytomas. Accordingly, late-stage *Nf1*-OPGs display a 2-fold increase in GFAP$^+$ astrocytes with increasingly thickened processes and a very disorganized pattern (Figures 6A and 6B). Several analyses of human pilocytic astrocytomas have revealed that they include numerous cells that express Olig2 within the dense fibrillary region of the tumor (Mokhtari et al. 2005; Ligon et al. 2004; Reis et al. 2013). Furthermore, Olig2 transcription levels were found to be similarly high in both oligodendroglial and astrocytic tumors (Bouvier et al. 2003). Therefore, I decided to examine Olig2 expression in our *Nf1*-OPGs. Similar to the astrocytic population, I observed an almost 2-fold increase in Olig2$^+$ oligodendrocytes in tumor location (Figure 6B'). Recent unpublished findings in our lab have revealed that the transient Pax2$^+$ APC population ectopically express Olig2 (Pax2$^+$Olig2$^+$) following *Nf1* inactivation in the developing nerve. Pax2$^+$Olig2$^+$ cells later differentiate into GFAP$^+$Olig2$^+$ double positive cells. With this knowledge, I decided to investigate whether GFAP$^+$Olig2$^+$ double positive cells persist in late-stage tumors. In contrast to GFAP$^+$Olig2$^-$ and GFAP$^-$Olig2$^+$ cells which show only a modest increase (less than 2-fold), cells that express both GFAP and Olig2 marker (GFAP$^+$Olig2$^+$) underwent the biggest expansion in the tumors (5-fold increase) (Figures 6A' and 6B"). The percentage of Olig2-expressing cells in the population of GFAP$^+$ astrocytes (GFAP$^+$Olig2$^+$) was dramatically increased from 17% in controls to 38% in mutants. Similarly, within the Olig2$^+$ cells, the percentage of double-positive cells rose from 9% in the control nerves to 21% in mutant OPGs (Figures 6B and 6B'). These data suggest that abnormally differentiated GFAP$^+$Olig2$^+$ cells are the glia cell population that underwent the biggest expansion in late-stage OPG.

The extracellular signal-regulated kinase (ERK) subfamily of mitogen-activated protein kinases (MAPKs) is one of the major downstream effector pathway activated by RAS through indirect phosphorylation. We have previously demonstrated that neurofibromin loss results in increased RAS-Erk signaling in the brain and optic nerves of *Nf1*^{hGFAP}CKOs, as measured by the expression of phosphorylated Erk (p-Erk$^+$) (Kim et al. 2014; Zhu et al. 2005). To investigate whether the increase in GFAP$^+$Olig2$^+$ cells in late-stage *Nf1*-OPG is associated with the activation

of RAS-MAPK signaling, I performed triple-labeling immunofluorescence staining for p-Erk along with GFAP and Olig2. I observed a robust increase (7-fold) in p-Erk$^+$ cells in the tumors compared to similar section in control nerves (Figures 7A- 7A'"). In control nerves, the vast majority of cells with activated RAS-Erk signaling (82%) belonged to the astrocytic lineage (p-Erk$^+$GFAP$^+$Olig2$^-$). Remarkably, within p-Erk$^+$ cells in the tumors, Olig2$^+$ population constituted the cellular component with the most dramatic increase, either through GFAP$^+$Olig2$^+$ cells (42-fold) or Olig2$^+$ only cells (15-fold) (Figures 7A"- 7A'"). Importantly, p-Erk$^+$GFAP$^+$Olig2$^+$ triple-positive cells in controls were rare and showed weak Olig2 expression. In contrast, the majority of triple-positive cells in late-stage OPGs showed robust nuclear p-Erk and Olig2 expression (Figure 7A'). Previous studies have shown that *Nf1* loss could also activate the mammalian target of rapamycin (mTOR) signaling pathway which also plays an important role in regulating cell metabolism, growth, proliferation and survival (Mendoza, Er, and Blenis 2011). To investigate whether the mTORC1 signaling pathway was activated in these *Nf1*-OPGs, I used the expression of phosphorylated S6 (p70 ribosomal S6) as a readout for the activation of mTORC1 signaling. The number of pS6$^+$ cells was only slightly increased (statistically non-significant) in late-stage *Nf1*-OPGs compared to age-matched control nerves. This observation indicated that mTORC1 pathway was not activated in these tumors (Figures 7B-7B'). Taken together, these observations suggest that *Nf1* loss and activation of the RAS-Erk signaling pathway in mutant nerves leads to the expansion of a cell population which express markers of both astrocyte and oligodendrocyte lineages.

2.2.3 *Nf1* inactivation leads to Erk-associated persistence of glial-restricted progenitor cells in late-stage OPGs.

Our unpublished data has shown that embryonic *Nf1* loss resulted in the expansion of glia-restricted precursors originating from the brain. Indeed, it was reported that mutant optic nerves express glial-restricted progenitor cell markers such as the brain lipid binding protein (BLBP) and Pax2 (Zhu et al. 2005). Accordingly, BLBP$^+$ cells were increased approximately 10-fold in mutant *Nf1*-OPGs (Figures 8A-8A"). Unlike the brain where BLBP is typically considered an astrocytic precursor, immunolabeling in normal nerves reveal BLBP co-expression in both astrocytic and oligodendrocytic lineages (Figures 8A' and 8A"). Surprisingly, *Nf1* inactivation leads to a

dramatic increase in glial progenitor specification not only in double-positive $GFAP^+Olig2^+$ cells (10-fold) but also in $Olig2^+$ only cells (17-fold). This result was strikingly similar to the cellular distribution observed within p-Erk^+ cells following *Nf1* loss. To investigate whether the persistence of $BLBP^+$ progenitors in late-stage gliomas was associated with Erk activation, I examined whether $BLBP^+$ cells express p-Erk in the gliomas. Since the most specific antibodies for both BLBP and p-Erk are raised within the same species (rabbit), I was unable to perform direct co-labeling experiments. Fortunately, we have crossed the *Nf1*^{hGFAP}CKO with a mouse strain that contains a transgene encoding the green fluorescent protein (GFP) under the control of the BLBP promoter. The GFP reporter was shown to exclusively express in the majority of BLBP-positive glial progenitor cells in the brain (Schmid, Yokota, and Anton 2006) and the optic nerve. In contrast to normal nerves which showed very little colocalization between p-Erk and BLBP, nearly one third of p-Erk^+ cells in the gliomas also expressed the BLBP protein (Figure 8B, 8B').

The results described above suggest that the oligodendrocyte lineage was most severely affected in the tumors, either through expression of Olig2 in $GFAP^+$ cells ($GFAP^+Olig2^+$) or expansion of $BLBP^+Olig2^+$ progenitors. Therefore, I set out to investigate how *Nf1* inactivation also affected the more specific progenitor marker, PDGFRα, which exclusively labels oligodendrocyte precursor cells (OPCs). In control nerves, less than 10% of oligodendrocytes were OPCs. This percentage was dramatically increased in mutant nerves where 22% of oligodendrocytes retained PDGFRα expression (Figure 8C, 8C'). Surprisingly, 14% of OPCs in the tumor abnormally express the GFAP marker. These cells were never found in normal nerves and represent a de-novo population in *Nf*1-OPG (Figure 8C, 8C"). Lastly, about 15% of tumor OPCs express p-Erk which suggests that Erk signaling plays a role in their maintenance (Figure 8D, 8D'). Taken together, these data suggest that acute *Nf1* inactivation leads to Erk-dependent persistence of glial progenitors in late-stage OPGs.

2.2.4 Glial cell expansion in *Nf1*^{hGFAP}CKO is largely established during neonatal development.

Analysis of late-stage OPGs identified the abnormal expansion of double-positive $GFAP^+Olig2^+$ cells that hyper activate the RAS-Erk pathway and the persistence of glia-restricted

progenitors. Next, I investigated the timing and cellular mechanism underlying developmental changes that occur in the optic nerve upon biallelic *Nf1* loss function that contribute to OPG formation. To determine the chronological sequence of events from tumor formation cumulating in RGC loss, I chose three developmental time-points: P15, P21 and P60. The peak of myelination in murine models occurs around P15. Prior to that time, the optic nerve looks almost transparent due to lack of myelination and is very difficult to distinguish from the surrounding tissue, much less to dissect. Around the time of weaning (three weeks postnatal, P21), the development of the optic nerve is considered complete. At postnatal day 60 (P60), mice have reached maturity and are sexually active. Whole-mount comparison revealed that optic nerve enlargement was not apparent in *Nf1*^{hGFAP}CKOs before P21 (Figure 9A). This observation was confirmed by H&E histological analysis which showed significant increase in diameter starting at P21 (Figures 9B and 9B'). However, obvious bulging of prechiasmatic nerve was not seen until P60. Surprisingly, increase cellularity was established as early as P15, prior to nerve enlargement (Figure 9B"). Based on this finding, I investigated whether as a tumor suppressor, *Nf1* loss altered the growth potential of optic nerve glial cells that could contribute to the hypercellularity observed in mutant nerves at this developmental time-point. The proliferation rate was highest at P15 (~10%) but dramatically decreased one week later (~1%). However, no significant difference in proliferation was observed between controls and mutants at all time-points analyzed (Figure 9C and 9C'). This result suggests that the glial cell increase in *Nf1*^{hGFAP}CKO optic nerves must occur during early postnatal stage.

2.2.5 Aberrant glial specification and activation of RAS-Erk signaling pathway are evident at P15 in *Nf1*^{hGFAP}CKO optic nerves and persist throughout gliomagenesis.

Based on the above findings, I investigated the cellular and molecular mechanism underlying the cellular increase in P15 nerves following *Nf1* inactivation. I observed a greater than two-fold increase in the number of p-Erk^{+} cells in *Nf1*^{hGFAP}CKO optic nerves at 2-weeks old (Figures 10A and 10B). Interestingly, the phenotypic alteration in Olig2 expression resulting in double-positive GFAP^{+}Olig2^{+} cells observed in late-stage OPGs can be found as early as P15 in mutant nerves. Specifically, GFAP^{+}Olig2^{+} cells underwent the biggest expansion (10-fold increase) between the different glia cellular compartment analyzed at P15 and a majority of them were positive for p-Erk, consistent with late-stage tumor described previously (Figures 10C and

10C'). In agreement with p-Erk expression pattern in aged control nerves, the overwhelming majority of p-Erk^{+} cells in P15 normal nerves were GFAP^{+} astrocytes. Expectedly, P15 *Nf1*^{hGFAP}CKO nerves showed a robust increase in glia progenitor marker, BLBP, with some co-expressing markers for both GFAP and Olig2 (Figures 10D). Likewise, immunostaining for Olig2 and PDGFRα showed significant increase in OPCs in P15 mutant nerves (Figures 10E). Furthermore, consistent with the observation that end-stage OPGs had minimal activation of mTORC1 signaling pathway, the pS6 expression in mutant optic nerves was also very low, which was very similar to control nerves at P15 (Figures 10F).

I next investigated the remaining time-points (P21 and P60) to determine whether there was a dynamic change in glial cell specification and number throughout gliomagenesis. At both time-points, the number of p-Erk^{+} cells in mutant nerves remain very high and did not appear to fluctuate significantly over time. In contrast, p-Erk^{+} cells represent a rare population in normal nerves during development. In addition, triple-positive cells (p-Erk^{+}GFAP^{+}Olig2^{+}) were found consistently in mutant nerves with no obvious change in number or distribution during tumorigenesis (Figures 11A). Similarly, the number of BLBP^{+} progenitors was extremely low in control nerves but remained elevated at all time-points analyzed in the mutants and retained their expression pattern in the abnormally expanded GFAP^{+}Olig2^{+} cells (Figures 11B). Furthermore, BLBP^{+} progenitors in P60 mutant nerves also activated the RAS-Erk pathway as evidenced by p-Erk co-expression (Figures 11C). Although the number of OPCs decrease from P21 to P60 in both control and mutant nerves, over time, there were significantly more OPCs in mutants compared to controls. These results suggest that *Nf1* regulates progenitor cells expression in an Erk-dependent fashion during early optic nerve development. Combined with the Ki67 data which clearly shows minimal proliferation in mutant nerves after P15, these results support a model of *Nf1*-OPG as a neurodevelopmental disorder where the glia abnormalities described in late-stage OPGs are established in mutant nerves during early postnatal development and persist throughout tumor development.

2.2.6 The second phase of *Nf1*-OPG disease progression is characterized by optic nerve dysfunction and neuronal loss

Despite a high percentage of NF1-OPG patients (80-90%) achieving tumor stabilization following treatment with chemotherapeutic agents, few of them exhibited visual improvement. These observations suggest that the irreversible neuronal damage was established at the time treatment was initiated. However, it is unknown whether there exists a temporal window for therapeutic intervention before neuronal dysfunction. Based on the analysis of control and mutant nerves at P15, P21, P60 and late-stage OPGs, we determined that *Nf1*-related cellular pathogenesis is established in the nerve starting at within the first two weeks of postnatal development. I used the same samples to determine the timeline for nerve dysfunction relevant to vision loss during the gliomagenesis. Increased microglia infiltration is the earliest event observed in mutant nerves at P15 (Figures 12A, 12A'). But at this time point, the microglia in both control and mutant nerves appear to be in a similar resting, inactive phase. At P21, microglia in mutant optic nerves begin to show more amoeboid shape and thickened processes- an indication of monocyte activation. However, this increase in immune cells infiltration was not immediately accompanied by axonal damage. Indeed, neurofilament staining did not reveal obvious areas of axonal loss in P21 mutant nerves. About forty days later (P60), there were clear signs of nerve damage in the optic nerves of P60 *Nf1*^{hGFAP}CKOs, as evidenced by patterns of misaligned optic nerves fibers and axonal loss (Figure 12A). The process of myelination is not completed until the end of optic nerve development around P21-P30. At both P15 and P21, I did not observe any significant difference in myelination in mutant versus control nerves. Strikingly, there was significant myelin alterations in tumor-bearing mice at P60 similar to defects observed in late-stage tumors (Figure 12B). This result indicates that the myelination loss observed in the gliomas does not occur as a result of an increase number of immature OPCs that are unable to myelinate the axon fibers in mutant nerves, but rather is an indication of secondary nerve damage. Consistent with the timeline for axonal damage, there was no increase in apoptosis or RGC loss in P21 *Nf1*^{hGFAP}CKO retinas (Figures 12C, 12C'). As expected, there was progressive RGC loss in mutant retinas which displayed ~40% decrease in the number of RGC relative to normal retinas and culminated to 60% loss in aged mutants (Figures 12D and 12E). Collectively, these data demonstrate a specific temporal sequence of critical events that underlie OPG formation: abnormal glial expansion occurred first, followed by immune infiltration and RGC degeneration.

2.2.7 Bax-mediated apoptosis underlies progressive RGC loss in *Nf1*^{hGFAP}CKO mice

The evolutionary conserved process of apoptotic cell death plays a major role in the development of the central nervous system. Using a *Bax*$^{-/-}$ mouse model that was defective in the pro-apoptotic Bax protein, Pequignot et al. reported that the adult mutant retinas showed a thicker RGC layer with significantly more neurons that normal retinas. They concluded that Bax protein is essential for the modeling of functional vision during normal retinal development (Pequignot et al. 2003). To determine whether Bax-mediated apoptosis is the mechanism involved in the progressive RGC loss observed in tumor-bearing mice, I decided to cross the *Nf1*^{hGFAP}CKO mice with *Bax*$^{-/-}$ mutants. The resulting double-mutants displayed similar phenotypes as *Nf1*^{hGFAP}CKOs. Four months old *Bax*$^{-/-}$ single mutants had thicker retinas and double the number of RGCs stacked in multiple rows in the GCL compared to age-matched control retinas (Figures 13A and 13A'). This finding is consistent with the previous report describing *Bax* mutant retinal phenotype. Strikingly, there was no decrease in the number of RGCs in the double mutant retinas compared to *Bax* mutant. Furthermore, the double mutants presented similar phenotype as Bax mutants such as increased RGCs and thicker ganglion cell layer. This finding suggests that retinal cell death was prevented in the *Bax* and *Nf1-Bax* double mutants.

The absence of RGC loss in the double mutants could be due to these mice not developing *Nf1*-OPGs, thus unrelated to our study. To explore this possibility, I performed whole-mount and histological analysis in the prechiasmatic optic nerve of *Bax* mutants and *Nf1-Bax* double mutants compared to *Nf1*^{hGFAP}CKOs and controls. Overall, both *Bax*$^{-/-}$ single mutants and *Nf1-Bax* double mutants displayed noticeable increase in thickness throughout the length of the optic nerves compared to *Nf1*^{hGFAP}CKOs and controls. However, only the double mutants showed significant optic nerve volume enlargement (bulging) in the prechiasmatic area (Figures 13B). Although, H&E staining revealed higher cellularity in *Bax*$^{-/-}$ single mutants the cellular density was not significantly different than control nerves. This result suggests that the increased nerve volume in the *Bax* mutants is contributed by the increase in axon numbers from the excess RGCs in the retina and not by an increase in glial cell in the nerve. However, the cellular density in the double mutants was statistically similar to *Nf1* single mutants, suggesting a local increase in glial cells in that region. To determine whether double mutants presented *Nf1*-OPG nerve damage, I performed

immunostaining for microglia, axonal marker and GFAP immunoreactivity. The increase in nerve volume in single *Bax* mutants did not invoke an immune response, axonal damage or increase in $GFAP^+$ astrocytes. In contrast, double mutants displayed clear tumor phenotypes such as increase microglia infiltration, axonal loss and increased in astrocytes with thicken processes and disorganized pattern reminiscent of OPGs in *Nf1* mutants (Figures 13C). Collectively, these data elucidate that the mechanism of progressive RGC loss in tumor bearing $Nf1^{hGFAP}$CKOs is dependent on Bax-mediated apoptosis.

2.2.8 MADM-based lineage tracing confirms dramatic overexpansion of $Olig2^+$ cells in *Nf1*-OPGs

Our early postnatal study suggests two major phenotypic consequences of *Nf1* loss during optic nerve development: 1- the ectopic Olig2 expression in $Pax2^+$ transient progenitor cells ($Pax2^+Olig2^+$) and 2- the expansion of $BLBP^+Olig2^+$ cells. Both mechanisms and subsequent late-stage tumor study hint at the oligodendrocyte lineage as the cellular compartment which is most affected by *Nf1* inactivation. In order to investigate the cell-type specific function of *Nf1* at a single cell resolution, I used a MADM-based mouse model under the hGFAP-cre promoter (Zong et al. 2005). Mosaic analysis with double markers (MADM) is a mouse genetic modeling system that allows for the direct comparison of the behavior of siblings wild-type (Green, $Nf1^{+/+}$) and mutant (Red, $Nf1^{-/-}$) cells that are derived from common stem/progenitors at the population level in their native environment (Figure 14A). The MADM mutants were analyzed at P60 and did not display any overt mutant phenotype (*Nf1* gene is heterozygous). When I analyzed the optic nerves, I found a dramatic overexpansion of red mutant cells compared to their green wild-type counterparts (Figure 14B). The difference was even more pronounced in the ventral brain, near the III-VZ adjacent to the chiasm. Because mutant and wild-type sibling cells come from the same mother cell in equal number at the beginning, their distribution should be similar if *Nf1* loss does not confer a growth advantage to mutant cells. Strikingly, red cells accounted for an astonishing 11% of total cells quantified compared to less than 1% for the green cells. The ratio of red to green cells number (R/G) enables the quantitative analysis of the extent of mutant cells expansion, whereas a R/G ratio of >1 signifies overexpansion or mutant cells growth advantage. The overall R/G ratio in P60 MADM nerves was about 8 (Figure 14C). These data corroborate the well-described role

of NF1 as a tumor suppressor because *Nf1* deficiency confers a clear growth advantage to the mutant cells in both the brain and nerves.

Out of 4 MADM mutants analyzed, all display significant enlargement in the prechiasmatic optic nerves with concurrent increase in $Olig2^+$ cells and $GFAP^+$ cells in a disorganized pattern suggestive of OPG (Figure 14D). To confirm whether MADM mutants develop OPGs, I evaluated the nerves for microglia infiltration, a clear sign of tumor presence. Compared to aged-matched control nerves, MADM nerves had double the number of $Iba1^+$ cells with most displaying amoeboid-like appearance (Figures 14E and 14F). Therefore, I concluded MADM mutants develop OPGs with similar timeline as $Nf1^{hGFAP}$CKOs. Next, I decided to investigate which cellular compartment underwent the most extensive expansion in mutant cells at P60. Immunostaining for GFAP revealed that a relatively higher number of mutant cells co-stained for GFAP (arrows) compared to wild-type cells (arrowhead) (Figure 14G). However, the difference did not appear to be overly dramatic, suggesting $GFAP^+$ astrocytes did not gain significant growth advantage following NF1 loss. Interestingly, $BLBP^+$ progenitors in MADM nerves were increased compared to controls and were overrepresented in the mutant cells (Figure 14H). Of note, $BLBP^+$ progenitor specification was disproportionally shifted towards oligodendrocyte lineage in OPGs from $Nf1^{hGFAP}$CKOs. Finally, I investigated the overall distribution of oligodendrocytes in both wild-type and mutant cells. In green, wild-type cells, Olig2 accounted only for 31% of the cells. This data indicates that hGFAP-cre normally targets few oligodendrocytes and is mainly in the astrocytic lineage. However, $Olig2^+$ cells were overexpanded in mutant cells and contributed to a whopping 75% in the increased cell number (Figures 14I and 14J). Similarly, the percentage of mutant cells in the Olig2 population rose to 33% compare to the 3% of wild-type, green cells in the same population (Figure 14K). Collectively, these data substantiate that the oligodendrocyte lineage represent the most susceptible lineage that manifest dramatic overexpansion following neurofibromin loss. In addition, the fact that MADM mutants were able to develop OPGs with similar temporal course and characteristics as conventional $Nf1^{hGFAP}$CKOs despite the low efficiency and sparse labelling (0.1%-1% or lower) afforded by the MADM system, underscores the notion that biallelic NF1 inactivation must occur in a progenitor cell during a critical early window of optic nerve development. This supports the clinical observation that NF1-OPGs arise from children with a peak incidence between 4-5 years and rarely over 7 years of age.

2.2.9 Dose-dependent genetic inactivation of *Mek1/2* prevents *Nf1*-OPG formation

The RAS/MEK/ERK pathway is known to play a critical role in cell proliferation, differentiation and function. Genetic modifications in various components of the core pathway cause RASopathies, a group of syndromes associated with severe cognitive impairment in humans. Recent works from our lab and others have highlighted the importance of this signaling pathway in regulating proper cortical and cerebellar development through the use of inhibitors of MEK (MEKi) (Wang et al. 2012; Kim et al. 2014; Sanchez-Ortiz et al. 2014). Through genetic manipulation of *Mek1/2*, Li et al. has demonstrated that gliogenesis during cortical development is tightly regulated by MEK activity (Li et al. 2012). In my data described previously, I have shown that MEK pathway is associated with glial abnormalities ($GFAP^{+}Olig2^{+}$, $BLBP^{+}$) in $Nf1^{hGFAP}$CKOs at all time-points analyzed. However, it remains unclear whether MAPK pathway activation is the main/sole molecular mechanism responsible for optic gliomagenesis. To answer this question, I crossed the $Nf1^{hGFAP}$CKO mutants with different levels of genetic inactivation of *Mek1* exon-3 floxed ($Mek1^{fl/fl}$) and $Mek2^{-/-}$. While the three-allele deletion of either *Mek1* or *Mek2* mutants bred in hGFAP-cre were viable and fertile, complete *Mek1/2* deletion (M4: $Mek1/2^{hGFAP}$CKO) resulted in pup mortality around P10. This result suggests that inactivation of all four alleles is necessary to achieve complete blockage of the pathway function and that MEK1 and MEK2 can successfully compensate for each other. To study the function of MEK1/2 in *Nf1*-OPG, I generated three groups of *Nf1* mutants with various degrees of *Mek1/2* allele inactivation. The first group, called M1, had a single remaining wild-type allele of *Mek1* or *Mek2* ($Nf1^{hGFAP}$CKO, $Mek1^{fl/fl}$, $Mek2^{-/+}$ or $Mek1^{fl/+}$, $Mek2^{-/-}$). The second group, M2, had two remaining wild-type *Mek1/2* alleles ($Nf1^{hGFAP}$CKO, $Mek1^{fl/+}$, $Mek2^{-/+}$; $Mek1^{fl/fl}$, $Mek2^{+/+}$; $Mek1^{+/+}$, $Mek2^{-/-}$). The last group, M3, retained three wild-type *Mek1/2* alleles ($Nf1^{hGFAP}$CKO, $Mek1^{fl/+}$, $Mek^{+/+}$ or $Mek1^{+/+}$, $Mek2^{-/+}$). To study the rescue effect of *Mek1/2* inactivation on *Nf1*-OPG, I performed H&E histological analyses and immunostaining on prechiasmatic nerves of all three groups and their littermate controls between 4 to 8 months of age, with a minimum of 8 representatives for each group. The overwhelming majority of M1 mutants with three alleles *Mek1/2* deletion displayed normal-looking nerves without gross morphological abnormalities (nerve enlargement) on the H&E staining (10 out of 11, 91% rescued). This result was reinforced by assessing markers

for tumor phenotype. M1 mutants displayed no sign of axonal damage (NF68K) or increase microglia infiltration, indicative of the second phase of OPG progression (Figure 15A). Accordingly, phase I glial abnormalities such as increase in $Olig2^+$ and $GFAP^+$ cells, as well as the persistence of $GFAP^+Olig2^+$ cells and $BLBP^+$ progenitors (data not shown) were completely rescued. These observations correlated very well with p-Erk activation in M1 mutants which show similar number of $p\text{-}Erk^+$ cells as age-matched controls. To my surprise, I noticed a dose-dependent rescue in *Nf1*-OPG corresponding to increasing number of wild-type *Mek1/2* alleles. In effect, less than half of the M2 mutants (4 out of 9, 44%) were rescued, with a further decrease to 38% (3 out of 8) rescued in M3 mutants. The non-rescued M2 and M3 mutants displayed severe OPGs with obvious glial abnormalities and nerve damage (Figure 16A). Furthermore, there was a clear association between the levels of phosphorylated Erk protein and the degree of rescue where M2 and M3 mutants with low number of $p\text{-}Erk^+$ cells showed near complete rescue of tumor phenotype (Figure 15B). Lastly, the phenotype rescue was not limited to the optic nerve. *Nf1*^{hGFAP}CKOs exhibit growth retardation and weight about half as much as littermate controls. This phenotype was readily identified in non-rescued M2 and M3 mutants. However, the majority of M1 mutants were indistinguishable in appearance and weight from control littermates (Figure 15C). Amazingly, rescued M1 mutants were fertile and bred normally, which was rarely observed in *Nf1*^{hGFAP}CKOs.

To determine whether the dose-dependent rescue in the nerve following *Mek1/2* genetic inactivation translated into neuronal protection in the retina, I examined the GCL of all three groups. I observed a complete rescue in RGC loss in M1 mutant, corroborating the observations from the optic nerve. There was a distribution observed in M2 and M3 mice where, the rescued animals consistently show RGC numbers within the normal range, and the majority tumor-bearing animals exhibited extensive RGC loss (Figures 16A and 16B). The same result was observed with the analysis of apoptosis. Indeed, the rescued and non-rescued animals in groups M2 and M3 could clearly be separated in the graph (Figure 16C). Taken together, these results demonstrated that MEK signaling is the major signaling pathway underlying *Nf1*-OPG formation. Furthermore, these results suggest that the pathway must be inactivated to a high enough degree (3 alleles) to achieve consistent and significant rescue.

2.3 Discussion

In this chapter, based on two independent genetic systems (conventional CKOs and the genetic mosaic system MADM) driven by hGFAP-cre, I identified essential roles of the *Nf1* tumor suppressor gene in regulating proper glial specification during early optic nerve development. In addition, my study broadly defined the two-step mechanism of optic gliomagenesis. Step 1, disease initiation: biallelic inactivation of *Nf1* during embryonic development results in expansion and persistence of glia-restricted progenitors and the generation of abnormally differentiated $GFAP^{+}Olig2^{+}$ cells through Erk-dependent mechanism. Step 2, disease progression: abnormal glial expansion leads to immune cell infiltration and activation, followed by axonal damage and myelin loss and culminating in Bax-dependent progressive RGC apoptosis.

2.3.1 *Nf1* regulates glial fate specification in the optic nerve

The prevalent view of NSCs as the cell of origin for OPGs has been perpetuated by their persistent proliferative capacity throughout neurodevelopment and into adulthood. In addition, their self-renewal and multilineage differentiation potential renders NSCs uniquely susceptible to oncogenic transformation. Indeed, Lee et al. have proposed NSC from the third ventricle zone as the cell of origin of NF1-OPG due to their proximity to the optic nerve, their proliferative potential and multilineage potential and preferential sensitivity to NF1 loss (Lee, Gianino, and Gutmann 2012). However, many of the same features are shared by glial-restricted precursors. For example, recent studies have revealed that glial progenitors constitute the largest proliferative pool in brain of both rodents and humans (Dawson et al. 2003; Geha et al. 2010). Furthermore, it was reported that *NF1* mutation alone is sufficient to promote OPC proliferation across different species (Bennett et al. 2003; Lee et al. 2010). Intriguingly, Lui et al. demonstrated that OPCs, unlike NSCs and other brain cell types, are particularly sensitive to *NF1* mutations (Liu et al. 2011). Together, these studies suggest a pivotal role for NF1 in regulating glial progenitor proliferation in the brain.

The most well-known genetic and molecular mechanism of the disease is the biallelic inactivation of NF1 gene. However, the phenotypical consequence of NF1 loss during optic nerve development remains elusive. Early postnatal optic nerve studies in our lab have revealed several

intriguing findings. Embryonic *Nf1* inactivation leads to the expansion of $BLBP^{+}Olig2^{+}$ progenitors from the brain which then migrate into the nerve. In the developing nerve, *Nf1* loss results in Erk-dependent transcriptional activation of Olig2 in $Pax2^{+}$ astrocyte precursor cells (APCs). $Pax2^{+}Olig2^{+}$ cells later differentiate into $GFAP^{+}Olig2^{+}$ cells. Lastly, these data suggest that $BLBP^{+}Olig2^{+}$ progenitors and $Pax2^{+}Olig2^{+}$ cells represent transient populations during normal development and are the most affected by NF1 deficiency. In this study, I extend these findings by demonstrating that $GFAP^{+}Olig2^{+}$ and $BLBP^{+}Olig2^{+}$ cells are the most expanded cellular compartment in late-stage tumors. Furthermore, I established that *Nf1*-OPGs represent a developmental defect with abnormal glial cell expansion occurring during the early postnatal period, followed by an immune response, nerve damage and progressive, Bax-dependent RGC apoptosis. Moreover, these findings provide a potential therapeutic window to prevent and treat visual impairments before irreversible neurological deficits. Using the hGFAP-cre-induced MADM labeling system, I demonstrated that *Nf1* mutant cells (red) displayed a growth advantage over their *Nf1* wild-type siblings (green). Furthermore, this growth advantage was conferred to the oligodendrocyte lineage as evidence by the overexpansion of mutant $Olig2^{+}$ cells (Red^{+}/ $Olig2^{+}$) as well as $BLBP^{+}$ glial progenitor cells. Importantly, both the conventional CKO and the MADM system fit with the current understanding of NF1-OPG as a neurodevelopmental disorder where biallelic NF1 inactivation must occur in a transient, progenitor cell during an early time window of CNS development. Accordingly, NF1-OPGs rarely arise in children over 7 years of age, with a peak incidence between 4-5 years.

2.3.2 Hyperactive MEK-Erk signaling underlies glial defects in *Nf1*^{hGFAP}CKOs and offers a platform for future clinical studies

A large body of work has revealed several signaling pathways that are known to regulate Olig2 expression in the CNS, such as epidermal growth factor, platelet-derived growth factor (PDGF), sonic hedgehog (Shh), canonical Wnt and Notch. Ortega et al. demonstrated, through infusion in the lateral ventricle and focal expression in the SVZ using lentiviral expression vector, that the signaling protein Wnt3a controls oligodendrogliogenesis from NSCs in the adult mouse (Ortega et al. 2013). Similarly, Brunet and colleagues have shown that loss of the protein deacetylase, Sirt1, increased OPC proliferation and oligodendrocyte production in the adult brain

through upregulation of PDGFRα (Rafalski et al. 2013). Indeed, overexpression of PDGFRα leads to an increase in production of $Olig2^+$ cells in the SVZ (Jackson et al. 2006). Of note, MAPK pathway is a critical signaling pathway working downstream of PDGFRα. Shh has been shown to promote OPC production and Olig2 expression in neocortical progenitors (Lu et al. 2002; Zhou and Anderson 2002). Importantly, the regulatory function of Shh depends on Erk signaling (Kessaris et al. 2004). In this study, I show that *Nf1* regulates glial specification in the developing nerve through MEK-ERK signaling. In control nerves, p-Erk activation is limited and restricted to the astrocyte lineage. *Nf1* loss resulted in the ectopic Olig2 expression in the astrocytic lineage, generating $GFAP^+Olig2^+$ cells that were enriched in the tumors. In addition, I showed that *Nf1* directly regulates $BLBP^+Olig2^+$ progenitor production. Importantly, both processes were modulated by MEK-Erk signaling activity as demonstrated by the dose-dependent rescue of glial abnormalities by genetic *Mek1/2* inactivation. Of note, the rescue of phase I Erk-dependent glial defects subsequently prevented phase II microglia infiltration, axonal and myelin degeneration and neuronal loss. These observations suggest that the glial abnormalities that occur during neonatal stages are both necessary and sufficient to induce neuronal death in the second phase of disease pathogenesis. Recently, the use of compounds targeting MEK1 and MEK2, such as MEK inhibitors, has shown promising clinical activity in a number of tumor types. In light of the availability of these agents, $Nf1^{hGFAP}$CKO mice can offer an attractive preclinical platform to investigate the potential for MEK inhibition in the prevention and treatment of NF1-OPGs. This will be the focus of the following chapter (Chapter III) of my thesis.

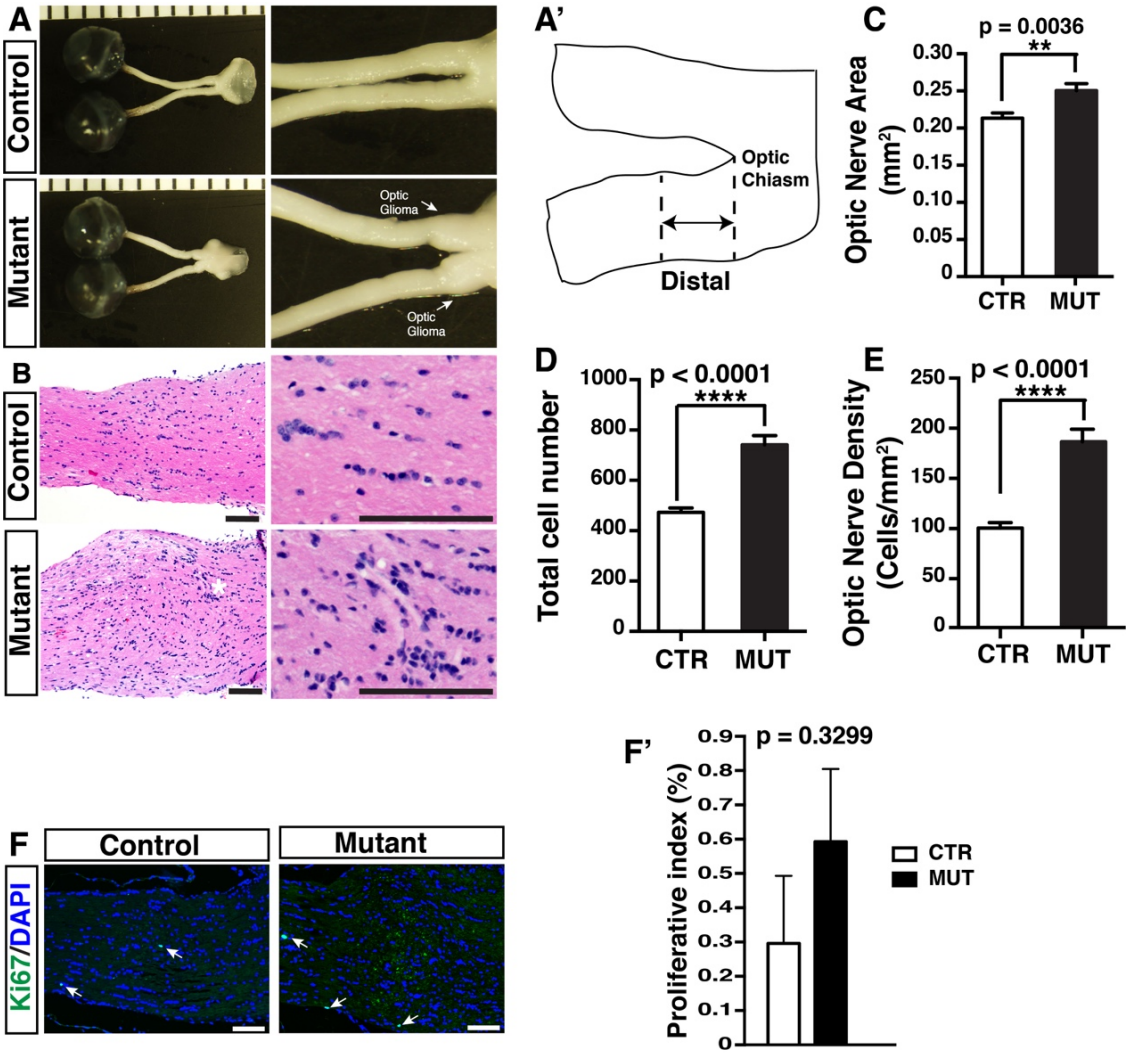

Figure 3. *Nf1*^{hGFAP}CKOs develop OPGs in the prechiasmatic optic nerve.

Whole mount optic nerves from control and *Nf1*^{hGFAP}CKO mice at 6 months of age or older were dissected, fixed in 4% PFA and imaged under the dissection microscope **(A)**. OPGs characterized by increase in volume (gross fusiform enlargement) form at the distal nerve, in an area immediately adjacent to the chiasm (prechiasmatic area) **(A')**. Sections from optic nerves of control and *Nf1* mutants were stained with H&E**. (B)**. The total cell number, optic nerve area and optic nerve density of controls and mutants were quantified. **(C, D, E)**. Comparison of the proliferation index between controls and mutant nerves revealed no significant increase in aged mice **(F, F')**. Arrows point to Ki67^{+} cells. DAPI labels for nuclei. Asterisks denote statistically significant differences (*p < 0.05, ** p < 0.01, *** p < 0.001; paired t-test). All the data are presented as mean ± SEM. Scale bars: 1 mm (A) and 50 μm.

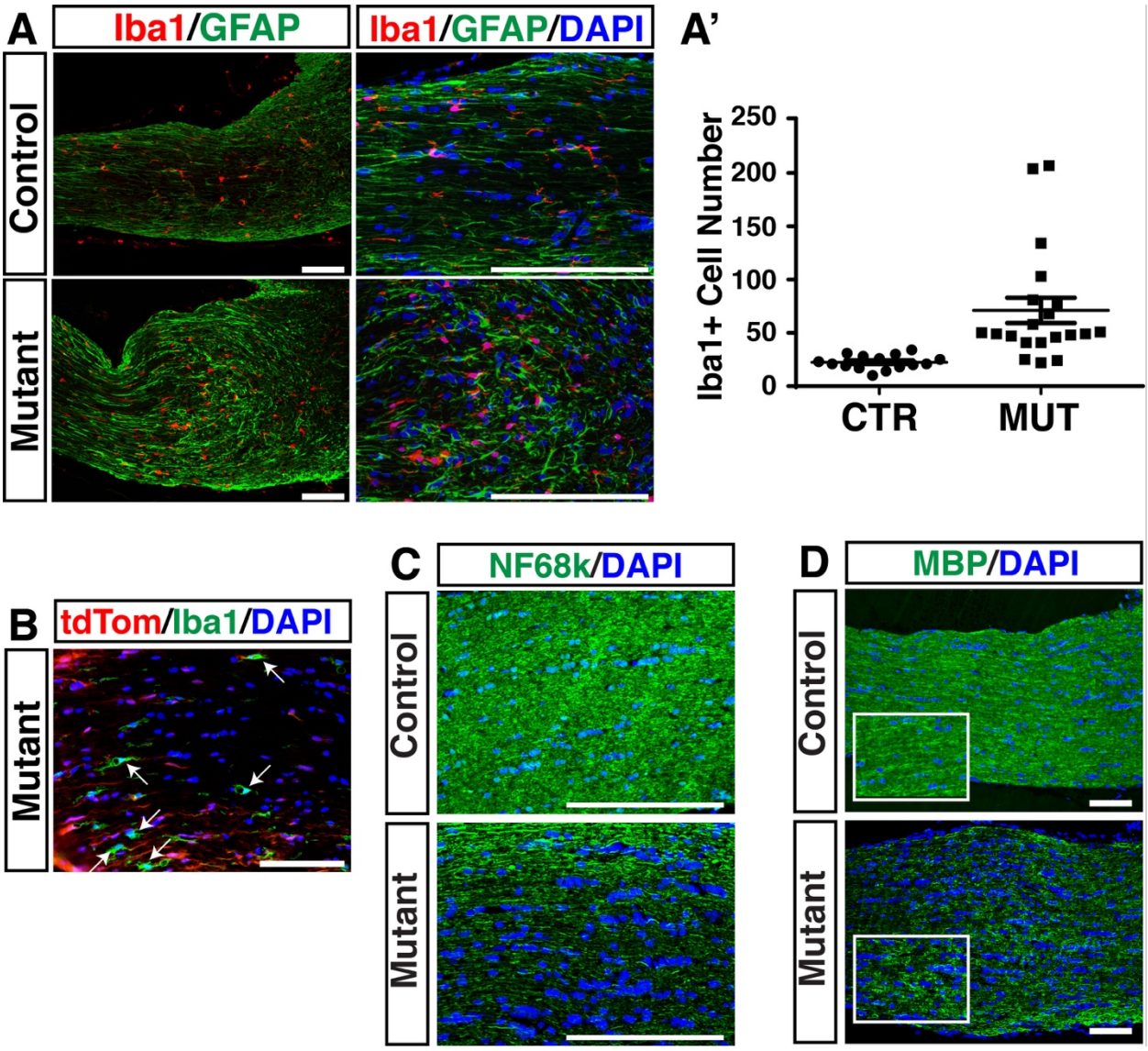

Figure 4. Late-stage OPG in *Nf1*^{hGFAP}CKOs is characterized by microglia infiltration and nerve damage.

Sections from optic nerves of control and *Nf1*^{hGFAP}CKO mice at 6 months of age or older were fluorescently labeled by anti-Iba1 (a marker for microglia) and anti-GFAP to show immune cell infiltration and activation in tumor **(A)**. Quantification of Iba^{+} cells show significant increase in late-stage OPG **(A')**. Immunostaining of distal nerve for Iba1 and tdTomato reporter revealed that microglia are not a target for cre recombination in *Nf1*^{hGFAP}CKO mice (arrows, non-recombined Iba1^{+} cells) **(B)**. Neurofilament staining (anti-NF68K) and myelin staining (anti-MBP) highlight the axonal and myelin defects in longitudinal sections of the prechiasmatic optic in tumor-bearing *Nf1* mutants **(C, D)**. All the data are presented as mean ± SEM. Scale bars: 5, 20 μm.

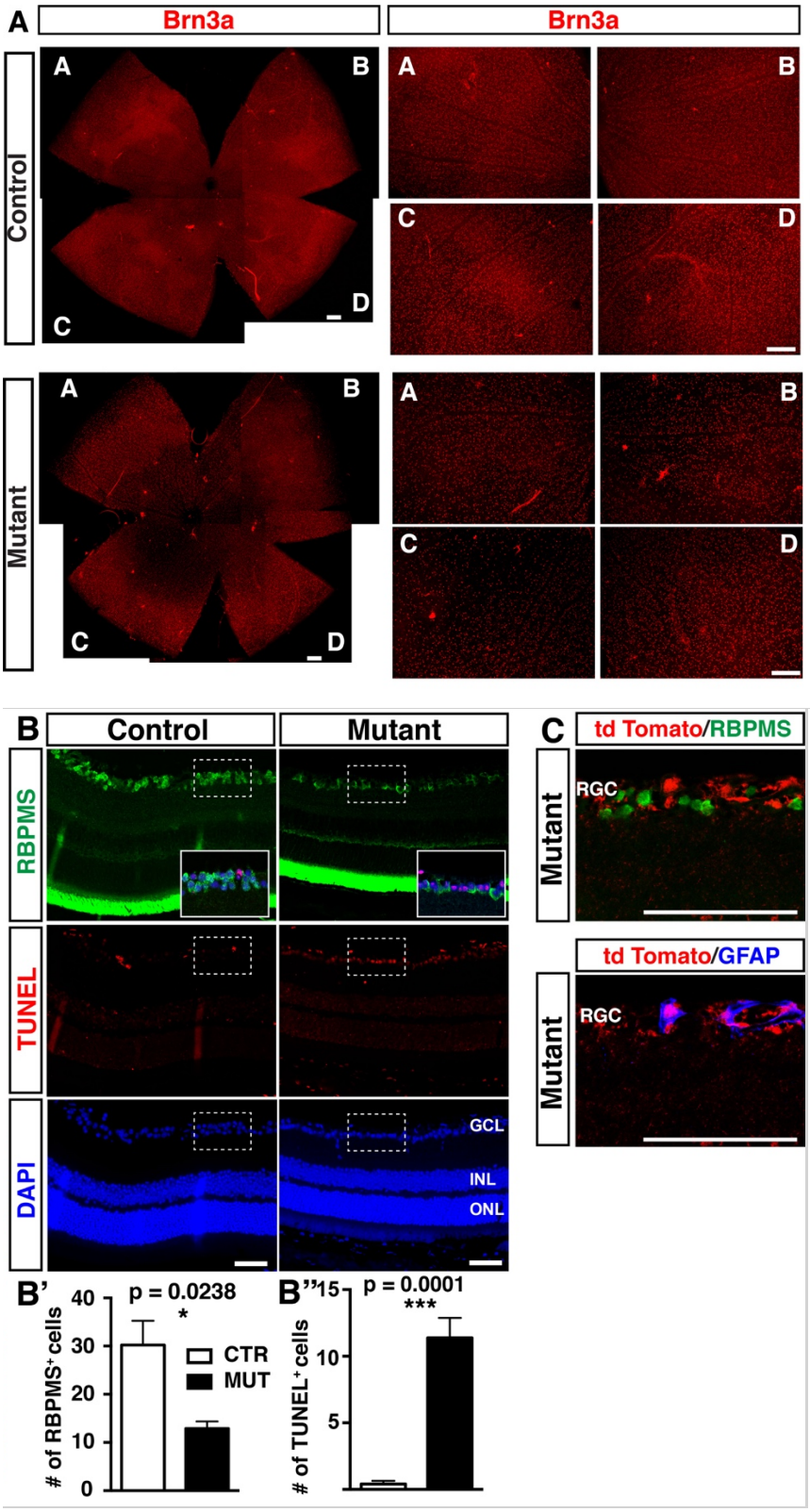
A
Brn3a
Brn3a
Control
Mutant
A
B
C
D
B
Control
Mutant
RBPMS
TUNEL
DAPI
GCL
INL
ONL
C
td Tomato/RBPMS
td Tomato/GFAP
RGC
Mutant
B'
p = 0.0238
*
CTR
MUT
# of RBPMS+ cells
B''
p = 0.0001
***
# of TUNEL+ cells

Figure 5. Retinal ganglion cell death in *Nf1*^{hGFAP}CKOs is non-cell autonomous.

Retinal flat-munts from littermate control and *Nf1* mutant retinas were stained for Brn3a to identify RGC somata (*red dots*) (**A**). Sections of retinas from controls and *Nf1* mutants with OPGs were doubly labeled by RBPMS (a marker for RGCs) and TUNEL (for apoptosis) **(B)**. The number of RGCs **(B')** and apoptotic cells in the RGC layer **(B")** were quantified for control and mutant mice. Inserts show apoptosis in the GCL. Immunostaining of retinas from *Nf1*^{hGFAP}CKO; tdTomato reporter mice demonstrates that recombination occurred in GFAP^{+} astrocytes, but not in RGCs **(C)**. All the data are presented as mean ± SEM. Scale bars: 2, 5 and 20 μm.

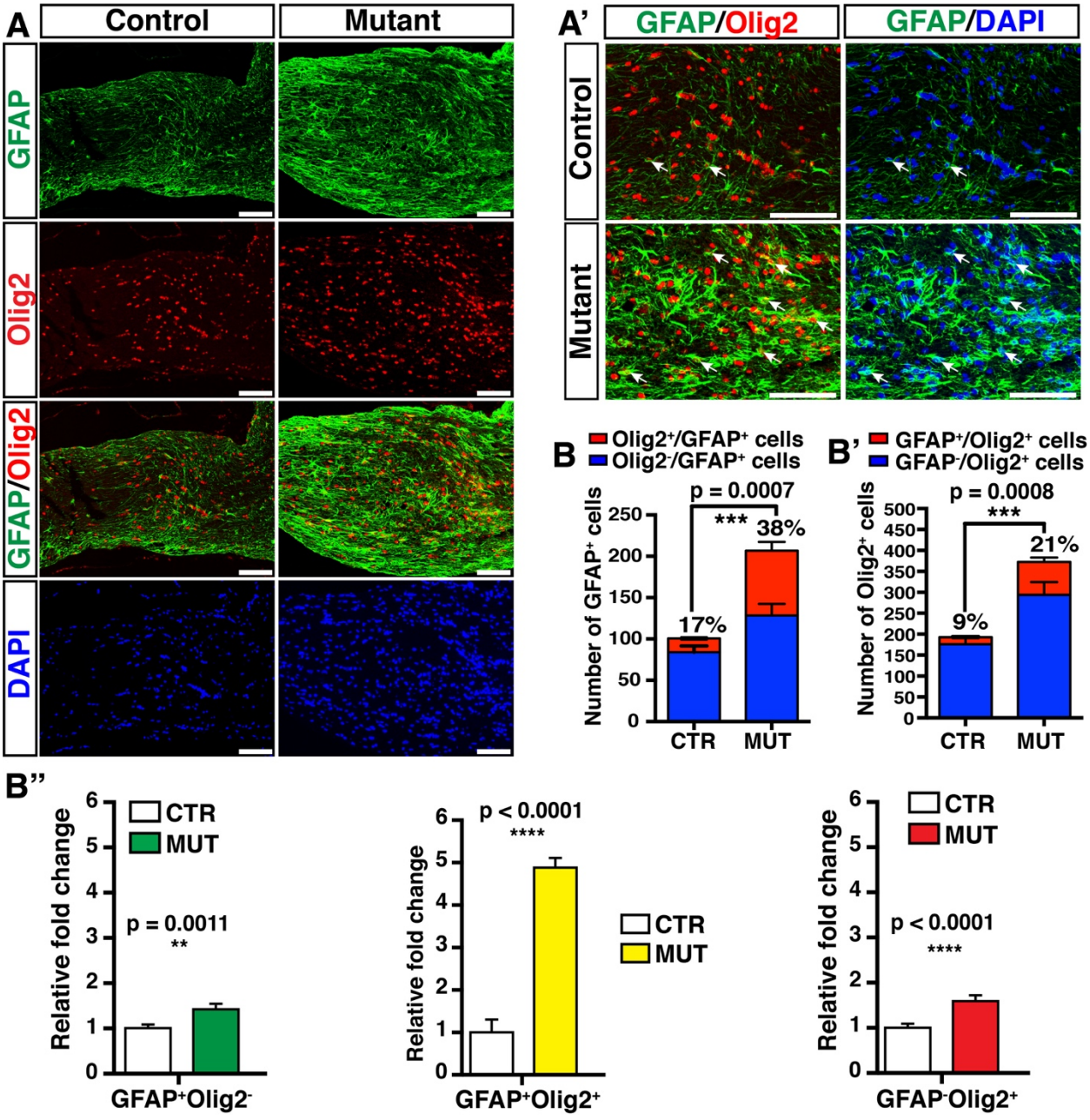
A
Control
Mutant
GFAP
Olig2
GFAP/Olig2
DAPI
A'
GFAP/Olig2
GFAP/DAPI
Control
Mutant
B
Olig2+/GFAP+ cells
Olig2-/GFAP+ cells
Number of GFAP+ cells
p = 0.0007
***
38%
17%
CTR
MUT
B'
GFAP+/Olig2+ cells
GFAP-/Olig2+ cells
Number of Olig2+ cells
p = 0.0008
***
21%
9%
CTR
MUT
B''
Relative fold change
CTR
MUT
p = 0.0011
**
GFAP+Olig2-
p < 0.0001
****
GFAP+Olig2+
p < 0.0001
****
GFAP-Olig2+

Figure 6. $GFAP^{+}Olig2^{+}$ cells underwent the biggest expansion in late-stage OPGs.

Representative images were taken from sections doubly stained with GFAP and Olig2 of control and mutant optic nerves at 6 months or older **(A)**. Arrows point to $GFAP^{+}Olig2^{+}$ cells **(A')**. The number and percentage of each of the 3 cell populations with different GFAP and Olig2 expression were quantified (**B**, **B')**. The 3 cellular compartments $GFAP^{+}Olig2^{-}$ cells, $GFAP^{+}Olig2^{+}$ cells and $GFAP^{-}Olig2^{+}$ cells were plotted as relative fold change (mutant/control) **(B")**. All the data are presented as mean ± SEM. Scale bars: 5 and 20 μm.

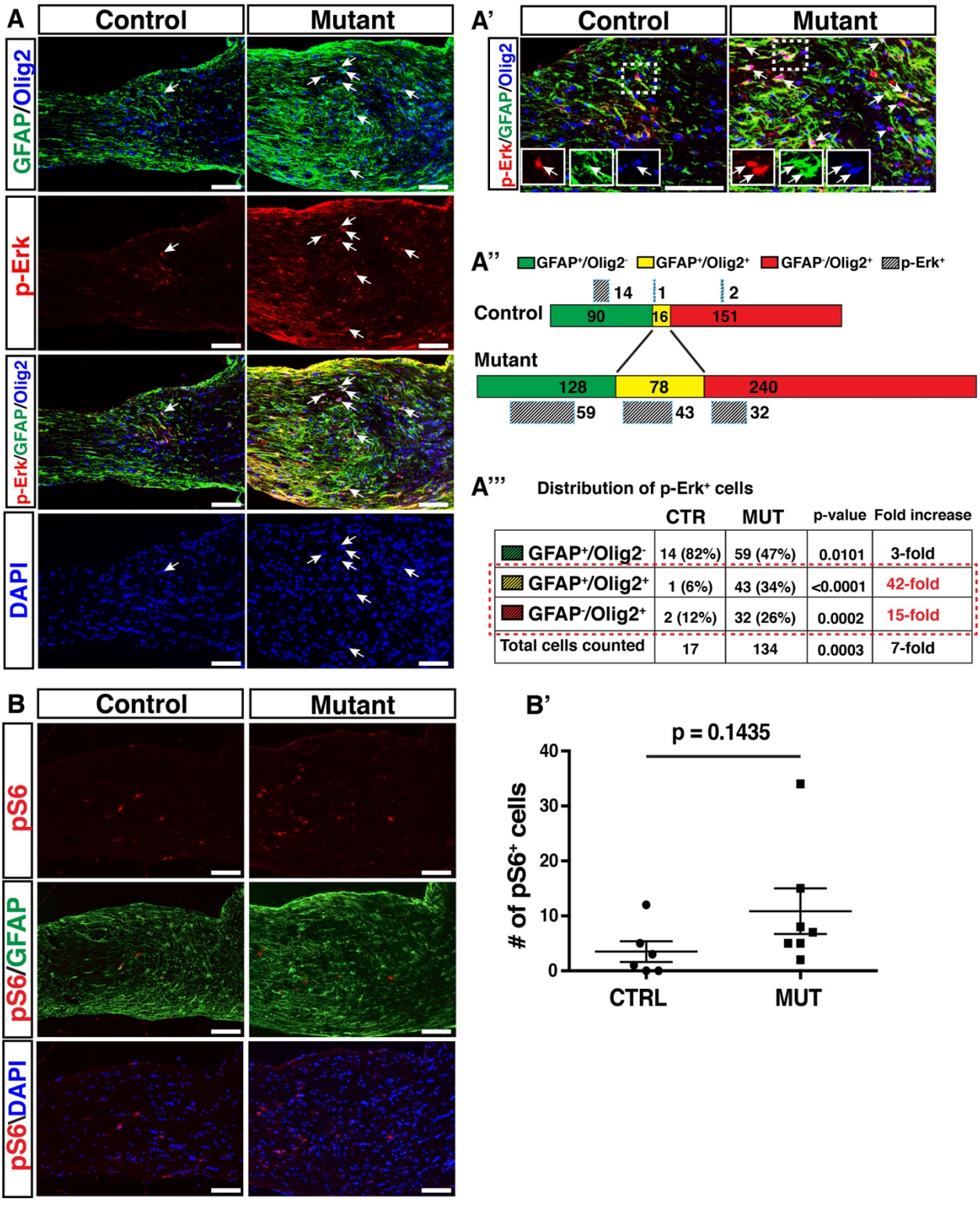
A
Control
Mutant
GFAP/Olig2
p-Erk
p-Erk/GFAP/Olig2
DAPI
A'
Control
Mutant
p-Erk/GFAP/Olig2
A''
GFAP+/Olig2-
GFAP+/Olig2+
GFAP-/Olig2+
p-Erk+
14
1
2
Control
90
16
151
Mutant
128
78
240
59
43
32
A'''
Distribution of p-Erk+ cells
CTR
MUT
p-value
Fold increase
GFAP+/Olig2-
14 (82%)
59 (47%)
0.0101
3-fold
GFAP+/Olig2+
1 (6%)
43 (34%)
<0.0001
42-fold
GFAP-/Olig2+
2 (12%)
32 (26%)
0.0002
15-fold
Total cells counted
17
134
0.0003
7-fold
B
Control
Mutant
pS6
pS6/GFAP
pS6\DAPI
B'
p = 0.1435
# of pS6+ cells
40
30
20
10
0
CTRL
MUT

Figure 7. *Nf1*-deficiency leads to specific p-Erk activation in GFAP$^+$Olig2$^+$ cells and GFAP$^-$ Olig2$^+$ cells.

Triple labeling p-Erk/Olig2/GFAP staining was performed on prechiasmatic optic nerve sections from aged *Nf1*^{hGFAP}CKO mice and their littermate controls **(A)**. Higher magnification view of the images in (A). Arrows indicate p-Erk$^+$/Olig2$^+$/GFAP$^+$ cells. Notice high expression of all 3 markers in triple-positive cells in the mutant OPGs **(A')**. Quantification and characterization of p-Erk$^+$ cells based on their expression of GFAP only (green), both GFAP and Olig2 (yellow), Olig2 only (red) **(A")**. Table of distribution of p-Erk$^+$ cells quantified in (A") demonstrate that triple-positive cells underwent the most dramatic increase (42-fold) between controls and age-matched *Nf1*^{hGFAP}CKO mice. p-S6 and GFAP double-labeling **(B)** and quantification **(B')** revealed that mTORC1 signaling pathway was not significantly activated in late-stage OPGs. Scale bars: 5, 20 μm. All the data are presented as mean ± SEM.

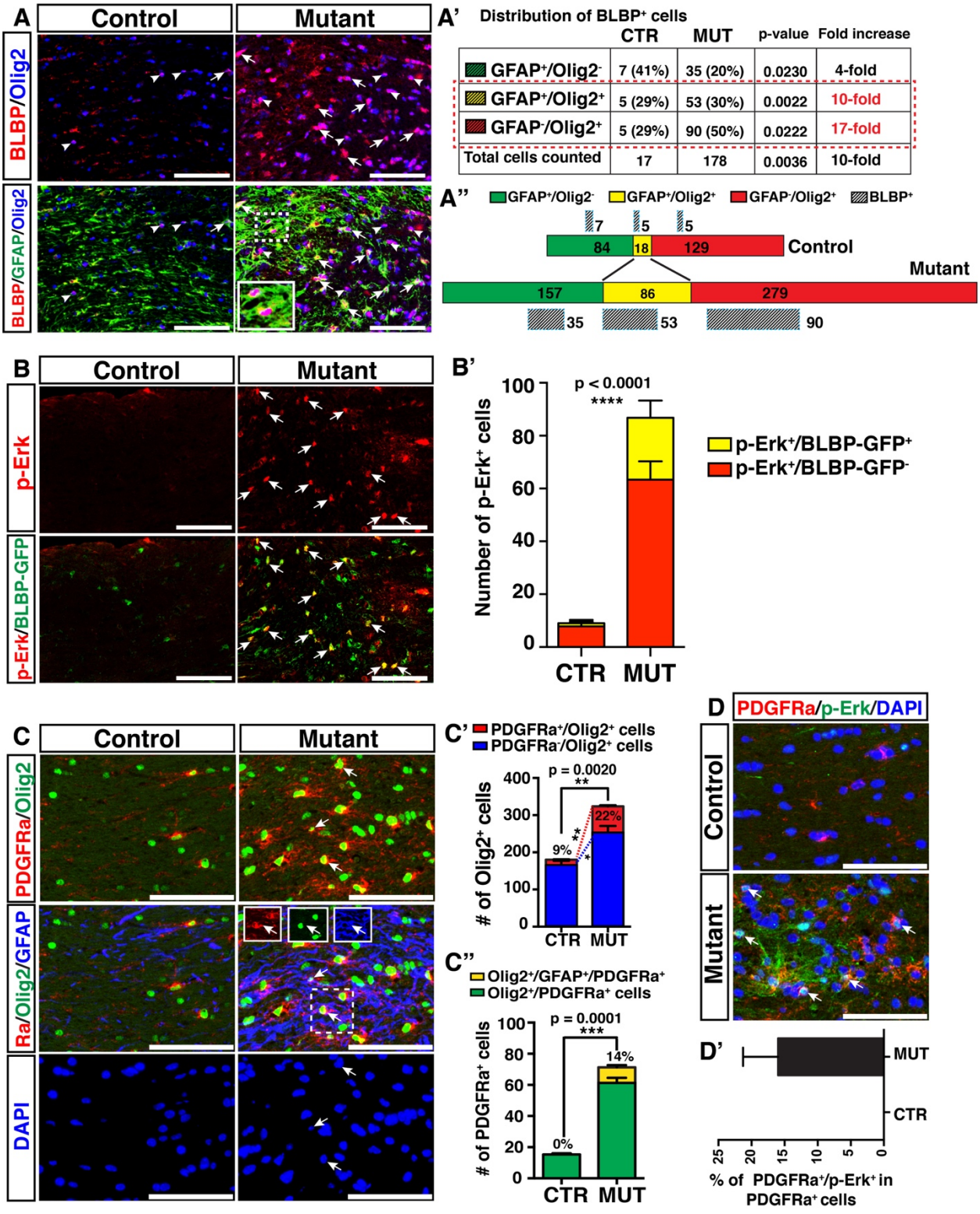
A
Control
Mutant
BLBP/Olig2
BLBP/GFAP/Olig2
A'
Distribution of BLBP+ cells
CTR
MUT
p-value
Fold increase
GFAP+/Olig2-
7 (41%)
35 (20%)
0.0230
4-fold
GFAP+/Olig2+
5 (29%)
53 (30%)
0.0022
10-fold
GFAP-/Olig2+
5 (29%)
90 (50%)
0.0222
17-fold
Total cells counted
17
178
0.0036
10-fold
A''
GFAP+/Olig2-
GFAP+/Olig2+
GFAP-/Olig2+
BLBP+
7
5
5
84
18
129
Control
Mutant
157
86
279
35
53
90
B
Control
Mutant
p-Erk
p-Erk/BLBP-GFP
B'
p < 0.0001
****
Number of p-Erk+ cells
p-Erk+/BLBP-GFP+
p-Erk+/BLBP-GFP-
CTR
MUT
C
Control
Mutant
PDGFRa/Olig2
Ra/Olig2/GFAP
DAPI
C'
PDGFRa+/Olig2+ cells
PDGFRa-/Olig2+ cells
p = 0.0020
**
# of Olig2+ cells
9%
22%
CTR
MUT
C''
Olig2+/GFAP+/PDGFRa+
Olig2+/PDGFRa+ cells
p = 0.0001
***
# of PDGFRa+ cells
0%
14%
CTR
MUT
D
PDGFRa/p-Erk/DAPI
Control
Mutant
D'
MUT
CTR
% of PDGFRa+/p-Erk+ in PDGFRa+ cells

Figure 8. *Nf1* loss causes Erk-dependent persistence of glial-restricted progenitor cells in late-stage OPGs.

Triple labeling immunofluorescence with glial progenitor marker BLBP and GFAP and Olig2. Arrowheads indicate $BLBP^+Olig2^+$ cells and arrows point to triple-positive $BLBP^+/Olig2^+/GFAP^+$ cells **(A)**. Quantification and characterization of $BLBP^+$ cells based on their expression of GFAP only (green), both GFAP and Olig2 (yellow), Olig2 only (red) revealed that the $Olig2^+$ population had the most dramatic increase, either through $GFAP^+Olig2^+$ cells or (10-fold) or $Olig2^+$ only cells (17-fold) within $BLBP^+$ cells **(A', A")**. Characterization of p-Erk expression in $BLBP^+$ cells tagged with the GFP reporter **(B)**. Arrows indicate $BLBP^+$ cells that activate p-Erk. Co-localization between p-Erk and GFP-BLBP was rarely detected in controls nerves but nearly 1/3 of p-Erk^+ cells in the gliomas were $BLBP^+$ progenitors **(B')**. Triple labeling immunofluorescence with OPC marker PDGFRα and GFAP and Olig2. Inserts and arrows indicate triple-positive cells that are exclusively found in the mutants **(C)**. Quantification of $Olig2^+$ and $PDGFR\alpha^+$ cells showed a greater than 2-fold increase in the percentage of OPCs in the late-stage OPGs **(C')**. Quantification of $PDGFR\alpha^+$ cells revealed a *de novo* OPC population that abnormally co-express GFAP in *Nf1*^{hGFAP}CKO nerves **(C")**. Double-labeling for PDGFRα and p-Erk show that 15% of tumor OPCs express p-Erk (arrows, $PDGFR\alpha^+$/p-Erk^+ cells) **(D, D')**. All the data are presented as mean ± SEM. Scale bars: 20, 50 μm.

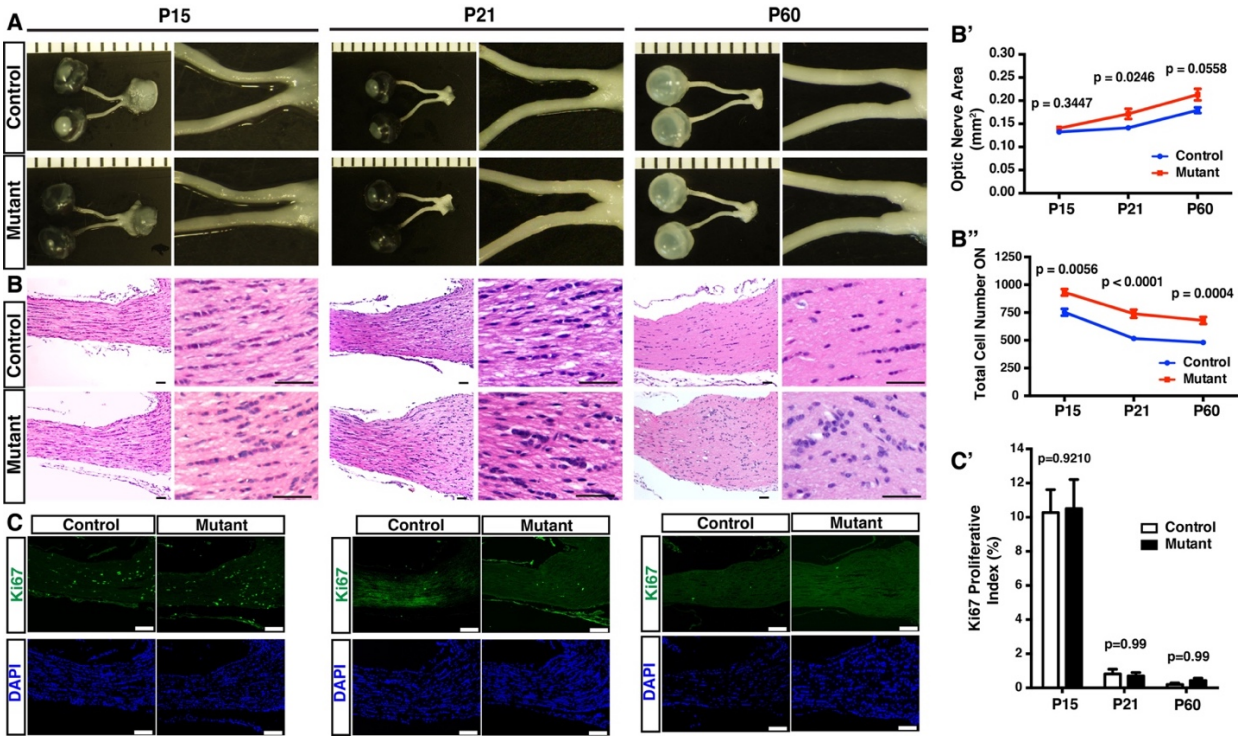

Figure 9. Expansion of glial cells in optic nerves of *Nf1*^{hGFAP}CKO mice is largely established during neonatal stages.

Whole-mount images from *Nf1*^{hGFAP}CKO and control prechiasmatic optic nerves at different ages: P15, P21, P60 show evidence of nerve enlargement at P21 **(A)**. Sections from control and mutant optic nerves were stained with H&E at the 3 time-points **(B)** and quantified to illustrate significant increase in nerve diameter at P21 and cellularity at P15 in mutant nerves compared to age-matched controls **(B', B")**. Comparison of the time course of proliferation in optic nerves illustrate that after P15, the proliferation levels decrease significantly, though the proliferation rate remains similar between control and mutant nerves at all time points. All the data are presented as mean ± SEM. Scale bars, 1 mm, 5 and 50 μm.

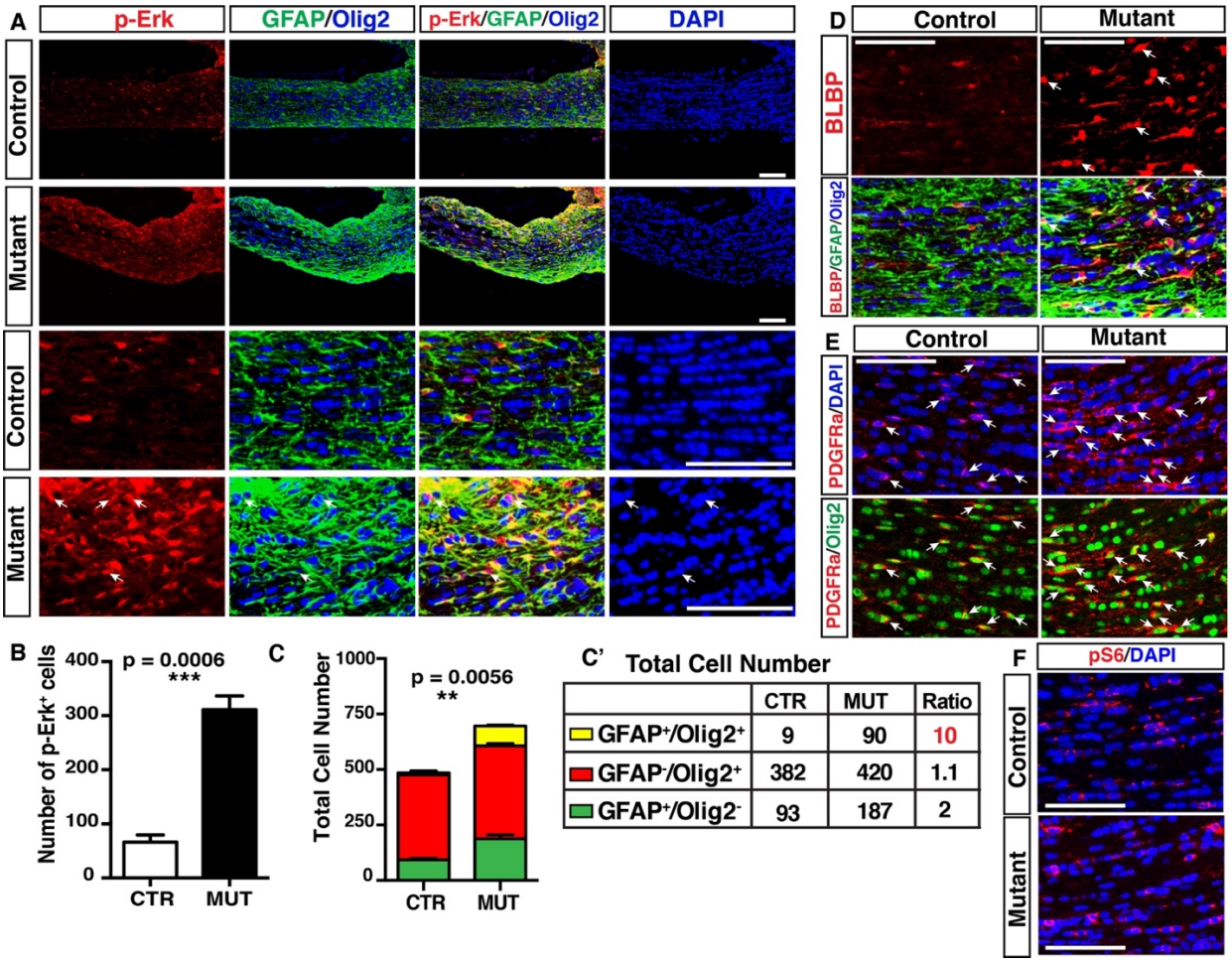

	CTR	MUT	Ratio
GFAP+/Olig2+	9	90	10
GFAP-/Olig2+	382	420	1.1
GFAP+/Olig2-	93	187	2

Figure 10. Abnormal glial specification and activation of RAS-Erk signaling pathway in P15 *Nf1*^{hGFAP}CKO optic nerves.

Triple labeling p-Erk/Olig2/GFAP staining was performed on prechiasmatic optic nerve sections from P15 *Nf1*^{hGFAP}CKO mice and their littermate controls **(A)**. Arrows point to triple-positive p-Erk^{+}/Olig2^{+}/GFAP^{+} cells. Mutants nerves contain more three times the number of p-Erk^{+} cells compared to controls **(B)**. Quantification and distribution of the 3 cell compartments GFAP^{+}Olig2^{-} (green), GFAP^{-}Olig2^{+} (red) and GFAP^{+}Olig2^{+} (yellow) cells revealed that GFAP^{+}Olig2^{+} cells displayed the most dramatic increase as early as P15 **(C, C')**. BLBP^{+} glial progenitors are expanded at P15 and co-localize with abnormal GFAP^{+}Olig2^{+} cells in the mutant nerves **(D)**. Double-labeling PDGFRα and Olig2 staining showed early expansion of OPCs **(E)**. Staining for pS6 show no significant overactivation of the signaling pathway in P15 *Nf1* mutant nerves **(F)**. All the data are presented as mean ± SEM. Scale bars: 5 and 50 μm.

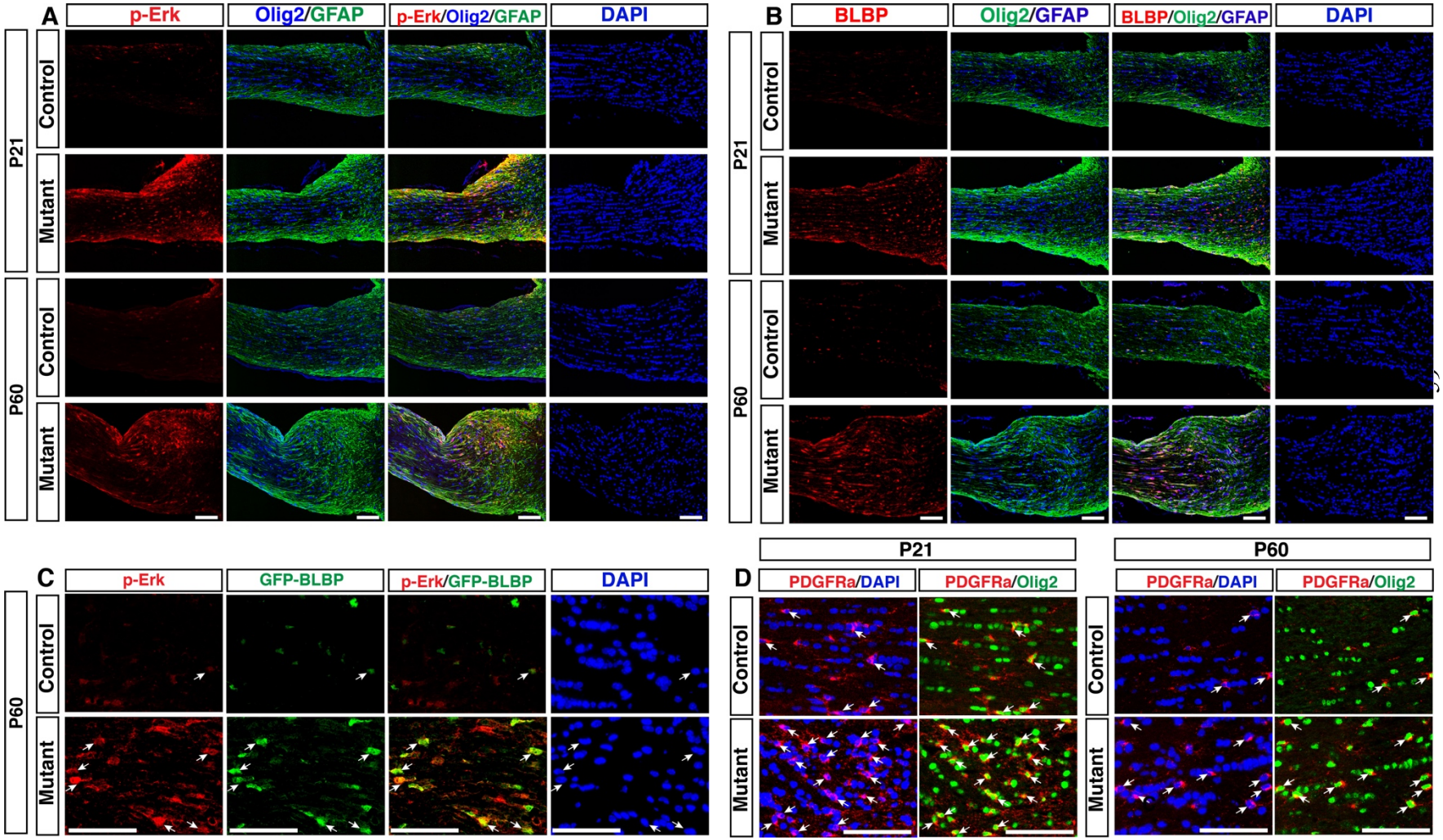
A
p-Erk
Olig2/GFAP
p-Erk/Olig2/GFAP
DAPI
P21
P60
Control
Mutant
B
BLBP
Olig2/GFAP
BLBP/Olig2/GFAP
DAPI
C
p-Erk
GFP-BLBP
p-Erk/GFP-BLBP
DAPI
D
P21
P60
PDGFRa/DAPI
PDGFRa/Olig2

Figure 11. Erk activation and glial abnormalities persist throughout gliomagenesis.
Triple labeling p-Erk/Olig2/GFAP staining was performed on prechiasmatic optic nerve sections from P21 and P60 *Nf1*^{hGFAP}CKO mice and their littermate controls **(A)**. Triple labeling immunofluorescence with glial progenitor marker BLBP and GFAP and Olig2 was performed at the same time-points **(B)**. p-Erk and BLBP co-labeling at P60 revealed that glial progenitors upregulate the MAPK pathway in mutants **(C)**. Staining of the number of prechiasmatic optic nerve sections with PDGFRα and Olig2 showed that OPCs decreased from P21 to P60 in both control and mutant nerves, but there was a greater number OPCs in mutants compared to controls in both time-points **(D)**. Scale bars: 5 and 50 μm.

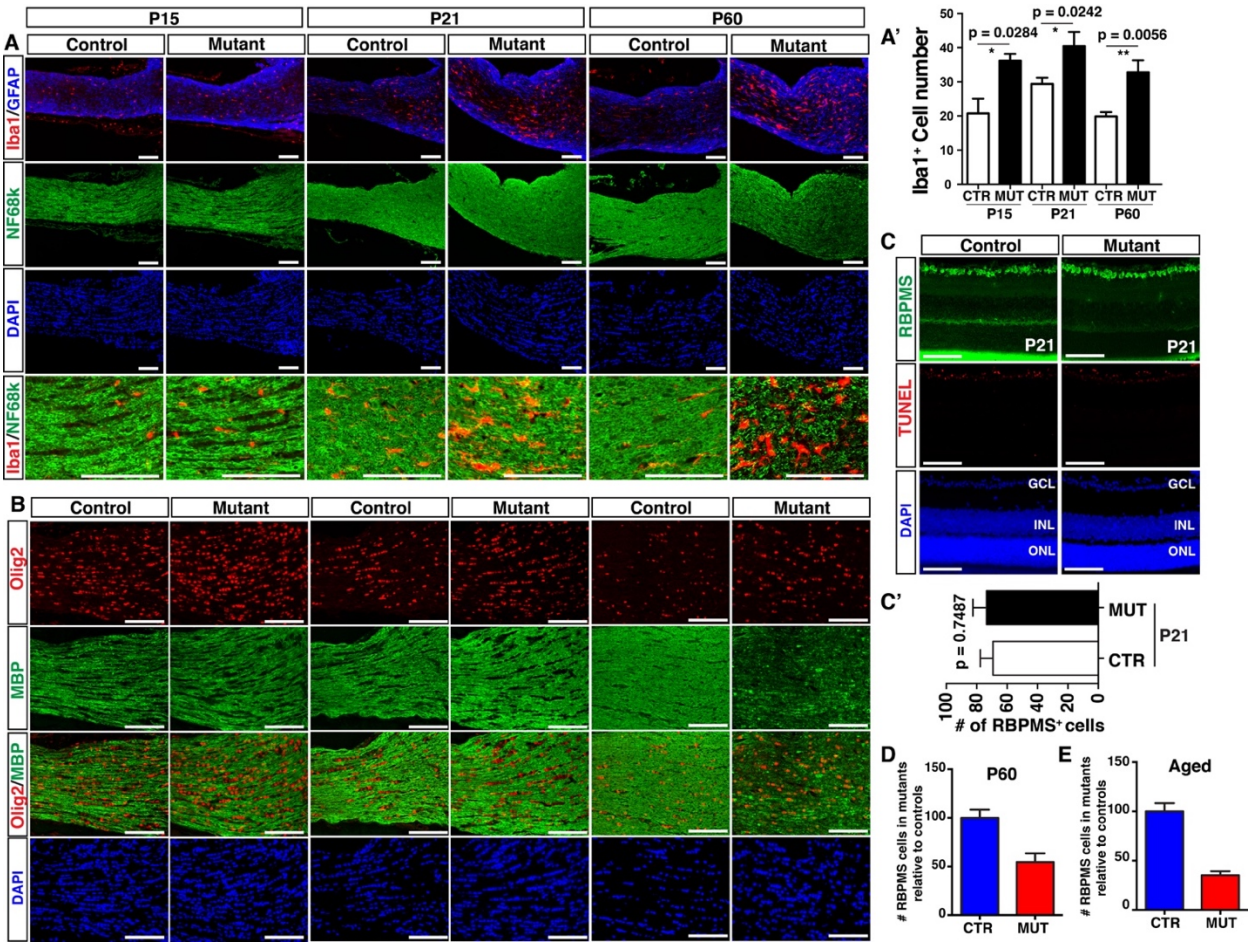

Figure 12. The second phase of *Nf1*-OPG disease pathogenesis involves optic nerve dysfunction and neuronal loss.

Sections from optic nerves of control and *Nf1*^{hGFAP}CKO mice at P15, P21 and P60 were fluorescently labeled with Iba1, NF68K and GFAP antibodies to study the time-course for optic nerve dysfunction **(A)**. Although the increase in microglia infiltration was noticed already at P15 **(A')**, they did not adopt an activated morphology with thickened processes until P21 **(A)**. Olig2 and MBP double-labeling staining at all 3 time-points demonstrate that myelin alteration did not become evident until P60 **(B)**. Staining for RBPMS and TUNEL show no increase in apoptosis or RGC loss in P21 *Nf1*^{hGFAP}CKO retinas **(C, C')**. The number of RBPMS cells in the mutant retinas relative to controls was quantified and showed progressive RGC loss over time **(D, E)**. DAPI labels for nuclei. All the data are presented as mean ± SEM. Scale bars: 5, 20 and 50 μm.

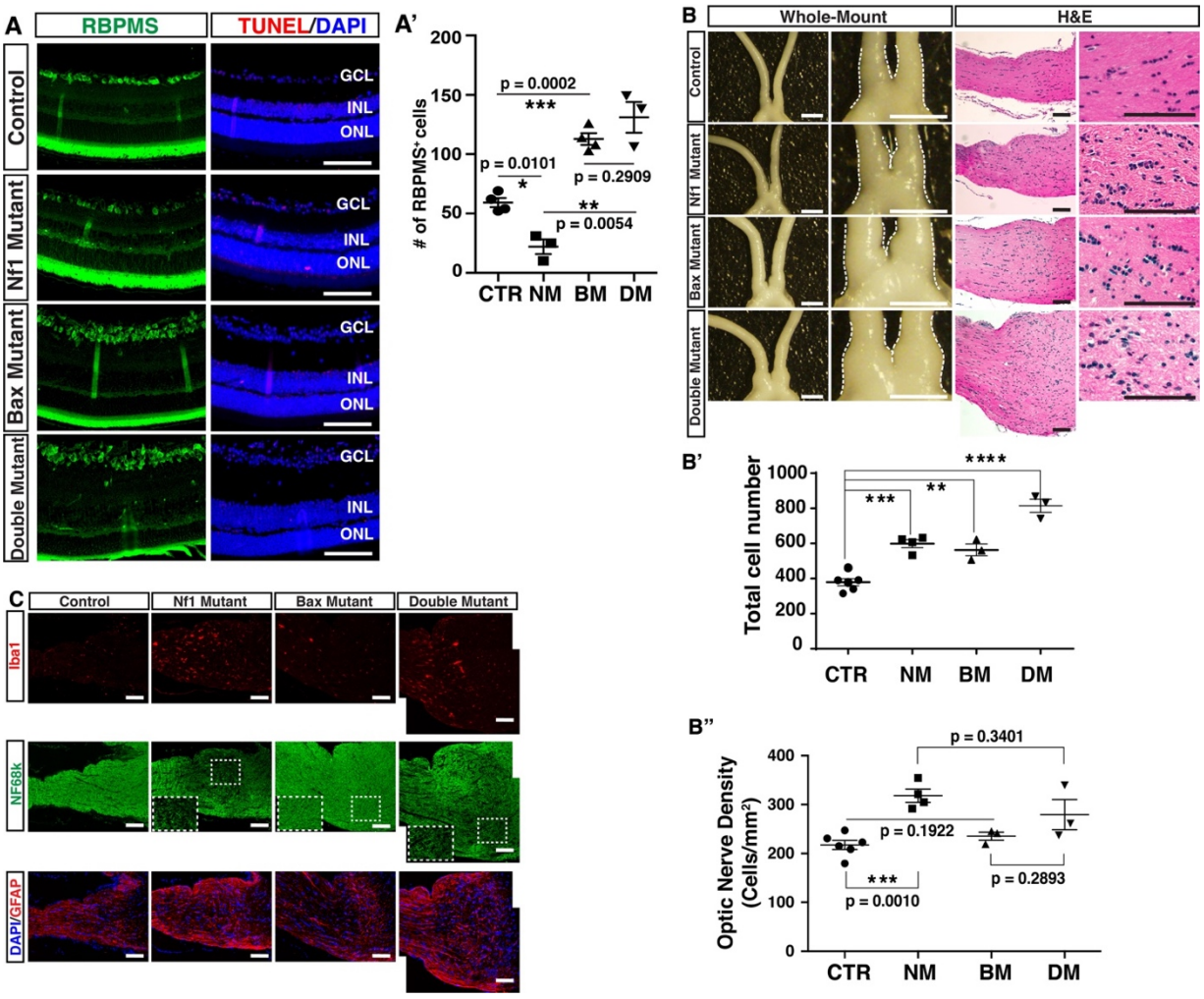

Figure 13. *Bax*-mediated apoptosis underlies progressive RGC loss in *Nf1*^{hGFAP}CKO mice. Sections of retinas from 4-month old controls and *Nf1* mutants (NM), *Bax* mutants (BM) and *Nf1*-*Bax* double mutants (DM) were doubly labeled by RBPMS and TUNEL **(A)**. The number of RGCs in the RGC layer were quantified **(A')**. Whole mount optic nerves from control and the 3 mutant genotypes were dissected and imaged under the dissection microscope, then sections from the optic nerves were stained with H&E **(B)**. Both BM and DM displayed noticeable increase in thickness throughout the whole length of the optic nerves. The total cell number and optic nerve density of controls and all 3 mutants were quantified. **(B', B")**. Triple labeling with Iba1, NF68K and GFAP show increased microglia infiltration and nerve damage in NM and DM, but not in BM **(C)**. All the data are presented as mean ± SEM. Scale bars: 5, 20 and 50 μm.

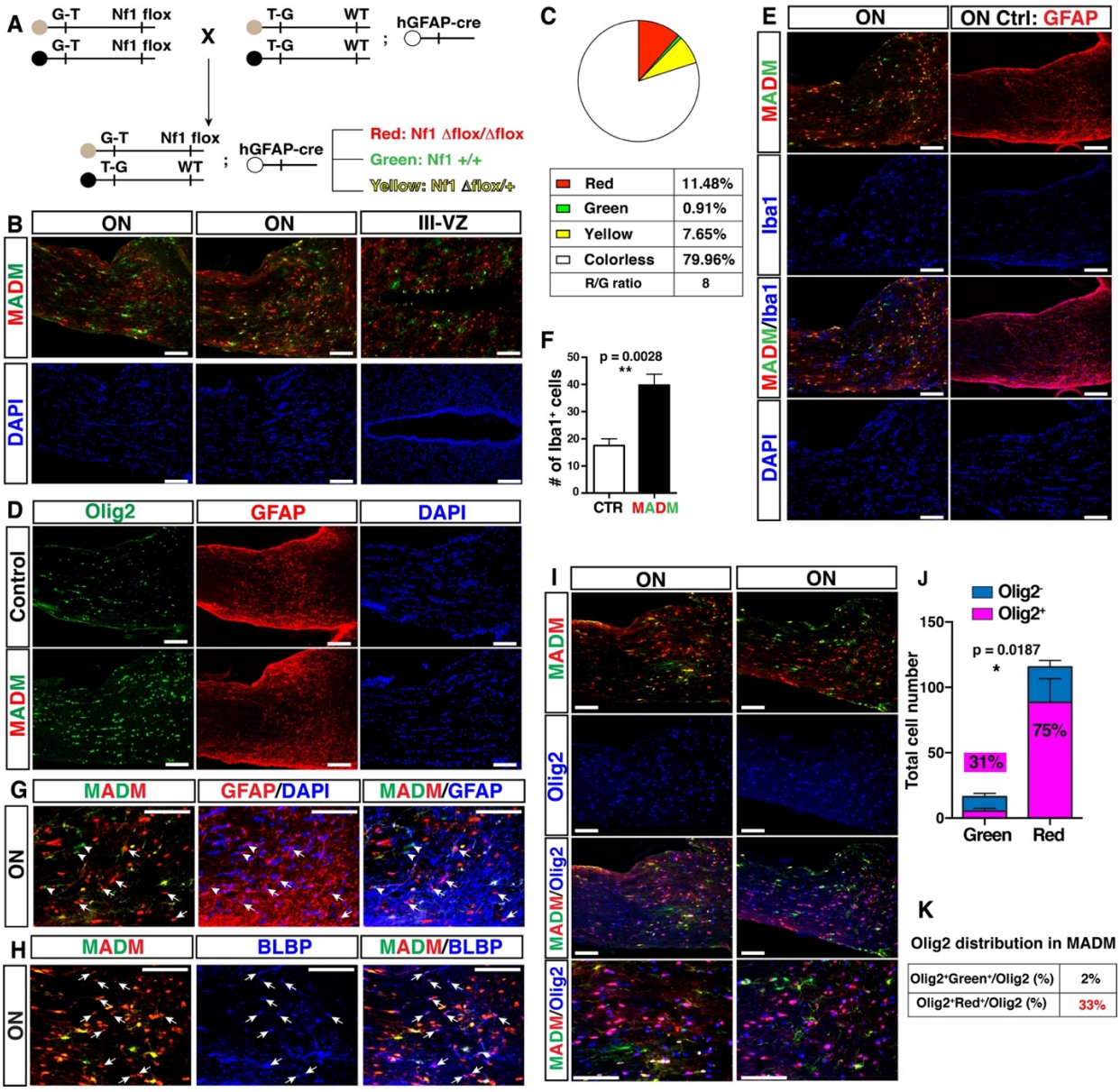
A
G-T Nf1 flox
G-T Nf1 flox
X
T-G WT
T-G WT
; hGFAP-cre
G-T Nf1 flox
T-G WT
; hGFAP-cre
Red: Nf1 Δflox/Δflox
Green: Nf1 +/+
Yellow: Nf1 Δflox/+
B
ON
ON
III-VZ
MADM
DAPI
C
Red 11.48%
Green 0.91%
Yellow 7.65%
Colorless 79.96%
R/G ratio 8
E
ON
ON Ctrl: GFAP
MADM
Iba1
MADM/Iba1
DAPI
F
p = 0.0028
**
# of Iba1+ cells
CTR MADM
D
Olig2
GFAP
DAPI
Control
MADM
G
MADM
GFAP/DAPI
MADM/GFAP
ON
H
MADM
BLBP
MADM/BLBP
ON
I
ON
ON
MADM
Olig2
MADM/Olig2
MADM/Olig2
J
Olig2-
Olig2+
p = 0.0187
*
Total cell number
31%
75%
Green
Red
K
Olig2 distribution in MADM
Olig2+Green+/Olig2 (%) 2%
Olig2+Red+/Olig2 (%) 33%

Figure 14. MADM-based lineage tracing reveals that *Nf1* loss confers growth advantage to Olig2$^+$ cells.

Scheme of MADM-based mouse model under the hGFAP-cre promoter illustrates how MADM concurrently mutates and labels cells **(A)**. Representative images from longitudinal sections of the prechiasmatic optic nerve and the III-VZ of P60 MADM mutants **(B)**. Distribution of the red, green yellow and colorless cells and quantification of the R/G ratio in P60 MADM mutants **(C)**. Olig2 and GFAP staining in MADM mutants shows increase in Olig2 and disorganized GFAP pattern compared to age-matched controls **(D)**. Iba1$^+$ microglia are not targeted by cre recombination in the MADM system **(E)**, but the number of immune cells is doubled compared to controls **(F)**. Staining of GFAP together with MADM shows distribution of astrocytes within red and green cells **(G)**. Arrowheads point to GFAP$^+$ cells expressing green label and arrows point to those expressing red label. BLBP staining with MADM shows the majority of BLBP glial progenitors are *Nf1* mutants (arrows) **(H)**. Compared to green wild-type cells where Olig2 accounted only for 31% of the cells, Olig2$^+$ cells were overexpanded in mutant cells (75%) **(I, J)**. Table representative of the increase in the percentage of mutant Olig2 (red) vs control Olig2 (green) within the oligodendrocyte lineage **(K)**. Four MADM mutants were analyzed at P60. All the data are presented as mean ± SEM. Scale bars: 5, 20 and 50 μm.

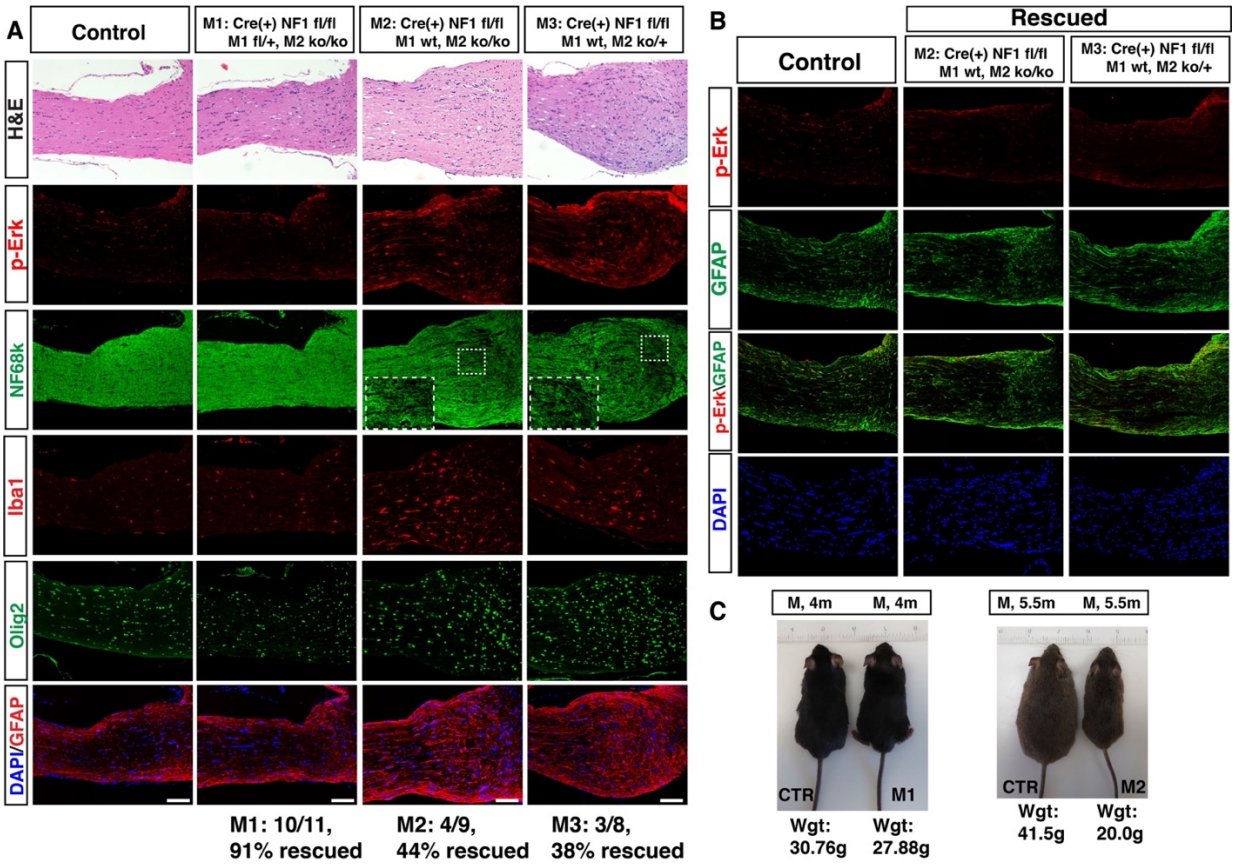

Figure 15. Dose-dependent genetic inactivation of *Mek1/2* prevents OPG formation in *Nf1*^{hGFAP}CKO mice

Adjacent sections of prechiasmatic optic nerves at 4-8 months of age from controls, M1 (1 remaining wild-type *MEK1/2* allele), M2 (2 remaining wild-type *MEK1/2* alleles) and M3 (3 remaining wild-type *MEK1/2* alleles) mutants stained with H&E, p-Erk, NF68K, Iba1, Olig2 and GFAP to show the degree of OPG rescue with increasing number of *MEK1/2* allele deletion (M1: 10/11, 91% rescued; M2: 4/9, 44% rescued; M3: 3/8, 38% rescued) **(A)**. Rescued M2 and M3 mutants showed concurrent decrease in the number of p-Erk^{+} cells and GFAP^{+} astrocyte organization indistinguishable from controls **(B)**. Comparison between M1 and M2 and their age-matched, littermate controls reveal rescue in appearance and weight with 3-allele *MEK1/2* deletion (M1) **(C)**. Scale bars: 1 cm, 5 μm.

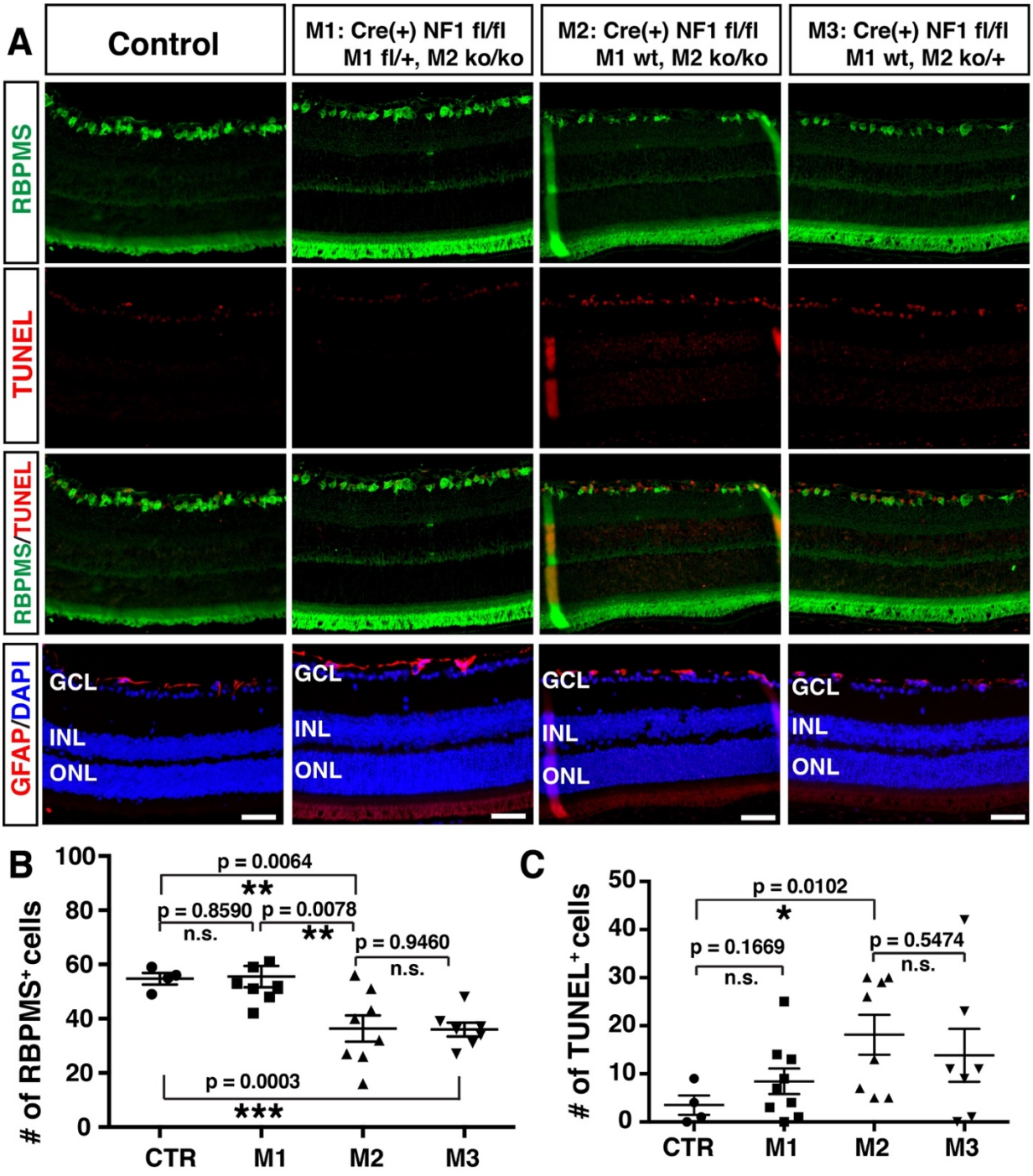

Figure 16. Dose-dependent neuronal protection with genetic inactivation of *Mek1/2*.

Representative cross-sections of control and M1, M2 and M3 retinas stained with RBPMS, TUNEL and GFAP **(A)**. The number of RGCs **(B)** and apoptotic cells in the RGC layer **(C)** were quantified for control and all 3 genotypes. All the data are presented as mean ± SEM. Scale bar: 20 μm.

2.4 References

Aguzzi, A., B. A. Barres, and M. L. Bennett. 2013. 'Microglia: scapegoat, saboteur, or something else?', *Science*, 339: 156-61.

Anthony, T. E., C. Klein, G. Fishell, and N. Heintz. 2004. 'Radial glia serve as neuronal progenitors in all regions of the central nervous system', *Neuron*, 41: 881-90.

Ater, J. L., C. Xia, C. M. Mazewski, T. N. Booth, D. R. Freyer, R. J. Packer, R. Sposto, G. Vezina, and I. F. Pollack. 2016. 'Nonrandomized comparison of neurofibromatosis type 1 and non-neurofibromatosis type 1 children who received carboplatin and vincristine for progressive low-grade glioma: A report from the Children's Oncology Group', *Cancer*, 122: 1928-36.

Ater, J. L., T. Zhou, E. Holmes, C. M. Mazewski, T. N. Booth, D. R. Freyer, K. H. Lazarus, R. J. Packer, M. Prados, R. Sposto, G. Vezina, J. H. Wisoff, and I. F. Pollack. 2012. 'Randomized study of two chemotherapy regimens for treatment of low-grade glioma in young children: a report from the Children's Oncology Group', *J Clin Oncol*, 30: 2641-7.

Avery, R. A., A. Cnaan, J. S. Schuman, C. Trimboli-Heidler, C. L. Chen, R. J. Packer, and H. Ishikawa. 2015. 'Longitudinal Change of Circumpapillary Retinal Nerve Fiber Layer Thickness in Children With Optic Pathway Gliomas', *Am J Ophthalmol*, 160: 944-52 e1.

Avery, R. A., A. Mansoor, R. Idrees, E. Biggs, M. A. Alsharid, R. J. Packer, and M. G. Linguraru. 2016. 'Quantitative MRI criteria for optic pathway enlargement in neurofibromatosis type 1', *Neurology*, 86: 2264-70.

Avery, R. A., A. Mansoor, R. Idrees, C. Trimboli-Heidler, H. Ishikawa, R. J. Packer, and M. G. Linguraru. 2016. 'Optic pathway glioma volume predicts retinal axon degeneration in neurofibromatosis type 1', *Neurology*, 87: 2403-07.

Bajenaru, M. L., J. R. Garbow, A. Perry, M. R. Hernandez, and D. H. Gutmann. 2005. 'Natural history of neurofibromatosis 1-associated optic nerve glioma in mice', *Ann Neurol*, 57: 119-27.

Bajenaru, M. L., M. R. Hernandez, A. Perry, Y. Zhu, L. F. Parada, J. R. Garbow, and D. H. Gutmann. 2003. 'Optic nerve glioma in mice requires astrocyte Nf1 gene inactivation and Nf1 brain heterozygosity', *Cancer Res*, 63: 8573-7.

Balcer, L. J., G. T. Liu, G. Heller, L. Bilaniuk, N. J. Volpe, S. L. Galetta, P. T. Molloy, P. C. Phillips, A. J. Janss, S. Vaughn, and M. G. Maguire. 2001. 'Visual loss in children with neurofibromatosis type 1 and optic pathway gliomas: relation to tumor location by magnetic resonance imaging', *Am J Ophthalmol*, 131: 442-5.

Ballester, R., D. Marchuk, M. Boguski, A. Saulino, R. Letcher, M. Wigler, and F. Collins. 1990. 'The NF1 locus encodes a protein functionally related to mammalian GAP and yeast IRA proteins', *Cell*, 63: 851-9.

Bao, S., Q. Wu, R. E. McLendon, Y. Hao, Q. Shi, A. B. Hjelmeland, M. W. Dewhirst, D. D. Bigner, and J. N. Rich. 2006. 'Glioma stem cells promote radioresistance by preferential activation of the DNA damage response', *Nature*, 444: 756-60.

Belanger, L. F., S. Roy, M. Tremblay, B. Brott, A. M. Steff, W. Mourad, P. Hugo, R. Erikson, and J. Charron. 2003. 'Mek2 is dispensable for mouse growth and development', *Mol Cell Biol*, 23: 4778-87.

Bennett, M. R., T. A. Rizvi, S. Karyala, R. D. McKinnon, and N. Ratner. 2003. 'Aberrant growth and differentiation of oligodendrocyte progenitors in neurofibromatosis type 1 mutants', *J Neurosci*, 23: 7207-17.

Bergthold, G., P. Bandopadhayay, W. L. Bi, L. Ramkissoon, C. Stiles, R. A. Segal, R. Beroukhim, K. L. Ligon, J. Grill, and M. W. Kieran. 2014. 'Pediatric low-grade gliomas: how modern biology reshapes the clinical field', *Biochim Biophys Acta*, 1845: 294-307.

Bertrand, V., C. Hudson, D. Caillol, C. Popovici, and P. Lemaire. 2003. 'Neural tissue in ascidian embryos is induced by FGF9/16/20, acting via a combination of maternal GATA and Ets transcription factors', *Cell*, 115: 615-27.

Bissonauth, V., S. Roy, M. Gravel, S. Guillemette, and J. Charron. 2006. 'Requirement for Map2k1 (Mek1) in extra-embryonic ectoderm during placentogenesis', *Development*, 133: 3429-40.

Bouvier, C., C. Bartoli, L. Aguirre-Cruz, I. Virard, C. Colin, C. Fernandez, J. Gouvernet, and D. Figarella-Branger. 2003. 'Shared oligodendrocyte lineage gene expression in gliomas and oligodendrocyte progenitor cells', *J Neurosurg*, 99: 344-50.

Brannan, C. I., A. S. Perkins, K. S. Vogel, N. Ratner, M. L. Nordlund, S. W. Reid, A. M. Buchberg, N. A. Jenkins, L. F. Parada, and N. G. Copeland. 1994. 'Targeted disruption of the neurofibromatosis type-1 gene leads to developmental abnormalities in heart and various neural crest-derived tissues', *Genes Dev*, 8: 1019-29.

Brown, A. P., T. C. Carlson, C. M. Loi, and M. J. Graziano. 2007. 'Pharmacodynamic and toxicokinetic evaluation of the novel MEK inhibitor, PD0325901, in the rat following oral and intravenous administration', *Cancer Chemother Pharmacol*, 59: 671-9.

Burkhard, C., P. L. Di Patre, D. Schuler, G. Schuler, M. G. Yasargil, Y. Yonekawa, U. M. Lutolf, P. Kleihues, and H. Ohgaki. 2003. 'A population-based study of the incidence and survival rates in patients with pilocytic astrocytoma', *J Neurosurg*, 98: 1170-4.

Chen, C., W. Ouyang, V. Grigura, Q. Zhou, K. Carnes, H. Lim, G. Q. Zhao, S. Arber, N. Kurpios, T. L. Murphy, A. M. Cheng, J. A. Hassell, V. Chandrashekar, M. C. Hofmann, R. A. Hess, and K. M. Murphy. 2005. 'ERM is required for transcriptional control of the spermatogonial stem cell niche', *Nature*, 436: 1030-4.

Chen, Y. H., S. M. Gianino, and D. H. Gutmann. 2015. 'Neurofibromatosis-1 regulation of neural stem cell proliferation and multilineage differentiation operates through distinct RAS effector pathways', *Genes Dev*, 29: 1677-82.

Chen, Y. H., L. D. McGowan, P. J. Cimino, S. Dahiya, J. R. Leonard, D. Y. Lee, and D. H. Gutmann. 2015. 'Mouse low-grade gliomas contain cancer stem cells with unique molecular and functional properties', *Cell Rep*, 10: 1899-912.

Cichowski, K., and T. Jacks. 2001. 'NF1 tumor suppressor gene function: narrowing the GAP', *Cell*, 104: 593-604.

Cin, H., C. Meyer, R. Herr, W. G. Janzarik, S. Lambert, D. T. Jones, K. Jacob, A. Benner, H. Witt, M. Remke, S. Bender, F. Falkenstein, T. N. Van Anh, H. Olbrich, A. von Deimling, A. Pekrun, A. E. Kulozik, A. Gnekow, W. Scheurlen, O. Witt, H. Omran, N. Jabado, V. P. Collins, T. Brummer, R. Marschalek, P. Lichter, A. Korshunov, and S. M. Pfister. 2011. 'Oncogenic FAM131B-BRAF fusion resulting from 7q34 deletion comprises an alternative mechanism of MAPK pathway activation in pilocytic astrocytoma', *Acta Neuropathol*, 121: 763-74.

Collins, V. P., D. T. Jones, and C. Giannini. 2015. 'Pilocytic astrocytoma: pathology, molecular mechanisms and markers', *Acta Neuropathol*, 129: 775-88.

Colman, S. D., C. A. Williams, and M. R. Wallace. 1995. 'Benign neurofibromas in type 1 neurofibromatosis (NF1) show somatic deletions of the NF1 gene', *Nat Genet*, 11: 90-2.

Coniglio, S. J., E. Eugenin, K. Dobrenis, E. R. Stanley, B. L. West, M. H. Symons, and J. E. Segall. 2012. 'Microglial stimulation of glioblastoma invasion involves epidermal growth factor receptor (EGFR) and colony stimulating factor 1 receptor (CSF-1R) signaling', *Mol Med*, 18: 519-27.

Cui, Y., R. M. Costa, G. G. Murphy, Y. Elgersma, Y. Zhu, D. H. Gutmann, L. F. Parada, I. Mody, and A. J. Silva. 2008. 'Neurofibromin regulation of ERK signaling modulates GABA release and learning', *Cell*, 135: 549-60.

Daginakatte, G. C., S. M. Gianino, N. W. Zhao, A. S. Parsadanian, and D. H. Gutmann. 2008. 'Increased c-Jun-NH2-kinase signaling in neurofibromatosis-1 heterozygous microglia drives microglia activation and promotes optic glioma proliferation', *Cancer Res*, 68: 10358-66.

Daginakatte, G. C., and D. H. Gutmann. 2007. 'Neurofibromatosis-1 (Nf1) heterozygous brain microglia elaborate paracrine factors that promote Nf1-deficient astrocyte and glioma growth', *Hum Mol Genet*, 16: 1098-112.

Dakubo, G. D., S. T. Beug, C. J. Mazerolle, S. Thurig, Y. Wang, and V. A. Wallace. 2008. 'Control of glial precursor cell development in the mouse optic nerve by sonic hedgehog from retinal ganglion cells', *Brain Res*, 1228: 27-42.

Dakubo, G. D., Y. P. Wang, C. Mazerolle, K. Campsall, A. P. McMahon, and V. A. Wallace. 2003. 'Retinal ganglion cell-derived sonic hedgehog signaling is required for optic disc and stalk neuroepithelial cell development', *Development*, 130: 2967-80.

Dasgupta, B., and D. H. Gutmann. 2005. 'Neurofibromin regulates neural stem cell proliferation, survival, and astroglial differentiation in vitro and in vivo', *J Neurosci*, 25: 5584-94.

Daston, M. M., H. Scrable, M. Nordlund, A. K. Sturbaum, L. M. Nissen, and N. Ratner. 1992. 'The protein product of the neurofibromatosis type 1 gene is expressed at highest abundance in neurons, Schwann cells, and oligodendrocytes', *Neuron*, 8: 415-28.

Dawson, M. R., A. Polito, J. M. Levine, and R. Reynolds. 2003. 'NG2-expressing glial progenitor cells: an abundant and widespread population of cycling cells in the adult rat CNS', *Mol Cell Neurosci*, 24: 476-88.

Diggs-Andrews, K. A., J. A. Brown, S. M. Gianino, J. B. Rubin, D. F. Wozniak, and D. H. Gutmann. 2014. 'Sex Is a major determinant of neuronal dysfunction in neurofibromatosis type 1', *Ann Neurol*, 75: 309-16.

Fangusaro, Jason, Arzu Onar-Thomas, Tina Y. Poussaint, Shengjie Wu, Azra H. Ligon, Neal Lindeman, Anu Banerjee, Roger J. Packer, Lindsay B. Kilburn, Ian F. Pollack, Regina I. Jakacki, Ibrahim Qaddoumi, Paul G. Fisher, Girish Dhall, Patricia Baxter, Susan G. Kreissman, Clinton F. Stewart, Stefan M. Pfister, David T. W. Jones, Gilbert Vezina, Jessica Stern, Ashok Panigrahy, Blaise V. Jones, Zoltan Patay, Benita Tamrazi, Jeremy Y. Jones, Sofia S. Haque, David S. Enterline, Soonmee Cha, Laurence A. Doyle, Malcolm Smith, James M. Boyett, Ira J. Dunkel, and Maryam Fouladi. 2017. 'LGG-08. A PHASE II PROSPECTIVE STUDY OF SELUMETINIB IN CHILDREN WITH RECURRENT OR REFRACTORY LOW-GRADE GLIOMA (LGG): A PEDIATRIC BRAIN TUMOR CONSORTIUM (PBTC) STUDY', *Neuro-Oncology*, 19: iv34-iv35.

Fisher, M. J., M. Loguidice, D. H. Gutmann, R. Listernick, R. E. Ferner, N. J. Ullrich, R. J. Packer, U. Tabori, R. O. Hoffman, S. L. Ardern-Holmes, T. R. Hummel, D. R. Hargrave, E. Bouffet, J. Charrow, L. T. Bilaniuk, L. J. Balcer, and G. T. Liu. 2012. 'Visual outcomes in

children with neurofibromatosis type 1-associated optic pathway glioma following chemotherapy: a multicenter retrospective analysis', *Neuro Oncol*, 14: 790-7.

Forshew, T., R. G. Tatevossian, A. R. Lawson, J. Ma, G. Neale, B. W. Ogunkolade, T. A. Jones, J. Aarum, J. Dalton, S. Bailey, T. Chaplin, R. L. Carter, A. Gajjar, A. Broniscer, B. D. Young, D. W. Ellison, and D. Sheer. 2009. 'Activation of the ERK/MAPK pathway: a signature genetic defect in posterior fossa pilocytic astrocytomas', *J Pathol*, 218: 172-81.

Freeman, C. R., J. P. Farmer, and J. Montes. 1998. 'Low-grade astrocytomas in children: evolving management strategies', *Int J Radiat Oncol Biol Phys*, 41: 979-87.

Fried, I., U. Tabori, T. Tihan, A. Reginald, and E. Bouffet. 2013. 'Optic pathway gliomas: a review', *CNS Oncol*, 2: 143-59.

Friedlander, M. 2007. 'Fibrosis and diseases of the eye', *J Clin Invest*, 117: 576-86.

Friedman, J. M. 1999. 'Epidemiology of neurofibromatosis type 1', *Am J Med Genet*, 89: 1-6.

Galli, R., E. Binda, U. Orfanelli, B. Cipelletti, A. Gritti, S. De Vitis, R. Fiocco, C. Foroni, F. Dimeco, and A. Vescovi. 2004. 'Isolation and characterization of tumorigenic, stem-like neural precursors from human glioblastoma', *Cancer Res*, 64: 7011-21.

Gao, L., and R. H. Miller. 2006. 'Specification of optic nerve oligodendrocyte precursors by retinal ganglion cell axons', *J Neurosci*, 26: 7619-28.

Geha, S., J. Pallud, M. P. Junier, B. Devaux, N. Leonard, F. Chassoux, H. Chneiweiss, C. Daumas-Duport, and P. Varlet. 2010. 'NG2+/Olig2+ cells are the major cycle-related cell population of the adult human normal brain', *Brain Pathol*, 20: 399-411.

Gilmartin, A. G., M. R. Bleam, A. Groy, K. G. Moss, E. A. Minthorn, S. G. Kulkarni, C. M. Rominger, S. Erskine, K. E. Fisher, J. Yang, F. Zappacosta, R. Annan, D. Sutton, and S. G. Laquerre. 2011. 'GSK1120212 (JTP-74057) is an inhibitor of MEK activity and activation with favorable pharmacokinetic properties for sustained in vivo pathway inhibition', *Clin Cancer Res*, 17: 989-1000.

Glover, T. W., C. K. Stein, E. Legius, L. B. Andersen, A. Brereton, and S. Johnson. 1991. 'Molecular and cytogenetic analysis of tumors in von Recklinghausen neurofibromatosis', *Genes Chromosomes Cancer*, 3: 62-70.

Gutmann, D. H., A. Aylsworth, J. C. Carey, B. Korf, J. Marks, R. E. Pyeritz, A. Rubenstein, and D. Viskochil. 1997. 'The diagnostic evaluation and multidisciplinary management of neurofibromatosis 1 and neurofibromatosis 2', *JAMA*, 278: 51-7.

Gutmann, D. H., M. D. McLellan, I. Hussain, J. W. Wallis, L. L. Fulton, R. S. Fulton, V. Magrini, R. Demeter, T. Wylie, C. Kandoth, J. R. Leonard, A. Guha, C. A. Miller, L. Ding, and E. R. Mardis. 2013. 'Somatic neurofibromatosis type 1 (NF1) inactivation characterizes NF1-associated pilocytic astrocytoma', *Genome Res*, 23: 431-9.

Hanahan, D., and R. A. Weinberg. 2000. 'The hallmarks of cancer', *Cell*, 100: 57-70.

Hegedus, B., B. Dasgupta, J. E. Shin, R. J. Emnett, E. K. Hart-Mahon, L. Elghazi, E. Bernal-Mizrachi, and D. H. Gutmann. 2007. 'Neurofibromatosis-1 regulates neuronal and glial cell differentiation from neuroglial progenitors in vivo by both cAMP- and Ras-dependent mechanisms', *Cell Stem Cell*, 1: 443-57.

Hegedus, B., F. W. Hughes, J. R. Garbow, S. Gianino, D. Banerjee, K. Kim, M. H. Ellisman, M. A. Brantley, Jr., and D. H. Gutmann. 2009. 'Optic nerve dysfunction in a mouse model of neurofibromatosis-1 optic glioma', *J Neuropathol Exp Neurol*, 68: 542-51.

Hemmati, H. D., I. Nakano, J. A. Lazareff, M. Masterman-Smith, D. H. Geschwind, M. Bronner-Fraser, and H. I. Kornblum. 2003. 'Cancerous stem cells can arise from pediatric brain tumors', *Proc Natl Acad Sci U S A*, 100: 15178-83.

Huson, S. M., P. S. Harper, and D. A. Compston. 1988. 'Von Recklinghausen neurofibromatosis. A clinical and population study in south-east Wales', *Brain*, 111 (Pt 6): 1355-81.

Hyman, S. L., A. Shores, and K. N. North. 2005. 'The nature and frequency of cognitive deficits in children with neurofibromatosis type 1', *Neurology*, 65: 1037-44.

Jacks, T., T. S. Shih, E. M. Schmitt, R. T. Bronson, A. Bernards, and R. A. Weinberg. 1994. 'Tumour predisposition in mice heterozygous for a targeted mutation in Nf1', *Nat Genet*, 7: 353-61.

Jackson, E. L., J. M. Garcia-Verdugo, S. Gil-Perotin, M. Roy, A. Quinones-Hinojosa, S. VandenBerg, and A. Alvarez-Buylla. 2006. 'PDGFR alpha-positive B cells are neural stem cells in the adult SVZ that form glioma-like growths in response to increased PDGF signaling', *Neuron*, 51: 187-99.

Jacob, K., S. Albrecht, C. Sollier, D. Faury, E. Sader, A. Montpetit, D. Serre, P. Hauser, M. Garami, L. Bognar, Z. Hanzely, J. L. Montes, J. Atkinson, J. P. Farmer, E. Bouffet, C. Hawkins, U. Tabori, and N. Jabado. 2009. 'Duplication of 7q34 is specific to juvenile pilocytic astrocytomas and a hallmark of cerebellar and optic pathway tumours', *Br J Cancer*, 101: 722-33.

Jacob, K., D. A. Quang-Khuong, D. T. Jones, H. Witt, S. Lambert, S. Albrecht, O. Witt, C. Vezina, M. Shirinian, D. Faury, M. Garami, P. Hauser, A. Klekner, L. Bognar, J. P. Farmer, J. L. Montes, J. Atkinson, C. Hawkins, A. Korshunov, V. P. Collins, S. M. Pfister, U. Tabori, and N. Jabado. 2011. 'Genetic aberrations leading to MAPK pathway activation mediate oncogene-induced senescence in sporadic pilocytic astrocytomas', *Clin Cancer Res*, 17: 4650-60.

Jones, D. T., B. Hutter, N. Jager, A. Korshunov, M. Kool, H. J. Warnatz, T. Zichner, S. R. Lambert, M. Ryzhova, D. A. Quang, A. M. Fontebasso, A. M. Stutz, S. Hutter, M. Zuckermann, D. Sturm, J. Gronych, B. Lasitschka, S. Schmidt, H. Seker-Cin, H. Witt, M. Sultan, M. Ralser, P. A. Northcott, V. Hovestadt, S. Bender, E. Pfaff, S. Stark, D. Faury, J. Schwartzentruber, J. Majewski, U. D. Weber, M. Zapatka, B. Raeder, M. Schlesner, C. L. Worth, C. C. Bartholomae, C. von Kalle, C. D. Imbusch, S. Radomski, C. Lawerenz, P. van Sluis, J. Koster, R. Volckmann, R. Versteeg, H. Lehrach, C. Monoranu, B. Winkler, A. Unterberg, C. Herold-Mende, T. Milde, A. E. Kulozik, M. Ebinger, M. U. Schuhmann, Y. J. Cho, S. L. Pomeroy, A. von Deimling, O. Witt, M. D. Taylor, S. Wolf, M. A. Karajannis, C. G. Eberhart, W. Scheurlen, M. Hasselblatt, K. L. Ligon, M. W. Kieran, J. O. Korbel, M. L. Yaspo, B. Brors, J. Felsberg, G. Reifenberger, V. P. Collins, N. Jabado, R. Eils, P. Lichter, S. M. Pfister, and Project International Cancer Genome Consortium PedBrain Tumor. 2013. 'Recurrent somatic alterations of FGFR1 and NTRK2 in pilocytic astrocytoma', *Nat Genet*, 45: 927-32.

Jones, D. T. W., M. W. Kieran, E. Bouffet, S. Alexandrescu, P. Bandopadhayay, M. Bornhorst, D. Ellison, J. Fangusaro, M. J. Fisher, N. Foreman, M. Fouladi, D. Hargrave, C. Hawkins, N. Jabado, M. Massimino, S. Mueller, G. Perilongo, A. Y. N. Schouten van Meeteren, U. Tabori, K. Warren, A. J. Waanders, D. Walker, W. Weiss, O. Witt, K. Wright, Y. Zhu, D. C. Bowers, S. M. Pfister, and R. J. Packer. 2018. 'Pediatric low-grade gliomas: next biologically driven steps', *Neuro Oncol*, 20: 160-73.

Kalamarides, M., A. O. Stemmer-Rachamimov, M. Niwa-Kawakita, F. Chareyre, E. Taranchon, Z. Y. Han, C. Martinelli, E. A. Lusis, B. Hegedus, D. H. Gutmann, and M. Giovannini. 2011. 'Identification of a progenitor cell of origin capable of generating diverse meningioma histological subtypes', *Oncogene*, 30: 2333-44.

Kaul, A., J. A. Toonen, P. J. Cimino, S. M. Gianino, and D. H. Gutmann. 2015. 'Akt- or MEK-mediated mTOR inhibition suppresses Nf1 optic glioma growth', *Neuro Oncol*, 17: 843-53.

Kessaris, N., F. Jamen, L. L. Rubin, and W. D. Richardson. 2004. 'Cooperation between sonic hedgehog and fibroblast growth factor/MAPK signalling pathways in neocortical precursors', *Development*, 131: 1289-98.

Kim, E., Y. Wang, S. J. Kim, M. Bornhorst, E. S. Jecrois, T. E. Anthony, C. Wang, Y. E. Li, J. L. Guan, G. G. Murphy, and Y. Zhu. 2014. 'Transient inhibition of the ERK pathway prevents cerebellar developmental defects and improves long-term motor functions in murine models of neurofibromatosis type 1', *Elife*, 3.

Klaes, A., T. Menne, A. Stollewerk, H. Scholz, and C. Klambt. 1994. 'The Ets transcription factors encoded by the Drosophila gene pointed direct glial cell differentiation in the embryonic CNS', *Cell*, 78: 149-60.

Kluwe, L., C. Hagel, M. Tatagiba, S. Thomas, D. Stavrou, H. Ostertag, A. von Deimling, and V. F. Mautner. 2001. 'Loss of NF1 alleles distinguish sporadic from NF1-associated pilocytic astrocytomas', *J Neuropathol Exp Neurol*, 60: 917-20.

Kondo, T., and M. Raff. 2000. 'Oligodendrocyte precursor cells reprogrammed to become multipotential CNS stem cells', *Science*, 289: 1754-7.

Ku, M. C., S. A. Wolf, D. Respondek, V. Matyash, A. Pohlmann, S. Waiczies, H. Waiczies, T. Niendorf, M. Synowitz, R. Glass, and H. Kettenmann. 2013. 'GDNF mediates glioblastoma-induced microglia attraction but not astrogliosis', *Acta Neuropathol*, 125: 609-20.

Kuwabara, T. 1975. 'Development of the optic nerve of the rat', *Invest Ophthalmol*, 14: 732-45.

Kwon, C. H., D. Zhao, J. Chen, S. Alcantara, Y. Li, D. K. Burns, R. P. Mason, E. Y. Lee, H. Wu, and L. F. Parada. 2008. 'Pten haploinsufficiency accelerates formation of high-grade astrocytomas', *Cancer Res*, 68: 3286-94.

Lau, N., M. M. Feldkamp, L. Roncari, A. H. Loehr, P. Shannon, D. H. Gutmann, and A. Guha. 2000. 'Loss of neurofibromin is associated with activation of RAS/MAPK and PI3-K/AKT signaling in a neurofibromatosis 1 astrocytoma', *J Neuropathol Exp Neurol*, 59: 759-67.

Lee, D. Y., S. M. Gianino, and D. H. Gutmann. 2012. 'Innate neural stem cell heterogeneity determines the patterning of glioma formation in children', *Cancer Cell*, 22: 131-8.

Lee, D. Y., T. H. Yeh, R. J. Emnett, C. R. White, and D. H. Gutmann. 2010. 'Neurofibromatosis-1 regulates neuroglial progenitor proliferation and glial differentiation in a brain region-specific manner', *Genes Dev*, 24: 2317-29.

Lee, J. S., A. Padmanabhan, J. Shin, S. Zhu, F. Guo, J. P. Kanki, J. A. Epstein, and A. T. Look. 2010. 'Oligodendrocyte progenitor cell numbers and migration are regulated by the zebrafish orthologs of the NF1 tumor suppressor gene', *Hum Mol Genet*, 19: 4643-53.

Legius, E., D. A. Marchuk, F. S. Collins, and T. W. Glover. 1993. 'Somatic deletion of the neurofibromatosis type 1 gene in a neurofibrosarcoma supports a tumour suppressor gene hypothesis', *Nat Genet*, 3: 122-6.

Li, X., J. M. Newbern, Y. Wu, M. Morgan-Smith, J. Zhong, J. Charron, and W. D. Snider. 2012. 'MEK Is a Key Regulator of Gliogenesis in the Developing Brain', *Neuron*, 75: 1035-50.

Li, Y., Y. Li, R. M. McKay, D. Riethmacher, and L. F. Parada. 2012. 'Neurofibromin modulates adult hippocampal neurogenesis and behavioral effects of antidepressants', *J Neurosci*, 32: 3529-39.

Ligon, K. L., J. A. Alberta, A. T. Kho, J. Weiss, M. R. Kwaan, C. L. Nutt, D. N. Louis, C. D. Stiles, and D. H. Rowitch. 2004. 'The oligodendroglial lineage marker OLIG2 is universally expressed in diffuse gliomas', *J Neuropathol Exp Neurol*, 63: 499-509.

Lim, D. A., S. Cha, M. C. Mayo, M. H. Chen, E. Keles, S. VandenBerg, and M. S. Berger. 2007. 'Relationship of glioblastoma multiforme to neural stem cell regions predicts invasive and multifocal tumor phenotype', *Neuro Oncol*, 9: 424-9.

Listernick, R. 2016. 'Predicting which NF1 optic pathway gliomas will require treatment', *Neurology*, 87: 2389-90.

Listernick, R., J. Charrow, and D. H. Gutmann. 1999. 'Intracranial gliomas in neurofibromatosis type 1', *Am J Med Genet*, 89: 38-44.

Listernick, R., R. E. Ferner, G. T. Liu, and D. H. Gutmann. 2007. 'Optic pathway gliomas in neurofibromatosis-1: controversies and recommendations', *Ann Neurol*, 61: 189-98.

Listernick, R., R. E. Ferner, L. Piersall, S. Sharif, D. H. Gutmann, and J. Charrow. 2004. 'Late-onset optic pathway tumors in children with neurofibromatosis 1', *Neurology*, 63: 1944-6.

Listernick, R., D. N. Louis, R. J. Packer, and D. H. Gutmann. 1997. 'Optic pathway gliomas in children with neurofibromatosis 1: consensus statement from the NF1 Optic Pathway Glioma Task Force', *Ann Neurol*, 41: 143-9.

Liu, C., J. C. Sage, M. R. Miller, R. G. Verhaak, S. Hippenmeyer, H. Vogel, O. Foreman, R. T. Bronson, A. Nishiyama, L. Luo, and H. Zong. 2011. 'Mosaic analysis with double markers reveals tumor cell of origin in glioma', *Cell*, 146: 209-21.

Lu, Q. R., T. Sun, Z. Zhu, N. Ma, M. Garcia, C. D. Stiles, and D. H. Rowitch. 2002. 'Common developmental requirement for Olig function indicates a motor neuron/oligodendrocyte connection', *Cell*, 109: 75-86.

Lush, M. E., Y. Li, C. H. Kwon, J. Chen, and L. F. Parada. 2008. 'Neurofibromin is required for barrel formation in the mouse somatosensory cortex', *J Neurosci*, 28: 1580-7.

Macdonald, R., J. Scholes, U. Strahle, C. Brennan, N. Holder, M. Brand, and S. W. Wilson. 1997. 'The Pax protein Noi is required for commissural axon pathway formation in the rostral forebrain', *Development*, 124: 2397-408.

Malatesta, P., M. A. Hack, E. Hartfuss, H. Kettenmann, W. Klinkert, F. Kirchhoff, and M. Gotz. 2003. 'Neuronal or glial progeny: regional differences in radial glia fate', *Neuron*, 37: 751-64.

Marchuk, D. A., A. M. Saulino, R. Tavakkol, M. Swaroop, M. R. Wallace, L. B. Andersen, A. L. Mitchell, D. H. Gutmann, M. Boguski, and F. S. Collins. 1991. 'cDNA cloning of the type 1 neurofibromatosis gene: complete sequence of the NF1 gene product', *Genomics*, 11: 931-40.

Marshall, C. A., B. G. Novitch, and J. E. Goldman. 2005. 'Olig2 directs astrocyte and oligodendrocyte formation in postnatal subventricular zone cells', *J Neurosci*, 25: 7289-98.

Mendoza, M. C., E. E. Er, and J. Blenis. 2011. 'The Ras-ERK and PI3K-mTOR pathways: cross-talk and compensation', *Trends Biochem Sci*, 36: 320-8.

Menn, B., J. M. Garcia-Verdugo, C. Yaschine, O. Gonzalez-Perez, D. Rowitch, and A. Alvarez-Buylla. 2006. 'Origin of oligodendrocytes in the subventricular zone of the adult brain', *J Neurosci*, 26: 7907-18.

Messersmith, W. A., M. Hidalgo, M. Carducci, and S. G. Eckhardt. 2006. 'Novel targets in solid tumors: MEK inhibitors', *Clin Adv Hematol Oncol*, 4: 831-6.

Mi, H., and B. A. Barres. 1999. 'Purification and characterization of astrocyte precursor cells in the developing rat optic nerve', *J Neurosci*, 19: 1049-61.

Miller, R. H., S. David, R. Patel, E. R. Abney, and M. C. Raff. 1985. 'A quantitative immunohistochemical study of macroglial cell development in the rat optic nerve: in vivo evidence for two distinct astrocyte lineages', *Dev Biol*, 111: 35-41.

Mokhtari, K., S. Paris, L. Aguirre-Cruz, N. Privat, E. Criniere, Y. Marie, J. J. Hauw, M. Kujas, D. Rowitch, K. Hoang-Xuan, J. Y. Delattre, and M. Sanson. 2005. 'Olig2 expression, GFAP, p53 and 1p loss analysis contribute to glioma subclassification', *Neuropathol Appl Neurobiol*, 31: 62-9.

Mui, S. H., J. W. Kim, G. Lemke, and S. Bertuzzi. 2005. 'Vax genes ventralize the embryonic eye', *Genes Dev*, 19: 1249-59.

Murphy, E. S., H. Xie, T. E. Merchant, J. S. Yu, S. T. Chao, and J. H. Suh. 2015. 'Review of cranial radiotherapy-induced vasculopathy', *J Neurooncol*, 122: 421-9.

Nadal-Nicolas, F. M., M. Jimenez-Lopez, P. Sobrado-Calvo, L. Nieto-Lopez, I. Canovas-Martinez, M. Salinas-Navarro, M. Vidal-Sanz, and M. Agudo. 2009. 'Brn3a as a marker of retinal ganglion cells: qualitative and quantitative time course studies in naive and optic nerve-injured retinas', *Invest Ophthalmol Vis Sci*, 50: 3860-8.

Newbern, J. M., X. Li, S. E. Shoemaker, J. Zhou, J. Zhong, Y. Wu, D. Bonder, S. Hollenback, G. Coppola, D. H. Geschwind, G. E. Landreth, and W. D. Snider. 2011. 'Specific functions for ERK/MAPK signaling during PNS development', *Neuron*, 69: 91-105.

Niihori, T., Y. Aoki, Y. Narumi, G. Neri, H. Cave, A. Verloes, N. Okamoto, R. C. Hennekam, G. Gillessen-Kaesbach, D. Wieczorek, M. I. Kavamura, K. Kurosawa, H. Ohashi, L. Wilson, D. Heron, D. Bonneau, G. Corona, T. Kaname, K. Naritomi, C. Baumann, N. Matsumoto, K. Kato, S. Kure, and Y. Matsubara. 2006. 'Germline KRAS and BRAF mutations in cardio-facio-cutaneous syndrome', *Nat Genet*, 38: 294-6.

Ohren, J. F., H. Chen, A. Pavlovsky, C. Whitehead, E. Zhang, P. Kuffa, C. Yan, P. McConnell, C. Spessard, C. Banotai, W. T. Mueller, A. Delaney, C. Omer, J. Sebolt-Leopold, D. T. Dudley, I. K. Leung, C. Flamme, J. Warmus, M. Kaufman, S. Barrett, H. Tecle, and C. A. Hasemann. 2004. 'Structures of human MAP kinase kinase 1 (MEK1) and MEK2 describe novel noncompetitive kinase inhibition', *Nat Struct Mol Biol*, 11: 1192-7.

Ohyama, T., and A. K. Groves. 2004. 'Generation of Pax2-Cre mice by modification of a Pax2 bacterial artificial chromosome', *Genesis*, 38: 195-9.

Ono, K., H. Takebayashi, K. Ikeda, M. Furusho, T. Nishizawa, K. Watanabe, and K. Ikenaka. 2008. 'Regional- and temporal-dependent changes in the differentiation of Olig2 progenitors in the forebrain, and the impact on astrocyte development in the dorsal pallium', *Dev Biol*, 320: 456-68.

Ono, K., Y. Yasui, U. Rutishauser, and R. H. Miller. 1997. 'Focal ventricular origin and migration of oligodendrocyte precursors into the chick optic nerve', *Neuron*, 19: 283-92.

Ono, K., K. Yoshii, H. Tominaga, H. Gotoh, T. Nomura, H. Takebayashi, and K. Ikenaka. 2017. 'Oligodendrocyte precursor cells in the mouse optic nerve originate in the preoptic area', *Brain Struct Funct*, 222: 2441-48.

Ortega, F., S. Gascon, G. Masserdotti, A. Deshpande, C. Simon, J. Fischer, L. Dimou, D. Chichung Lie, T. Schroeder, and B. Berninger. 2013. 'Oligodendrogliogenic and neurogenic adult subependymal zone neural stem cells constitute distinct lineages and exhibit differential responsiveness to Wnt signalling', *Nat Cell Biol*, 15: 602-13.

Ostrom, Q. T., H. Gittleman, P. Liao, C. Rouse, Y. Chen, J. Dowling, Y. Wolinsky, C. Kruchko, and J. Barnholtz-Sloan. 2014. 'CBTRUS statistical report: primary brain and central

nervous system tumors diagnosed in the United States in 2007-2011', *Neuro Oncol*, 16 Suppl 4: iv1-63.

Packer, R. J., J. Ater, J. Allen, P. Phillips, R. Geyer, H. S. Nicholson, R. Jakacki, E. Kurczynski, M. Needle, J. Finlay, G. Reaman, and J. M. Boyett. 1997. 'Carboplatin and vincristine chemotherapy for children with newly diagnosed progressive low-grade gliomas', *J Neurosurg*, 86: 747-54.

Packer, R. J., S. Pfister, E. Bouffet, R. Avery, P. Bandopadhayay, M. Bornhorst, D. C. Bowers, D. Ellison, J. Fangusaro, N. Foreman, M. Fouladi, A. Gajjar, D. Haas-Kogan, C. Hawkins, C. Y. Ho, E. Hwang, N. Jabado, L. B. Kilburn, A. Lassaletta, K. L. Ligon, M. Massimino, S. V. Meeteren, S. Mueller, T. Nicolaides, G. Perilongo, U. Tabori, G. Vezina, K. Warren, O. Witt, Y. Zhu, D. T. Jones, and M. Kieran. 2017. 'Pediatric low-grade gliomas: implications of the biologic era', *Neuro Oncol*, 19: 750-61.

Paolicelli, R. C., K. Bisht, and M. E. Tremblay. 2014. 'Fractalkine regulation of microglial physiology and consequences on the brain and behavior', *Front Cell Neurosci*, 8: 129.

Parsa, C. F., C. S. Hoyt, R. L. Lesser, J. M. Weinstein, C. M. Strother, R. Muci-Mendoza, M. Ramella, R. S. Manor, W. A. Fletcher, M. X. Repka, J. A. Garrity, R. N. Ebner, M. L. Monteiro, R. M. McFadzean, I. V. Rubtsova, and W. F. Hoyt. 2001. 'Spontaneous regression of optic gliomas: thirteen cases documented by serial neuroimaging', *Arch Ophthalmol*, 119: 516-29.

Pasmant, E., M. Vidaud, D. Vidaud, and P. Wolkenstein. 2012. 'Neurofibromatosis type 1: from genotype to phenotype', *J Med Genet*, 49: 483-9.

Pequignot, M. O., A. C. Provost, S. Salle, P. Taupin, K. M. Sainton, D. Marchant, J. C. Martinou, J. C. Ameisen, J. P. Jais, and M. Abitbol. 2003. 'Major role of BAX in apoptosis during retinal development and in establishment of a functional postnatal retina', *Dev Dyn*, 228: 231-8.

Pfister, S., and O. Witt. 2009. 'Pediatric gliomas', *Recent Results Cancer Res*, 171: 67-81.

Platten, M., A. Kretz, U. Naumann, S. Aulwurm, K. Egashira, S. Isenmann, and M. Weller. 2003. 'Monocyte chemoattractant protein-1 increases microglial infiltration and aggressiveness of gliomas', *Ann Neurol*, 54: 388-92.

Pong, W. W., S. B. Higer, S. M. Gianino, R. J. Emnett, and D. H. Gutmann. 2013. 'Reduced microglial CX3CR1 expression delays neurofibromatosis-1 glioma formation', *Ann Neurol*, 73: 303-8.

Preusser, M., H. Budka, K. Rossler, and J. A. Hainfellner. 2007. 'OLIG2 is a useful immunohistochemical marker in differential diagnosis of clear cell primary CNS neoplasms', *Histopathology*, 50: 365-70.

Rafalski, V. A., P. P. Ho, J. O. Brett, D. Ucar, J. C. Dugas, E. A. Pollina, L. M. Chow, A. Ibrahim, S. J. Baker, B. A. Barres, L. Steinman, and A. Brunet. 2013. 'Expansion of oligodendrocyte progenitor cells following SIRT1 inactivation in the adult brain', *Nat Cell Biol*, 15: 614-24.

Raff, M. C., E. R. Abney, J. Cohen, R. Lindsay, and M. Noble. 1983. 'Two types of astrocytes in cultures of developing rat white matter: differences in morphology, surface gangliosides, and growth characteristics', *J Neurosci*, 3: 1289-300.

Raff, M. C., E. R. Abney, and R. H. Miller. 1984. 'Two glial cell lineages diverge prenatally in rat optic nerve', *Dev Biol*, 106: 53-60.

Reis, G. F., M. M. Bloomer, A. Perry, J. J. Phillips, J. P. Grenert, A. N. Karnezis, and T. Tihan. 2013. 'Pilocytic astrocytomas of the optic nerve and their relation to pilocytic astrocytomas elsewhere in the central nervous system', *Mod Pathol*, 26: 1279-87.

Rickert, C. H., and W. Paulus. 2001. 'Epidemiology of central nervous system tumors in childhood and adolescence based on the new WHO classification', *Childs Nerv Syst*, 17: 503-11.

Rodriguez, A. R., L. P. de Sevilla Muller, and N. C. Brecha. 2014. 'The RNA binding protein RBPMS is a selective marker of ganglion cells in the mammalian retina', *J Comp Neurol*, 522: 1411-43.

Rodriguez-Viciana, P., O. Tetsu, W. E. Tidyman, A. L. Estep, B. A. Conger, M. S. Cruz, F. McCormick, and K. A. Rauen. 2006. 'Germline mutations in genes within the MAPK pathway cause cardio-facio-cutaneous syndrome', *Science*, 311: 1287-90.

Sanchez-Ortiz, E., W. Cho, I. Nazarenko, W. Mo, J. Chen, and L. F. Parada. 2014. 'NF1 regulation of RAS/ERK signaling is required for appropriate granule neuron progenitor expansion and migration in cerebellar development', *Genes Dev*, 28: 2407-20.

Schindler, G., D. Capper, J. Meyer, W. Janzarik, H. Omran, C. Herold-Mende, K. Schmieder, P. Wesseling, C. Mawrin, M. Hasselblatt, D. N. Louis, A. Korshunov, S. Pfister, C. Hartmann, W. Paulus, G. Reifenberger, and A. von Deimling. 2011. 'Analysis of BRAF V600E mutation in 1,320 nervous system tumors reveals high mutation frequencies in pleomorphic xanthoastrocytoma, ganglioglioma and extra-cerebellar pilocytic astrocytoma', *Acta Neuropathol*, 121: 397-405.

Schmid, R. S., Y. Yokota, and E. S. Anton. 2006. 'Generation and characterization of brain lipid-binding protein promoter-based transgenic mouse models for the study of radial glia', *Glia*, 53: 345-51.

Schwarz, M., F. Cecconi, G. Bernier, N. Andrejewski, B. Kammandel, M. Wagner, and P. Gruss. 2000. 'Spatial specification of mammalian eye territories by reciprocal transcriptional repression of Pax2 and Pax6', *Development*, 127: 4325-34.

Sebolt-Leopold, J. S., D. T. Dudley, R. Herrera, K. Van Becelaere, A. Wiland, R. C. Gowan, H. Tecle, S. D. Barrett, A. Bridges, S. Przybranowski, W. R. Leopold, and A. R. Saltiel. 1999. 'Blockade of the MAP kinase pathway suppresses growth of colon tumors in vivo', *Nat Med*, 5: 810-6.

Sebolt-Leopold, J. S., and R. Herrera. 2004. 'Targeting the mitogen-activated protein kinase cascade to treat cancer', *Nat Rev Cancer*, 4: 937-47.

Serra, E., T. Rosenbaum, U. Winner, R. Aledo, E. Ars, X. Estivill, H. G. Lenard, and C. Lazaro. 2000. 'Schwann cells harbor the somatic NF1 mutation in neurofibromas: evidence of two different Schwann cell subpopulations', *Hum Mol Genet*, 9: 3055-64.

Shannon, K. M., P. O'Connell, G. A. Martin, D. Paderanga, K. Olson, P. Dinndorf, and F. McCormick. 1994. 'Loss of the normal NF1 allele from the bone marrow of children with type 1 neurofibromatosis and malignant myeloid disorders', *N Engl J Med*, 330: 597-601.

Sharif, S., R. Ferner, J. M. Birch, J. E. Gillespie, H. R. Gattamaneni, M. E. Baser, and D. G. Evans. 2006. 'Second primary tumors in neurofibromatosis 1 patients treated for optic glioma: substantial risks after radiotherapy', *J Clin Oncol*, 24: 2570-5.

Sharif, S., A. Moran, S. M. Huson, R. Iddenden, A. Shenton, E. Howard, and D. G. Evans. 2007. 'Women with neurofibromatosis 1 are at a moderately increased risk of developing breast cancer and should be considered for early screening', *J Med Genet*, 44: 481-4.

Sielska, M., P. Przanowski, B. Wylot, K. Gabrusiewicz, M. Maleszewska, M. Kijewska, M. Zawadzka, J. Kucharska, K. Vinnakota, H. Kettenmann, K. Kotulska, W. Grajkowska, and B. Kaminska. 2013. 'Distinct roles of CSF family cytokines in macrophage infiltration and activation in glioma progression and injury response', *J Pathol*, 230: 310-21.

Simmons, G. W., W. W. Pong, R. J. Emnett, C. R. White, S. M. Gianino, F. J. Rodriguez, and D. H. Gutmann. 2011. 'Neurofibromatosis-1 heterozygosity increases microglia in a spatially and temporally restricted pattern relevant to mouse optic glioma formation and growth', *J Neuropathol Exp Neurol*, 70: 51-62.

Singh, S. K., C. Hawkins, I. D. Clarke, J. A. Squire, J. Bayani, T. Hide, R. M. Henkelman, M. D. Cusimano, and P. B. Dirks. 2004. 'Identification of human brain tumour initiating cells', *Nature*, 432: 396-401.

Small, R. K., P. Riddle, and M. Noble. 1987. 'Evidence for migration of oligodendrocyte--type-2 astrocyte progenitor cells into the developing rat optic nerve', *Nature*, 328: 155-7.

Solga, A. C., J. A. Toonen, Y. Pan, P. J. Cimino, Y. Ma, G. A. Castillon, S. M. Gianino, M. H. Ellisman, D. Y. Lee, and D. H. Gutmann. 2017. 'The cell of origin dictates the temporal course of neurofibromatosis-1 (Nf1) low-grade glioma formation', *Oncotarget*, 8: 47206-15.

Soukkarieh, C., E. Agius, C. Soula, and P. Cochard. 2007. 'Pax2 regulates neuronal-glial cell fate choice in the embryonic optic nerve', *Dev Biol*, 303: 800-13.

Stiller, C. A., J. M. Chessells, and M. Fitchett. 1994. 'Neurofibromatosis and childhood leukaemia/lymphoma: a population-based UKCCSG study', *Br J Cancer*, 70: 969-72.

Sun, G. J., Y. Zhou, S. Ito, M. A. Bonaguidi, G. Stein-O'Brien, N. K. Kawasaki, N. Modak, Y. Zhu, G. L. Ming, and H. Song. 2015. 'Latent tri-lineage potential of adult hippocampal neural stem cells revealed by Nf1 inactivation', *Nat Neurosci*, 18: 1722-4.

Surawicz, T. S., F. Davis, S. Freels, E. R. Laws, Jr., and H. R. Menck. 1998. 'Brain tumor survival: results from the National Cancer Data Base', *J Neurooncol*, 40: 151-60.

Surawicz, T. S., B. J. McCarthy, V. Kupelian, P. J. Jukich, J. M. Bruner, and F. G. Davis. 1999. 'Descriptive epidemiology of primary brain and CNS tumors: results from the Central Brain Tumor Registry of the United States, 1990-1994', *Neuro Oncol*, 1: 14-25.

Tatsumi, K., H. Takebayashi, T. Manabe, K. F. Tanaka, M. Makinodan, T. Yamauchi, E. Makinodan, H. Matsuyoshi, H. Okuda, K. Ikenaka, and A. Wanaka. 2008. 'Genetic fate mapping of Olig2 progenitors in the injured adult cerebral cortex reveals preferential differentiation into astrocytes', *J Neurosci Res*, 86: 3494-502.

Taylor, M. D., H. Poppleton, C. Fuller, X. Su, Y. Liu, P. Jensen, S. Magdaleno, J. Dalton, C. Calabrese, J. Board, T. Macdonald, J. Rutka, A. Guha, A. Gajjar, T. Curran, and R. J. Gilbertson. 2005. 'Radial glia cells are candidate stem cells of ependymoma', *Cancer Cell*, 8: 323-35.

Tihan, T., P. G. Fisher, J. L. Kepner, C. Godfraind, R. D. McComb, P. T. Goldthwaite, and P. C. Burger. 1999. 'Pediatric astrocytomas with monomorphous pilomyxoid features and a less favorable outcome', *J Neuropathol Exp Neurol*, 58: 1061-8.

Torres, M., E. Gomez-Pardo, and P. Gruss. 1996. 'Pax2 contributes to inner ear patterning and optic nerve trajectory', *Development*, 122: 3381-91.

Ueda, H., J. M. Levine, R. H. Miller, and B. D. Trapp. 1999. 'Rat optic nerve oligodendrocytes develop in the absence of viable retinal ganglion cell axons', *J Cell Biol*, 146: 1365-74.

Viti, J., A. Feathers, J. Phillips, and L. Lillien. 2003. 'Epidermal growth factor receptors control competence to interpret leukemia inhibitory factor as an astrocyte inducer in developing cortex', *J Neurosci*, 23: 3385-93.

Vlenterie, M., U. Flucke, L. C. Hofbauer, H. J. Timmers, J. Gastmeier, D. E. Aust, W. T. van der Graaf, P. Wesseling, G. Eisenhofer, and J. W. Lenders. 2013. 'Pheochromocytoma and

gastrointestinal stromal tumors in patients with neurofibromatosis type I', *Am J Med*, 126: 174-80.

Wallace, V. A., and M. C. Raff. 1999. 'A role for Sonic hedgehog in axon-to-astrocyte signalling in the rodent optic nerve', *Development*, 126: 2901-9.

Wang, Y., E. Kim, X. Wang, B. G. Novitch, K. Yoshikawa, L. S. Chang, and Y. Zhu. 2012. 'ERK inhibition rescues defects in fate specification of Nf1-deficient neural progenitors and brain abnormalities', *Cell*, 150: 816-30.

Wang, Y., J. Yang, H. Zheng, G. J. Tomasek, P. Zhang, P. E. McKeever, E. Y. Lee, and Y. Zhu. 2009. 'Expression of mutant p53 proteins implicates a lineage relationship between neural stem cells and malignant astrocytic glioma in a murine model', *Cancer Cell*, 15: 514-26.

Watters, J. J., J. M. Schartner, and B. Badie. 2005. 'Microglia function in brain tumors', *J Neurosci Res*, 81: 447-55.

Xu, G. F., P. O'Connell, D. Viskochil, R. Cawthon, M. Robertson, M. Culver, D. Dunn, J. Stevens, R. Gesteland, R. White, and et al. 1990. 'The neurofibromatosis type 1 gene encodes a protein related to GAP', *Cell*, 62: 599-608.

Xu, W., L. M. Mulligan, M. A. Ponder, L. Liu, B. A. Smith, C. G. Mathew, and B. A. Ponder. 1992. 'Loss of NF1 alleles in phaeochromocytomas from patients with type I neurofibromatosis', *Genes Chromosomes Cancer*, 4: 337-42.

Yalon, M., B. Rood, T. J. MacDonald, G. McCowage, R. Kane, S. Constantini, and R. J. Packer. 2013. 'A feasibility and efficacy study of rapamycin and erlotinib for recurrent pediatric low-grade glioma (LGG)', *Pediatr Blood Cancer*, 60: 71-6.

Yeh, T. C., V. Marsh, B. A. Bernat, J. Ballard, H. Colwell, R. J. Evans, J. Parry, D. Smith, B. J. Brandhuber, S. Gross, A. Marlow, B. Hurley, J. Lyssikatos, P. A. Lee, J. D. Winkler, K. Koch, and E. Wallace. 2007. 'Biological characterization of ARRY-142886 (AZD6244), a potent, highly selective mitogen-activated protein kinase kinase 1/2 inhibitor', *Clin Cancer Res*, 13: 1576-83.

Yue, T., K. Xian, E. Hurlock, M. Xin, S. G. Kernie, L. F. Parada, and Q. R. Lu. 2006. 'A critical role for dorsal progenitors in cortical myelination', *J Neurosci*, 26: 1275-80.

Zhang, J., G. Wu, C. P. Miller, R. G. Tatevossian, J. D. Dalton, B. Tang, W. Orisme, C. Punchihewa, M. Parker, I. Qaddoumi, F. A. Boop, C. Lu, C. Kandoth, L. Ding, R. Lee, R. Huether, X. Chen, E. Hedlund, P. Nagahawatte, M. Rusch, K. Boggs, J. Cheng, J. Becksfort, J. Ma, G. Song, Y. Li, L. Wei, J. Wang, S. Shurtleff, J. Easton, D. Zhao, R. S. Fulton, L. L. Fulton, D. J. Dooling, B. Vadodaria, H. L. Mulder, C. Tang, K. Ochoa, C. G. Mullighan, A. Gajjar, R. Kriwacki, D. Sheer, R. J. Gilbertson, E. R. Mardis, R. K. Wilson, J. R. Downing, S. J. Baker, D. W. Ellison, and Project St. Jude Children's Research Hospital-Washington University Pediatric Cancer Genome. 2013. 'Whole-genome sequencing identifies genetic alterations in pediatric low-grade gliomas', *Nat Genet*, 45: 602-12.

Zheng, H., L. Chang, N. Patel, J. Yang, L. Lowe, D. K. Burns, and Y. Zhu. 2008. 'Induction of abnormal proliferation by nonmyelinating schwann cells triggers neurofibroma formation', *Cancer Cell*, 13: 117-28.

Zhou, Q., and D. J. Anderson. 2002. 'The bHLH transcription factors OLIG2 and OLIG1 couple neuronal and glial subtype specification', *Cell*, 109: 61-73.

Zhu, Y., T. Harada, L. Liu, M. E. Lush, F. Guignard, C. Harada, D. K. Burns, M. L. Bajenaru, D. H. Gutmann, and L. F. Parada. 2005. 'Inactivation of NF1 in CNS causes increased glial progenitor proliferation and optic glioma formation', *Development*, 132: 5577-88.

Zhuo, L., M. Theis, I. Alvarez-Maya, M. Brenner, K. Willecke, and A. Messing. 2001. 'hGFAP-cre transgenic mice for manipulation of glial and neuronal function in vivo', *Genesis*, 31: 85-94.

Zong, H., J. S. Espinosa, H. H. Su, M. D. Muzumdar, and L. Luo. 2005. 'Mosaic analysis with double markers in mice', *Cell*, 121: 479-92.

Chapter III: Transient pharmacological inhibition of the MAPK pathway prevents optic nerve glioma formation in a dose-dependent manner

3.1 Introduction

Despite the great progress made in unraveling the mysteries of cancer genetics, the daunting task facing researchers and clinicians remains the translation of these exciting discoveries into novel therapeutics that will ameliorate patient outcomes. Many of the genetic mutations found in cancers involve genes whose products are involved in regulating signal transduction (Hanahan and Weinberg 2000). As a result, much of the focus of target-based therapies has been on inhibitors of signal transduction molecules such as protein kinases. The process of signal transduction involves an extracellular signaling molecule activating a specific receptor on the cell surface which in turn triggers a biochemical chain of events inside the cell cumulating in cellular response. All multicellular organisms possess the evolutionary conserved four subfamilies of mitogen-activated protein kinases (MAPKs), which play an essential role in numerous normal cellular processes, such as gene expression regulation, progression of the G1 stage of the cell cycle before DNA replication, and spindle assembly during both meiotic and mitotic cell division. The RAS–RAF–MEK–ERK pathway (ERK signaling) is generally considered the 'classical MAPK pathway' and is the most characterized. The main components include the RAS family of small GTPases. In normal physiological conditions, feedback loops at multiple levels tightly control ERK signaling. When stimulated by upstream receptors through stimuli such as extracellular mitogens, growth factors, and cytokines, RAS switches from the inactive (GDP-bound) to the active (GTP-bound) form. This conformational change leads to its binding to RAF, the first kinase in the signaling cascade. RAS subsequently recruits RAF to the membrane and promotes its dimerization and activation. The activated form of RAF phosphorylates and activates the MEK kinase, which in turn phosphorylates and activates ERK kinase. Activated ERK can then translocate to the nucleus and is able to phosphorylate several substrates, such as kinases and transcription factors that are in

charge of regulating cell cycle progression, differentiation, protein translation and escape from apoptosis.

Germline mutational activation of RAS, B-RAF, MEK1 and MEK2 has been discovered in patients that encompass a group of related developmental disorders (Costello, cardio-facial-cutaneous and Noonan syndromes) (Rodriguez-Viciana et al. 2006; Niihori et al. 2006). Lastly, neurofibromin, the protein encoded by NF1, negatively regulates the RAS-MEK-ERK signaling cascade by activating RAS GTPase and precipitating the transformation of RAS from its active, GTP-bound form to inactive GDP-bound form (Ballester et al. 1990). Thus, inactivation of the NF1 gene is directly linked to the dysregulation of the MAPK signaling pathway. There is ample evidence that support the essential role of MEK in malignant transformation and tumorigenesis. MEK1 and MEK2 are highly homologous, dual-specificity kinases, capable of phosphorylating both serine/threonine and tyrosine residues of their substrates ERK1 and ERK2 and possess a distinctive pocket structure located next to the ATP-binding site. Moreover, due to their unique structural characteristics and narrow substrate specificities, MEK1 and MEK2 represent ideal targets for drug development in cancer and developmental disorders.

The first MEK inhibitor (MEKi) to enter phase I clinical study was, CI-1040 (also known as PD0184352), a highly potent and selective inhibitor of MEK1 and MEK2 developed by Pfizer (Sebolt-Leopold et al. 1999). One of the reasons for MEKis target selectivity is the fact that they are non-ATP competitive, but instead bind to a unique inhibitor binding pocket adjacent to the ATP-binding site (Ohren et al. 2004). Since that first breakthrough, several other highly specific and potent MEK1/2 inhibitors have been developed and evaluated in clinical studies (Table 1). Three MEK inhibitors are of particular interest due to their superior pharmacological and biopharmaceutical properties and their promising status in clinical trials: PD0325901, selumetinib (AZD6244) and trametinib (GSK1120212). PD0325901 is a derivative of CI-1040 in which modifications in the chemical structure of the molecule has yielded a more than a 50-fold increase in potency for MEK inhibition, higher bioavailability, and longer duration of target suppression (Sebolt-Leopold and Herrera 2004). Remarkably, a phase 2 study in adolescents and adults NF1 patients with plexiform neurofibromas is currently ongoing with an expected completion date at the end of 2018 (ClinicalTrials.gov number, NCT02096471). Selumetinib is an effective, highly

selective, non-ATP-competitive MEK1 inhibitor developed by Array Biopharma and then licensed to AstraZeneca. Early results in a phase 2 clinical study showed that selumetinib was effective in treating children with recurrent/refractory low-grade glioma (LGG), including those with NF1-associated LGG (Fangusaro et al. 2017). Trametinib is an allosteric, non-ATP-competitive MEK1 and MEK2 inhibitor that was approved in 2003 by the FDA for melanoma treatment. Unlike Selumetinib which is available only in capsule form, trametinib is available as an oral solution and can be used in children as young as one year of age. Chemotherapeutic agents have shown very high efficacy in the management of clinically progressive OPGs, but provided variable outcomes in vision improvement. Therefore, the most critical challenge in the field is to develop preventive or early interventional therapies to be delivered before irreversible neurological deficits such as axonal degeneration and RGC loss.

Recently, the use of MEK inhibitors in children with NF1 and LGGs has received tremendous undertaking. In the past 3 years, there have been three consensus conferences on pediatric low-grade gliomas in collaboration with Children's National Medical Hospital (Washington, D.C.), the Hospital for Sick Children (Toronto), the Children's Hospital in Boston and the DKFZ group led by Dr. Stefan Pfister in Germany. The goals of these international conferences were to assess the body of information related to molecularly-targeted therapies in children with newly diagnosed with LGGs, and to determine new treatment paradigms. The general consensus is that MEKis should be used, not only in progressive and recurrent disease but also in newly diagnosed individuals (Jones et al. 2018). Thereby, a major objective of this study is to provide enough data and incentive towards this treatment transition.

In chapter II of my thesis, I use GEM models to demonstrate that hyperactivation of the MAPK pathway is responsible for NF1-assiociated glial abnormalities, leading to tumor formation. In the present study, I utilize the *Nf1*^{hGFAP}CKOs as a preclinical model to investigate pharmacological inhibition of MEK as a therapeutic strategy for NF1-OPGs. By comparing three clinically relevant MEKis, PD0325901 (PD901), selumetinib and trametinib, I first show that both PD901 and trametinib can achieve greater inhibition outside the central nervous system compared to selumetinib. However, PD901 is far superior at crossing the blood-brain barrier than trametinib. Based on these results, I chose PD901 to screen for optimal dose and delivery method and as the

benchmark for the preclinical study. Using three doses of PD901, 5 mg/kg, 10 mg/kg and 20mg/kg, I demonstrate that transient MEK inhibition during a neonatal window (P0.5-P21) prevents OPG formation in a dose-dependent fashion. This study, in conjunction with the previous chapter, underscores the essential role of the MAPK signaling pathway in the formation and maintenance of NF1-OPG and the need to target it in early interventional treatments.

3.2 Results

3.2.1 Biological effect of MEK-inhibitors: screening for the optimal dose and delivery method

The majority of MEKis were developed to suppress MEK activity in tumor tissues outside the central nervous system (melanoma, pancreatic cancer, ovarian cancer, non-small cell lung cancer). Therefore, their potential to cross the blood-brain barrier (BBB) has not been systematically investigated. To study the ability of the three MEKis to cross into the brain and the extent of p-Erk inhibition, I treated groups of P30 mice by oral gavage with doses of the agents previously used in preclinical studies (Gilmartin et al. 2011; Brown et al. 2007; Yeh et al. 2007). Mice treated with GSK were given two different doses: 3 mg/kg and 5 mg/kg. Mice treated with AZD were given the maximum tolerated dose (MTD) of 100 mg/kg and mice treated with PD901 were administered 5 mg/kg dose. Four hours after treatment, mice were sacrificed and the cerebellum and spleen were collected to determine MEK inhibition by western blot analysis. Both PD901 and GSK achieved excellent inhibition in the spleen (between 80% to nearly 100%). In contrast, the spleens of AZD treated mice showed significantly less p-Erk inhibition (about 40%), even though the mice were treated with the MTD dose (Figures 17A and 17C). However, AZD was able to efficiently cross the BBB, as evidence by the cerebellum which showed similar levels of p-Erk inhibition as the spleen. Likewise, the PD901 agent demonstrated great potential to cross in the CNS (greater than 80% p-Erk inhibition in the cerebellum). Although, GSK was highly potent at p-Erk inhibition outside the CNS, its ability to inhibit the pathway in the brain was greatly limited, indicating that the drug cannot efficiently cross the BBB (Figure 17B). Based on its combined potency in inhibiting the MAPK pathway and efficiency at crossing the BBB, I selected the PD901 agent to continue with my preclinical study.

In Chapter II, I demonstrated that the NF1-associated glial abnormalities are established within the first three weeks of postnatal development. Therefore, I set out to establish a treatment protocol to efficiently and consistently inhibit p-Erk in young pups. First, I used an established protocol in the Zhu laboratory of administering MEKi through lactation ("MEKi in the milk") by treating the nursing mothers via oral gavage. To determine the duration of p-Erk inhibition in the brain, lactating mothers were treated with a dose of 5 mg/kg of PD901 and cerebella were collected in both mothers and P8 pups at different time intervals: 4hr, 8hr, 10hr and 12hr. Four hours after gavage, the cerebellum in treated pups showed close to 60% inhibition (Figure 18A). This was the highest reduction in Erk phosphorylation observed at all time-points with a dose of 5 mg/kg in the pups. Consistently, treated cerebella in the mothers achieved near complete p-Erk inhibition with this dose (data not shown). Inhibition of p-Erk in the cerebellum was no longer detected 10 hours following treatment. These data indicate that the peak inhibition time in the pups after oral gavage lies around 4 hours and that a lower dose than administered will reach the pups through lactation. To investigate whether higher inhibition can be achieved with a different route of administration, I decided to treat P8 pups via single intraperitoneal injection (IP) with reduced dosages of 0.125 mg/kg, 0.25 mg/kg, 0.5 mg/kg and 1 mg/kg and harvested the cerebella at 2hrs and 4hrs after treatment (Figure 18B). A dose of 1 mg/kg almost completely eliminated p-Erk signal at both 2 and 4hrs after treatment (Figure 18C). There was a dose-dependent inhibition of p-Erk with decreasing doses of the drug. Of note, treatment with 0.125 mg/kg through IP injection achieved the same level of p-Erk inhibition as gavage treatment with 5 mg/kg within the same time frame (4hrs after treatment). Following these results, I decided to treat a cohort of pups from P0.5 to P8 via IP injection with a dose of 0.5 mg/kg of PD901 to test for toxicity and sustainability. Unfortunately, this treatment modality resulted in very high mortality level in the pups due to a combination of drug toxicity and repeated handling of the mice at such a young age.

3.2.2 A dose of 10 mg/kg of PD901 through "MEKi in the milk" can inhibit hyperactive p-Erk in *Nf1*^{hGFAP}CKOs to the level of controls

As a result of the failure of the IP treatments, I decided to increase the oral gavage dosage from 5 mg/kg to 10 mg/kg in order to achieve greater inhibition in the brain. To test the extent of

inhibition that can be achieved with PD901 treatment in *Nf1*^{hGFAP}CKOs, I treated mothers with P8 litters that were capable of generating three different genotypes: *Nf1*$^{+/+}$ (wild-type), *Nf1*$^{fl/+}$ (heterozygous) and *Nf1*$^{fl/fl}$ (mutant). Vehicle-treated *Nf1*^{hGFAP}CKOs showed an 80% increase in Erk phosphorylation in the cerebellum compared to either *Nf1* heterozygous or wild-type pups. Treatment with 10 mg/kg of PD901 resulted in about 40% inhibition of p-Erk in both wild-type and heterozygous mice. Remarkably, treatment of *Nf1* mutants with the same dosage decrease Erk phosphorylation to the same level as controls (Figures 19A and 19B). There was no significant change in the levels of phosphorylated AKT in *Nf1*^{hGFAP}CKOs and PD901 did not appear to target this downstream effector of RAS-mediated signaling pathway (Figure 19C). There appears to be an increase in phosphorylation of S6, a readout for the mTORC1 pathway, in the cerebella of P8 mutants. Interestingly, the MEKi treatment also inhibited the p-S6 signal to the level of controls (Figure 19D). Together, these results confirm that MEK-Erk pathway is the downstream signaling pathway that is the most hyperactivated in *Nf1*^{hGFAP}CKOs and that a dose of 10 mg/kg of PD901 through "MEKi in the milk" can successfully inhibit the pathway to the level of controls.

3.2.3 A three-week MEKi treatment during early postnatal stages suppresses Erk activation and rescues hypercellularity in *Nf1*^{hGFAP}CKOs

To test whether hyperactive Erk signaling is responsible for glia abnormalities in *Nf1*-deficient nerves, I treated newborn control and *Nf1*^{hGFAP}CKO pups with 10 mg/kg PD901 or vehicle from P0.5 to P21 for 3 weeks with the "MEKi in the milk" protocol (Figure 20A). This 3-week treatment protocol exhibited very little adverse effects on the pups. When I analyzed the prechiasmatic nerve of PD treated *Nf1*^{hGFAP}CKOs at P21, there was a complete rescue of the increase in cell number and cell density compared to vehicle-treated mutants (Figures 20B-20B"). Strikingly, MEK inhibition significantly reduced p-Erk expression in treated mutants as well as the number of abnormal generated GFAP^{+}Olig2^{+} double-positive cells (Figure 20C). These results demonstrate that inhibition of *Nf1*-mediated MEK-Erk is the major mechanism underlying the ectopic Olig2 expression in GFAP^{+} cells and the hypercellularity in the developing nerves of *Nf1*^{hGFAP}CKOs.

3.2.4 Transient, neonatal inhibition of the MEK-ERK pathway prevents the formation of optic nerve glioma formation in a dose-dependent manner

To determine whether the transient P0.5-P21 MEKi treatment protocol can provide long-term and sustained therapeutic benefits in a dose-dependent fashion, I treated groups of litter with either 5, 10 or 20 mg/kg doses of PD901 and analyzed the optic nerves at P60, about 40 days after treatment was terminated (Figure 21A). Mice treated with the 20 mg/kg dose displayed the most clinical signs of toxicity in both mothers and pups. Specifically, this high dosage negatively affected lactation in the mothers resulting in pups that looked malnourished and sickly, leading to high mortality. Therefore, I was only able to analyze three surviving mice treated at this high dose. Decreasing dose levels reduced this problem in a dose-dependent fashion. H&E analysis also revealed a dose-dependent decrease in cellularity in PD-treated mice with the 20 mg/kg dose providing the most complete and consistent rescue (Figures 21A and 22A'). The 5 mg/kg dose did not appear to provide significant rescue effect as evidence by the majority of mice (4 out of 5) displaying cellularity level similar to untreated mutants. Consistent with the results from P21 analysis, the vast majority of 10 mg/kg treated mutants showed rescue in cellularity to the level of controls, indicating the long-term benefit of transient MEKi treatment. Next, I performed immunofluorescence experiments to examine whether the MAPK pathway is reactivated 40 days after the MEKi treatment. The majority of mutants treated with either 5 mg/kg and 10 mg/kg showed a reduction in the number of p-Erk$^+$ cells when analyzed at P60. However, there was a cluster of poor-responders that still maintained high p-Erk activity (Figures 21B and 21B'). These poor-responders also corresponded to the mice that displayed higher cellularity after treatment. Remarkably, the group treated with 20 mg/kg PD did not have any poor-responder and achieved consistent p-Erk inhibition almost to the level of controls.

To evaluate whether the sustained p-Erk inhibition resulted in overall improvement in the glial abnormalities, I examined the different doses treated mice for decrease in the number of GFAP$^+$Olig2$^+$ cells. Although there was dose-dependent variation in the p-Erk rescue, all three doses showed significant reduction in the number of abnormal GFAP$^+$Olig2$^+$ cells (Figure 21B"). Furthermore, only a small number of the remaining double-positive cells showed Erk activation (arrows, Figure 21B). Similarly, there was a complete rescue in the number of BLBP$^+$ progenitors

in the nerves of mutants treated with 10 mg/kg dose of PD (Figures 21C and 21C'). Out of the 11 MEKi-treated mutants with 10 mg/kg of PD, only 1 showed clear signs of non-rescue and exhibited an OPG. A comparison between this non-rescued mouse and the remaining rescued group revealed a strong correlation between the degree of p-Erk inhibition and the rescue of glial abnormalities (Figure 22A). Together, these results demonstrate that transient MEKi treatment during neonatal stages prevents NF1-dependent glial abnormalities and provides long-term, sustained benefits in a dose-dependent manner.

3.2.5 Neonatal MEKi treatment rescues nerve damage and RGC loss in *Nf1*^{hGFAP}CKO mice

The second phase of NF1-OPG disease pathogenesis is manifested after the establishment of glial abnormalities and is characterized by immune cell activation, axonal and myelin defects and RGC apoptosis. Based on the success of the MEKi treatment in rescuing the glial defects in *Nf1*^{hGFAP}CKOs, I investigated whether the transient P0.5-P21 treatment protocol could also prevent the nerve degeneration and the death of RGCs observed in the second phase of the disease. When analyzed 40 days after the last 10 mg/kg PD treatment, MEKi-treated mutant nerves displayed a complete rescue of the increase in immune cell infiltration compared to vehicle-treated mutants (Figures 23 A and 23A'). Furthermore, the Iba^{+} microglia present in the nerves after treatment did not exhibit the "activated" morphology typically found in the tumors (amoeboid-like shape). In contrast to the disoriented axonal fibers associated with axonal swelling and loss observed in the OPGs of vehicle-treated animals, MEKi treatment completely restored the axonal architecture of the mutant nerve to the level of controls (Figure 23A). Similarly, MBP staining revealed no disruption of myelin or the presence of blebs in MEKi treated mutants (Figure 23B). Lastly, I investigated the rescue in neuronal loss in P60 mutants following neonatal treatment. As expected tumor-bearing, vehicle-treated mutants exhibited significant reduction in the number of RGC neurons compared to controls. The 10 mg/kg PD901 treatment completely rescued neuronal loss by preventing apoptosis in the GCL (Figures 23C-23C"). Collectively, these findings indicate that by rescuing the Phase I NF1-associated glial abnormalities, the transient, neonatal MEKi treatment can prevent the nerve damage and neuronal loss characteristic of the Phase II disease pathogenesis.

3.2.6 The first postnatal week represents a critical period in NF1-OPG formation

The P0.5-P21 MEKi treatment protocol clearly demonstrate that the neonatal stage is an important period in OPG formation. However, it remains unclear which week has the most critical need for NF1 function. The period of P0.5-P5 highlights two major events in optic nerve development: 1) peak time when $Pax2^+$ cells acquire astrocyte specification, 2) oligodendrocyte precursors migrate in the nerve from the chiasm. Our previous findings have shown that NF1 plays an important role in suppressing Olig2 expression in $Pax2^+$ APCs and mediating gliogenesis in the first week of postnatal development. To confirm the essential requirement of NF1 during this period, I administered the "MEKi in the milk" protocol to mice from P5 to P21 with the highest dose of PD901 (20 mg/kg) and analyzed the optic nerves at P60. Although this shortened protocol resulted in increased survival of the pups, most of the treated mice in this group developed OPG under histological analysis. When I directly compared P5-P21 to the conventional three-week protocol (P0.5-P21) at the same dose, I observed that the number of p-Erk^+ cells in the majority of P5-P21 treated mice was significantly higher than P0.5-P21 group and even reached the level of untreated mutants (Figure 24A). Furthermore, triple-positive (p-$Erk^+GFAP^+Olig2^+$) cells could be readily detected in this group whereas they were almost completely eliminated with the P0.5-P21 treatment protocol. Unsurprisingly, the number of $BLBP^+$ progenitors remained elevated in the P5-P21 treated group with the majority of them co-localizing with $Olig2^+$ cells (Figure 24B). These results demonstrate that ERK signaling plays a critical role in normal gliogenesis during the first postnatal week of optic nerve development.

3.3 Discussion

The goal of molecularly-targeted treatment strategies is to achieve long-term tumor control in patients with LGGs while simultaneously having less negative impact on their developing brain compared to conventional genotoxic therapies. In the context of NF1-OPGs, the most pressing challenge, in addition to tumor shrinkage, is to develop early interventional therapies in newly diagnosed patients before irreversible neuronal loss. The use of cell lines from patient tumors would be ideal for testing preclinical drugs because of the fact that they closely resemble actual human tumors and would therefore provide a more accurate response to a particular treatment.

Despite the combine efforts of many research groups, human NF1-pylocitic astrocytoma cell cultures have not yet been successfully established. Several factors could underlie this failure such as issues with cellular senescence or the lack of trophic growth factors from the tumor microenvironment.

3.3.1 Screening for the most potent MEKi in the CNS

In the absence of patient-derived cell lines, the availability of accurate preclinical mouse models together with a deeper understanding of neurofibromin function can offer the opportunity to develop treatments tailored to specific features of NF1-associated medical problems. In this study, I employ pharmacological inhibition of MEK to demonstrate the critical role that the MEK-Erk signaling pathway plays in NF1-OPG formation. In a proof of concept study, I tested three clinically relevant MEKis, PD0325901, selumetinib (AZD6244) and trametinib (GSK1120212), for their potential to cross the blood-brain-barrier. Oral gavage of P30 mice with both PD901 and GSK can achieve excellent inhibition outside the central nervous system (between 80-100% in the spleen). AZD showed significantly less inhibition in the spleen (up to 40%), even at the maximum tolerated dose. However, AZD was able to efficiently cross to the brain where comparable level of inhibition as the spleen was observed. Similarly, PD901 showed excellent affinity at crossing the blood-brain barrier. Although GSK can efficiently inhibit p-Erk signal in the body, it displayed poor ability to reach the cerebellum. As a result, the level of inhibition decreased to about 50% in the brain compared to the spleen. Consistent with my findings, AZD was shown to be 10 times less potent, with a relatively poor bioavailability, and lower p-Erk inhibition in tumor biopsies than PD901 in clinical testing (Messersmith et al. 2006). Based on these results, the agent PD901 was selected for the remaining study. Drug administration via repeated intraperitoneal injections proved to be too toxic for the pups, even at very low dose. Our laboratory is one of the first to use MEKi to treat NF1-associated diseases in GEM models using the “MEK in the milk” protocol by treating lactating mothers via oral gavage. This protocol allows the pups to receive a relatively low dose of the drug (about 1-5% of the administered dose reached the CNS in the pups) without added physical distress. By using this strategy in P8 pups, I determined that the highest reduction in Erk phosphorylation with PD901 was achieved at 4-5 hours after treatment. The duration of inhibition in the brain was about 10 hours.

3.3.2 The use of *Nf1*^{hGFAP}CKO mice for preclinical drug evaluation

Previously published studies in our lab have demonstrated a transient MEK inhibition during a neonatal window can rescue forebrain and cerebellum defects in *Nf1*^{hGFAP}CKO mice (Wang et al. 2012; Kim et al. 2014). Based on the success of these treatments and my genetic inhibition studies, I decided to use the *Nf1*^{hGFAP}CKOs to evaluate MEKi treatment as targeted therapy for NF1-OPG. The *Nf1*^{hGFAP}CKO mice provide several advantages as a model to study NF1-OPG. First, their OPGs share similar histopathological features and similar disease progression as the human disease. Second, the mice develop tumors predictably in the prechiasmatic area in complete penetrance. Third, the cellular and molecular targets of *Nf1* loss during development have been identified (GFAP^{+}Olig2^{+}, BLBP^{+} and p-Erk^{+} cells) and can be used as readout for treatment efficacy. Lastly, I have established the time course of visual impairment during OPG progression in *Nf1*^{hGFAP}CKO mice. I first began by showing that a single dose of 10 mg/kg of PD901 through "MEKi in the milk" can inhibit hyperactive p-Erk in the *Nf1* mutants to the level of controls. Next, I revealed that P0.5-P21 MEKi treatment protocol can prevent cell increase and GFAP^{+}Olig2^{+} glial abnormalities at P21 by suppressing p-Erk signaling. In particular, the 3-week transient, neonatal inhibition of the MEK-Erk pathway also provided long-term and sustained therapeutic benefits, even 40 days after last treatment. In the treated P60 *Nf1* mutants, there was a dose-dependent rescue in the tumor phenotype, with 20 mg/kg dose of PD901 providing the most consistent rescue in glial defects but with the highest toxicity. In addition, the neonatal MEKi treatment prevented the nerve damage and neuronal loss that characterize the second phase of disease pathogenesis. These results suggest that the neurological deficits including axonal degeneration and RGC loss are a direct consequence of the NF1-associated glial abnormalities. A possible implication of a cross-talk between neoplastic glial cells and microglia will be further explored in Chapter IV. To improve the translational potential for these preclinical findings from our mouse studies, it is essential to determine whether the prevention of neuroanatomic deficits by the "MEKi in Milk" protocol can also provide visual and behavioral improvement to *Nf1*^{hGFAP}CKO mice. Additional behavioral, imaging, and electrophysiological tests will help to examine whether these preclinical findings can be translated rapidly and reliably to clinical testing in NF1 patients. However, as most clinical studies with MEKis are still

underway, we will have to learn how to integrate promising preliminary results into clinical practice while waiting for long-term toxicity and outcome data.

Agents	Dose-limiting toxicities in phase I studies	Phase (Disease)
AZD8330 (ARRY-424704); AstraZeneca, UK and Array Biopharma, USA	Change in mental status and rash	Phase I
Refametinib (BAY 86-9766, RDEA119); Bayer, Germany and Ardea Bioscience, USA	Diarrhea, elevated lipase levels, somnolence, rash	Phase II (in hepatocellular carcinoma)
Cobimetinib (GDC-0973, XL-518, RG7421); Exelixis, USA and Hoffmann-La Roche, Switzerland	Elevated levels of lipase and CPK	Phase III (in melanoma)
E6201; Eisai, USA	QTc prolongation (grade 3) and confusion	Phase I
MEK162 (ARRY-438162); Array Biopharma, USA and Norvartis, Switzerland	Retinopathy, dermatitis, CPK elevation	Phase III (in melanoma, low-grade serous ovarian, fallopian tube, or peritoneal cancer)
PD0325901; Pfizer, USA	Rash, diarrhea, unsteady gait, fatigue, dizziness, confusion, blurry vision	Phase II (in NSCLC, CRC, and pancreatic cancer)
Pimasertib (AS703026, MSC1936369B); EMD Serono, USA	Liver function test elevation, retinal vein occlusion, skin rash, serous retinal detachment, and macular oedema	Phase II (in melanoma, CRC, pancreatic cancer, and ovarian cancer)
RO4987655 (CH4987655); Hoffmann-La Roche, Switzerland	Blurred vision and elevated CPK levels	Phase I
RO5126766 (CH5126766); Hoffmann-La Roche, Switzerland	Blurred vision and elevated CPK levels	Phase I
Selumetinib (AZD6244, ARRY-142,886); AstraZeneca, UK and Array Biopharma, USA	Rash, hypoxia, diarrhea, and xerostomia	Phase III (in NSCLC)
TAK-733; Takeda, Japan	Acneiform dermatitis, pustular rash	Phase I
Trametinib (GSK1120212); GlaxoSmithKline, UK	Rash, diarrhea and retinopathy	Phase III (in melanoma)
GDC-0623; Genentech, USA	CPK elevation, transient visual disturbance, dehydration, thrombocytopenia, retinal pigment epithelial detachment	Phase I
WX-554; Wilex, Germany	Not reported	Phase I/II

Table 3. MEK inhibitors in clinical trials. (See text for details)

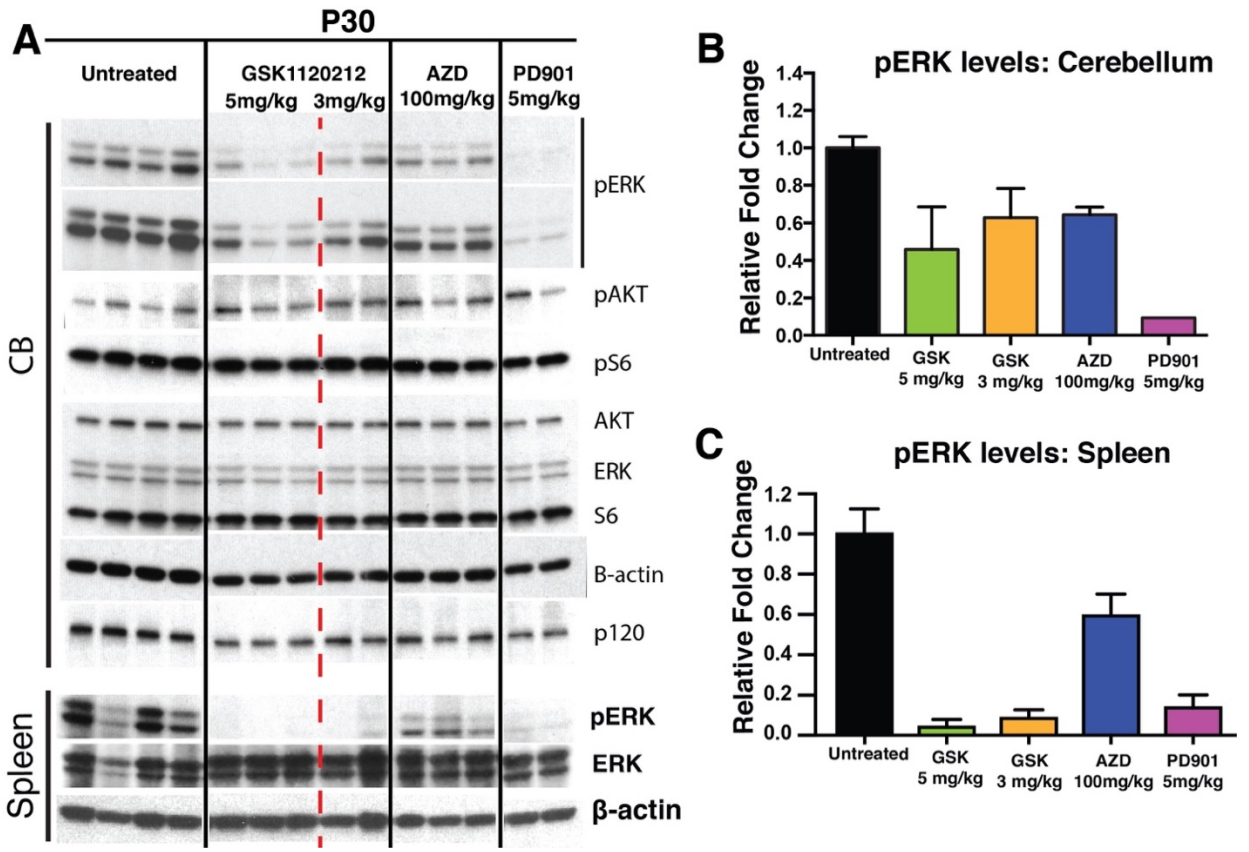

Figure 17. Comparison of three different MEKis administered by oral gavage to P30 wild-type mice

P30 wild-type mice were treated by oral gavage with a single dose of different MEKis at the following doses: GSK 5 or 3 mg/kg of body weight (BW), AZD 100 mg/kg BW and PD 5 mg/kg BW. Mice were sacrificed between 4-6hrs after treatment. Western blot (WB) analysis was performed on whole cerebellar lysates and spleen lysates from treated mice and compared to untreated wild-type to evaluate inhibition in downstream effectors of the RAS pathway **(A)**. Other pathways were not activated as evidence by no change in p-AKT and p-S6 levels. Each lane represents a sample from an individual animal. Quantification of the relative fold change in p-Erk level for each MEKi in the cerebellum **(B)** and the spleen **(C)**.

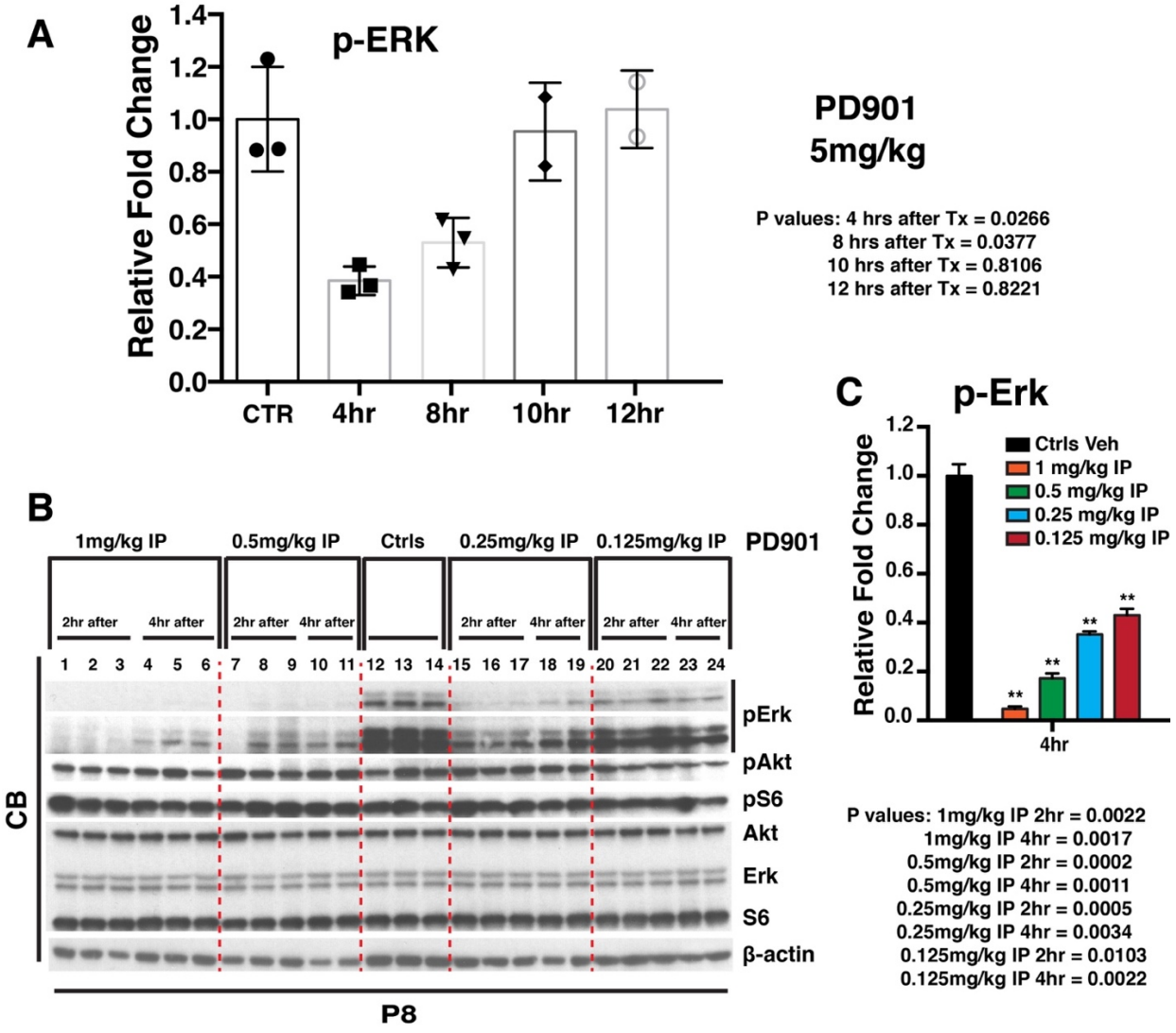

Figure 18. Time-course of MEK inhibition in the brain and degree of inhibition via IP injection

Quantification of relative fold change in p-Erk level in P8 pups after "MEKi in the milk" treatment with PD901 at 5 mg/kg BW and cerebella harvested at different time-points: 4, 8, 10, 12hrs for WB analysis **(A)**. Western blot analysis was performed on cerebella of P8 pups treated with PD901 at different doses via IP injection and collected at 2hrs and 4hrs after treatment **(B)**. Relative fold change in p-Erk level in the cerebellum in treated pups compared to untreated littermate controls 4hrs after treatment **(C)**. Asterisks denote statistically significant differences (** $p < 0.01$; paired t-test). All the data are presented as mean ± SEM.

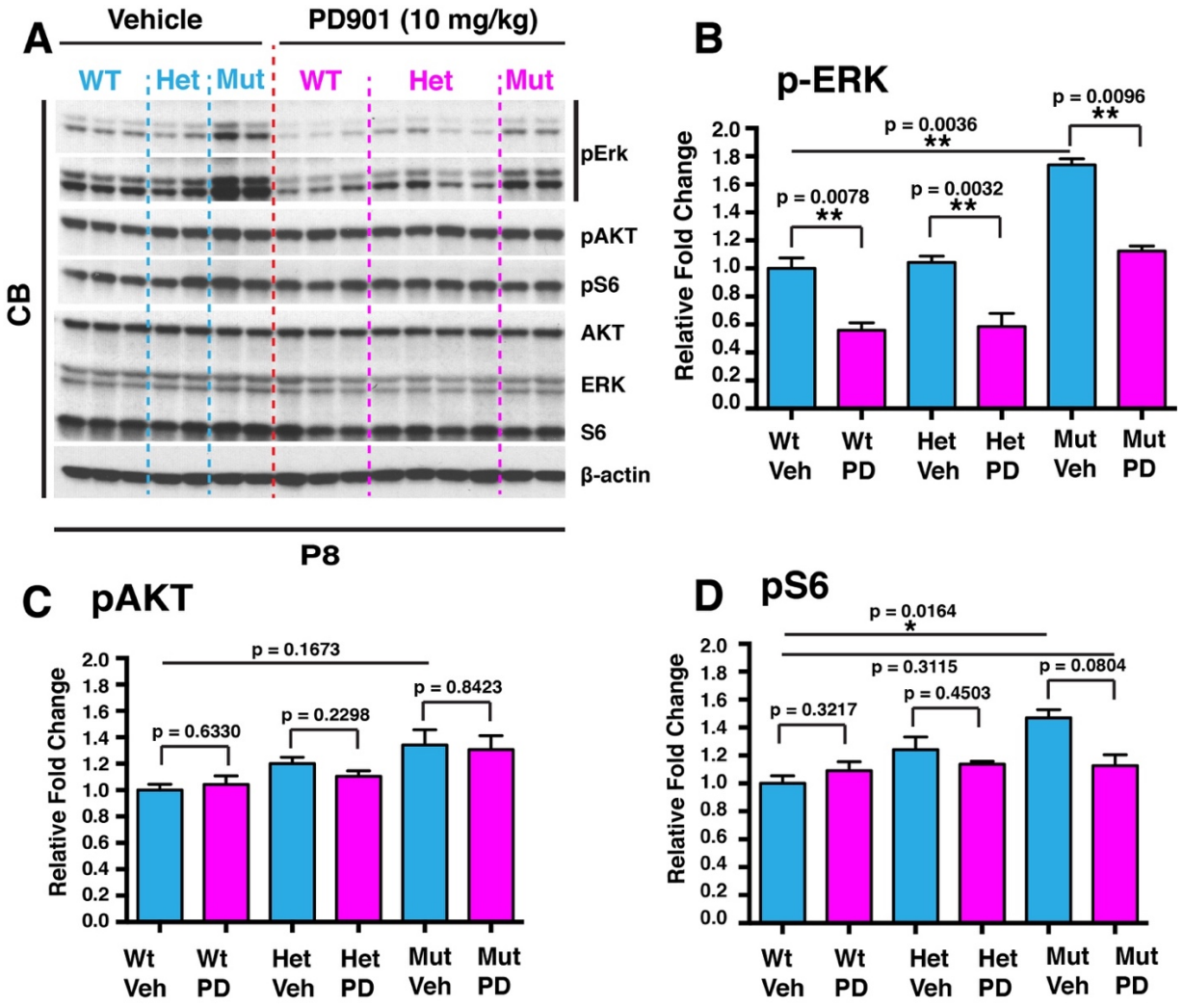

Figure 19. 10 mg/kg of PD901 can inhibit p-Erk in *Nf1*^{hGFAP}CKOs to the level of controls. Western blot analysis of cerebella of P8 pups from different genotypes (WT, Het, Mut) treated with either vehicle or 10 mg/kg PD901 via "MEKi in the milk" protocol **(A)**. Quantification of the relative fold change in p-Erk in the cerebellum revealed that this dose inhibits p-Erk activation in *Nf1*^{hGFAP}CKOs to the level of controls **(B)**. No significant change in p-AKT activation was detected in mutants before or after treatment **(C)**. Increase in pS6 level in *Nf1*^{hGFAP}CKOs was also inhibited with the treatment **(D)**. All the data are presented as mean ± SEM.

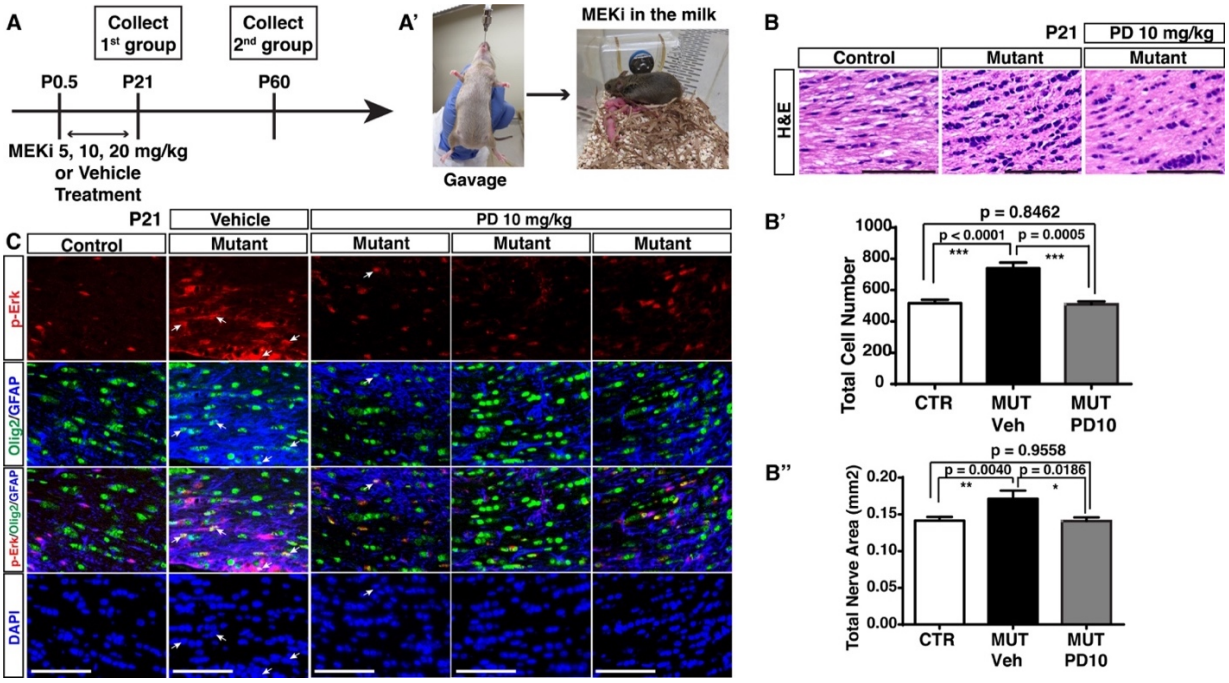

Figure 20. A three-week MEKi treatment rescues glia defects in the *Nf1*^{hGFAP}CKOs

Schematic representation of the P0.5-P21 "MEKi in the milk" PD901 treatment at different dosages. Cohorts of vehicle or PD treated mice were collected at either P21 (4hrs after last treatment) or 40 days later at P60 for long-term analysis **(A, A')**. H&E staining on paraffin sections of optic nerve of P21 vehicle-treated and 10 mg/kg PD-treated mice **(B)**. Quantification of the cell number **(B')** and optic nerve diameter **(B")** demonstrate complete rescue in PD-treated mutants versus vehicle-treated mutants. Triple labeling p-Erk/Olig2/GFAP staining on adjacent sections demonstrated that MEKi treatment inhibits ERK signaling and decreased the number of GFAP^{+}Olig2^{+} cells in the mutants **(C)**. All the data are presented as mean ± SEM. Scale bar: 50 μm.

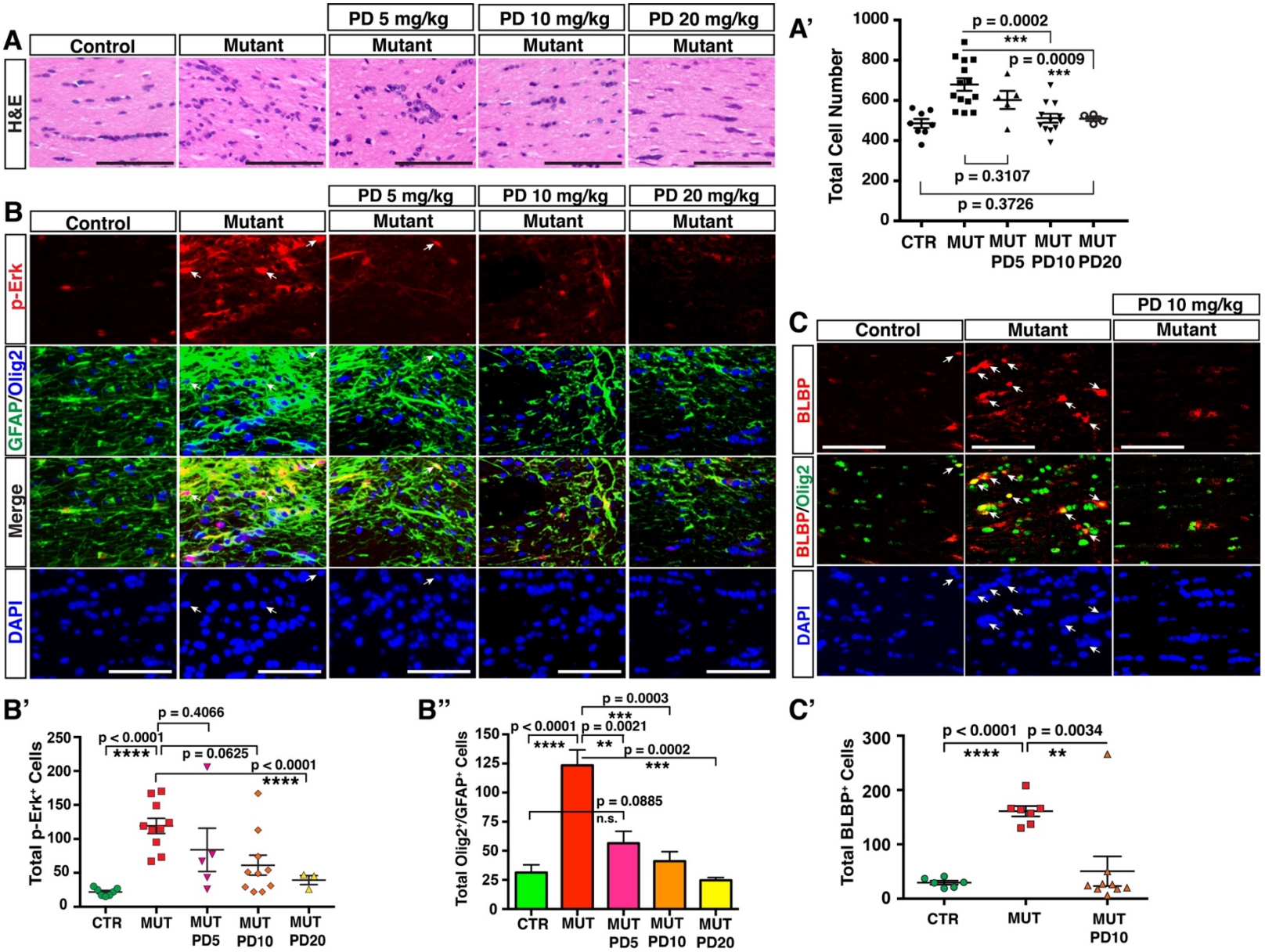
A
Control
Mutant
PD 5 mg/kg
Mutant
PD 10 mg/kg
Mutant
PD 20 mg/kg
Mutant
H&E
A'
Total Cell Number
p = 0.0002
***
p = 0.0009
***
p = 0.3107
p = 0.3726
CTR
MUT
MUT PD5
MUT PD10
MUT PD20
B
p-Erk
GFAP/Olig2
Merge
DAPI
C
PD 10 mg/kg
BLBP
BLBP/Olig2
DAPI
B'
Total p-Erk+ Cells
p = 0.4066
p < 0.0001
****
p = 0.0625
p < 0.0001
****
B''
Total Olig2+/GFAP+ Cells
p = 0.0003
***
p < 0.0001
****
p = 0.0021
**
p = 0.0002
***
p = 0.0885
n.s.
C'
Total BLBP+ Cells
p < 0.0001
****
p = 0.0034
**

Figure 21. Neonatal MEK inhibition provides long-term rescue of *Nf1*-associated glial defects in a dose-dependent manner.

Control and *Nf1*^{hGFAP}CKO mice were treated with vehicle or PD901 at different doses from P0.5–P21 and paraffin sections of the prechiasmatic optic nerve were analyzed by H&E at P60 **(A)**. The total cell number in controls, vehicle-treated mutants and 5, 10 and 20 mg/kg PD-treated mutants were quantified, respectively (**A′**). Triple labeling p-Erk/Olig2/GFAP staining was performed on adjacent sections **(B)**. Arrows highlight triple-positive (p-Erk^{+}Olig2^{+}GFAP^{+}) cells present in untreated P60 mutant nerves. The number of p-Erk^{+} cells **(B')** and Olig2^{+}GFAP^{+} cells **(B")** were quantified and compared. Optic nerves sections from controls, vehicle- and 10 mg/kg PD-treated mutants were stained for BLBP/Olig2 **(C)**. Arrows denote BLBP^{+}Olig2^{+} cells in vehicle-treated mutants. Quantification of BLBP^{+} cells in all three groups at P60 **(C')**. All the data are presented as mean ± SEM. Scale bar: 50 μm.

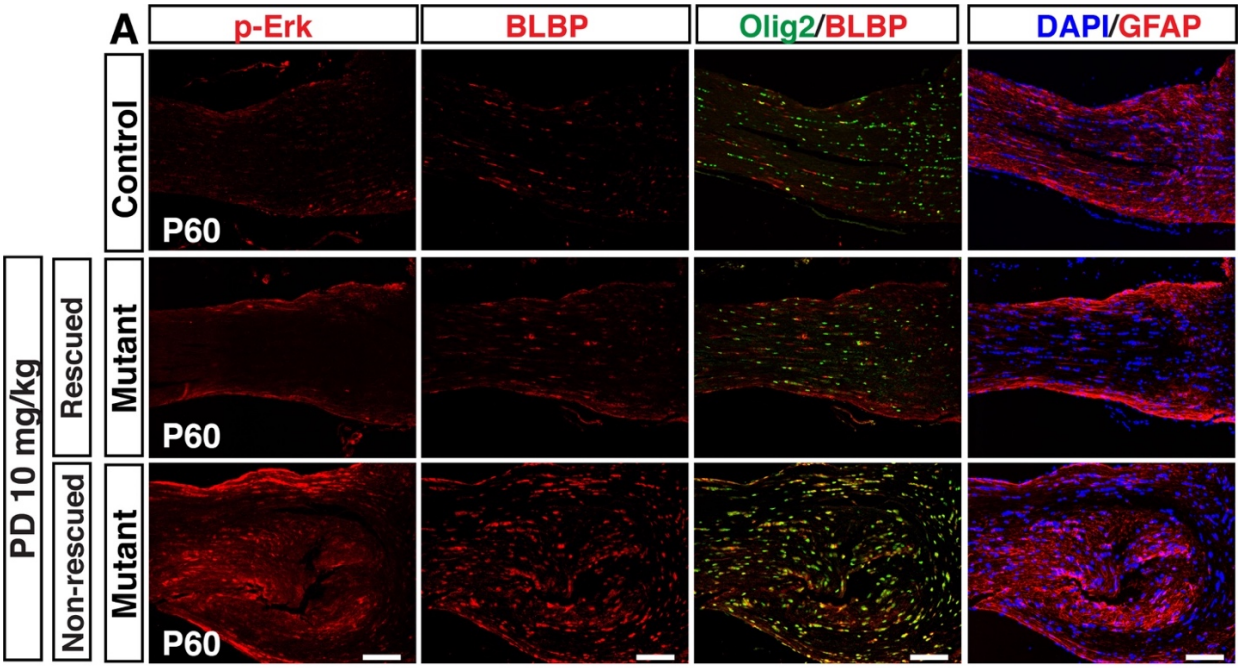

Figure 22. Correlation between decrease in p-Erk activation and long-term rescue of glia abnormalities after transient MEKi treatment.

Adjacent paraffin sections of optic nerves from controls and 10 mg/kg PD-treated mutants were strained for p-Erk, BLBP/Olig2 and GFAP **(A)**. There was a strong correlation between the degree of p-Erk inhibition (number of p-Erk^{+} cells) and the rescue in glial abnormalities 21 days after last treatment. DAPI labels the nuclei. Scale bar: 20, 50 μm.

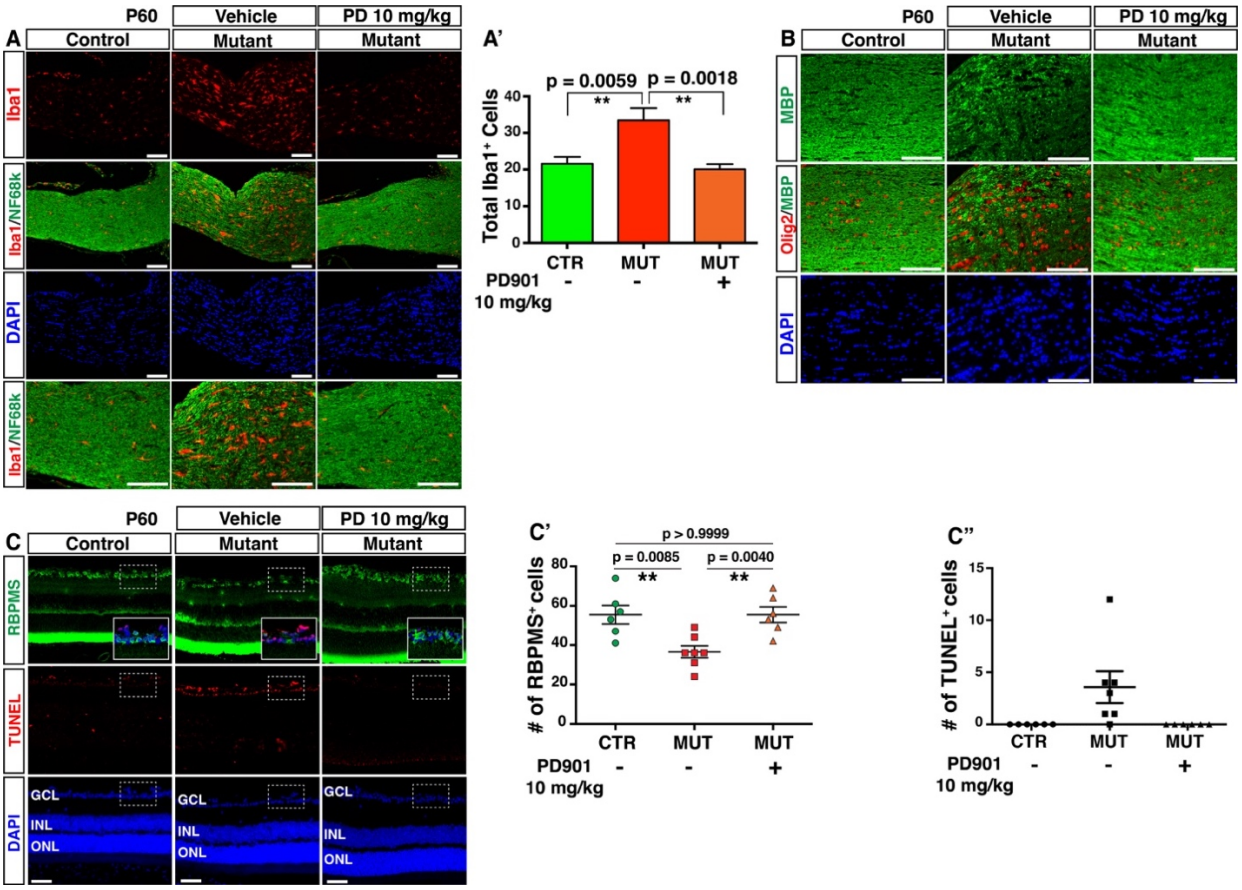

Figure 23. Transient MEKi treatment prevents nerve degeneration and neuronal loss in *Nf1*^{hGFAP}CKO mice.

Control and *Nf1*^{hGFAP}CKO mice were treated with vehicle or 10 mg/kg PD901 from P0.5–P21 and paraffin sections of the prechiasmatic optic nerve were analyzed for Iba1/NF68k at P60. The last row represents high magnification images highlighting rescue in microglia number/activation and neurofilament loss in PD-treated mutants compared to vehicle-treated mutants **(A)**. The total number of Iba1$^+$ cells in all three groups were quantified **(A')**. Double-labeling staining for MBP and Olig2 show complete rescue in myelin defect in PD-treated mice **(B)**. Sections of retinas were doubly labeled by RBPMS and TUNEL **(C)**. The insets are the high magnification images of the boxed areas representing TUNEL$^+$ cells in the GCL. The number of RBPMS$^+$ RGCs **(C')** and TUNEL$^+$ cells in the GCL were quantified respectively. All the data are presented as mean ± SEM. Scale bars: 5, 20, 50 μm.

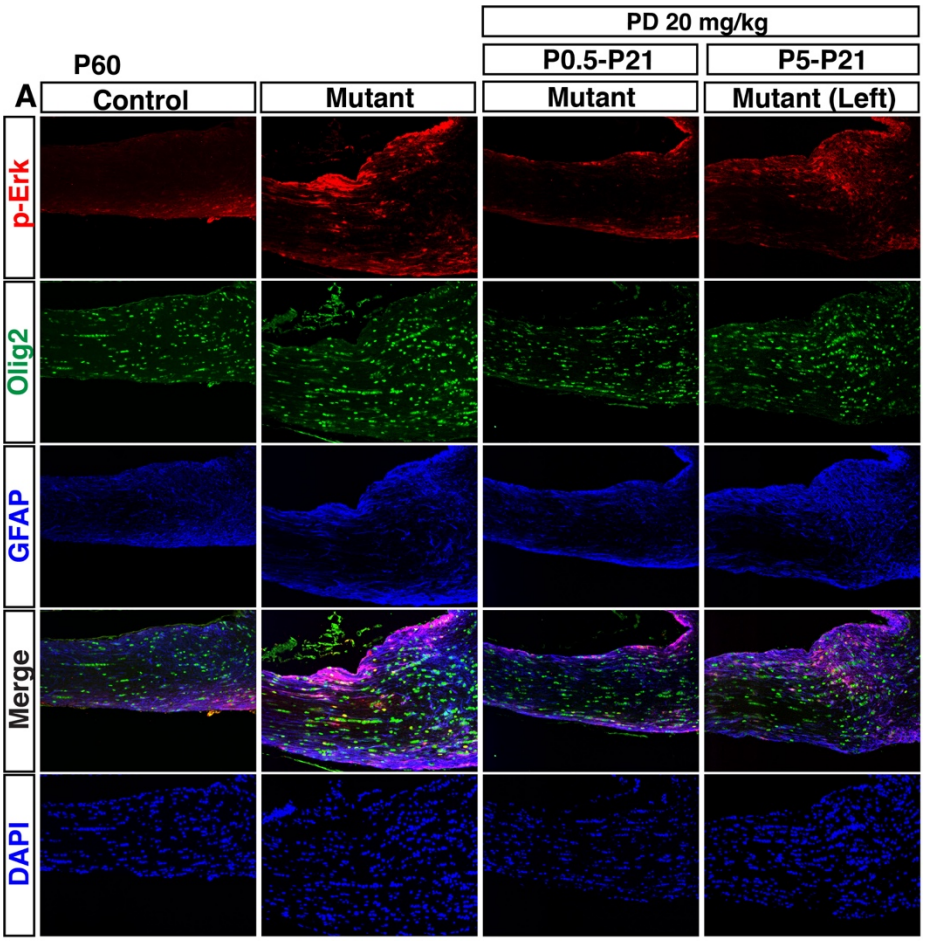
PD 20 mg/kg
P0.5-P21
P5-P21
P60
A
Control
Mutant
Mutant
Mutant (Left)
p-Erk
Olig2
GFAP
Merge
DAPI

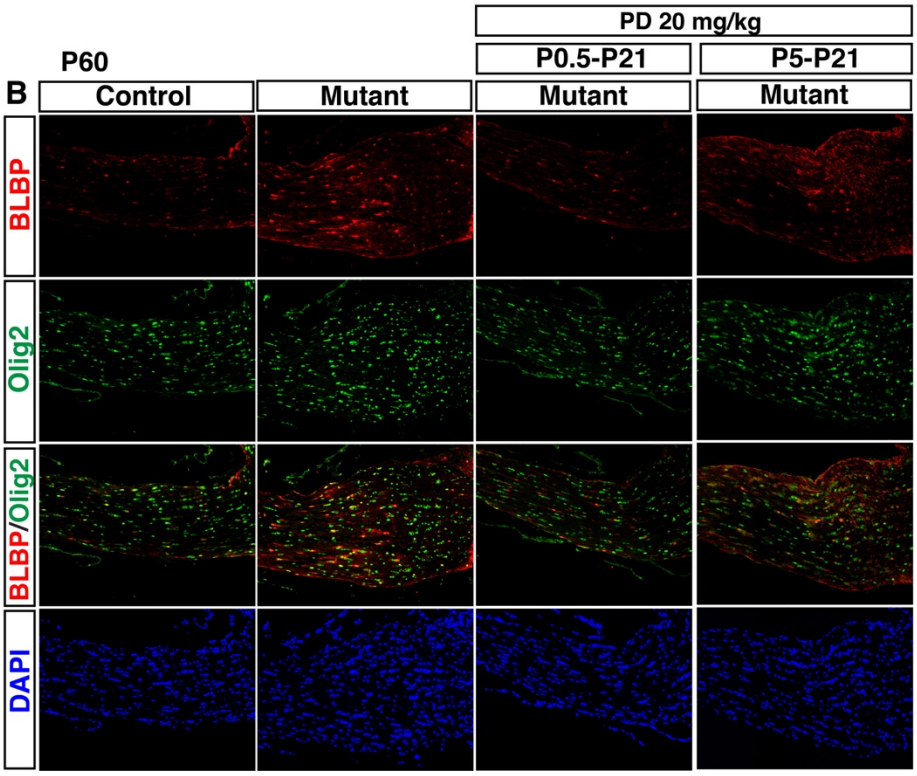
PD 20 mg/kg
P0.5-P21
P5-P21
P60
B
Control
Mutant
Mutant
Mutant
BLBP
Olig2
BLBP/Olig2
DAPI

Figure 24. The first postnatal week represents a critical time-point for *Nf1* requirement in the developing optic nerve.

Control and *Nf1*^{hGFAP}CKO mice were treated with 20 mg/kg PD901 from P0.5–P21 or P5-P21 and paraffin sections of the prechiasmatic optic nerve were triple labeled for p-Erk/Olig2/GFAP at P60 **(A)**. Adjacent sections were immunostained for BLBP/Olig2 and analyzed **(B)**. MEKi treatment initiated after the first postnatal week is not sufficient to rescue glial abnormalities in the mutant optic nerve. DAPI labels the nuclei.

3.4 References

Ballester, R., D. Marchuk, M. Boguski, A. Saulino, R. Letcher, M. Wigler, and F. Collins. 1990. 'The NF1 locus encodes a protein functionally related to mammalian GAP and yeast IRA proteins', *Cell*, 63: 851-9.

Brown, A. P., T. C. Carlson, C. M. Loi, and M. J. Graziano. 2007. 'Pharmacodynamic and toxicokinetic evaluation of the novel MEK inhibitor, PD0325901, in the rat following oral and intravenous administration', *Cancer Chemother Pharmacol*, 59: 671-9.

Fangusaro, Jason, Arzu Onar-Thomas, Tina Y. Poussaint, Shengjie Wu, Azra H. Ligon, Neal Lindeman, Anu Banerjee, Roger J. Packer, Lindsay B. Kilburn, Ian F. Pollack, Regina I. Jakacki, Ibrahim Qaddoumi, Paul G. Fisher, Girish Dhall, Patricia Baxter, Susan G. Kreissman, Clinton F. Stewart, Stefan M. Pfister, David T. W. Jones, Gilbert Vezina, Jessica Stern, Ashok Panigrahy, Blaise V. Jones, Zoltan Patay, Benita Tamrazi, Jeremy Y. Jones, Sofia S. Haque, David S. Enterline, Soonmee Cha, Laurence A. Doyle, Malcolm Smith, James M. Boyett, Ira J. Dunkel, and Maryam Fouladi. 2017. 'LGG-08. A PHASE II PROSPECTIVE STUDY OF SELUMETINIB IN CHILDREN WITH RECURRENT OR REFRACTORY LOW-GRADE GLIOMA (LGG): A PEDIATRIC BRAIN TUMOR CONSORTIUM (PBTC) STUDY', *Neuro-Oncology*, 19: iv34-iv35.

Gilmartin, A. G., M. R. Bleam, A. Groy, K. G. Moss, E. A. Minthorn, S. G. Kulkarni, C. M. Rominger, S. Erskine, K. E. Fisher, J. Yang, F. Zappacosta, R. Annan, D. Sutton, and S. G. Laquerre. 2011. 'GSK1120212 (JTP-74057) is an inhibitor of MEK activity and activation with favorable pharmacokinetic properties for sustained in vivo pathway inhibition', *Clin Cancer Res*, 17: 989-1000.

Hanahan, D., and R. A. Weinberg. 2000. 'The hallmarks of cancer', *Cell*, 100: 57-70.

Jones, D. T. W., M. W. Kieran, E. Bouffet, S. Alexandrescu, P. Bandopadhayay, M. Bornhorst, D. Ellison, J. Fangusaro, M. J. Fisher, N. Foreman, M. Fouladi, D. Hargrave, C. Hawkins, N. Jabado, M. Massimino, S. Mueller, G. Perilongo, A. Y. N. Schouten van Meeteren, U. Tabori, K. Warren, A. J. Waanders, D. Walker, W. Weiss, O. Witt, K. Wright, Y. Zhu, D. C. Bowers, S. M. Pfister, and R. J. Packer. 2018. 'Pediatric low-grade gliomas: next biologically driven steps', *Neuro Oncol*, 20: 160-73.

Kim, E., Y. Wang, S. J. Kim, M. Bornhorst, E. S. Jecrois, T. E. Anthony, C. Wang, Y. E. Li, J. L. Guan, G. G. Murphy, and Y. Zhu. 2014. 'Transient inhibition of the ERK pathway prevents cerebellar developmental defects and improves long-term motor functions in murine models of neurofibromatosis type 1', *Elife*, 3.

Messersmith, W. A., M. Hidalgo, M. Carducci, and S. G. Eckhardt. 2006. 'Novel targets in solid tumors: MEK inhibitors', *Clin Adv Hematol Oncol*, 4: 831-6.

Niihori, T., Y. Aoki, Y. Narumi, G. Neri, H. Cave, A. Verloes, N. Okamoto, R. C. Hennekam, G. Gillessen-Kaesbach, D. Wieczorek, M. I. Kavamura, K. Kurosawa, H. Ohashi, L. Wilson, D. Heron, D. Bonneau, G. Corona, T. Kaname, K. Naritomi, C. Baumann, N. Matsumoto, K. Kato, S. Kure, and Y. Matsubara. 2006. 'Germline KRAS and BRAF mutations in cardio-facio-cutaneous syndrome', *Nat Genet*, 38: 294-6.

Ohren, J. F., H. Chen, A. Pavlovsky, C. Whitehead, E. Zhang, P. Kuffa, C. Yan, P. McConnell, C. Spessard, C. Banotai, W. T. Mueller, A. Delaney, C. Omer, J. Sebolt-Leopold, D. T. Dudley, I. K. Leung, C. Flamme, J. Warmus, M. Kaufman, S. Barrett, H. Tecle, and C. A.

Hasemann. 2004. 'Structures of human MAP kinase kinase 1 (MEK1) and MEK2 describe novel noncompetitive kinase inhibition', *Nat Struct Mol Biol*, 11: 1192-7.

Rodriguez-Viciana, P., O. Tetsu, W. E. Tidyman, A. L. Estep, B. A. Conger, M. S. Cruz, F. McCormick, and K. A. Rauen. 2006. 'Germline mutations in genes within the MAPK pathway cause cardio-facio-cutaneous syndrome', *Science*, 311: 1287-90.

Sebolt-Leopold, J. S., D. T. Dudley, R. Herrera, K. Van Becelaere, A. Wiland, R. C. Gowan, H. Tecle, S. D. Barrett, A. Bridges, S. Przybranowski, W. R. Leopold, and A. R. Saltiel. 1999. 'Blockade of the MAP kinase pathway suppresses growth of colon tumors in vivo', *Nat Med*, 5: 810-6.

Sebolt-Leopold, J. S., and R. Herrera. 2004. 'Targeting the mitogen-activated protein kinase cascade to treat cancer', *Nat Rev Cancer*, 4: 937-47.

Wang, Y., E. Kim, X. Wang, B. G. Novitch, K. Yoshikawa, L. S. Chang, and Y. Zhu. 2012. 'ERK inhibition rescues defects in fate specification of Nf1-deficient neural progenitors and brain abnormalities', *Cell*, 150: 816-30.

Yeh, T. C., V. Marsh, B. A. Bernat, J. Ballard, H. Colwell, R. J. Evans, J. Parry, D. Smith, B. J. Brandhuber, S. Gross, A. Marlow, B. Hurley, J. Lyssikatos, P. A. Lee, J. D. Winkler, K. Koch, and E. Wallace. 2007. 'Biological characterization of ARRY-142886 (AZD6244), a potent, highly selective mitogen-activated protein kinase kinase 1/2 inhibitor', *Clin Cancer Res*, 13: 1576-83.

Chapter IV: Discussion and Future Directions

4.1 NF1 serves as a potent regulator of gliogenesis during optic nerve development

Besides the loss of the remaining *NF1* wild-type allele (LOH) in NF1 patients who already sustain germline *NF1* heterozygous mutations, there is limited knowledge about the genetic and molecular basis for NF1-OPG disease pathogenesis. One of the main objectives of my thesis project is to determine the cellular and molecular mechanisms underlying *Nf1* loss in the developing optic nerve that induce tumor formation and neurological deficits at later stages. By using two independent genetic systems (conventional CKOs and MADM CKO) under the hGFAP-cre promoter, I demonstrated in Chapter II that *Nf1* loss lead to Erk-dependent abnormal glial cell expansion in the optic nerve during neonatal development. The phase I glial abnormalities are followed by a second phase of NF1-OPG disease progression characterized by immune cell infiltration and activation, axonal degeneration, myelin loss and Bax-dependent, progressive apoptosis of RGCs. These observations suggest that *Nf1*-dependent glial defects are directly responsible for tumor initiation and progression and represent an attractive target for preventative and early interventional therapies. In Chapter III, I tested this possibility by using MEK inhibitors to treat the glial defects during a critical developmental window (P0.5-P21). This treatment protocol resulted in long-term benefits by preventing nerve damage and RGC loss. Collectively, these results indicate that transient, glial restricted precursor cells ($Pax2^{+}Olig2^{+}$ that differentiate into $GFAP^{+}Olig2^{+}$ cells and $BLBP^{+}Olig2^{+}$ cells) are the cellular compartment most susceptible to *Nf1* deficiency.

4.1.1 A case for glial restricted progenitors as the cell of origin of *Nf1*-OPG

In patients with familiar cancer syndromes like NF1, even though every cell harbors the initial mutation “first-hit”, only biallelic inactivation in a specific cell type can trigger tumor formation. In the context of NF1-OPG, the early childhood-onset of the disease suggests that the

somatic "second-hit" event must occur in early stem and/or precursor cells during a critical window of optic nerve development. Therefore, identification of this "putative" cell of origin susceptible to *NF1* loss could provide valuable insights for understanding disease pathogenesis and for developing rational therapeutic strategies. Due to the substantial self-renewal and multilineage capacities possessed by developing neural stem cell (NSC) populations, they have been proposed as the cell of origin of NF1-OPG. In support of this theory, it was demonstrated that *Nf1* heterozygosity ($Nf1^{+/-}$) and absence ($Nf1^{-/-}$) in NSCs increased stem cell proliferation *in vitro* and *in vivo* (Dasgupta and Gutmann 2005). Additionally, Chen et al. reported that neurofibromin regulates NSC differentiation and multilineage differentiation through different arms of RAS downstream effector pathways (Chen, Gianino, and Gutmann 2015). Through the use of *Nf1* GEM and pharmacological inhibition, they showed that neurofibromin controls NSC proliferation through the PI3K/AKT pathway, but multilineage differentiation was MEK-ERK dependent. Furthermore, successful isolation of tumor cells with stem cell features (cancer stem cells) such as expression of CD133 from a mouse model of low grade glioma suggests NSCs as the cell of origin (Chen et al. 2015). Additional evidence supporting the NSC origin *Nf1*-OPG came from the same research group. By comparing NSCs from germinal zones in the lateral ventricle and the third ventricle, they showed that only NSCs from the III-VZ display increase proliferation following mutations characteristic of childhood glioma. Next, they reported that OPG developed in a GFAP-cre^{ER} mouse model only when *Nf1* mutation was introduced at E16.5, but not after postnatal stage (Lee, Gianino, and Gutmann 2012). Based on these observations, they concluded that the III-VZ NSCs was the source of mouse *Nf1*-OPG. However, the cells that initially acquire the mutation may not necessarily be the cell of origin. Therefore, it remains unclear whether NSCs or their more restricted glial progeny are the most susceptible to *Nf1* loss and represent the actual cell of origin. Although it is difficult to distinguish the cell of origin, the natural history of NF1-OPGs as slowly progressing benign tumors suggests that they are more likely to arise from glial restricted progenitors (GRPs) during postnatal development instead of NSCs from early embryonic stages.

Many of the features that make NSCs susceptible to oncogenic mutations are also shared by GRPs such as oligodendrocyte precursor cells (OPCs). In both adult rodent and human brains, OPCs make up the largest proliferative cell population (Dawson et al. 2003; Geha et al. 2010).

During early developmental stages, OPCs have been found to express common stem cell markers nestin and Sox2. Remarkably, OPCs isolated from the rodent optic nerve acquire multipotent NSC-like features when reprogrammed under in vitro conditions (Kondo and Raff 2000). Olig2 expression was shown to be both necessary and sufficient in directing SVZ progenitors toward glial fates, while preventing neuronal differentiation, in neonatal and adult brain (Marshall, Novitch, and Goldman 2005; Menn et al. 2006). OPCs have been shown to be particularly sensitive to neurofibromin loss. Dr. Ratner's group showed that *Nf1* mutation alone was sufficient to promote OPC proliferation in mice (Bennett et al. 2003). In the adult hippocampus, NF1 has been shown to suppress the OPC lineage potential of NSCs (Sun et al. 2015). Importantly, our lab demonstrated that *Nf1* suppresses Olig2 expression in neonatal and adult SVZ progenitor cells (Wang et al. 2012). Thus, *Nf1* functions as a negative regulator of Olig2 specifically in both neonatal and adult brain.

Examination of the effect of *Nf1* loss during early postnatal stages in our lab has revealed several intriguing findings. hGFAP-cre is known to be expressed in multi-potent radial glial cells in the dorsal brain. However, our findings indicate that cre expression is restricted to glia precursors already committed to the glial lineage in the ventral brain, including the III-VZ. Furthermore, embryonic analysis uncovered that cre-mediated recombination does not occur until E15.5 in the optic nerve, long after the neuronal-to-glial transition of neural stem cells in the ventral forebrain (E12.5). Our unpublished findings revealed that embryonic *Nf1* inactivation leads to the expansion of $BLBP^{+}Olig2^{+}$ progenitors from the ventral brain which then migrate into the nerve. Astrocytes in the optic nerve, unlike brain-derived oligodendrocytes, arise form locally generated neuroepithelial cells that produce APCs. These optic nerve-derived APCs only differentiate into mature astrocytes in the direction from the eye to the brain. In the developing nerve, *Nf1* loss results in Erk-dependent transcriptional activation of Olig2 in $Pax2^{+}$ APCs. $Pax2^{+}Olig2^{+}$ cells later differentiate into $GFAP^{+}Olig2^{+}$ cells (unpublished findings from Zhu laboratory). Taken together, these data suggest that glial progenitor populations are the most affected by *Nf1* deficiency. My study further extends the consequences from these findings in OPG formation. By studying the optic nerve at different time-points during development (P15, P21, P60, and 6 months or older), I determined that $GFAP^{+}Olig2^{+}$ and $BLBP^{+}Olig2^{+}$ cells represent transient populations that are present in the normal nerve during a short, early developmental window and become rare later on.

However, these cells are maintained throughout gliomagenesis in *Nf1* mutant nerves and are the most expanded cellular compartment in late-stage tumors. The MADM system has provided the definitive evidence that *Nf1* inactivation gave a growth advantage to Olig2 cells. Indeed, Olig2$^+$ cells were overexpanded in MADM OPGs and contributed to an astonishing 75% in the increased cell number in mutant (red) cells compared to only 31% of the wild-type cells (green). Similarly, the percentage of mutant cells in the Olig2 population rose to 33% compare to the 3% of wild-type cells in the same population. These findings suggest over proliferation of Olig2$^+$ cells as a major underlying mechanism for overabundance of glia. It also suggests that Olig2 cells are the most sensitive cellular compartment to *Nf1* inactivation. Pediatric gliomas such as NF1-OPGs are classified as neurodevelopmental disorders based on their cellular composition, growth environment, early timing of development and low proliferation rates. Consistently, the rate of proliferation in the *Nf1*^{hGFAP}CKO mice was highest at P15 (about 10%) but decreased dramatically at P21 and later stages (~ 1%). Together with the observation that the proportion of abnormal glial cells does not significantly fluctuate over time, these results indicate that the glial abnormalities are established during a specific window of neonatal development, mimicking the early childhood-onset of the human disease. They also suggest a clear requirement for neurofibromin to serve as a potent regulator of gliogenesis during early optic nerve development.

4.1.2 Understanding the mechanism underlying the generation of GFAP$^+$Olig2$^+$ double-positive glial cells in the developing optic nerve

Previous studies have reported an abnormal increase of glial cells in *Nf1*-deficient mouse brain (Dasgupta and Gutmann 2005; Zhu et al. 2005; Hegedus et al. 2007). In the neonatal forebrain, *Nf1* was found to regulate fate specification in neuroglial progenitor. Specifically, *Nf1* functions as a negative regulator of Olig2 in SVZ Ascl1$^+$ cells to repress glial fate determination (Wang et al. 2012). In the ventral brain, *Nf1* loss only results in increase OPC proliferation at E17.5, after the neuronal-to-glial transition of neural stem cells but not at E15.5 (unpublished data from Dr. Miriam Bornhorst). Therefore, neurofibromin acts to regulate OPC proliferation during embryonic development in the ventral brain, including III-VZ. However, little is known about the role of neurofibromin on optic nerve-derived glial progenitor cells. Findings from the early postnatal study in our lab revealed glial cell expansion accompanied by increase cell proliferation

in optic nerve of *Nf1*^{hGFAP}CKO mice at P0.5, when the first wave of OPCs begin to migrate in the distal portion of the nerve. In fact, the expansion of Pax2^{+} APCs in the mutants stemmed from an increase in Pax2^{+}Olig2^{+} cells at the expense of Pax2^{+}Olig2^{-} cells. Pax2^{+} cells later differentiate into GFAP^{+} astrocytes and retain abnormal Olig2 expression (GFAP^{+}Olig2^{+}) in the *Nf1* mutants. These findings are more consistent with a model where *Nf1* loss results in two critical events in the developing nerve: 1- Pax2^{+} APCs ectopically acquire Olig2 expression and 2- Pax2^{+}Olig2^{+} cells transiently expand during neonatal stages and differentiate into abnormal GFAP^{+}Olig2^{+} cells. However, the fact the expansion of Pax2^{+}Olig2^{+} cells coincides with the time when the first wave of OPCs start to migrate in the optic nerve from the brain at P0.5 coupled with the knowledge that hGFAP-cre targets both astrocyte and oligodendrocyte lineages make it harder to dissect the exact phenotypic consequence of *Nf1* loss on locally arising astrocytic lineage cells. Therefore, GFAP^{+}Olig2^{+} cells could conceivably arise by non-cell autonomous mechanism of *Nf1* inactivation on the astrocytic lineage triggered by the influx of mutant Olig2 cells. One way to address this possibility is to target *Nf1* mutation specifically in the astrocyte or oligodendrocyte lineage by different genetic strategies. To target the astrocyte lineage specifically in the nerve, we could use the Pax-cre promoter which is specifically expressed in APCs (Ohyama and Groves 2004). In this model, the Olig2^{+} cells coming from the brain will remain wild-type and thus should not impact the nerve-derived APCs. Analysis of neonatal optic nerve from these *Nf1*^{Pax2}CKOs at P0.5 could reveal the effect of neurofibromin loss on the astrocyte lineage alone and elucidate their potential to generate GFAP^{+}Olig2^{+} cells. Alternatively, we could use an inducible Cre/estrogen receptor fusion strain under the Olig2 promoter (Olig2-cre^{ER}) to inactivate *Nf1* in the oligodendrocyte lineage at specific developmental time-points (Ono et al. 2008). By administering Tamoxifen injection at E17.5, we could target *Nf1* mutation in Olig2^{+} cells in the ventral brain before they enter the optic nerve. These two genetic strategies will allow us to investigate the mechanisms by which *Nf1*-deficient astrocyte and oligodendrocyte lineage cells cooperatively and individually contribute to OPG formation.

Finally, due to paucity of human NF1-OPGs tissues, it is unclear whether GFAP^{+}Olig2^{+} cells are a feature of the human disease. OLIG2 is expressed in human ventral neural progenitor cells and oligodendroglia (Ligon et al. 2004). Historically, NF1-OPGs have been classified as pilocytic astrocytomas based of the strong immunostaining for GFAP. However, numerous recent

studies have shown that a significant proportion of gliomas show ambiguous histological features that make classification as either oligodendroglial or astrocytic difficult. In fact, pilocytic astrocytomas, diffuse low-grade astrocytomas (grade II) and anaplastic astrocytomas (grade III) all contained numerous $OLIG2^{+}$ cells with large irregular nuclei within the dense fibrillary areas (Ligon et al. 2004; Reis et al. 2013; Mokhtari et al. 2005). Likewise, semi-quantitative RT-PCR analysis and in situ hybridization demonstrated that pilocytic astrocytomas contain the highest expression of OLIG2 genes (Bouvier et al. 2003). Strong co-expression of GFAP and Olig2 was found in gliomas that contain gliofibrillary features (Preusser et al. 2007). The neurodevelopmental basis for NF1-OPGs and their benign nature make it very unlikely that expression of OLIG2 is aberrant in these tumors and results from genomic instability or rearrangements. In the future, it would be helpful to obtain samples of PAs from other brain sites (cerebellum, brainstem) in NF1 patients in order to validate the presence of $GFAP^{+}OLIG2^{+}$ double-positive cells.

4.1.3 The natural history of *Nf1*-OPG in the mouse offers a window of opportunity for therapeutic treatment.

The majority of NF1-OPGs are diagnosed in children before the age of 6 years. Of these patients, less than half will develop vision loss. As a consequence, initial management typically involves close observation. When therapy is advised, chemotherapy is usually the treatment of choice. There is currently no general consensus regarding treatment protocol for the disease. Some clinicians advocate treatment when there is radiographic progression or visual deterioration. On the other hand, the remaining health care professionals promote treatment only for patients with documented visual deterioration. Much of the confusion stems from the heterogeneous nature of disease progression in NF1-OPG patients and the lack of reliable markers to predict which patients will develop vision loss. Furthermore, there is a poor correlation between radiographic response and visual acuity outcomes with only a third of chemotherapy-treated patients showing improvement in vision (Fisher et al. 2012). Since chemotherapy is not expected to regenerate RGCs or re-establish neuronal circuits, the most critical challenge for the field is to develop preventive or early interventional therapies before irreversible neurological deficits such as axonal degeneration and RGC loss occur (Listernick 2016). In Chapter II, I used the *Nf1*^{hGFAP}CKO mice to delineate the cellular and molecular events that underlie *Nf1*-OPG development and vision loss

and identify critical window for neuroprotective intervention. First, I showed that *Nf1*-associated glial defects are established during early neonatal development. Specifically, aberrant $GFAP^{+}Olig2^{+}$ cells that activate the RAS-Erk signaling pathway and increased glial progenitors are evident at P15 in $Nf1^{hGFAP}$CKO optic nerves and persist throughout gliomagenesis (P21, P60 and 6 months or older). Although increased microglia infiltration was observed in mutant nerves as early as P15, it did not result in immediate nerve damage. Accordingly, no increase in apoptosis or RGC loss was detected in P21 $Nf1^{hGFAP}$CKO retinas. About forty days later, there were clear signs of nerve damage in optic nerves of P60 *Nf1* mutants as evidence by patterns of misaligned optic nerves fibers and axonal and myelin loss. The resulting RGC loss in mutant retinas was progressive over time with ~40% decrease relative to normal retinas at P60 and culminating to 60% loss in aged mutants. By crossing the $Nf1^{hGFAP}$CKO mice with $Bax^{-/-}$ mutants, I demonstrated that the mechanism of progressive RGC loss in tumor bearing $Nf1^{hGFAP}$CKOs is dependent on Bax-mediated apoptosis. Collectively, my findings provide a specific temporal sequence of events that underlie OPG progression following abnormal glial expansion (Phase I), from immune infiltration to RGC degeneration (Phase II). Furthermore, I established that the first three weeks of postnatal development represent a critical window for therapeutic intervention before neuronal loss. However, it remains unclear how the phase I glial abnormalities can lead to subsequent nerve degeneration.

One possible explanation could be a cross talk between neoplastic cells and microglia. It is well documented that gliomas microenvironment is composed of neoplastic and non-neoplastic cells that contribute to cancer formation, progression and response to treatment. In PAs, the percentage of microglia can be as high as 35% to 50% (Gutmann et al. 2013). Numerous studies using models of pharmacological (minocycline, c-Jun-NH(2)-kinase inhibition) or genetic inactivation (ganciclovir treatment of CD11b−thymidine kinase–expressing mouse line, CX3CR1) have established the critical role of microglia in mediating glioma formation and maintenance (Daginakatte and Gutmann 2007; Daginakatte et al. 2008; Simmons et al. 2011; Pong et al. 2013). Gliomas are known to attract microglia and reprogram them into immunosuppressive, pro-invasive cells. There are many factors that mediate microglia chemoattraction such as chemokines, cytokines, growth factors, neurotransmitters and ATP. However, the distinct factors that recruit microglia to the tumor site are currently unknown. One potential player could be monocyte

chemoattractant protein-1 (MCP-1), also known as CCL2. Indeed, ectopic expression of CCL2 in rat glioma cells resulted in a three-fold increase in tumor size (Platten et al. 2003). CX3CR1 (the receptor for the cytokine CX3CL1), another potent microglia chemoattractant, is mostly expressed by microglial cells and is critical for neuron-microglia communication (Paolicelli, Bisht, and Tremblay 2014). Genetic inhibition of CX3CR1 delays glioma formation in a mouse model of *Nf1*-OPG. The growth factor glial cell–derived neurotrophic factor (GDNF) is secreted by both mouse and human gliomas and has been shown to be a strong chemoattractant for microglia (Ku et al. 2013). Colony stimulating factor 1 (CSF-1) is another microglia chemoattractant secreted by glioma cells that is capable of converting microglia into a pro-tumorigenic phenotype. Inhibition of its receptor, CSF-1R, decreased the number of tumor-associated microglia (TAM) and inhibited glioblastoma invasion (Coniglio et al. 2012). Lastly, granulocyte-macrophage colony-stimulating factor (GM-CSF) was shown to recruit and activate microglia and thereby promote glioma growth (Sielska et al. 2013). Collectively, these studies help to establish that a critical step in creating a supportive microenvironment for tumor growth involves microglial recruitment and activation. In turn, glioma-associated microglia can secrete a large number of cytokines, interleukins, and growth factors (such as IL-6, TGFβ, TNFα, STI1) to directly stimulate glioma cell growth and invasion.

The observation that there is a temporal window between microglia infiltration/activation and axonal loss opens the possibility that microglia recruited by the neoplastic cells release soluble factors that promote nerve damage. To investigate this hypothesis, we could perform an assay for cytokines using a Multi-Analyte ELIS Array kit (Qiagen, CA, USA) to check the concentration of 12 inflammatory cytokines (IL1-α, IL-1β, IL-2, IL-4, IL-6, IL-10, IL-12, IL-13, IFNγ, TNF-α, GM-CSF, and RANTES) in tissue supernatant from P21-P30 *Nf1* mutant nerves compared to age-matched littermate controls. These experiments would enable us to explore the mechanism for the delay from abnormal cell expansion to nerve degeneration and the role of microglia in tumor progression. Additionally, anatomical assays such as optical coherence tomography (OCT), retinal nerve fiber layer (RNFL) and ganglion cell complex (GCC) thickness can provide automated, high resolution *in vivo* quantification of the relationship between RGC axon number and cell survival to further delineate the time course of visual impairment during OPG progression. Due to their important role in influencing tumor growth, microglia represent an attractive target for incorporation into future clinical therapies for low grade gliomas.

4.2 MEK-ERK signaling is the major signaling pathway underlying *Nf1*-OPG formation.

The RAS-MEK-ERK pathway is known to play a critical role in cell proliferation, differentiation and function. In the mammalian spinal cord, oligodendrocyte proliferation was shown to be at least partially controlled by RAS-Erk signaling pathway (Newbern et al. 2011). Li et al. have shown that blockage of MAPK signaling pathway through genetic deletion of *Mek1/2* prevents the generation of OPCs in the developing cortex (Li et al. 2012). Several studies have also implicated a role for the signaling pathway in regulating *Nf1*-deficient neural progenitor cell growth and differentiation in the forebrain and the cerebellum (Sanchez-Ortiz et al. 2014; Wang et al. 2012; Kim et al. 2014). Specifically, our lab has shown that neurofibromin regulates Olig2 expression in SVZ Ascl1$^+$ cells through RAS-Erk signaling. In my study, I have shown that MAPK pathway activation is associated with glial abnormalities (GFAP$^+$Olig2$^+$, BLBP$^+$) in *Nf1*^{hGFAP}CKOs throughout gliomagenesis. Furthermore, I demonstrated that MAPK pathway activation is the main/sole molecular mechanism responsible for optic gliomagenesis. This conclusion is based on clear-cut in vivo findings in genetically induced loss of function model (*Mek1/2* genetic inactivation) and MEK pharmacological inhibition in the *Nf1*^{hGFAP}CKO mice. First, I crossed the *Nf1* mutants with *Mek1/2* mice with different levels of genetic inactivation. Three alleles *Mek1/2* deletion prevented nerve enlargement and abnormal glial cell increase in aged *Nf1*^{hGFAP}CKO mice. Importantly, the rescue in glial abnormalities such as GFAP$^+$Olig2$^+$ cells and BLBP$^+$ progenitors were correlated with decreased MEK-Erk activation. Of note, there was a dose-dependent rescue in *Nf1*-OPG phenotypes corresponding to increasing number of wild-type *Mek1/2* alleles. When 2 alleles of *Mek1/2* were deleted (M2), less than half of the M2 mutants (4 out of 9, 44%) were rescued, with a further decrease to 38% rescued with one allele deletion (M3). Consistently, the degree of rescue in M2 and M3 mutants was associated the levels of phosphorylated Erk protein (low number of p-Erk$^+$ cells correlated to complete rescue of tumor phenotype). Finally, I also observed a dose-dependent rescue in nerve degeneration and RGC apoptosis corresponding to degree of *Mek1/2* inactivation. These results demonstrate that MEK-ERK signaling is essential in regulating gliogenesis in the developing optic nerve and raise significant clinical implications for optic glioma treatment (Figure 25).

Based on the successful use of MEK inhibitors to rescue forebrain and cerebellum defects in *Nf1*^{hGFAP}CKO mice, I then investigated the potential for pharmacological MEK inhibition in the prevention and treatment of *Nf1*-OPGs. Initial screening showed that PD901 displayed the most potent inhibition inside and outside the CNS compared to two clinically relevant MEKis (selumetinib (AZD6244) and trametinib (GSK1120212)). Remarkably, a twenty-one days' treatment "MEKi in the milk" protocol during neonatal development (P0.5-P21) not only repressed abnormal Olig2 expression in the astrocytic lineage, but also provided long-term rescue of the subsequent phase II nerve damage and neuronal loss by suppressing Erk activation. Similar to the results from genetic *Mek1/2* inactivation, I noted a dose-dependent (5, 10, 20 mg/kg) rescue in the tumor phenotype, with 20 mg/kg dose of PD901 providing the most consistent rescue in glial defects but with high toxicity. My findings are most consistent with a model where neurofibromin downregulate bipotency of Pax2^{+} APCs by inhibiting Olig2 expression through MEK-Erk inactivation during early postnatal optic nerve development. As such, *Nf1* is a key regulator of glial fate specification in the developing nerve. In the ventral brain, *Nf1* inactivation leads to abnormal expansion of BLBP^{+}Olig2^{+} glia progenitors that migrate into the nerve and persist throughout development (Figure 25). Although this model addresses the role of *Nf1* in progenitor fate specification, the mechanism of MAPK regulation of gliogenesis is less defined. Several studies have implicated members of the Ets family transcription factor in regulation of gliogenesis. Ets transcription factors are targets of FGF and can be phosphorylated and activated by MAPK pathway (Bertrand et al. 2003; Chen et al. 2005). The Pointed domain, named after the Drosophila Ets protein Pointed, is the docking site for ERK1/2 and plays an important role in glial differentiation in the developing Drosophila brain (Klaes et al. 1994). In the mammalian brain, overexpression of Etv5/Erm, a member of Ets transcription factor, in radial progenitors induces glial progenitor specification. MEK was shown to be a key regulator of *Erm* expression in radial progenitors (Li et al. 2012). Another possible mechanism is through MEK modulation of *Egfr* expression which increases during late embryonic development. EGFR is known to regulate the competence of gliogenic progenitors in vivo (Viti et al. 2003). One important future direction would be to use FACS techniques to isolate *Nf1*$^{-/-}$ and *Nf1*$^{+/+}$ cells based on their genetically coupled RFP (red) and GFP (green) from optic nerves of MADM-*Nf1*^{hGFAP}CKO mice during early postnatal development (P0.5, P5 and P15) when the majority of abnormal expansion of *Nf1*$^{-/-}$ glial cell populations occurs compared to their sibling *Nf1*$^{+/+}$ cells. Next, we could extract total RNAs

and mRNAs for library construct and RNA sequencing analysis to identify potential targets that are differentially expressed between sibling *Nf1*$^{-/-}$ cells and *Nf1*$^{+/+}$ cells isolated from different stages of the developing optic nerve.

4.3 Clinical implications for NF1-associated OPG

The progression-free survival (PFS) for pediatric LGG patients with unresectable/residual disease requiring treatment is approximately 40% (Ater et al. 2012). Radiotherapy treatment has been shown to cause neurocognitive and neuroendocrine dysfunction, ototoxicity, vasculopathy, and secondary neoplasms. Although chemotherapeutic strategies can achieve tumor stabilization in 80–90% of patients, they are often only transiently effective and visual outcomes are variable. Over the past several years, several groups and institutions have undertaken and completed multiple clinical trials on NF1 children with progressive LGGs using mTOR inhibitors. However, improvement in vision was infrequently observed. The use of MEK inhibitors has been greatly advocated in NF1 patients with recurrent disease. Preliminary data from clinical studies suggest that MEKis are not only effective in tumor shrinkage, but they can also ameliorate vision. Over the past four years, several national consensus conferences have advocated for the use of MEKis in NF1 patients with newly diagnosed disease, not just recurrent disease (Jones et al. 2018). Amendments in the eligibility criteria are being investigated for current clinical studies to allow children as young as one-year-old to participate. Although the MEKi treatment was shown to be very effective in preventing tumor formation, the functional consequences of these anatomic outcomes remain unknown. Therefore, we must examine whether the prevention of neurologic deficits by the "MEKi in milk" protocol can provide improvement in functional outcomes and behavioral impairment in *Nf1*^{hGFAP}CKO mice. One possible method is to measure optomotor and optokinetic responses (OMR & OKR) in order to evaluate visual acuity and contrast sensitivity in MEKi-treated versus untreated mutants at P60. Optical coherence tomography (OCT) has been used as a biomarker for vision loss in patients with NF1-OPG and can detect thinning of the retinal nerve fiber layer (RNFL) and ganglion cell complex (GCC). OCT measurements after treatment would therefore provide automated and precise *in vivo* quantification for RGC survival in *Nf1* mutants. Finally, electrophysiological studies using multielectrode array (MEA) to simultaneous record 50-200 RGCs can be performed to measure spontaneous activity (number of action

potentials per second), light-evoked responses (strength, latency and duration) between treated versus untreated mutants. These studies can provide the foundation for developing MEKi-based early intervention therapies for NF1-OPG.

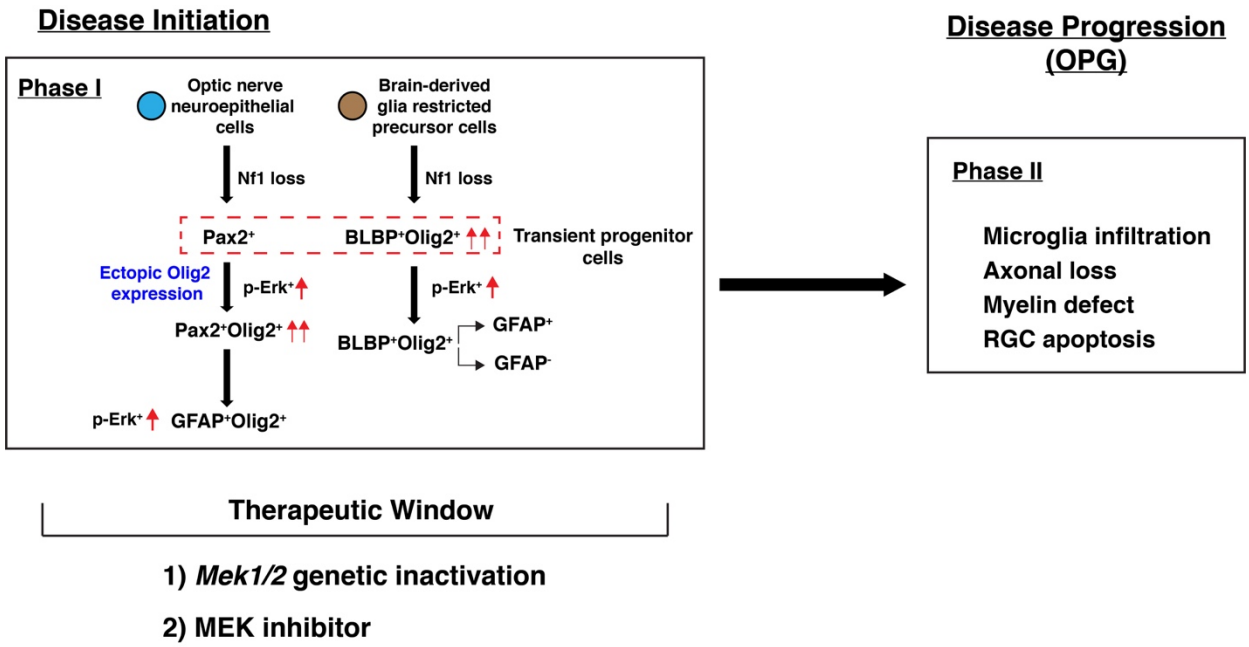

Figure 25. Proposed model of how *Nf1* loss affects transient brain-derived and optic nerve-derived glial precursor cells during optic nerve development.

During neonatal stage, *Nf1* loss causes the ectopic expression of Olig2 in nerve-derived transient $Pax2^+$ APCs and the expansion $Pax2^+Olig2^+$ cells which later differentiate into $GFAP^+Olig2^+$ cells. In the embryonic brain, *Nf1* inactivation leads to the expansion of $BLBP^+Olig2^+$ glia-restricted progenitors which migrate in the developing optic nerve and a portion of these cells express GFAP marker later on. $Pax2^+Olig2^+$ and $BLBP^+Olig2^+$ cells represent transient glial progenitor populations that are present in the normal nerve during a short, early developmental window and become rare later on. These cells are maintained throughout gliomagenesis in *Nf1* mutant nerves through p-Erk activation and are the most expanded cellular compartment in late-stage tumors. The second phase of disease progression is characterized by microglia infiltration, axonal and myelin defects and RGC loss. Phase I abnormal glial expansion represent an attractive therapeutic window that can be targeted by genetic and pharmacological MEK inhibition.

4.4 References

Ater, J. L., T. Zhou, E. Holmes, C. M. Mazewski, T. N. Booth, D. R. Freyer, K. H. Lazarus, R. J. Packer, M. Prados, R. Sposto, G. Vezina, J. H. Wisoff, and I. F. Pollack. 2012. 'Randomized study of two chemotherapy regimens for treatment of low-grade glioma in young children: a report from the Children's Oncology Group', *J Clin Oncol*, 30: 2641-7.

Bennett, M. R., T. A. Rizvi, S. Karyala, R. D. McKinnon, and N. Ratner. 2003. 'Aberrant growth and differentiation of oligodendrocyte progenitors in neurofibromatosis type 1 mutants', *J Neurosci*, 23: 7207-17.

Bertrand, V., C. Hudson, D. Caillol, C. Popovici, and P. Lemaire. 2003. 'Neural tissue in ascidian embryos is induced by FGF9/16/20, acting via a combination of maternal GATA and Ets transcription factors', *Cell*, 115: 615-27.

Bouvier, C., C. Bartoli, L. Aguirre-Cruz, I. Virard, C. Colin, C. Fernandez, J. Gouvernet, and D. Figarella-Branger. 2003. 'Shared oligodendrocyte lineage gene expression in gliomas and oligodendrocyte progenitor cells', *J Neurosurg*, 99: 344-50.

Chen, C., W. Ouyang, V. Grigura, Q. Zhou, K. Carnes, H. Lim, G. Q. Zhao, S. Arber, N. Kurpios, T. L. Murphy, A. M. Cheng, J. A. Hassell, V. Chandrashekar, M. C. Hofmann, R. A. Hess, and K. M. Murphy. 2005. 'ERM is required for transcriptional control of the spermatogonial stem cell niche', *Nature*, 436: 1030-4.

Chen, Y. H., S. M. Gianino, and D. H. Gutmann. 2015. 'Neurofibromatosis-1 regulation of neural stem cell proliferation and multilineage differentiation operates through distinct RAS effector pathways', *Genes Dev*, 29: 1677-82.

Chen, Y. H., L. D. McGowan, P. J. Cimino, S. Dahiya, J. R. Leonard, D. Y. Lee, and D. H. Gutmann. 2015. 'Mouse low-grade gliomas contain cancer stem cells with unique molecular and functional properties', *Cell Rep*, 10: 1899-912.

Coniglio, S. J., E. Eugenin, K. Dobrenis, E. R. Stanley, B. L. West, M. H. Symons, and J. E. Segall. 2012. 'Microglial stimulation of glioblastoma invasion involves epidermal growth factor receptor (EGFR) and colony stimulating factor 1 receptor (CSF-1R) signaling', *Mol Med*, 18: 519-27.

Daginakatte, G. C., S. M. Gianino, N. W. Zhao, A. S. Parsadanian, and D. H. Gutmann. 2008. 'Increased c-Jun-NH2-kinase signaling in neurofibromatosis-1 heterozygous microglia drives microglia activation and promotes optic glioma proliferation', *Cancer Res*, 68: 10358-66.

Daginakatte, G. C., and D. H. Gutmann. 2007. 'Neurofibromatosis-1 (Nf1) heterozygous brain microglia elaborate paracrine factors that promote Nf1-deficient astrocyte and glioma growth', *Hum Mol Genet*, 16: 1098-112.

Dasgupta, B., and D. H. Gutmann. 2005. 'Neurofibromin regulates neural stem cell proliferation, survival, and astroglial differentiation in vitro and in vivo', *J Neurosci*, 25: 5584-94.

Dawson, M. R., A. Polito, J. M. Levine, and R. Reynolds. 2003. 'NG2-expressing glial progenitor cells: an abundant and widespread population of cycling cells in the adult rat CNS', *Mol Cell Neurosci*, 24: 476-88.

Fisher, M. J., M. Loguidice, D. H. Gutmann, R. Listernick, R. E. Ferner, N. J. Ullrich, R. J. Packer, U. Tabori, R. O. Hoffman, S. L. Ardern-Holmes, T. R. Hummel, D. R. Hargrave, E. Bouffet, J. Charrow, L. T. Bilaniuk, L. J. Balcer, and G. T. Liu. 2012. 'Visual outcomes in

children with neurofibromatosis type 1-associated optic pathway glioma following chemotherapy: a multicenter retrospective analysis', *Neuro Oncol*, 14: 790-7.

Geha, S., J. Pallud, M. P. Junier, B. Devaux, N. Leonard, F. Chassoux, H. Chneiweiss, C. Daumas-Duport, and P. Varlet. 2010. 'NG2+/Olig2+ cells are the major cycle-related cell population of the adult human normal brain', *Brain Pathol*, 20: 399-411.

Gutmann, D. H., M. D. McLellan, I. Hussain, J. W. Wallis, L. L. Fulton, R. S. Fulton, V. Magrini, R. Demeter, T. Wylie, C. Kandoth, J. R. Leonard, A. Guha, C. A. Miller, L. Ding, and E. R. Mardis. 2013. 'Somatic neurofibromatosis type 1 (NF1) inactivation characterizes NF1-associated pilocytic astrocytoma', *Genome Res*, 23: 431-9.

Hegedus, B., B. Dasgupta, J. E. Shin, R. J. Emnett, E. K. Hart-Mahon, L. Elghazi, E. Bernal-Mizrachi, and D. H. Gutmann. 2007. 'Neurofibromatosis-1 regulates neuronal and glial cell differentiation from neuroglial progenitors in vivo by both cAMP- and Ras-dependent mechanisms', *Cell Stem Cell*, 1: 443-57.

Jones, D. T. W., M. W. Kieran, E. Bouffet, S. Alexandrescu, P. Bandopadhayay, M. Bornhorst, D. Ellison, J. Fangusaro, M. J. Fisher, N. Foreman, M. Fouladi, D. Hargrave, C. Hawkins, N. Jabado, M. Massimino, S. Mueller, G. Perilongo, A. Y. N. Schouten van Meeteren, U. Tabori, K. Warren, A. J. Waanders, D. Walker, W. Weiss, O. Witt, K. Wright, Y. Zhu, D. C. Bowers, S. M. Pfister, and R. J. Packer. 2018. 'Pediatric low-grade gliomas: next biologically driven steps', *Neuro Oncol*, 20: 160-73.

Kim, E., Y. Wang, S. J. Kim, M. Bornhorst, E. S. Jecrois, T. E. Anthony, C. Wang, Y. E. Li, J. L. Guan, G. G. Murphy, and Y. Zhu. 2014. 'Transient inhibition of the ERK pathway prevents cerebellar developmental defects and improves long-term motor functions in murine models of neurofibromatosis type 1', *Elife*, 3.

Klaes, A., T. Menne, A. Stollewerk, H. Scholz, and C. Klambt. 1994. 'The Ets transcription factors encoded by the Drosophila gene pointed direct glial cell differentiation in the embryonic CNS', *Cell*, 78: 149-60.

Kondo, T., and M. Raff. 2000. 'Oligodendrocyte precursor cells reprogrammed to become multipotential CNS stem cells', *Science*, 289: 1754-7.

Ku, M. C., S. A. Wolf, D. Respondek, V. Matyash, A. Pohlmann, S. Waiczies, H. Waiczies, T. Niendorf, M. Synowitz, R. Glass, and H. Kettenmann. 2013. 'GDNF mediates glioblastoma-induced microglia attraction but not astrogliosis', *Acta Neuropathol*, 125: 609-20.

Lee, D. Y., S. M. Gianino, and D. H. Gutmann. 2012. 'Innate neural stem cell heterogeneity determines the patterning of glioma formation in children', *Cancer Cell*, 22: 131-8.

Li, X., J. M. Newbern, Y. Wu, M. Morgan-Smith, J. Zhong, J. Charron, and W. D. Snider. 2012. 'MEK Is a Key Regulator of Gliogenesis in the Developing Brain', *Neuron*, 75: 1035-50.

Ligon, K. L., J. A. Alberta, A. T. Kho, J. Weiss, M. R. Kwaan, C. L. Nutt, D. N. Louis, C. D. Stiles, and D. H. Rowitch. 2004. 'The oligodendroglial lineage marker OLIG2 is universally expressed in diffuse gliomas', *J Neuropathol Exp Neurol*, 63: 499-509.

Listernick, R. 2016. 'Predicting which NF1 optic pathway gliomas will require treatment', *Neurology*, 87: 2389-90.

Marshall, C. A., B. G. Novitch, and J. E. Goldman. 2005. 'Olig2 directs astrocyte and oligodendrocyte formation in postnatal subventricular zone cells', *J Neurosci*, 25: 7289-98.

Menn, B., J. M. Garcia-Verdugo, C. Yaschine, O. Gonzalez-Perez, D. Rowitch, and A. Alvarez-Buylla. 2006. 'Origin of oligodendrocytes in the subventricular zone of the adult brain', *J Neurosci*, 26: 7907-18.

Mokhtari, K., S. Paris, L. Aguirre-Cruz, N. Privat, E. Criniere, Y. Marie, J. J. Hauw, M. Kujas, D. Rowitch, K. Hoang-Xuan, J. Y. Delattre, and M. Sanson. 2005. 'Olig2 expression, GFAP, p53 and 1p loss analysis contribute to glioma subclassification', *Neuropathol Appl Neurobiol*, 31: 62-9.

Newbern, J. M., X. Li, S. E. Shoemaker, J. Zhou, J. Zhong, Y. Wu, D. Bonder, S. Hollenback, G. Coppola, D. H. Geschwind, G. E. Landreth, and W. D. Snider. 2011. 'Specific functions for ERK/MAPK signaling during PNS development', *Neuron*, 69: 91-105.

Ohyama, T., and A. K. Groves. 2004. 'Generation of Pax2-Cre mice by modification of a Pax2 bacterial artificial chromosome', *Genesis*, 38: 195-9.

Ono, K., H. Takebayashi, K. Ikeda, M. Furusho, T. Nishizawa, K. Watanabe, and K. Ikenaka. 2008. 'Regional- and temporal-dependent changes in the differentiation of Olig2 progenitors in the forebrain, and the impact on astrocyte development in the dorsal pallium', *Dev Biol*, 320: 456-68.

Paolicelli, R. C., K. Bisht, and M. E. Tremblay. 2014. 'Fractalkine regulation of microglial physiology and consequences on the brain and behavior', *Front Cell Neurosci*, 8: 129.

Platten, M., A. Kretz, U. Naumann, S. Aulwurm, K. Egashira, S. Isenmann, and M. Weller. 2003. 'Monocyte chemoattractant protein-1 increases microglial infiltration and aggressiveness of gliomas', *Ann Neurol*, 54: 388-92.

Pong, W. W., S. B. Higer, S. M. Gianino, R. J. Emnett, and D. H. Gutmann. 2013. 'Reduced microglial CX3CR1 expression delays neurofibromatosis-1 glioma formation', *Ann Neurol*, 73: 303-8.

Preusser, M., H. Budka, K. Rossler, and J. A. Hainfellner. 2007. 'OLIG2 is a useful immunohistochemical marker in differential diagnosis of clear cell primary CNS neoplasms', *Histopathology*, 50: 365-70.

Reis, G. F., M. M. Bloomer, A. Perry, J. J. Phillips, J. P. Grenert, A. N. Karnezis, and T. Tihan. 2013. 'Pilocytic astrocytomas of the optic nerve and their relation to pilocytic astrocytomas elsewhere in the central nervous system', *Mod Pathol*, 26: 1279-87.

Sanchez-Ortiz, E., W. Cho, I. Nazarenko, W. Mo, J. Chen, and L. F. Parada. 2014. 'NF1 regulation of RAS/ERK signaling is required for appropriate granule neuron progenitor expansion and migration in cerebellar development', *Genes Dev*, 28: 2407-20.

Sielska, M., P. Przanowski, B. Wylot, K. Gabrusiewicz, M. Maleszewska, M. Kijewska, M. Zawadzka, J. Kucharska, K. Vinnakota, H. Kettenmann, K. Kotulska, W. Grajkowska, and B. Kaminska. 2013. 'Distinct roles of CSF family cytokines in macrophage infiltration and activation in glioma progression and injury response', *J Pathol*, 230: 310-21.

Simmons, G. W., W. W. Pong, R. J. Emnett, C. R. White, S. M. Gianino, F. J. Rodriguez, and D. H. Gutmann. 2011. 'Neurofibromatosis-1 heterozygosity increases microglia in a spatially and temporally restricted pattern relevant to mouse optic glioma formation and growth', *J Neuropathol Exp Neurol*, 70: 51-62.

Sun, G. J., Y. Zhou, S. Ito, M. A. Bonaguidi, G. Stein-O'Brien, N. K. Kawasaki, N. Modak, Y. Zhu, G. L. Ming, and H. Song. 2015. 'Latent tri-lineage potential of adult hippocampal neural stem cells revealed by Nf1 inactivation', *Nat Neurosci*, 18: 1722-4.

Viti, J., A. Feathers, J. Phillips, and L. Lillien. 2003. 'Epidermal growth factor receptors control competence to interpret leukemia inhibitory factor as an astrocyte inducer in developing cortex', *J Neurosci*, 23: 3385-93.

Wang, Y., E. Kim, X. Wang, B. G. Novitch, K. Yoshikawa, L. S. Chang, and Y. Zhu. 2012. 'ERK inhibition rescues defects in fate specification of Nf1-deficient neural progenitors and brain abnormalities', *Cell*, 150: 816-30.

Zhu, Y., T. Harada, L. Liu, M. E. Lush, F. Guignard, C. Harada, D. K. Burns, M. L. Bajenaru, D. H. Gutmann, and L. F. Parada. 2005. 'Inactivation of NF1 in CNS causes increased glial progenitor proliferation and optic glioma formation', *Development*, 132: 5577-88.

Chapter V: Materials and Methods

5.1 Mouse Models

Nf1^{hGFAP}CKO

The control mice used in this study are a pool of phenotypically indistinguishable mice with genotypes *Nf1*$^{flox/flox}$; *Nf1*$^{flox/+}$; and hGFAP-cre^{+}; *Nf1*$^{flox/+}$. The mutant *Nf1*^{hGFAP}CKO used was of the genotype hGFAP-cre^{+}; *Nf1*$^{flox/flox}$ and was maintained in the mixed backgrounds of C57Bl6, 129Svj, and FVB, which resulted in improvement of the overall health and life span of the mutant mice. Age and littermate-matched control and mutant mice were used for the developmental analyses to minimize the impact of modifier genes. All mice in this study were cared for according to the guidelines that were approved by the Animal Care and Use Committees of the University of Michigan at Ann Arbor as well as the Institutional Animal Care and Use Committee of Children's National Medical Center in Washington DC.

Mek1/2^{hGFAP}CKO

Mek1$^{flox/flox}$ mice were generated by flanking the ATP-binding site for the kinase in the third exon with LoxP sites (Bissonauth et al. 2006). The *Mek2*$^{-/-}$ mice were generated by replacing exon VI-IV with a reversed neo cassette in the middle of the gene coding sequence (Belanger et al. 2003). They were later crossed with *Nf1* mice to generate three groups of *Nf1* mutants with various degrees of *Mek1/2* allele inactivation: M1 (*Nf1*^{hGFAP}CKO, *Mek1*$^{fl/fl}$, *Mek2*$^{-/+}$ or *Mek1*$^{fl/+}$, *Mek2*$^{-/-}$); M2 (*Nf1*^{hGFAP}CKO, *Mek1*$^{fl/+}$, *Mek2*$^{-/+}$; *Mek1*$^{fl/fl}$, *Mek2*$^{+/+}$; *Mek1*$^{+/+}$, *Mek2*$^{-/-}$); M3 (*Nf1*^{hGFAP}CKO, *Mek1*$^{fl/+}$, *Mek*$^{+/+}$ or *Mek1*$^{+/+}$, *Mek2*$^{-/+}$).

MADM hGFAP-cre, *Nf1*$^{fl/+}$

RG mice were crossed with hGFAP-cre^{+}; *Nf1*$^{flox/+}$ mice. They were subsequently crossed with GR mice to generate RG/GR hGFAP-cre^{+}; *Nf1*$^{flox/+}$ mice for MADM analysis. Cre negative mice were used for controls.

5.2 Genotyping and PCR

Genetic analysis of mice in the colony used genomic DNA extracted from P18-P21 tail snips incubated overnight at 50ºC in SDS-EDTA TAE Buffer with Proteinase K (Roche Diagnostics). The resulting solution was mixed with 70% isopropanol (1:1) to allow DNA to precipitate. The precipitate was then transferred and diluted into ultrapure water before PCR analysis was performed for the Cre insert, NF1 recombination and tdTomato and GFP reporters using the Taq 2X MeanGreen Master Mix (Empyrical BioScience) or 2X PCR Super Master Mix (Bimake) in conjuncture with the following primers:

Cre primers

Icres 5'-CCG TTT GCC GGT CGT GGG-3'

IcreAs 5'-CG TAT ATC CTG GCA GCG ATC- 3'

NF1 Primers

Yuan 11 5'-CTT CAG ACT GAT TGT TGT ACC TGA- 3'

Yuan 6.1 5'-AAA TCA GCA GAG GTT GTC AGA ATC- 3'

Yuan 6.2 5'-AGT TCC ATC ACA CGT AAA ATT GAG- 3'

tdTomato Primers

5'-AAG GGA GCT GCA GFG GAG TA- 3'

RT 1	
RT 2	5'-CCG AAA ATC TGT GGG AAG TC- 3'
RT 3	5'-GGC ATT AAA GCA GCG TAT CC- 3'
RT 4	5'-CTG TTC CTG TAC GGC ATG G- 3'
GFP Primers	
eGFP-F	5'-GAG CTG GAC GGC GAC GTA AAC- 3'
eGFP-R	5'-CGT TGT GGC TGT TGT TAG TGT TAC- 3'
Mek1/2 Primers	
Mek1-Olig9	5'-CAG AAG TTC CCA CGA CAC TA- 3'
Mek1-2772Flox	5'-GTC TGT CAC TTG TCT TCT GG- 3'
Mek2WT-13131	5'-CTG ACC TTC CTG TAG GTG- 3'
Mek2WT-13424	5'-ACT CAC GGA CAT GTA GGA- 3'
Mek2KO-Neo25	5'-CGT GCA ATC CAT CTT GTT C- 3'
MADM primers	
Chr11_CS1	5-TGGAGGAGGACAAACTGGTCAC-3
Rosa4	5-TCAATGGGCGGGG GTCGTT-3

Chr11_CS2 5-TTCCCTTTCTGCTTCATCTTGC-3

5.3 Tissue preparation

Mice were perfused with 4% paraformaldehyde (PFA) and optic nerves and brains were dissected, followed by overnight post-fixation in 4% PFA at 4ºC. Following sacrifice, chiasms and optic nerves were micro dissected, cleaned and imaged using an Olympus DP70 camera. Optic nerves, retinas and brains were processed through a sequence of dehydration steps prior to paraffin embedding. Brains were divided into two hemispheres along the midline and each hemisphere was embedded. Optic nerves were separated into 2 portions: the distal nerves including prechiasmatic nerve and chiasm were embedded separately from the proximal portion which included the retina and optic nerve head. Embedded tissue was sectioned sagittally at 5 μm for paraffin sections or 10 μm for cryostat sections. Serial sections were prepared at 5 μm for paraffin sections or 10~14 μm for cryostat sections. Slides from histologically comparable positions were stained by hematoxylin and eosin (H&E). Adjacent sections were subjected to immunohistochemical or immunofluorescence analysis.

5.4 Immunohistochemistry/immunofluorescence

Paraffin sections were deparaffinized through Xylene, 100% ethanol, 95% ethanol, 50% ethanol and 30% ethanol and rehydrated in distilled water. Antigen retrieval was performed with Retrieve-all antigen retrieval solution (BioLegend) in heated coplin jars. Cryosections do not require deparaffinization or antigen retrieval steps and were directly fixed in 4% PFA for 15 minutes. Sections were then permeabilized by 0.3% Triton-X (Sigma) solution for 20 minutes and blocked for 1 hour with 3% normal goat/horse/donkey serum (Sigma) depending on the secondary antibody selection. Slides were put in humidified chamber and incubated in primary antibodies dissolved in the blocking solution at 4ºC overnight. The visualization of primary antibodies was performed with either a horseradish peroxidase system using a diaminobenzidine-based (DAB) peroxidase substrate (Vectastain ABC kit, Vector) or immunofluorescence by using Cy2 (or Alexa 488), Cy3 (or Alexa 555) and Cy5 (Alexa 647)-conjugated secondary antibodies at 1:200 dilution for 1 hour incubation (Cy2/Cy3/Cy5, Jackson Immunoresearch; Alexa 488/555/647, Invitrogen).

Slides were washed in between the steps with 1X PBS. The dilutions of primary antibodies were as followed:

GFAP (1:2000, mouse, BD Pharmingen),
GFAP (1:2000, mouse, DAKO),
Olig2 (1:2000, rabbit, Millipore),
Olig2 (1:300, mouse, Millipore),
Olig2 (1:10000, guinea pig, a kind gift from Dr. B. Novitch),
Iba-1 (1:2000, rabbit, Wako),
PDGFRα (1:1000, goat, RD)
MBP (1:500, rat, Chemicon),
BLBP (1:100, rabbit, Abcam),
Ki-67 (1:500, mouse, BD Pharmingen),
Ki-67 (1:500, rabbit,),
p-ERK (1:200, rabbit, Cell Signaling),
p-S6 (1:1000, rabbit, Cell Signaling),
RBPMS (1:250, guinea pig, Cedarlane).
GFP (1:500, rabbit, Molecular Probes)
GFP (1:500, chicken, Abcam)

Terminal deoxynucleotidyl transferase (TdT) dUTP Nick-End Labeling (**TUNEL**) assay was performed using the Click-iT® TUNEL Alexa Fluor® Imaging kit from Thermo-Fisher according to manufacturer's recommendations.
Sections were examined under either a light or a fluorescence microscope (Olympus).

MADM staining design

Fluorescence involving MADM (for GFP and RFP) occupied the commonly used green (488 nm laser) and red (555 nm laser) channels in fluorescent microscope. Marker staining other than MADM was applied in either the Far-red channel (635 nm laser). When a single marker was stained along with MADM (three-channel staining), I stained this marker with the appropriate secondary antibody to visualize it in the Far-red channel (Alexa Fluor 647 secondary antibody).

5.5 Retinal analyses

For whole-mount retinal staining, special care was taken to maintain the orientation of the eyes by the following methods. After anesthesia and before perfusion a suture was placed on the superior pole of each eye. Upon dissection of the eyeball, the rectus muscle insertion into the superior part of the eye and the nasal caruncle were used as additional landmarks. Both retinas were dissected and prepared as flattened whole-mounts by making four radial cuts (the deepest one in the superior pole), post-fixed for an additional hour, rinsed in 1X PBS, mounted vitreal side up on subbed slides and covered with anti-fading mounting media containing 50% glycerol and 0.04% p-phenylenediamine in 0.1 M sodium carbonate buffer (pH 9).

For cross-sectional analysis, eyes from pigmented mice were enucleated and immunostained for RBPMS (retinal ganglion cells) following previously described methods for immunofluorescence. TUNEL-positive cells were quantified by counting the number of cells positive for TUNEL staining within the $DAPI^+$ cells in the retinal ganglion cell layer. The total number of $RBPMS^+$ cells was counted per section starting from area adjacent to the optic nerve head.

5.6 MEK inhibitor treatment

MEK inhibitor (MEKi) PD0325901 (Sigma, PZ0162-25MG) was dissolved in 0.5% hydroxypropyl methyl-cellulose plus 0.2% Tween 80 (Sigma) at a concentration of 1mg/ml. The solution was administered by oral gavage at the dosage of 5, 10 or 20 mg/kg (body weight) every day from P0.5-P21 to lactating females ("MEKi in the milk"). Mice that receive vehicle (0.5% hydroxypropyl methyl-cellulose plus 0.2% Tween 80) treatment were used as controls. MEKi-treated mice were collected and compared to control mice and vehicle-treated mice.

5.7 Western blotting

Snap-frozen tissue samples from wild-type control brains and tumors were homogenized

in Pierce RIPA Buffer (Thermo Scientific) (10 µl buffer/1 mg tissue), mixed 1:1 with Laemmli Sample Buffer (BioRad, Hercules, CA) for 20 minutes on ice, subjected to centrifugation at 14,000 rpm for 10 min at 4°C and boiled at 100°C for 10 minutes. Equal amounts of protein samples were mixed with 1X SDS loading buffer [50 mM Tris-HCL (pH6.8), 2% SDS, 0.05% bromophenol blue, 10% glycerol, 100 mM β-mercaptoethanol] (BioRad). Samples were then subjected to SDS-PAGE using the Criterion TGX Precast gels (BioRad) and transferred onto PVDF membranes (Millipore). Membranes were blocked in 5% non-fat milk (BioRad) prepared in 1X TBST and incubated with primary antibodies at 4°C overnight. The following day, the membranes were washed with TBST and incubated in horseradish peroxidase (HRP)- conjugated secondary antibodies at room temperature for 1 hour. The membranes were then exposed to Pierce ECL western blotting substrate (Thermo Scientific) for 3-5 minutes to detect signal by film development in dark room. The primary antibodies used in this study were as follows:

pAkt^{S473} (1:1,000, rabbit, Cell Signaling),
Akt (1:1,000, rabbit, Cell Signaling),
β-Actin (1:5,000-10,000, mouse, Sigma-Aldrich),
pS6^{KT389} (1:1,000, rabbit, Cell Signaling),
S6 (1:2,000, rabbit, Cell Signaling),
pErk1/2$^{T202/Ty204}$ (1:1,000, rabbit, Cell Signaling),
Erk1/2 (1:1,000, rabbit, Cell Signaling),
P120 (1:1000, mouse, BD Biosciences)
NF1 (1:1000, rabbit, Upstate, Lake Placid, NY)
HRP-conjugated secondary antibodies were anti-mouse (1:5,000-1: 10,000, goat, BioRad) and anti-rabbit (1: 5,000-1: 10,000, goat, BioRad).

5.8 Quantification and Statistical analyses

Anatomically comparable sections from control and mutant prechiasmatic nerves were visualized using an Olympus BX51 microscope. Images were captured and subjected to double-blinded counting. Lengths, areas and the number of cells were quantified by the NIH software, ImageJ. Control and mutant groups were compared, and statistical analysis was carried out using two-tailed Student's t-test. At least three animals from each group were used for quantification. Data were

presented as mean ± Standard Error Mean (SEM). $p < 0.05$ was considered to be statistically significant.

5.9 References

Aguzzi, A., B. A. Barres, and M. L. Bennett. 2013. 'Microglia: scapegoat, saboteur, or something else?', *Science*, 339: 156-61.

Anthony, T. E., C. Klein, G. Fishell, and N. Heintz. 2004. 'Radial glia serve as neuronal progenitors in all regions of the central nervous system', *Neuron*, 41: 881-90.

Ater, J. L., C. Xia, C. M. Mazewski, T. N. Booth, D. R. Freyer, R. J. Packer, R. Sposto, G. Vezina, and I. F. Pollack. 2016. 'Nonrandomized comparison of neurofibromatosis type 1 and non-neurofibromatosis type 1 children who received carboplatin and vincristine for progressive low-grade glioma: A report from the Children's Oncology Group', *Cancer*, 122: 1928-36.

Ater, J. L., T. Zhou, E. Holmes, C. M. Mazewski, T. N. Booth, D. R. Freyer, K. H. Lazarus, R. J. Packer, M. Prados, R. Sposto, G. Vezina, J. H. Wisoff, and I. F. Pollack. 2012. 'Randomized study of two chemotherapy regimens for treatment of low-grade glioma in young children: a report from the Children's Oncology Group', *J Clin Oncol*, 30: 2641-7.

Avery, R. A., A. Cnaan, J. S. Schuman, C. Trimboli-Heidler, C. L. Chen, R. J. Packer, and H. Ishikawa. 2015. 'Longitudinal Change of Circumpapillary Retinal Nerve Fiber Layer Thickness in Children With Optic Pathway Gliomas', *Am J Ophthalmol*, 160: 944-52 e1.

Avery, R. A., A. Mansoor, R. Idrees, E. Biggs, M. A. Alsharid, R. J. Packer, and M. G. Linguraru. 2016. 'Quantitative MRI criteria for optic pathway enlargement in neurofibromatosis type 1', *Neurology*, 86: 2264-70.

Avery, R. A., A. Mansoor, R. Idrees, C. Trimboli-Heidler, H. Ishikawa, R. J. Packer, and M. G. Linguraru. 2016. 'Optic pathway glioma volume predicts retinal axon degeneration in neurofibromatosis type 1', *Neurology*, 87: 2403-07.

Bajenaru, M. L., J. R. Garbow, A. Perry, M. R. Hernandez, and D. H. Gutmann. 2005. 'Natural history of neurofibromatosis 1-associated optic nerve glioma in mice', *Ann Neurol*, 57: 119-27.

Bajenaru, M. L., M. R. Hernandez, A. Perry, Y. Zhu, L. F. Parada, J. R. Garbow, and D. H. Gutmann. 2003. 'Optic nerve glioma in mice requires astrocyte Nf1 gene inactivation and Nf1 brain heterozygosity', *Cancer Res*, 63: 8573-7.

Balcer, L. J., G. T. Liu, G. Heller, L. Bilaniuk, N. J. Volpe, S. L. Galetta, P. T. Molloy, P. C. Phillips, A. J. Janss, S. Vaughn, and M. G. Maguire. 2001. 'Visual loss in children with neurofibromatosis type 1 and optic pathway gliomas: relation to tumor location by magnetic resonance imaging', *Am J Ophthalmol*, 131: 442-5.

Ballester, R., D. Marchuk, M. Boguski, A. Saulino, R. Letcher, M. Wigler, and F. Collins. 1990. 'The NF1 locus encodes a protein functionally related to mammalian GAP and yeast IRA proteins', *Cell*, 63: 851-9.

Belanger, L. F., S. Roy, M. Tremblay, B. Brott, A. M. Steff, W. Mourad, P. Hugo, R. Erikson, and J. Charron. 2003. 'Mek2 is dispensable for mouse growth and development', *Mol Cell Biol*, 23: 4778-87.

Bennett, M. R., T. A. Rizvi, S. Karyala, R. D. McKinnon, and N. Ratner. 2003. 'Aberrant growth and differentiation of oligodendrocyte progenitors in neurofibromatosis type 1 mutants', *J Neurosci*, 23: 7207-17.

Bergthold, G., P. Bandopadhayay, W. L. Bi, L. Ramkissoon, C. Stiles, R. A. Segal, R. Beroukhim, K. L. Ligon, J. Grill, and M. W. Kieran. 2014. 'Pediatric low-grade gliomas: how modern biology reshapes the clinical field', *Biochim Biophys Acta*, 1845: 294-307.

Bertrand, V., C. Hudson, D. Caillol, C. Popovici, and P. Lemaire. 2003. 'Neural tissue in ascidian embryos is induced by FGF9/16/20, acting via a combination of maternal GATA and Ets transcription factors', *Cell*, 115: 615-27.

Bissonauth, V., S. Roy, M. Gravel, S. Guillemette, and J. Charron. 2006. 'Requirement for Map2k1 (Mek1) in extra-embryonic ectoderm during placentogenesis', *Development*, 133: 3429-40.

Bouvier, C., C. Bartoli, L. Aguirre-Cruz, I. Virard, C. Colin, C. Fernandez, J. Gouvernet, and D. Figarella-Branger. 2003. 'Shared oligodendrocyte lineage gene expression in gliomas and oligodendrocyte progenitor cells', *J Neurosurg*, 99: 344-50.

Brannan, C. I., A. S. Perkins, K. S. Vogel, N. Ratner, M. L. Nordlund, S. W. Reid, A. M. Buchberg, N. A. Jenkins, L. F. Parada, and N. G. Copeland. 1994. 'Targeted disruption of the neurofibromatosis type-1 gene leads to developmental abnormalities in heart and various neural crest-derived tissues', *Genes Dev*, 8: 1019-29.

Brown, A. P., T. C. Carlson, C. M. Loi, and M. J. Graziano. 2007. 'Pharmacodynamic and toxicokinetic evaluation of the novel MEK inhibitor, PD0325901, in the rat following oral and intravenous administration', *Cancer Chemother Pharmacol*, 59: 671-9.

Burkhard, C., P. L. Di Patre, D. Schuler, G. Schuler, M. G. Yasargil, Y. Yonekawa, U. M. Lutolf, P. Kleihues, and H. Ohgaki. 2003. 'A population-based study of the incidence and survival rates in patients with pilocytic astrocytoma', *J Neurosurg*, 98: 1170-4.

Chen, C., W. Ouyang, V. Grigura, Q. Zhou, K. Carnes, H. Lim, G. Q. Zhao, S. Arber, N. Kurpios, T. L. Murphy, A. M. Cheng, J. A. Hassell, V. Chandrashekar, M. C. Hofmann, R. A. Hess, and K. M. Murphy. 2005. 'ERM is required for transcriptional control of the spermatogonial stem cell niche', *Nature*, 436: 1030-4.

Chen, Y. H., S. M. Gianino, and D. H. Gutmann. 2015. 'Neurofibromatosis-1 regulation of neural stem cell proliferation and multilineage differentiation operates through distinct RAS effector pathways', *Genes Dev*, 29: 1677-82.

Chen, Y. H., L. D. McGowan, P. J. Cimino, S. Dahiya, J. R. Leonard, D. Y. Lee, and D. H. Gutmann. 2015. 'Mouse low-grade gliomas contain cancer stem cells with unique molecular and functional properties', *Cell Rep*, 10: 1899-912.

Cichowski, K., and T. Jacks. 2001. 'NF1 tumor suppressor gene function: narrowing the GAP', *Cell*, 104: 593-604.

Cin, H., C. Meyer, R. Herr, W. G. Janzarik, S. Lambert, D. T. Jones, K. Jacob, A. Benner, H. Witt, M. Remke, S. Bender, F. Falkenstein, T. N. Van Anh, H. Olbrich, A. von Deimling, A. Pekrun, A. E. Kulozik, A. Gnekow, W. Scheurlen, O. Witt, H. Omran, N. Jabado, V. P. Collins, T. Brummer, R. Marschalek, P. Lichter, A. Korshunov, and S. M. Pfister. 2011. 'Oncogenic FAM131B-BRAF fusion resulting from 7q34 deletion comprises an alternative mechanism of MAPK pathway activation in pilocytic astrocytoma', *Acta Neuropathol*, 121: 763-74.

Collins, V. P., D. T. Jones, and C. Giannini. 2015. 'Pilocytic astrocytoma: pathology, molecular mechanisms and markers', *Acta Neuropathol*, 129: 775-88.

Colman, S. D., C. A. Williams, and M. R. Wallace. 1995. 'Benign neurofibromas in type 1 neurofibromatosis (NF1) show somatic deletions of the NF1 gene', *Nat Genet*, 11: 90-2.

Coniglio, S. J., E. Eugenin, K. Dobrenis, E. R. Stanley, B. L. West, M. H. Symons, and J. E. Segall. 2012. 'Microglial stimulation of glioblastoma invasion involves epidermal growth factor

receptor (EGFR) and colony stimulating factor 1 receptor (CSF-1R) signaling', *Mol Med*, 18: 519-27.

Cui, Y., R. M. Costa, G. G. Murphy, Y. Elgersma, Y. Zhu, D. H. Gutmann, L. F. Parada, I. Mody, and A. J. Silva. 2008. 'Neurofibromin regulation of ERK signaling modulates GABA release and learning', *Cell*, 135: 549-60.

Daginakatte, G. C., S. M. Gianino, N. W. Zhao, A. S. Parsadanian, and D. H. Gutmann. 2008. 'Increased c-Jun-NH2-kinase signaling in neurofibromatosis-1 heterozygous microglia drives microglia activation and promotes optic glioma proliferation', *Cancer Res*, 68: 10358-66.

Daginakatte, G. C., and D. H. Gutmann. 2007. 'Neurofibromatosis-1 (Nf1) heterozygous brain microglia elaborate paracrine factors that promote Nf1-deficient astrocyte and glioma growth', *Hum Mol Genet*, 16: 1098-112.

Dakubo, G. D., S. T. Beug, C. J. Mazerolle, S. Thurig, Y. Wang, and V. A. Wallace. 2008. 'Control of glial precursor cell development in the mouse optic nerve by sonic hedgehog from retinal ganglion cells', *Brain Res*, 1228: 27-42.

Dakubo, G. D., Y. P. Wang, C. Mazerolle, K. Campsall, A. P. McMahon, and V. A. Wallace. 2003. 'Retinal ganglion cell-derived sonic hedgehog signaling is required for optic disc and stalk neuroepithelial cell development', *Development*, 130: 2967-80.

Dasgupta, B., and D. H. Gutmann. 2005. 'Neurofibromin regulates neural stem cell proliferation, survival, and astroglial differentiation in vitro and in vivo', *J Neurosci*, 25: 5584-94.

Daston, M. M., H. Scrable, M. Nordlund, A. K. Sturbaum, L. M. Nissen, and N. Ratner. 1992. 'The protein product of the neurofibromatosis type 1 gene is expressed at highest abundance in neurons, Schwann cells, and oligodendrocytes', *Neuron*, 8: 415-28.

Dawson, M. R., A. Polito, J. M. Levine, and R. Reynolds. 2003. 'NG2-expressing glial progenitor cells: an abundant and widespread population of cycling cells in the adult rat CNS', *Mol Cell Neurosci*, 24: 476-88.

Diggs-Andrews, K. A., J. A. Brown, S. M. Gianino, J. B. Rubin, D. F. Wozniak, and D. H. Gutmann. 2014. 'Sex Is a major determinant of neuronal dysfunction in neurofibromatosis type 1', *Ann Neurol*, 75: 309-16.

Fangusaro, Jason, Arzu Onar-Thomas, Tina Y. Poussaint, Shengjie Wu, Azra H. Ligon, Neal Lindeman, Anu Banerjee, Roger J. Packer, Lindsay B. Kilburn, Ian F. Pollack, Regina I. Jakacki, Ibrahim Qaddoumi, Paul G. Fisher, Girish Dhall, Patricia Baxter, Susan G. Kreissman, Clinton F. Stewart, Stefan M. Pfister, David T. W. Jones, Gilbert Vezina, Jessica Stern, Ashok Panigrahy, Blaise V. Jones, Zoltan Patay, Benita Tamrazi, Jeremy Y. Jones, Sofia S. Haque, David S. Enterline, Soonmee Cha, Laurence A. Doyle, Malcolm Smith, James M. Boyett, Ira J. Dunkel, and Maryam Fouladi. 2017. 'LGG-08. A PHASE II PROSPECTIVE STUDY OF SELUMETINIB IN CHILDREN WITH RECURRENT OR REFRACTORY LOW-GRADE GLIOMA (LGG): A PEDIATRIC BRAIN TUMOR CONSORTIUM (PBTC) STUDY', *Neuro-Oncology*, 19: iv34-iv35.

Fisher, M. J., M. Loguidice, D. H. Gutmann, R. Listernick, R. E. Ferner, N. J. Ullrich, R. J. Packer, U. Tabori, R. O. Hoffman, S. L. Ardern-Holmes, T. R. Hummel, D. R. Hargrave, E. Bouffet, J. Charrow, L. T. Bilaniuk, L. J. Balcer, and G. T. Liu. 2012. 'Visual outcomes in children with neurofibromatosis type 1-associated optic pathway glioma following chemotherapy: a multicenter retrospective analysis', *Neuro Oncol*, 14: 790-7.

Forshew, T., R. G. Tatevossian, A. R. Lawson, J. Ma, G. Neale, B. W. Ogunkolade, T. A. Jones, J. Aarum, J. Dalton, S. Bailey, T. Chaplin, R. L. Carter, A. Gajjar, A. Broniscer, B. D.

Young, D. W. Ellison, and D. Sheer. 2009. 'Activation of the ERK/MAPK pathway: a signature genetic defect in posterior fossa pilocytic astrocytomas', *J Pathol*, 218: 172-81.
Freeman, C. R., J. P. Farmer, and J. Montes. 1998. 'Low-grade astrocytomas in children: evolving management strategies', *Int J Radiat Oncol Biol Phys*, 41: 979-87.
Fried, I., U. Tabori, T. Tihan, A. Reginald, and E. Bouffet. 2013. 'Optic pathway gliomas: a review', *CNS Oncol*, 2: 143-59.
Friedlander, M. 2007. 'Fibrosis and diseases of the eye', *J Clin Invest*, 117: 576-86.
Friedman, J. M. 1999. 'Epidemiology of neurofibromatosis type 1', *Am J Med Genet*, 89: 1-6.
Galli, R., E. Binda, U. Orfanelli, B. Cipelletti, A. Gritti, S. De Vitis, R. Fiocco, C. Foroni, F. Dimeco, and A. Vescovi. 2004. 'Isolation and characterization of tumorigenic, stem-like neural precursors from human glioblastoma', *Cancer Res*, 64: 7011-21.
Gao, L., and R. H. Miller. 2006. 'Specification of optic nerve oligodendrocyte precursors by retinal ganglion cell axons', *J Neurosci*, 26: 7619-28.
Geha, S., J. Pallud, M. P. Junier, B. Devaux, N. Leonard, F. Chassoux, H. Chneiweiss, C. Daumas-Duport, and P. Varlet. 2010. 'NG2+/Olig2+ cells are the major cycle-related cell population of the adult human normal brain', *Brain Pathol*, 20: 399-411.
Gilmartin, A. G., M. R. Bleam, A. Groy, K. G. Moss, E. A. Minthorn, S. G. Kulkarni, C. M. Rominger, S. Erskine, K. E. Fisher, J. Yang, F. Zappacosta, R. Annan, D. Sutton, and S. G. Laquerre. 2011. 'GSK1120212 (JTP-74057) is an inhibitor of MEK activity and activation with favorable pharmacokinetic properties for sustained in vivo pathway inhibition', *Clin Cancer Res*, 17: 989-1000.
Glover, T. W., C. K. Stein, E. Legius, L. B. Andersen, A. Brereton, and S. Johnson. 1991. 'Molecular and cytogenetic analysis of tumors in von Recklinghausen neurofibromatosis', *Genes Chromosomes Cancer*, 3: 62-70.
Gutmann, D. H., A. Aylsworth, J. C. Carey, B. Korf, J. Marks, R. E. Pyeritz, A. Rubenstein, and D. Viskochil. 1997. 'The diagnostic evaluation and multidisciplinary management of neurofibromatosis 1 and neurofibromatosis 2', *JAMA*, 278: 51-7.
Gutmann, D. H., M. D. McLellan, I. Hussain, J. W. Wallis, L. L. Fulton, R. S. Fulton, V. Magrini, R. Demeter, T. Wylie, C. Kandoth, J. R. Leonard, A. Guha, C. A. Miller, L. Ding, and E. R. Mardis. 2013. 'Somatic neurofibromatosis type 1 (NF1) inactivation characterizes NF1-associated pilocytic astrocytoma', *Genome Res*, 23: 431-9.
Hanahan, D., and R. A. Weinberg. 2000. 'The hallmarks of cancer', *Cell*, 100: 57-70.
Hegedus, B., B. Dasgupta, J. E. Shin, R. J. Emnett, E. K. Hart-Mahon, L. Elghazi, E. Bernal-Mizrachi, and D. H. Gutmann. 2007. 'Neurofibromatosis-1 regulates neuronal and glial cell differentiation from neuroglial progenitors in vivo by both cAMP- and Ras-dependent mechanisms', *Cell Stem Cell*, 1: 443-57.
Hegedus, B., F. W. Hughes, J. R. Garbow, S. Gianino, D. Banerjee, K. Kim, M. H. Ellisman, M. A. Brantley, Jr., and D. H. Gutmann. 2009. 'Optic nerve dysfunction in a mouse model of neurofibromatosis-1 optic glioma', *J Neuropathol Exp Neurol*, 68: 542-51.
Hemmati, H. D., I. Nakano, J. A. Lazareff, M. Masterman-Smith, D. H. Geschwind, M. Bronner-Fraser, and H. I. Kornblum. 2003. 'Cancerous stem cells can arise from pediatric brain tumors', *Proc Natl Acad Sci U S A*, 100: 15178-83.
Huson, S. M., P. S. Harper, and D. A. Compston. 1988. 'Von Recklinghausen neurofibromatosis. A clinical and population study in south-east Wales', *Brain*, 111 (Pt 6): 1355-81.
Hyman, S. L., A. Shores, and K. N. North. 2005. 'The nature and frequency of cognitive deficits in children with neurofibromatosis type 1', *Neurology*, 65: 1037-44.

Jacks, T., T. S. Shih, E. M. Schmitt, R. T. Bronson, A. Bernards, and R. A. Weinberg. 1994. 'Tumour predisposition in mice heterozygous for a targeted mutation in Nf1', *Nat Genet*, 7: 353-61.

Jackson, E. L., J. M. Garcia-Verdugo, S. Gil-Perotin, M. Roy, A. Quinones-Hinojosa, S. VandenBerg, and A. Alvarez-Buylla. 2006. 'PDGFR alpha-positive B cells are neural stem cells in the adult SVZ that form glioma-like growths in response to increased PDGF signaling', *Neuron*, 51: 187-99.

Jacob, K., S. Albrecht, C. Sollier, D. Faury, E. Sader, A. Montpetit, D. Serre, P. Hauser, M. Garami, L. Bognar, Z. Hanzely, J. L. Montes, J. Atkinson, J. P. Farmer, E. Bouffet, C. Hawkins, U. Tabori, and N. Jabado. 2009. 'Duplication of 7q34 is specific to juvenile pilocytic astrocytomas and a hallmark of cerebellar and optic pathway tumours', *Br J Cancer*, 101: 722-33.

Jacob, K., D. A. Quang-Khuong, D. T. Jones, H. Witt, S. Lambert, S. Albrecht, O. Witt, C. Vezina, M. Shirinian, D. Faury, M. Garami, P. Hauser, A. Klekner, L. Bognar, J. P. Farmer, J. L. Montes, J. Atkinson, C. Hawkins, A. Korshunov, V. P. Collins, S. M. Pfister, U. Tabori, and N. Jabado. 2011. 'Genetic aberrations leading to MAPK pathway activation mediate oncogene-induced senescence in sporadic pilocytic astrocytomas', *Clin Cancer Res*, 17: 4650-60.

Jones, D. T., B. Hutter, N. Jager, A. Korshunov, M. Kool, H. J. Warnatz, T. Zichner, S. R. Lambert, M. Ryzhova, D. A. Quang, A. M. Fontebasso, A. M. Stutz, S. Hutter, M. Zuckermann, D. Sturm, J. Gronych, B. Lasitschka, S. Schmidt, H. Seker-Cin, H. Witt, M. Sultan, M. Ralser, P. A. Northcott, V. Hovestadt, S. Bender, E. Pfaff, S. Stark, D. Faury, J. Schwartzentruber, J. Majewski, U. D. Weber, M. Zapatka, B. Raeder, M. Schlesner, C. L. Worth, C. C. Bartholomae, C. von Kalle, C. D. Imbusch, S. Radomski, C. Lawerenz, P. van Sluis, J. Koster, R. Volckmann, R. Versteeg, H. Lehrach, C. Monoranu, B. Winkler, A. Unterberg, C. Herold-Mende, T. Milde, A. E. Kulozik, M. Ebinger, M. U. Schuhmann, Y. J. Cho, S. L. Pomeroy, A. von Deimling, O. Witt, M. D. Taylor, S. Wolf, M. A. Karajannis, C. G. Eberhart, W. Scheurlen, M. Hasselblatt, K. L. Ligon, M. W. Kieran, J. O. Korbel, M. L. Yaspo, B. Brors, J. Felsberg, G. Reifenberger, V. P. Collins, N. Jabado, R. Eils, P. Lichter, S. M. Pfister, and Project International Cancer Genome Consortium PedBrain Tumor. 2013. 'Recurrent somatic alterations of FGFR1 and NTRK2 in pilocytic astrocytoma', *Nat Genet*, 45: 927-32.

Jones, D. T. W., M. W. Kieran, E. Bouffet, S. Alexandrescu, P. Bandopadhayay, M. Bornhorst, D. Ellison, J. Fangusaro, M. J. Fisher, N. Foreman, M. Fouladi, D. Hargrave, C. Hawkins, N. Jabado, M. Massimino, S. Mueller, G. Perilongo, A. Y. N. Schouten van Meeteren, U. Tabori, K. Warren, A. J. Waanders, D. Walker, W. Weiss, O. Witt, K. Wright, Y. Zhu, D. C. Bowers, S. M. Pfister, and R. J. Packer. 2018. 'Pediatric low-grade gliomas: next biologically driven steps', *Neuro Oncol*, 20: 160-73.

Kalamarides, M., A. O. Stemmer-Rachamimov, M. Niwa-Kawakita, F. Chareyre, E. Taranchon, Z. Y. Han, C. Martinelli, E. A. Lusis, B. Hegedus, D. H. Gutmann, and M. Giovannini. 2011. 'Identification of a progenitor cell of origin capable of generating diverse meningioma histological subtypes', *Oncogene*, 30: 2333-44.

Kaul, A., J. A. Toonen, P. J. Cimino, S. M. Gianino, and D. H. Gutmann. 2015. 'Akt- or MEK-mediated mTOR inhibition suppresses Nf1 optic glioma growth', *Neuro Oncol*, 17: 843-53.

Kessaris, N., F. Jamen, L. L. Rubin, and W. D. Richardson. 2004. 'Cooperation between sonic hedgehog and fibroblast growth factor/MAPK signalling pathways in neocortical precursors', *Development*, 131: 1289-98.

Kim, E., Y. Wang, S. J. Kim, M. Bornhorst, E. S. Jecrois, T. E. Anthony, C. Wang, Y. E. Li, J. L. Guan, G. G. Murphy, and Y. Zhu. 2014. 'Transient inhibition of the ERK pathway prevents cerebellar developmental defects and improves long-term motor functions in murine models of neurofibromatosis type 1', *Elife*, 3.

Klaes, A., T. Menne, A. Stollewerk, H. Scholz, and C. Klambt. 1994. 'The Ets transcription factors encoded by the Drosophila gene pointed direct glial cell differentiation in the embryonic CNS', *Cell*, 78: 149-60.

Kluwe, L., C. Hagel, M. Tatagiba, S. Thomas, D. Stavrou, H. Ostertag, A. von Deimling, and V. F. Mautner. 2001. 'Loss of NF1 alleles distinguish sporadic from NF1-associated pilocytic astrocytomas', *J Neuropathol Exp Neurol*, 60: 917-20.

Kondo, T., and M. Raff. 2000. 'Oligodendrocyte precursor cells reprogrammed to become multipotential CNS stem cells', *Science*, 289: 1754-7.

Ku, M. C., S. A. Wolf, D. Respondek, V. Matyash, A. Pohlmann, S. Waiczies, H. Waiczies, T. Niendorf, M. Synowitz, R. Glass, and H. Kettenmann. 2013. 'GDNF mediates glioblastoma-induced microglia attraction but not astrogliosis', *Acta Neuropathol*, 125: 609-20.

Kuwabara, T. 1975. 'Development of the optic nerve of the rat', *Invest Ophthalmol*, 14: 732-45.

Kwon, C. H., D. Zhao, J. Chen, S. Alcantara, Y. Li, D. K. Burns, R. P. Mason, E. Y. Lee, H. Wu, and L. F. Parada. 2008. 'Pten haploinsufficiency accelerates formation of high-grade astrocytomas', *Cancer Res*, 68: 3286-94.

Lau, N., M. M. Feldkamp, L. Roncari, A. H. Loehr, P. Shannon, D. H. Gutmann, and A. Guha. 2000. 'Loss of neurofibromin is associated with activation of RAS/MAPK and PI3-K/AKT signaling in a neurofibromatosis 1 astrocytoma', *J Neuropathol Exp Neurol*, 59: 759-67.

Lee, D. Y., S. M. Gianino, and D. H. Gutmann. 2012. 'Innate neural stem cell heterogeneity determines the patterning of glioma formation in children', *Cancer Cell*, 22: 131-8.

Lee, J. S., A. Padmanabhan, J. Shin, S. Zhu, F. Guo, J. P. Kanki, J. A. Epstein, and A. T. Look. 2010. 'Oligodendrocyte progenitor cell numbers and migration are regulated by the zebrafish orthologs of the NF1 tumor suppressor gene', *Hum Mol Genet*, 19: 4643-53.

Legius, E., D. A. Marchuk, F. S. Collins, and T. W. Glover. 1993. 'Somatic deletion of the neurofibromatosis type 1 gene in a neurofibrosarcoma supports a tumour suppressor gene hypothesis', *Nat Genet*, 3: 122-6.

Li, X., J. M. Newbern, Y. Wu, M. Morgan-Smith, J. Zhong, J. Charron, and W. D. Snider. 2012. 'MEK Is a Key Regulator of Gliogenesis in the Developing Brain', *Neuron*, 75: 1035-50.

Ligon, K. L., J. A. Alberta, A. T. Kho, J. Weiss, M. R. Kwaan, C. L. Nutt, D. N. Louis, C. D. Stiles, and D. H. Rowitch. 2004. 'The oligodendroglial lineage marker OLIG2 is universally expressed in diffuse gliomas', *J Neuropathol Exp Neurol*, 63: 499-509.

Listernick, R. 2016. 'Predicting which NF1 optic pathway gliomas will require treatment', *Neurology*, 87: 2389-90.

Listernick, R., J. Charrow, and D. H. Gutmann. 1999. 'Intracranial gliomas in neurofibromatosis type 1', *Am J Med Genet*, 89: 38-44.

Listernick, R., R. E. Ferner, G. T. Liu, and D. H. Gutmann. 2007. 'Optic pathway gliomas in neurofibromatosis-1: controversies and recommendations', *Ann Neurol*, 61: 189-98.

Listernick, R., R. E. Ferner, L. Piersall, S. Sharif, D. H. Gutmann, and J. Charrow. 2004. 'Late-onset optic pathway tumors in children with neurofibromatosis 1', *Neurology*, 63: 1944-6.
Listernick, R., D. N. Louis, R. J. Packer, and D. H. Gutmann. 1997. 'Optic pathway gliomas in children with neurofibromatosis 1: consensus statement from the NF1 Optic Pathway Glioma Task Force', *Ann Neurol*, 41: 143-9.
Liu, C., J. C. Sage, M. R. Miller, R. G. Verhaak, S. Hippenmeyer, H. Vogel, O. Foreman, R. T. Bronson, A. Nishiyama, L. Luo, and H. Zong. 2011. 'Mosaic analysis with double markers reveals tumor cell of origin in glioma', *Cell*, 146: 209-21.
Lu, Q. R., T. Sun, Z. Zhu, N. Ma, M. Garcia, C. D. Stiles, and D. H. Rowitch. 2002. 'Common developmental requirement for Olig function indicates a motor neuron/oligodendrocyte connection', *Cell*, 109: 75-86.
Macdonald, R., J. Scholes, U. Strahle, C. Brennan, N. Holder, M. Brand, and S. W. Wilson. 1997. 'The Pax protein Noi is required for commissural axon pathway formation in the rostral forebrain', *Development*, 124: 2397-408.
Malatesta, P., M. A. Hack, E. Hartfuss, H. Kettenmann, W. Klinkert, F. Kirchhoff, and M. Gotz. 2003. 'Neuronal or glial progeny: regional differences in radial glia fate', *Neuron*, 37: 751-64.
Marchuk, D. A., A. M. Saulino, R. Tavakkol, M. Swaroop, M. R. Wallace, L. B. Andersen, A. L. Mitchell, D. H. Gutmann, M. Boguski, and F. S. Collins. 1991. 'cDNA cloning of the type 1 neurofibromatosis gene: complete sequence of the NF1 gene product', *Genomics*, 11: 931-40.
Marshall, C. A., B. G. Novitch, and J. E. Goldman. 2005. 'Olig2 directs astrocyte and oligodendrocyte formation in postnatal subventricular zone cells', *J Neurosci*, 25: 7289-98.
Mendoza, M. C., E. E. Er, and J. Blenis. 2011. 'The Ras-ERK and PI3K-mTOR pathways: cross-talk and compensation', *Trends Biochem Sci*, 36: 320-8.
Menn, B., J. M. Garcia-Verdugo, C. Yaschine, O. Gonzalez-Perez, D. Rowitch, and A. Alvarez-Buylla. 2006. 'Origin of oligodendrocytes in the subventricular zone of the adult brain', *J Neurosci*, 26: 7907-18.
Messersmith, W. A., M. Hidalgo, M. Carducci, and S. G. Eckhardt. 2006. 'Novel targets in solid tumors: MEK inhibitors', *Clin Adv Hematol Oncol*, 4: 831-6.
Mi, H., and B. A. Barres. 1999. 'Purification and characterization of astrocyte precursor cells in the developing rat optic nerve', *J Neurosci*, 19: 1049-61.
Miller, R. H., S. David, R. Patel, E. R. Abney, and M. C. Raff. 1985. 'A quantitative immunohistochemical study of macroglial cell development in the rat optic nerve: in vivo evidence for two distinct astrocyte lineages', *Dev Biol*, 111: 35-41.
Mokhtari, K., S. Paris, L. Aguirre-Cruz, N. Privat, E. Criniere, Y. Marie, J. J. Hauw, M. Kujas, D. Rowitch, K. Hoang-Xuan, J. Y. Delattre, and M. Sanson. 2005. 'Olig2 expression, GFAP, p53 and 1p loss analysis contribute to glioma subclassification', *Neuropathol Appl Neurobiol*, 31: 62-9.
Mui, S. H., J. W. Kim, G. Lemke, and S. Bertuzzi. 2005. 'Vax genes ventralize the embryonic eye', *Genes Dev*, 19: 1249-59.
Murphy, E. S., H. Xie, T. E. Merchant, J. S. Yu, S. T. Chao, and J. H. Suh. 2015. 'Review of cranial radiotherapy-induced vasculopathy', *J Neurooncol*, 122: 421-9.
Nadal-Nicolas, F. M., M. Jimenez-Lopez, P. Sobrado-Calvo, L. Nieto-Lopez, I. Canovas-Martinez, M. Salinas-Navarro, M. Vidal-Sanz, and M. Agudo. 2009. 'Brn3a as a marker of

retinal ganglion cells: qualitative and quantitative time course studies in naive and optic nerve-injured retinas', *Invest Ophthalmol Vis Sci*, 50: 3860-8.

Newbern, J. M., X. Li, S. E. Shoemaker, J. Zhou, J. Zhong, Y. Wu, D. Bonder, S. Hollenback, G. Coppola, D. H. Geschwind, G. E. Landreth, and W. D. Snider. 2011. 'Specific functions for ERK/MAPK signaling during PNS development', *Neuron*, 69: 91-105.

Niihori, T., Y. Aoki, Y. Narumi, G. Neri, H. Cave, A. Verloes, N. Okamoto, R. C. Hennekam, G. Gillessen-Kaesbach, D. Wieczorek, M. I. Kavamura, K. Kurosawa, H. Ohashi, L. Wilson, D. Heron, D. Bonneau, G. Corona, T. Kaname, K. Naritomi, C. Baumann, N. Matsumoto, K. Kato, S. Kure, and Y. Matsubara. 2006. 'Germline KRAS and BRAF mutations in cardio-facio-cutaneous syndrome', *Nat Genet*, 38: 294-6.

Ohren, J. F., H. Chen, A. Pavlovsky, C. Whitehead, E. Zhang, P. Kuffa, C. Yan, P. McConnell, C. Spessard, C. Banotai, W. T. Mueller, A. Delaney, C. Omer, J. Sebolt-Leopold, D. T. Dudley, I. K. Leung, C. Flamme, J. Warmus, M. Kaufman, S. Barrett, H. Tecle, and C. A. Hasemann. 2004. 'Structures of human MAP kinase kinase 1 (MEK1) and MEK2 describe novel noncompetitive kinase inhibition', *Nat Struct Mol Biol*, 11: 1192-7.

Ohyama, T., and A. K. Groves. 2004. 'Generation of Pax2-Cre mice by modification of a Pax2 bacterial artificial chromosome', *Genesis*, 38: 195-9.

Ono, K., H. Takebayashi, K. Ikeda, M. Furusho, T. Nishizawa, K. Watanabe, and K. Ikenaka. 2008. 'Regional- and temporal-dependent changes in the differentiation of Olig2 progenitors in the forebrain, and the impact on astrocyte development in the dorsal pallium', *Dev Biol*, 320: 456-68.

Ono, K., Y. Yasui, U. Rutishauser, and R. H. Miller. 1997. 'Focal ventricular origin and migration of oligodendrocyte precursors into the chick optic nerve', *Neuron*, 19: 283-92.

Ono, K., K. Yoshii, H. Tominaga, H. Gotoh, T. Nomura, H. Takebayashi, and K. Ikenaka. 2017. 'Oligodendrocyte precursor cells in the mouse optic nerve originate in the preoptic area', *Brain Struct Funct*, 222: 2441-48.

Ortega, F., S. Gascon, G. Masserdotti, A. Deshpande, C. Simon, J. Fischer, L. Dimou, D. Chichung Lie, T. Schroeder, and B. Berninger. 2013. 'Oligodendrogliogenic and neurogenic adult subependymal zone neural stem cells constitute distinct lineages and exhibit differential responsiveness to Wnt signalling', *Nat Cell Biol*, 15: 602-13.

Ostrom, Q. T., H. Gittleman, P. Liao, C. Rouse, Y. Chen, J. Dowling, Y. Wolinsky, C. Kruchko, and J. Barnholtz-Sloan. 2014. 'CBTRUS statistical report: primary brain and central nervous system tumors diagnosed in the United States in 2007-2011', *Neuro Oncol*, 16 Suppl 4: iv1-63.

Packer, R. J., J. Ater, J. Allen, P. Phillips, R. Geyer, H. S. Nicholson, R. Jakacki, E. Kurczynski, M. Needle, J. Finlay, G. Reaman, and J. M. Boyett. 1997. 'Carboplatin and vincristine chemotherapy for children with newly diagnosed progressive low-grade gliomas', *J Neurosurg*, 86: 747-54.

Packer, R. J., S. Pfister, E. Bouffet, R. Avery, P. Bandopadhayay, M. Bornhorst, D. C. Bowers, D. Ellison, J. Fangusaro, N. Foreman, M. Fouladi, A. Gajjar, D. Haas-Kogan, C. Hawkins, C. Y. Ho, E. Hwang, N. Jabado, L. B. Kilburn, A. Lassaletta, K. L. Ligon, M. Massimino, S. V. Meeteren, S. Mueller, T. Nicolaides, G. Perilongo, U. Tabori, G. Vezina, K. Warren, O. Witt, Y. Zhu, D. T. Jones, and M. Kieran. 2017. 'Pediatric low-grade gliomas: implications of the biologic era', *Neuro Oncol*, 19: 750-61.

Paolicelli, R. C., K. Bisht, and M. E. Tremblay. 2014. 'Fractalkine regulation of microglial physiology and consequences on the brain and behavior', *Front Cell Neurosci*, 8: 129.

Parsa, C. F., C. S. Hoyt, R. L. Lesser, J. M. Weinstein, C. M. Strother, R. Muci-Mendoza, M. Ramella, R. S. Manor, W. A. Fletcher, M. X. Repka, J. A. Garrity, R. N. Ebner, M. L. Monteiro, R. M. McFadzean, I. V. Rubtsova, and W. F. Hoyt. 2001. 'Spontaneous regression of optic gliomas: thirteen cases documented by serial neuroimaging', *Arch Ophthalmol*, 119: 516-29.

Pasmant, E., M. Vidaud, D. Vidaud, and P. Wolkenstein. 2012. 'Neurofibromatosis type 1: from genotype to phenotype', *J Med Genet*, 49: 483-9.

Pequignot, M. O., A. C. Provost, S. Salle, P. Taupin, K. M. Sainton, D. Marchant, J. C. Martinou, J. C. Ameisen, J. P. Jais, and M. Abitbol. 2003. 'Major role of BAX in apoptosis during retinal development and in establishment of a functional postnatal retina', *Dev Dyn*, 228: 231-8.

Pfister, S., and O. Witt. 2009. 'Pediatric gliomas', *Recent Results Cancer Res*, 171: 67-81.

Platten, M., A. Kretz, U. Naumann, S. Aulwurm, K. Egashira, S. Isenmann, and M. Weller. 2003. 'Monocyte chemoattractant protein-1 increases microglial infiltration and aggressiveness of gliomas', *Ann Neurol*, 54: 388-92.

Pong, W. W., S. B. Higer, S. M. Gianino, R. J. Emnett, and D. H. Gutmann. 2013. 'Reduced microglial CX3CR1 expression delays neurofibromatosis-1 glioma formation', *Ann Neurol*, 73: 303-8.

Preusser, M., H. Budka, K. Rossler, and J. A. Hainfellner. 2007. 'OLIG2 is a useful immunohistochemical marker in differential diagnosis of clear cell primary CNS neoplasms', *Histopathology*, 50: 365-70.

Rafalski, V. A., P. P. Ho, J. O. Brett, D. Ucar, J. C. Dugas, E. A. Pollina, L. M. Chow, A. Ibrahim, S. J. Baker, B. A. Barres, L. Steinman, and A. Brunet. 2013. 'Expansion of oligodendrocyte progenitor cells following SIRT1 inactivation in the adult brain', *Nat Cell Biol*, 15: 614-24.

Raff, M. C., E. R. Abney, J. Cohen, R. Lindsay, and M. Noble. 1983. 'Two types of astrocytes in cultures of developing rat white matter: differences in morphology, surface gangliosides, and growth characteristics', *J Neurosci*, 3: 1289-300.

Raff, M. C., E. R. Abney, and R. H. Miller. 1984. 'Two glial cell lineages diverge prenatally in rat optic nerve', *Dev Biol*, 106: 53-60.

Reis, G. F., M. M. Bloomer, A. Perry, J. J. Phillips, J. P. Grenert, A. N. Karnezis, and T. Tihan. 2013. 'Pilocytic astrocytomas of the optic nerve and their relation to pilocytic astrocytomas elsewhere in the central nervous system', *Mod Pathol*, 26: 1279-87.

Rickert, C. H., and W. Paulus. 2001. 'Epidemiology of central nervous system tumors in childhood and adolescence based on the new WHO classification', *Childs Nerv Syst*, 17: 503-11.

Rodriguez, A. R., L. P. de Sevilla Muller, and N. C. Brecha. 2014. 'The RNA binding protein RBPMS is a selective marker of ganglion cells in the mammalian retina', *J Comp Neurol*, 522: 1411-43.

Rodriguez-Viciana, P., O. Tetsu, W. E. Tidyman, A. L. Estep, B. A. Conger, M. S. Cruz, F. McCormick, and K. A. Rauen. 2006. 'Germline mutations in genes within the MAPK pathway cause cardio-facio-cutaneous syndrome', *Science*, 311: 1287-90.

Sanchez-Ortiz, E., W. Cho, I. Nazarenko, W. Mo, J. Chen, and L. F. Parada. 2014. 'NF1 regulation of RAS/ERK signaling is required for appropriate granule neuron progenitor expansion and migration in cerebellar development', *Genes Dev*, 28: 2407-20.

Schindler, G., D. Capper, J. Meyer, W. Janzarik, H. Omran, C. Herold-Mende, K. Schmieder, P. Wesseling, C. Mawrin, M. Hasselblatt, D. N. Louis, A. Korshunov, S. Pfister, C. Hartmann, W. Paulus, G. Reifenberger, and A. von Deimling. 2011. 'Analysis of BRAF V600E

mutation in 1,320 nervous system tumors reveals high mutation frequencies in pleomorphic xanthoastrocytoma, ganglioglioma and extra-cerebellar pilocytic astrocytoma', *Acta Neuropathol*, 121: 397-405.

Schmid, R. S., Y. Yokota, and E. S. Anton. 2006. 'Generation and characterization of brain lipid-binding protein promoter-based transgenic mouse models for the study of radial glia', *Glia*, 53: 345-51.

Schwarz, M., F. Cecconi, G. Bernier, N. Andrejewski, B. Kammandel, M. Wagner, and P. Gruss. 2000. 'Spatial specification of mammalian eye territories by reciprocal transcriptional repression of Pax2 and Pax6', *Development*, 127: 4325-34.

Sebolt-Leopold, J. S., D. T. Dudley, R. Herrera, K. Van Becelaere, A. Wiland, R. C. Gowan, H. Tecle, S. D. Barrett, A. Bridges, S. Przybranowski, W. R. Leopold, and A. R. Saltiel. 1999. 'Blockade of the MAP kinase pathway suppresses growth of colon tumors in vivo', *Nat Med*, 5: 810-6.

Sebolt-Leopold, J. S., and R. Herrera. 2004. 'Targeting the mitogen-activated protein kinase cascade to treat cancer', *Nat Rev Cancer*, 4: 937-47.

Serra, E., T. Rosenbaum, U. Winner, R. Aledo, E. Ars, X. Estivill, H. G. Lenard, and C. Lazaro. 2000. 'Schwann cells harbor the somatic NF1 mutation in neurofibromas: evidence of two different Schwann cell subpopulations', *Hum Mol Genet*, 9: 3055-64.

Shannon, K. M., P. O'Connell, G. A. Martin, D. Paderanga, K. Olson, P. Dinndorf, and F. McCormick. 1994. 'Loss of the normal NF1 allele from the bone marrow of children with type 1 neurofibromatosis and malignant myeloid disorders', *N Engl J Med*, 330: 597-601.

Sharif, S., R. Ferner, J. M. Birch, J. E. Gillespie, H. R. Gattamaneni, M. E. Baser, and D. G. Evans. 2006. 'Second primary tumors in neurofibromatosis 1 patients treated for optic glioma: substantial risks after radiotherapy', *J Clin Oncol*, 24: 2570-5.

Sharif, S., A. Moran, S. M. Huson, R. Iddenden, A. Shenton, E. Howard, and D. G. Evans. 2007. 'Women with neurofibromatosis 1 are at a moderately increased risk of developing breast cancer and should be considered for early screening', *J Med Genet*, 44: 481-4.

Sielska, M., P. Przanowski, B. Wylot, K. Gabrusiewicz, M. Maleszewska, M. Kijewska, M. Zawadzka, J. Kucharska, K. Vinnakota, H. Kettenmann, K. Kotulska, W. Grajkowska, and B. Kaminska. 2013. 'Distinct roles of CSF family cytokines in macrophage infiltration and activation in glioma progression and injury response', *J Pathol*, 230: 310-21.

Simmons, G. W., W. W. Pong, R. J. Emnett, C. R. White, S. M. Gianino, F. J. Rodriguez, and D. H. Gutmann. 2011. 'Neurofibromatosis-1 heterozygosity increases microglia in a spatially and temporally restricted pattern relevant to mouse optic glioma formation and growth', *J Neuropathol Exp Neurol*, 70: 51-62.

Singh, S. K., C. Hawkins, I. D. Clarke, J. A. Squire, J. Bayani, T. Hide, R. M. Henkelman, M. D. Cusimano, and P. B. Dirks. 2004. 'Identification of human brain tumour initiating cells', *Nature*, 432: 396-401.

Small, R. K., P. Riddle, and M. Noble. 1987. 'Evidence for migration of oligodendrocyte--type-2 astrocyte progenitor cells into the developing rat optic nerve', *Nature*, 328: 155-7.

Solga, A. C., J. A. Toonen, Y. Pan, P. J. Cimino, Y. Ma, G. A. Castillon, S. M. Gianino, M. H. Ellisman, D. Y. Lee, and D. H. Gutmann. 2017. 'The cell of origin dictates the temporal course of neurofibromatosis-1 (Nf1) low-grade glioma formation', *Oncotarget*, 8: 47206-15.

Soukkarieh, C., E. Agius, C. Soula, and P. Cochard. 2007. 'Pax2 regulates neuronal-glial cell fate choice in the embryonic optic nerve', *Dev Biol*, 303: 800-13.

Stiller, C. A., J. M. Chessells, and M. Fitchett. 1994. 'Neurofibromatosis and childhood leukaemia/lymphoma: a population-based UKCCSG study', *Br J Cancer*, 70: 969-72.

Sun, G. J., Y. Zhou, S. Ito, M. A. Bonaguidi, G. Stein-O'Brien, N. K. Kawasaki, N. Modak, Y. Zhu, G. L. Ming, and H. Song. 2015. 'Latent tri-lineage potential of adult hippocampal neural stem cells revealed by Nf1 inactivation', *Nat Neurosci*, 18: 1722-4.

Surawicz, T. S., F. Davis, S. Freels, E. R. Laws, Jr., and H. R. Menck. 1998. 'Brain tumor survival: results from the National Cancer Data Base', *J Neurooncol*, 40: 151-60.

Surawicz, T. S., B. J. McCarthy, V. Kupelian, P. J. Jukich, J. M. Bruner, and F. G. Davis. 1999. 'Descriptive epidemiology of primary brain and CNS tumors: results from the Central Brain Tumor Registry of the United States, 1990-1994', *Neuro Oncol*, 1: 14-25.

Tatsumi, K., H. Takebayashi, T. Manabe, K. F. Tanaka, M. Makinodan, T. Yamauchi, E. Makinodan, H. Matsuyoshi, H. Okuda, K. Ikenaka, and A. Wanaka. 2008. 'Genetic fate mapping of Olig2 progenitors in the injured adult cerebral cortex reveals preferential differentiation into astrocytes', *J Neurosci Res*, 86: 3494-502.

Taylor, M. D., H. Poppleton, C. Fuller, X. Su, Y. Liu, P. Jensen, S. Magdaleno, J. Dalton, C. Calabrese, J. Board, T. Macdonald, J. Rutka, A. Guha, A. Gajjar, T. Curran, and R. J. Gilbertson. 2005. 'Radial glia cells are candidate stem cells of ependymoma', *Cancer Cell*, 8: 323-35.

Tihan, T., P. G. Fisher, J. L. Kepner, C. Godfraind, R. D. McComb, P. T. Goldthwaite, and P. C. Burger. 1999. 'Pediatric astrocytomas with monomorphous pilomyxoid features and a less favorable outcome', *J Neuropathol Exp Neurol*, 58: 1061-8.

Torres, M., E. Gomez-Pardo, and P. Gruss. 1996. 'Pax2 contributes to inner ear patterning and optic nerve trajectory', *Development*, 122: 3381-91.

Ueda, H., J. M. Levine, R. H. Miller, and B. D. Trapp. 1999. 'Rat optic nerve oligodendrocytes develop in the absence of viable retinal ganglion cell axons', *J Cell Biol*, 146: 1365-74.

Viti, J., A. Feathers, J. Phillips, and L. Lillien. 2003. 'Epidermal growth factor receptors control competence to interpret leukemia inhibitory factor as an astrocyte inducer in developing cortex', *J Neurosci*, 23: 3385-93.

Vlenterie, M., U. Flucke, L. C. Hofbauer, H. J. Timmers, J. Gastmeier, D. E. Aust, W. T. van der Graaf, P. Wesseling, G. Eisenhofer, and J. W. Lenders. 2013. 'Pheochromocytoma and gastrointestinal stromal tumors in patients with neurofibromatosis type I', *Am J Med*, 126: 174-80.

Wallace, V. A., and M. C. Raff. 1999. 'A role for Sonic hedgehog in axon-to-astrocyte signalling in the rodent optic nerve', *Development*, 126: 2901-9.

Wang, Y., E. Kim, X. Wang, B. G. Novitch, K. Yoshikawa, L. S. Chang, and Y. Zhu. 2012. 'ERK inhibition rescues defects in fate specification of Nf1-deficient neural progenitors and brain abnormalities', *Cell*, 150: 816-30.

Wang, Y., J. Yang, H. Zheng, G. J. Tomasek, P. Zhang, P. E. McKeever, E. Y. Lee, and Y. Zhu. 2009. 'Expression of mutant p53 proteins implicates a lineage relationship between neural stem cells and malignant astrocytic glioma in a murine model', *Cancer Cell*, 15: 514-26.

Watters, J. J., J. M. Schartner, and B. Badie. 2005. 'Microglia function in brain tumors', *J Neurosci Res*, 81: 447-55.

Xu, G. F., P. O'Connell, D. Viskochil, R. Cawthon, M. Robertson, M. Culver, D. Dunn, J. Stevens, R. Gesteland, R. White, and et al. 1990. 'The neurofibromatosis type 1 gene encodes a protein related to GAP', *Cell*, 62: 599-608.

Xu, W., L. M. Mulligan, M. A. Ponder, L. Liu, B. A. Smith, C. G. Mathew, and B. A. Ponder. 1992. 'Loss of NF1 alleles in phaeochromocytomas from patients with type I neurofibromatosis', *Genes Chromosomes Cancer*, 4: 337-42.

Yalon, M., B. Rood, T. J. MacDonald, G. McCowage, R. Kane, S. Constantini, and R. J. Packer. 2013. 'A feasibility and efficacy study of rapamycin and erlotinib for recurrent pediatric low-grade glioma (LGG)', *Pediatr Blood Cancer*, 60: 71-6.

Yeh, T. C., V. Marsh, B. A. Bernat, J. Ballard, H. Colwell, R. J. Evans, J. Parry, D. Smith, B. J. Brandhuber, S. Gross, A. Marlow, B. Hurley, J. Lyssikatos, P. A. Lee, J. D. Winkler, K. Koch, and E. Wallace. 2007. 'Biological characterization of ARRY-142886 (AZD6244), a potent, highly selective mitogen-activated protein kinase kinase 1/2 inhibitor', *Clin Cancer Res*, 13: 1576-83.

Yue, T., K. Xian, E. Hurlock, M. Xin, S. G. Kernie, L. F. Parada, and Q. R. Lu. 2006. 'A critical role for dorsal progenitors in cortical myelination', *J Neurosci*, 26: 1275-80.

Zhang, J., G. Wu, C. P. Miller, R. G. Tatevossian, J. D. Dalton, B. Tang, W. Orisme, C. Punchihewa, M. Parker, I. Qaddoumi, F. A. Boop, C. Lu, C. Kandoth, L. Ding, R. Lee, R. Huether, X. Chen, E. Hedlund, P. Nagahawatte, M. Rusch, K. Boggs, J. Cheng, J. Becksfort, J. Ma, G. Song, Y. Li, L. Wei, J. Wang, S. Shurtleff, J. Easton, D. Zhao, R. S. Fulton, L. L. Fulton, D. J. Dooling, B. Vadodaria, H. L. Mulder, C. Tang, K. Ochoa, C. G. Mullighan, A. Gajjar, R. Kriwacki, D. Sheer, R. J. Gilbertson, E. R. Mardis, R. K. Wilson, J. R. Downing, S. J. Baker, D. W. Ellison, and Project St. Jude Children's Research Hospital-Washington University Pediatric Cancer Genome. 2013. 'Whole-genome sequencing identifies genetic alterations in pediatric low-grade gliomas', *Nat Genet*, 45: 602-12.

Zheng, H., L. Chang, N. Patel, J. Yang, L. Lowe, D. K. Burns, and Y. Zhu. 2008. 'Induction of abnormal proliferation by nonmyelinating schwann cells triggers neurofibroma formation', *Cancer Cell*, 13: 117-28.

Zhou, Q., and D. J. Anderson. 2002. 'The bHLH transcription factors OLIG2 and OLIG1 couple neuronal and glial subtype specification', *Cell*, 109: 61-73.

Zhu, Y., T. Harada, L. Liu, M. E. Lush, F. Guignard, C. Harada, D. K. Burns, M. L. Bajenaru, D. H. Gutmann, and L. F. Parada. 2005. 'Inactivation of NF1 in CNS causes increased glial progenitor proliferation and optic glioma formation', *Development*, 132: 5577-88.

Zhuo, L., M. Theis, I. Alvarez-Maya, M. Brenner, K. Willecke, and A. Messing. 2001. 'hGFAP-cre transgenic mice for manipulation of glial and neuronal function in vivo', *Genesis*, 31: 85-94.

Zong, H., J. S. Espinosa, H. H. Su, M. D. Muzumdar, and L. Luo. 2005. 'Mosaic analysis with double markers in mice', *Cell*, 121: 479-92.